TECHNISCHE UNIVERSITÄT MÜNCHEN

Fakultät für Maschinenwesen

Visual Augmentation for Rotorcraft Pilots in Degraded Visual Environment

Franz Xaver Viertler

Vollständiger Abdruck der von der Fakultät für Maschinenwesen der Technischen Universität München zur Erlangung des akademischen Grades eines

Doktor-Ingenieurs (Dr.-Ing.)

genehmigten Dissertation.

Vorsitzender:	Univ.-Prof. Dr.-Ing. Mirko Hornung
Prüfer der Dissertation:	1. Univ.-Prof. Dr.-Ing. Manfred Hajek
	2. Univ.-Prof. Dr. phil. Klaus Bengler

Die Dissertation wurde am 10.11.2016 bei der Technischen Universität München eingereicht und durch die Fakultät für Maschinenwesen am 06.03.2017 angenommen.

Abstract

Visual augmentation methods for rotorcraft pilots using a see-through head-mounted display have the potential to assist the pilot and to increase flight safety in severely degraded visual environments. This work investigates advanced 3D-conformal display concepts to improve the support of the pilot by showing terrain and obstacle data. A novel pilot-in-the-loop simulation experiment was designed and conducted to evaluate the display concepts in a safe environment at visual ranges below 800 meters. Sixteen professional pilots participated in this experiment to observe statistically significant results between different display variants and different visibility conditions. Two main tasks were considered, namely, low-altitude flight with obstacle avoidance and the rotorcraft stabilization during hover. The results showed that the pilot workload could be reduced using the advanced display concept for the obstacle avoidance task and the pilots were also able to fly faster and higher than without the assistance in low visibilities. However, the scenario regarding the hover task demonstrated limitations of the technology due to the limited available field-of-view of the head-mounted display.

Keywords:
Visual Augmentation, Degraded Visual Environment, Head-Mounted Display, Flight Simulation, Workload, Human-Machine-Interface, Pilot Assistance, Augmented Reality.

Zusammenfassung

Visuelle Methoden zur Erweiterung der Außensicht für Hubschrauberpiloten haben das Potential den Piloten durch ein Helmsichtsystem zu unterstützen und die Flugsicherheit in stark verschlechterten Sichtbedingungen zu erhöhen. Diese Arbeit untersucht hochentwickelte dreidimensionale, der Außensicht überlagerte Anzeigekonzepte zur Verbesserung der Unterstützungsmöglichkeiten für den Piloten durch die Darstellung von Gelände und Hindernis Informationen. Ein neuartiges Simulationsexperiment mit Piloten wurde entworfen und durchgeführt zur Bewertung der Anzeigekonzepte in einer sicheren Umgebung bei Sichtweiten unter 800 Meter. Sechzehn professionelle Piloten nahmen an dem Experiment teil, um statistisch signifikante Ergebnisse zwischen den Anzeigevarianten und den unterschiedlichen Sichtbedingungen beobachten zu können. Zwei Hauptaufgaben wurden betrachtet, und zwar der Flug in geringer Höhe mit Hindernisvermeidung und die Hubschrauberstabilisierung während dem Schwebeflug. Die Ergebnisse zeigten, dass die Arbeitsbelastung der Piloten mit dem fortschrittlichen Anzeigesystem für die Aufgabe der Hindernisvermeidung reduziert werden konnte und dass die Piloten bei geringen Sichtweiten schneller und höher fliegen konnten im Vergleich zum Fall ohne die Unterstützung. Die Schwebeflug Aufgabe veranschaulichte jedoch auch die Grenzen der Technologie durch den eingeschränkt verfügbaren Sichtbereich des Helmsichtsystems.

Schlüsselwörter:
Visuelle Erweiterung, Verschlechterte Sicht, Helmsichtsystem, Flugsimulation, Arbeitsbelastung, Mensch-Maschine-Interaktion, Pilotenunterstützung, Erweiterte Realität.

Acknowledgments

I sincerely like to thank all people who have supported me over the duration of this thesis, both through direct assistance with this study as well as through emotional support. First of all I would like to thank my supervisor Prof. Manfred Hajek for the opportunity to start this new field of research at the Institute of Helicopter Technology and for his support and constructive feedback. Moreover, I would like to thank Prof. Florian Holzapfel for pushing me into the right direction with his encouragement and for being a great mentor. I would also like to thank my second reviewer and supervisor Prof. Klaus Bengler for his assistance and effort.

I greatly appreciate the support from my colleagues at the Chair of Helicopter Technology, especially the team of our flight simulator, Ludwig Friedmann and Christian Spieß for their technical contribution as to the implementation of the simulation environment and all my other colleagues for their mental support and many fruitful discussions. Furthermore, special thanks to Martina Thieme for her administrative assistance, patience and very helpful tips during the time at the Institute. In addition, I would like to thank all my students for their support for the implementation of the tremendous amount of software required for this simulation study.

Special thanks to Sven Schmerwitz, Thomas Lüken and Patrizia Knabl from the German Aerospace Center for their valuable advice on the display concepts, the simulation scenarios and the experimental design. Moreover, I like to thank Andreas Haslbeck and Markus Zimmermann from the Chair of Ergonomics for challenging my ideas and providing insights from the human factors point of view.

A very special thanks to all participating pilots for spending long hours in the flight simulator and for giving immensely valuable feedback. In addition, I gratefully acknowledge the contribution of all operators who enabled the participation of their pilots in this simulation study.

Last but not least, I would like to thank my family for their unlimited support and their belief in me. Without their encouragement, this thesis would not have been possible.

Prior publications

Preliminary results of this work have been accepted for publication in the Journal of the American Helicopter Society:

Viertler, F., and Hajek, M., "Evaluation of Visual Augmentation Methods for Rotorcraft Pilots in Degraded Visual Environments," *Journal of the American Helicopter Society* (submitted: April 2016, accepted: August 2016).

Further results have been published at the following international conferences:

Viertler, F., and Hajek, M., "Requirements and Design Challenges in Rotorcraft Flight Simulations for Research Applications," Proc. of AIAA SciTech Modeling and Simulation Technologies Conference, Kissimmee, Florida, USA, January 2015.

Viertler, F., and Hajek, M., "Dynamic registration of an optical see-through HMD into a wide field-of-view rotorcraft flight simulation environment," Proc. of SPIE Vol. 9470, Head- and Helmet-Mounted Displays XX: Design and Applications, Baltimore, USA, April 2015.

Viertler, F., Krammer, C., and Hajek, M., "Analyzing Visual Clutter of 3D-Conformal HMD Solutions for Rotorcraft Pilots in Degraded Visual Environment," 41st European Rotorcraft Forum, Munich, Germany, September 2015.

Viertler, F., and Hajek, M., "Evaluation of Visual Augmentation Methods for Rotorcraft Pilots in Degraded Visual Environments," American Helicopter Society 72nd Annual Forum, West Palm Beach, Florida, USA, May 2016.

In addition, the following student theses have been supervised by the author at the Technical University of Munich within the scope of this work:

Groelly, Q., "Design of Sensor Fusion Architectures for enhanced Situational Awareness for all weather take-off and landing of Helicopters with unknown obstacles," Diploma's Thesis in cooperation with Eurocopter Germany, Ottobrunn, September 2011.

Kessner, M., "Development of a generic display system for a helicopter simulator," Bachelor's Thesis in cooperation with the Faculty of Informatics, Technical University of Munich, Garching, July 2012.

Pree, M., "4-PI Circumferential Visibility for Sensor Supported Helicopter Flight," Bachelor's Thesis in cooperation with Airbus Defence and Space, Unterschleißheim, September 2012.

Simm, A., "Development and Implementation of a Pilot Model to Quantify Situation Awareness of Helicopter Pilots," Diploma's Thesis, Garching, March 2013.

Kessner, B., “Development of an advanced helicopter instrumentation for flight simulation,” Bachelor’s Thesis in cooperation with the Faculty of Informatics, Technical University of Munich, Garching, April 2013.

Weber, W., “Follow-Up-Trim and Monitoring of Helicopter Simulator Flight Controls,” Bachelor’s Thesis, Garching, September 2013.

Reiß, P., “Experimental Setup for Mission Task Elements of the Aeronautical Design Standard 33,” Bachelor’s Thesis, Garching, January 2014.

Potyka, V., “All-Weather Hover Positioning of Helicopters – Feasibility Study for Offshore Wind Energy Plants,” Master’s Thesis in cooperation with Airbus Helicopters Germany, Donauwoerth, May 2014.

Ernst, J. M., “Design and Implementation of Virtual Aircraft-Fixed Cockpit Instruments,” Semesterarbeit in cooperation with the German Aerospace Center (DLR), Braunschweig, August 2014.

Krammer, C., “Three-dimensional visual flight guidance symbologies for helicopters,” Bachelor’s Thesis, Garching, September 2014.

Groetsch, D., “Evaluation Environment for Pilot-In-The-Loop Simulation Experiments,” Bachelor’s Thesis, Garching, October 2014.

Alves Ferreira Pinto, F., “Modeling the Visualization of Imaging and Ranging Sensors for Helicopter Flight,” Interdisciplinary project in cooperation with the Faculty of Informatics, Technical University of Munich, Garching, November 2014.

Ernst, J. M., “Visualization of Traffic Information in Head-Mounted Displays for Helicopter Navigation,” Master’s Thesis in cooperation with Airbus Defence and Space, Immenstaad, April 2015.

Lindemann, G., “Concept for improved safety during helicopter operations facing DVE, based on a new method RF sensor,” Master’s Thesis in cooperation with Airbus Defence and Space, Ottobrunn, October 2015.

Table of Contents

List of Figures

List of Tables

Abbreviations

AHRS	Attitude Heading Reference System
CIGI	Common Image Generator Interface
DLR	Deutsches Zentrum für Luft-und Raumfahrt e.V. (German Aerospace Center)
DOF	Degree of Freedom
DOP	Digital Ortho Photo
DSM	Digital Surface Model
DTED	Digital Terrain Elevation Data
DTM	Digital Terrain Model
DVE	Degraded Visual Environment
EASA	European Aviation Safety Agency
EGNOS	European Geostationary Navigation Overlay Service
EHEST	European Helicopter Safety Team
FAA	Federal Aviation Administration
FLIR	Forward Looking InfraRed
FOV	Field-of-View
FSTD	Flight Simulation Training Device
GNSS	Global Navigation Satellite System
HMD	Head-Mounted Display
HEMS	Helicopter Emergency Medical Services
HMI	Human-Machine-Interface
HQR	Cooper-Harper Handling Qualities Rating
HUD	Head-Up Display
IFR	Instrument Flight Rules
IG	Image Generator
ILS	Instrument Landing System
IMC	Instrument Meteorological Conditions
IOS	Instructor / Operator Station
IPD	Interpupillary Distance
LCD	Liquid Crystal Display
LED	Light-Emitting Diode
LOD	Level-of-Detail
MTE	Mission Task Element
MTF	Modulation Transfer Function
NIAG	NATO Industrial Advisory Group
NLR	Netherlands Aerospace Centre
NOE	Nap-of-the-Earth
NTSB	National Transportation Safety Board
NVG	Night Vision Goggles
OSG	OpenSceneGraph

PEP	Pilot Eye-Point
PHS	Precision Hover Symbology
PMMW	Passive Millimeter Wave
RMSE	Root-Mean-Square Error
ROSIE	Rotorcraft Simulation Environment
SFR	Simulation Fidelity Rating
SRTM	Shuttle Radar Topography Mission
TAWS	Terrain Awareness and Warning System
TFR	Time-Frequency Representation
UCE	Usable Cue Environment
UDP	User Datagram Protocol
VCR	Visual Cue Rating
VFR	Visual Flight Rules

1 Introduction

Helicopters allow the flight at low altitudes with take-off and landing at unprepared sites through their unique characteristics. However, rotorcraft pilots are exposed to high risks when flying in degraded visual environments (DVE). Low visibility conditions impact the environmental awareness of the pilot. At the same time the workload of the pilot increases with the attempt to retain enough visual cues to control the helicopter safely. Furthermore, without compensating for the reduction of visual cues, the pilot will not be able to conduct every requested mission in all visibility conditions or this would lead to a severe decrease in flight safety [99]. Unmanned or remote controlled systems will displace piloted systems for certain tasks which has been demonstrated in the research project for the unmanned operation in police missions (DemUEB [7]). Nevertheless, many helicopter operations, for example, helicopter emergency medical services (HEMS), police, commercial or military missions, will still be operated manned in the foreseeable future. Further endeavors were made to investigate a rescue infrastructure covering a large area solely relying on aeronautical systems without ground vehicle support (PrimAir [2]). This requires an all-weather capability of the helicopter under all circumstances, for instance, at night, in cloudy weather, in heavy rain, in snow or in fog. Thus, visual pilot assistance is required for both the reduction of helicopter accidents and for the extension of manned helicopter operations to bad-weather conditions [67] [68].

To increase the performance of the pilot in DVE, development efforts began three decades ago with the focus on control augmentation methods because of the restricted display performance at that time [76]. Thus, the developmental stage of control assistance systems including a four axis autopilot and hover hold functionality is far beyond the evolution of advanced display technologies. However, advanced head-mounted displays (HMD) and visual augmentation systems in general have reached a reasonable level of maturity over the last decades [16] [37] and a useful assistance has been provided to the pilot in the meantime. Nevertheless, zero-visibility conditions are still a big challenge when flying in low-altitude close to obstacles. Emerging low-cost systems are beginning to enable the use of HMDs also in civil operations, compared to the high-end systems applied in the military field. In addition, the increasing computational resources enable 3D-conformal (scene-linked) visualization concepts which add scenery content to the primary flight references. This approach provides an intuitive and safe assistance for terrain and obstacle collision avoidance, but is prone to visual clutter. To mitigate attention allocation problems a sophisticated visualization concept is required to enhance the capabilities of the pilot in DVE [93]. Hence, the question arises what a suitable visualization concept for different low-altitude helicopter flight tasks close to obstacles has to look like, and how this can be validated?

Consequently, this work aims to evaluate the measurable pilot control strategy together with subjective pilot ratings. This evaluation allows to draw conclusions about the impact on flight safety and the ability of the pilots to expand the flight envelope in severe degraded visual environments with these enhanced HMD concepts applied. A pilot-in-the-loop simulation experiment has been designed to investigate the emerging 3D-conformal obstacle displays under

DVE conditions in a safe and high-fidelity experimental environment. Sixteen pilots participated in the experiment to determine the quality of the visual augmentation approach and to provide meaningful conclusions. Therefore, existing visualization concepts which have been designed to present scenery information for collision avoidance and flight guidance references have been combined and extended. In addition, design properties to reduce visual clutter have been applied. The following sections provide some background information about the problem of helicopter flight in DVE and about the visual augmentation methods as a contribution to overcome those challenges.

1.1 Helicopter Flight in Degraded Visual Environments

For emergency medical services or other time critical tasks, it is desired to operate the helicopter twenty-four hours a day, seven days a week. With the increased navigation accuracy through the European Geostationary Navigation Overlay Service (EGNOS), for example, point-in-space procedures will become available for those helicopter operations [35]. Thereby, a large part of these missions can be conducted according to the instrument flight rules (IFR) with the assistance of an air-traffic controller and radar surveillance. During these phases of flight, the pilot relies solely on the cockpit instruments. Whereas from such a point-in-space the approach, take-off and landing at the target area at low altitudes and unknown terrain requires additional outside visual cues for the pilot to detect and avoid obstacles. These phases of flight, conducted according to the visual flight rules (VFR), are very demanding and hazardous for the pilots. Darkness, bad weather, dispersed snow (whiteout) or dust (brownout) during approach and landing impair the visual references and increase the risk of accidents (see Figure 1-1).

Figure 1-1: Whiteout during helicopter landing

Even though the most dangerous helicopter operations are those of personal helicopter flying by nonprofessionals, the fatal-accident rate for HEMS is very high. Reason for this is the operation at night or at degraded visibility conditions, where more than the half of the accidents occur [138]. In 2006, the National Transportation Safety Board (NTSB) stated an increase in HEMS accidents and recommended the use of terrain awareness and warning systems (TAWS) amongst other technologies to mitigate this trend [18]. The European Helicopter Safety Team (EHEST) has the objective to reduce the helicopter accident rate. Therefore, the Netherlands Aerospace Centre (NLR) has worked under the aegis of the EHEST on the mapping of safety issues with

technological solutions [164]. The potential of 145 technologies to mitigate helicopter accident factors has been investigated [165] with similar results demonstrated by the NTSB. According to this report from 2014, enhanced TAWS and obstacle detection systems for helicopter low-level flight guidance aids are ranked as the top three promising technologies to enhance safety. Those pilot assistance systems can increase pilot situation awareness, especially the awareness of the external environment, and they can improve pilot judgements and actions. Thus, the risk of obstacle collisions in bad visibility conditions can be reduced. These results encourage further investigations on pilot assistance systems, which increase the environmental awareness of the pilot. The NATO Industrial Advisory Subgroup 167 [9] determined three development areas, which require further advancements to solve the problem of DVE in low altitude, see Figure 1-2.

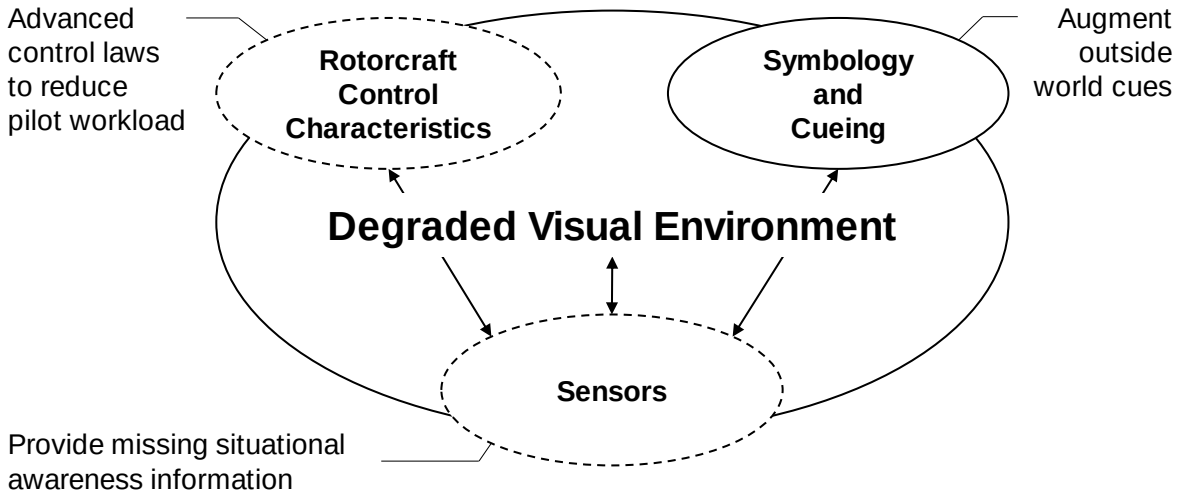

Figure 1-2: Development areas for the DVE solution (adapted from [9], [48] and [190])

The first objective aims to improve the rotorcraft control characteristics with advanced control laws. High level autopilot functions or advanced response characteristics, e.g. an Attitude Command Attitude Hold (ACAH) response or Translational Rate Command (TRC), reduce the pilot workload. With those control characteristics implemented the pilot does not need any mental or physical resources for the stabilization of the helicopter anymore. As a result, the pilot has more capacity for maintaining a sufficient situation awareness. The second objective addresses sensors to provide enough environmental data to prevent collisions with dynamic moving or static obstacles. These sensors are required to detect obstacles during all-weather conditions in order to assist the pilot with synthetic visual cues augmenting the degraded outside view. Finally, the third objective is the advancement of the symbology and visual cueing for the pilot. This includes all visually provided information for stabilization, flight guidance and navigation to ensure an obstacle free flight path. Many displays have been developed already, which provide useful information in moderate DVE conditions, e.g. a digital moving map showing weather and obstacles hazards head-down, or enhanced synthetic vision systems, including sensor information. In severe DVE below 800 m of visual range, the pilots are not able to spend enough time on head-down instruments to obtain all necessary information. Display solutions are required, which allow the pilots to fly head-out at all times [47] to conduct a safe flight in obstacle proximity. Therefore, this work focuses on the visual augmentation with a head-mounted display to account for that requirement in an intuitive manner.

Besides visual assistance and control augmentation, there exist alternative means to support other perceptional modes of the pilot in DVE, e.g. three-dimensional audio, tactile vests or haptic cueing [16]. 3D-audio [29] [66] and tactile vests [113] [114] can provide cues about the direction of an obstacle by providing acoustic warnings or vibrations to the human body. Both functions usually direct attention to the point of interest, but additional visual information is required to obtain enough awareness for proper actions. Haptic feedback from active control inceptors [64] can help the pilot to perceive flight envelope or engine limitations without visual cueing, but its usability is still very limited for obstacle detection.

Despite the limitations of each perceptional mode, the long-term goal should be to apply all these assistance functions in a suitable way in order to reduce the workload of the pilot. In addition, enhanced environmental awareness must be provided to the pilot during all flight phases [48]. Since the visual perception is a key element in the human-machine-interface regarding the helicopter flight in degraded visual environment, the objective of this work is to contribute to the maturity of visual augmentation methods.

1.2 Visual Augmentation with a Head-Mounted Display

The evolution of the cockpit environment of helicopters has run through similar development stages as in the fixed-wing domain (Figure 1-3). It began with analog round instruments and consists now of a glass cockpit with digital multi-function displays. In the future the alternative perceptional cues mentioned above might be integrated in a multi-sensory cockpit, providing advanced audio, tactile and haptic feedback with active inceptors, in addition to advanced control and visual augmentation methods. Current displays with weather radar information, digital moving maps, together with enhanced vision displays using forward looking infrared (FLIR) cameras, support pilots in good visual as well as degraded visual environments. Furthermore, terrain elevation database information as well as obstacle information detected by an obstacle warning sensor can be shown on the digital map to prevent controlled flight into terrain [87] [159] [161] [189]. Night vision goggles provide enhanced environmental awareness at night, at least at good weather conditions without clouds or fog. However, if visibility decreases the time to gather all necessary information in order to make decisions and to derive suitable actions diminishes. Below a certain visibility range the pilot is not able to gain information from the head-down instrumentation. A copilot is required to assist in a multi-crew concept or information must be provided by other means to the pilot, e.g. with a HMD. Conventional stationary head-up displays (HUD) applied for fixed-wing aircrafts are of limited use in the rotary wing domain by the fixed view in the forward direction. Despite of the relative small field of view provided by current HMDs, the field of regard is only limited by head motion. This makes a see-through HMD an advantageous aid for rotorcraft pilots. With the latter, the pilot can obtain primary flight references and the remaining outside cues, without the need of refocusing the eyes to head-down information. Thus, less time is required to switch physically and mentally between those references. However, it is still a difficult challenge to mitigate visual clutter and thus to avoid pilot confusion with the synthetic visualization, especially if a lot of information is overloading the display.

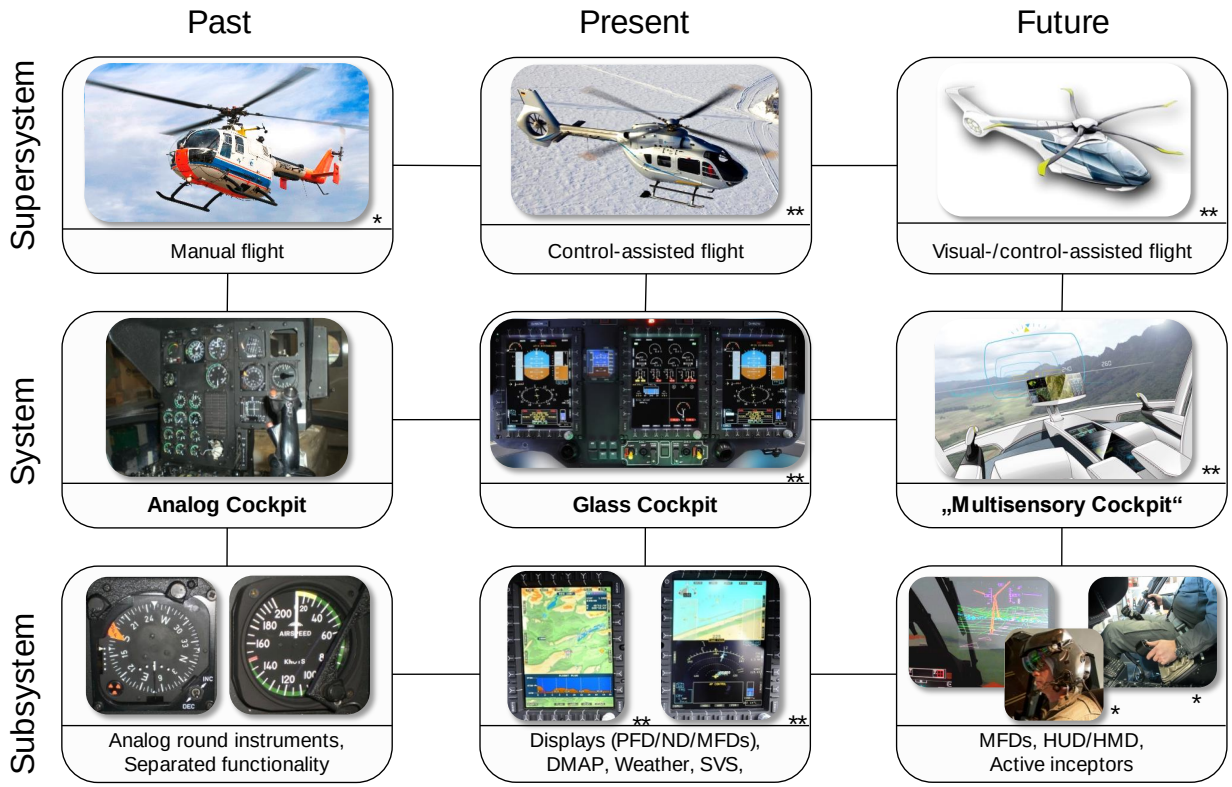

Figure 1-3: Helicopter cockpit evolution [*DLR, **Airbus Helicopters]

Up to present, two main approaches with a HMD have been investigated. On the one hand, a non-head-tracked application presenting primary flight references in a head-fixed frame of reference and secondly, a 3D-conformal extension with information presented in the geospatial or aircraft-fixed frame of reference with gaze direction considered from a head-tracking system [44] [199]. The latter is more complex but offers the feasibility to merge the synthetic visualization with the real world environment. Thus, missing references due to degraded visual conditions can be augmented with synthetic cues and attention switching problems between the two information sources can be minimized. Figure 1-4 shows a pilot with the applied HMD for this work and the view through the HMD with the visual augmentation of the degraded visual flight environment. The synthetic presentation extends the remaining outside cues at the region where no real world cues are visible. In addition to the mid- or long-term HMD solutions with 3D-conformal obstacle representations, a couple of short-term solutions have been developed by the NLR in a research project initiated by the European Aviation Safety Agency (EASA). The objective was to develop assistant functions for light, single-engine piston-powered rotorcraft with relatively inexperienced pilots [188]. These functionalities can help the pilot to maintain spatial attitude awareness with the “Malcolm Horizon” concept or by using LEDs to address peripheral vision. Furthermore, an arc segment attitude reference, called “HUD Orange Peel”, has been investigated to assist in recovering from unusual attitudes in case of an Inadvertent Entry into Instrument Meteorological Conditions (IIMC) for example, which has been adopted from the fighter aircraft domain. Besides the additional acoustic terrain warning concept, these attitude references do not provide any obstacle information for collision avoidance in DVE. Thus, they contribute only partially to solve the DVE problem.

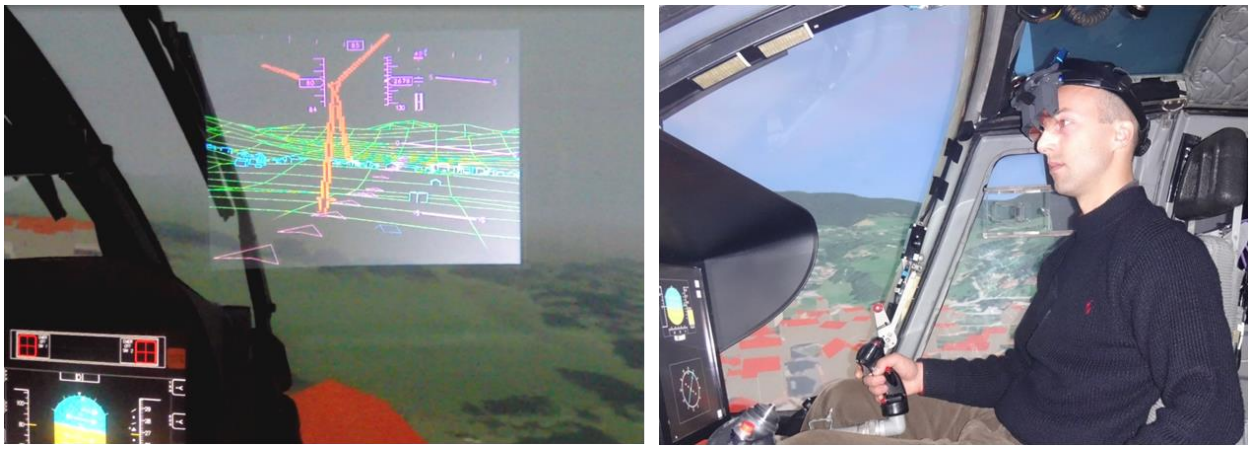

Figure 1-4: Visual augmentation of the environment (left), Pilot with a HMD (right)

Latest research investigations consider a 3D-conformal visualization of obstacles, mostly with a symbolic representation in the geospatial frame of reference, to provide sufficient collision avoidance awareness [44] [84] [121]. Considering these concepts, a lot of information is still presented in 2D and not 3D-conformal. Several primary rotorcraft states need to be perceived very precisely in a numerical way. Hence, information presented two-dimensional is still meaningful and can hardly be replaced completely with analog 3D-conformal symbols. Consequently, low-altitude flight guidance visualization is usually a mix of 2D flight references adapted from well-known and trained primary flight displays and 3D-conformal highways-in-the-sky [65] [152] [153] or pathways on the ground with navigation markers [90] [91]. A highway- or tunnel-in-the-sky is used to guide the pilot vertically and horizontally for the final approach with an Instrument Landing System (ILS) for example. For helicopter operations in unknown terrain without external navigation infrastructure such a guidance is under development, which provides collision free flight paths to the pilot with re-planning capability in real-time [201]. However, care must be taken in the design with respect to attentional tunneling effects [195]. Therefore, those alternative concepts with navigation markers in form of triangles or arrow-heads on the ground with horizontal guidance only, provide useful navigation assistance head-up, without capturing too much attention. Moreover, the pilot can maximize the amount of time searching for obstacles in DVE to prevent collisions.

For the task of landing in DVE, two main approaches have been developed over the last years. The first one provides rotorcraft state information, e.g. attitude, position, drift velocities and accelerations, with a mix of two dimensional views, forward view and bird’s eye view [43]. The second approach includes 3D-conformal landing zone visualizations to provide geospatial-fixed references in addition to the 2D flight references [80] [92] [120] [150] [169]. The latter requires the gaze direction of the pilot through a head-tracking system, but it enables a fusion of the synthetic references together with the remaining outside cues, for instance, micro-textures (fine grained surface details) or obstacles at the landing site. In addition, sensor information can be integrated to warn the pilot in case of hazards on the landing surface. The applied landing zones differ in their visualization details, but have a lot of features in common. They usually provide some pictorial references of the ground surface with a local terrain grid and a circle or a dog-house for marking the landing point, as in the Low Visibility Landing (LVL) Symbology [80], the Landing Zone (LZ) of Airbus Defense and Space [120] or the Three-Dimensional Landing Zone

(3D-LZ) of the Joint Capability Technology Demonstration (JCTD) [150]. The vertical velocity and height above ground can be assessed by the pilot through additional height bars, which are virtually placed around the landing site. The visualization concepts differ in the amount of 2D flight parameters displayed to the pilot, ranging from a minimum set of references to the full BrownOut Symbology System of the second generation (BOSS2) [171], including a velocity vector and acceleration cue symbols. The German Aerospace Center (DLR) implemented another approach presenting an open rectangle with longitudinal and lateral markers moving with the helicopter to show the current position with respect to the landing zone. They investigated a moving line and moving patterns on the ground to indicate the lateral drift of the helicopter [154] [155]. The latter motion is very hazardous in brownout or whiteout landings, since the dispersing dust or snow can lead to a confusing perception of drift velocities. Another interesting approach has been developed by Bachelder [24] [25] to assist in the hover task with night vision goggles applied. Here, the focus lied on the perception of the three dimensional synthetic cues with differences in the longitudinal and lateral gain, because of the very limited field-of-view available for presenting the cues.

The above explanations show that the maturity of the HMD technology and 3D-conformal visualizations increases in the aviation sector. A great leap forward may arise from the consumer market where HMD devices are under development for numerous augmented reality or mixed reality [119] applications. Microsoft's HoloLens or the Google Glasses are two famous developments in recent years to name. A lot of effort in the aviation domain is going into the certification of this technology for airborne use. The strict regulations do not allow yet to apply the HMD as primary flight reference. However, the usage as assistance system is conceivably, and progress is made with more and more guideline material developed, e.g. the SAE ARP6023 [14]. A number of committees globally are active working on updates for performance standards of vision systems [175]. The NATO Industrial Advisory Group (NIAG SG 193) is currently working on the airworthiness certification of rotorcraft Degraded Visual Environment Systems (DVES) including flight trials in 2016 and 2017 [174]. The group focuses on the development of recommendations for new policies in airworthiness certifications, the development of minimum key performance parameters required and the development of system installation safety concepts. Even though, the reliability of the system functionality is not in the scope of this thesis, the human factors experiment contributes to the means of compliance in order to ensure effective pilot assistance with increasing external environment awareness and decreasing pilot workload in DVE.

1.3 Previous Evaluation Methods

Evaluation methods of visual augmentation systems for rotorcraft pilots in degraded visual environment either concentrated on the assessment of the HMD symbology perception or on the control behavior of the pilot in severely degraded visual conditions. Several human factors experiments have been undertaken to evaluate these 3D-conformal HMD concepts in recent years. Attentional issues with a HMD in DVE have been examined by Knabl et al. [91]. Results demonstrated improved flight path tracking, but un-cued target detection was impaired with the HMD. Visual ranges of 800 m and 1200 m were investigated in this experiment. Kahana et al. [84]

conducted further experiments on 3D-conformal obstacle visualizations at night with 1000 m of visual range. Exposure time, reaction time and the rate of target detection were of primary interest amongst others with different display concepts at low altitude. In addition to those low altitude flights, Bachelder [24] developed an interesting approach to assist in DVE hover operations with NVG and conformal symbol elements in the form of cubes and rectangles, which change size depending on helicopter movements. He investigated the relation between the longitudinal and lateral perceptional issues and examined artificial gains to compensate differences in the resulting hover precision.

In the context of handling qualities evaluations three decades ago, Hoh [76] gathered experiences in low-altitude flight and hover in DVE, but without testing state-of-the-art 3D-conformal obstacle visualizations yet. One of the results was the linkage between the control augmentation methods and displays in the Usable Cue Environment (UCE) of the ADS-33E-PRF [5]. The display performance was not sufficient at that time and thus, general restricting factors to visual perception were investigated, for instance, field of view, macrotexture (large objects) and microtexture (fine-grained detail) [75]. Twenty years later, Gary Clark invented new mission task elements for the ADS-33E-PRF in order to develop vision aids for the pilot in DVE [36]. He subdivided the obstacle avoidance task into three possible basic maneuvers, in fact, climbing, turning and stopping. His experiments were conducted with visual ranges of 80 m, 240 m, 480 m and 720 m. The control strategy of the pilot was examined by the velocity in eye-heights and time-to-contact, in addition to the visual cue rating in order to determine a tau-guidance (τ-guidance) for pilot assistance. Padfield further investigated τ-guidance, based on time-to-contact and its derivative, to close several motion gaps [126] [128]. He applied τ-coupling with success in the area of deceleration maneuvers in order to analyze the flight strategies of pilots. The work on τ-guidance aimed to develop prospective displays, for example a “tunnel-in-the-sky” based on τ-control. However, 3D-conformal scenery content with a HMD was not yet examined in this context.

1.4 Research Objectives

This work aims to close the gap in the above mentioned evaluation methods and it intends to consider both aspects in one simulation experiment, the latest developments in visualization concepts using HMDs on the one hand, and low-visibility control strategy evaluations on the other hand. Therefore, degraded visual conditions below 800 m of visual range were examined, where this kind of visual pilot assistance was assumed to have a great beneficial impact on the control behavior and workload of the pilot. Below this visibility minimum, pilots are trained to fly according to the general rule of “low and slow” to ensure that they maintain sufficient reaction time and ground visibility at all times. However, the reduced visual cues decreased the safety margin and thus, increased both pilot workload and the risk of accidents. The scenarios developed for the conducted simulation experiment contain the following two main research objectives:

1) 3D-conformal terrain and obstacle representation for low-altitude flight

The first objective addressed whether a 3D-conformal terrain and obstacle representation is worth the cost of visual clutter by increasing the safety margin in the form of time-to-contact or by

changing this low and slow control strategy. Thus, for the flight phase in low-altitude and with obstacle hazards, two different display variants were compared at varying visual conditions of 100 m, 200 m, 400 m and 800 m. The advanced display variant contained flight guidance symbology and scenery information to sense and avoid obstacles (FGSA), while the basic reference display included only flight guidance information (FG). Below 200 m of visual range, the pilots were not able to fly the low altitude scenario tasks without a minimum amount of information presented head-up in the form of two-dimensional flight references, together with a 3D-conformal flight path for navigation. Figure 1-5 shows the scope of the anticipated pilot behavior on velocity control, depending on the visibility range and the display type. In general, with the terrain and obstacle information available on the HMD (FGSA), it was assumed that the pilots should be able to fly faster and higher compared to the variant with flight guidance information (FG) only. In addition to the velocity and height control, the obstacle avoidance maneuvers were analyzed according to the minimum distance to the obstacles, the point in time of the obstacle detection and the initiation of the avoidance maneuvers.

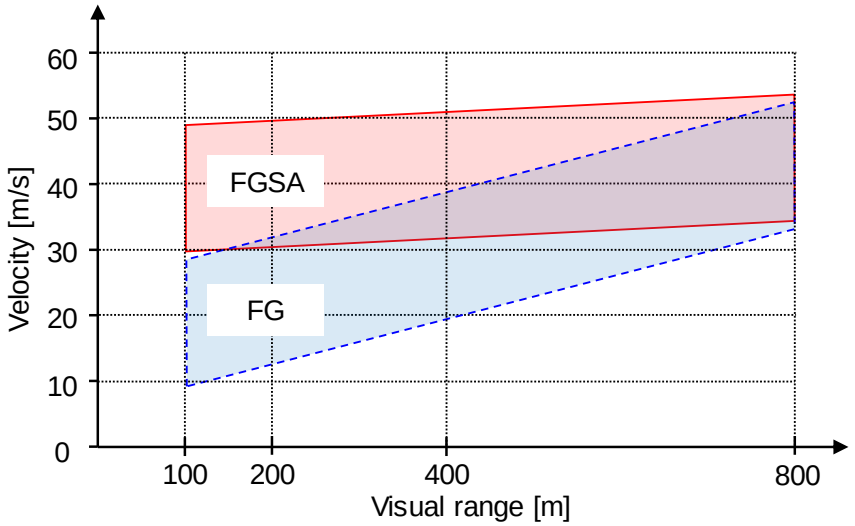

Figure 1-5: Anticipated pilot behavior on velocity control depending on visibility ranges and the display type basic (FG) or advanced (FGSA)

Besides the objective measurements on the pilots' control strategy, subjective workload ratings with the NASA Task Load Index (NASA-TLX) [70] were conducted. In addition to the performance evaluation of the visual augmentation assistance, the results further reveal the general pilot behavior in low-visibility contour flight with obstacle avoidance maneuvers.

2) 3D-conformal cues for stabilization and precise hover maneuvering

The second research objective was the investigation of a novel approach with 3D-conformal cues for the hover task in contrast to the low-altitude, obstacle avoidance task. A precise hover maneuver can be very demanding for the pilot, for instance, during winch operations or as preliminary phase for landings in DVE. Control augmentation can be very beneficial and can reduce workload, especially in rotorcraft stabilization, but visual references are still required in severe visibility conditions to maintain the position. Therefore, the pilots had to hover in different visual conditions in ground and out-of-ground within the second part of the experiment conducted.

For the hover display design, the reference elements of the ADS-33E-PRF mission task element with the hover boards were adopted and extended. The Visual Cue Rating (VCR) and a Handling Qualities Rating (HQR) was conducted, in addition to the evaluation of the pilot control activity and hover performance. The results demonstrate whether or not the macro-textures alone can assist the pilot, considering the very low field of view (23° x 17°) of the low-cost HMD applied and the missing micro-texture through DVE.

The hover task complements the low-altitude flight task and thus allows an extensive investigation of the benefits and limitations of the visual augmentation technology with a head-mounted display for helicopter flight in degraded visual environment.

1.5 Scope and Thesis Structure

This work considered the task of low altitude flight in the proximity of obstacles and the task of stabilization in hover, as part of the most hazardous situations during the final approach in DVE at unknown landing sites, when the pilots have to fly according to visual references. The transition to hover and the landing itself were not yet included in the experiments. Furthermore, only the assistance for visual perception with the synthetic augmentation of the degraded visual flight environment was considered. Control augmentation and audio cues were intentionally excluded to obtain results which rely solely on the visual channel. Thus, multimodal perception or even crew coordination were not included. Sensor technologies and database information are explained for the design and simulation of the display concept, but the experiment focused only on the human-machine-interface part.

Flight simulation is currently the only means to investigate severe degraded visual conditions without exposing the pilot to extreme risk of danger. Thus, obstacle avoidance maneuvers in low-altitude and DVE should be examined and trained first in a simulation environment, before going into flight test. This causes high demands on the simulation fidelity. However, simulation technology has improved in recent years and especially for this work, novel HMD integration methods have been applied to mitigate simulation induced errors, when simulating 3D-conformal visualizations in a dome-projected environment. These approaches not only increase the simulation fidelity of the experiment, they can also be useful for the quality and the transfer of synthetic training in simulators later on.

Figure 1-6 depicts the structure of this thesis. Chapter 2 reviews state-of-the-art technologies available for advanced human-machine-interface designs with respect to visual augmentation (2.1). Very useful or even mandatory systems for augmented vision are considered, especially head-mounted displays (HMD) with a head-tracking system and information recording and storing systems, such as sensors and databases. Moreover, this section reviews the scientific background (2.2). Hence, visual perception and control strategies are explained, in particular mechanisms of depth perception, the influence of micro- and macro-texture and the principle of optical-flow perception. The latter affects the control strategy of the pilots with time-to-contact as main control parameter. Thus, the basic control behavior considering displayed content is investigated. In addition, visual clutter and design properties to reduce this adverse effect are examined.

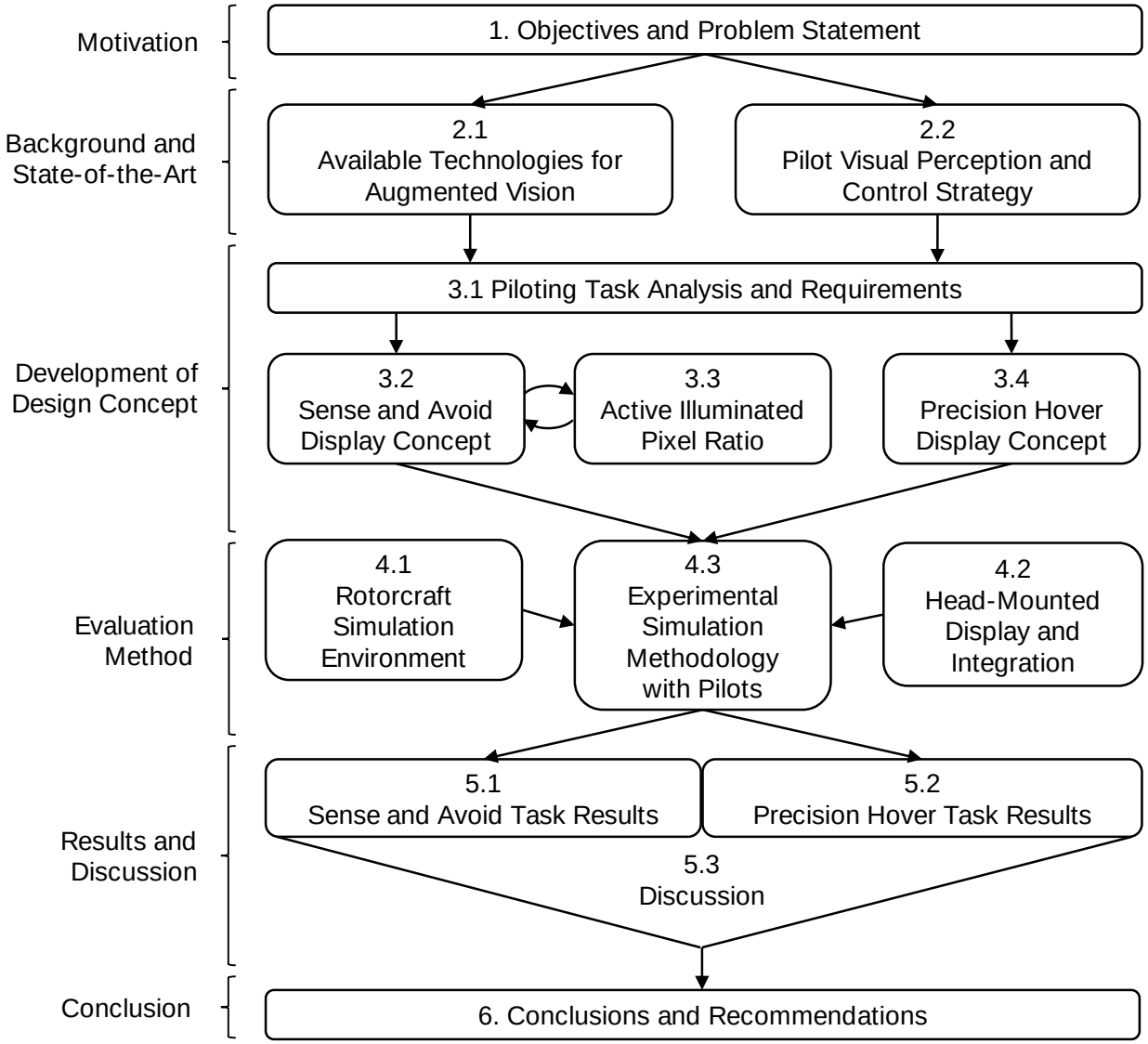

Figure 1-6. Structure of this thesis

Chapter 3 describes the development of the advanced display concepts evaluated and specifies the content displayed. Two challenging flight phases were selected following a piloting task analysis at the beginning (3.1). The first concept shall assist in low-altitude flight with improved detection and avoidance of obstacles (3.2). For analyzing visual clutter a new method was implemented, which determines the active illuminated pixel ratio in real-time (3.3). This enables a measurement of the amount of occlusion through the head-mounted display, when showing 3D-conformal scenery content. The second display concept aims to support the pilot in precise hover maneuvers (3.4).

To evaluate the control strategy of the pilot depending on the display concept and different visibility conditions, a pilot-in-the-loop simulation experiment was developed, which is explained in chapter 4. It starts with a specification of the applied Rotorcraft Simulation Environment (ROSIE) (4.1), followed by the integration of the head-mounted display (4.2). Two solutions have been tested to minimize the dynamic registration error of the HMD image against the multi-channel dome-projection system for an enhanced simulation fidelity. Furthermore, this chapter describes the newly developed low-level contour flight scenarios and tasks for obstacle detection,

avoidance and hover maneuvers (4.3). The description of the simulation procedure and the participating pilots together with the applied ratings and questionnaires complete the experimental design.

Results of the simulation experiment are presented in chapter 5, beginning with the sense and avoid scenarios in low-level contour flight (5.1), followed by the evaluation of the precise hover maneuvers (5.2). Finally, a discussion on the results is given with regard to the overall problem of helicopter flight in degraded visual environments (DVE) (5.3).

Chapter 6 summarizes the main contribution of this work to visual augmentation methods for helicopter pilots in DVE. Moreover, future research prospects and recommendations on this topic are presented.

2 Background and State-of-the-Art Technologies

This chapter provides an overview of the available technologies for augmented vision and scientific background on the visual perception and the control strategies of the pilot. It describes the main features of the HMD and sensor technologies and points out the state-of-the-art in HMI design concepts from the literature. The fundamentals on pilot visual perception and flight control strategies are essential for the development of the design concept in chapter 3. Different approaches of reducing visual clutter from previous work are explained, which were also applied in the final concept.

2.1 Available Technologies for Augmented Vision

The technologies for augmented vision contain the HMD itself, the local and global positioning systems and the information sources, which provide sufficient situational awareness about the environment, in fact, databases and sensors. For the obstacle detection, both imaging and ranging sensors are explained, but only range measuring sensors are simulated in the later experiment. Air-traffic or collision warning sensors are briefly explained for completeness, but are also not included yet in the experiment. Finally, state-of-the-art solutions from several research projects are described, as possible starting point for improvements.

2.1.1 Display Solutions

For the 3D-conformal visualization of scenery content or flight guidance symbols, a head-tracking system and global helicopter positioning sensors are required in addition to the HMD. In the real world application only angular head positions are usually required by the head-tracking system, because of the relative small translational head movements of a few centimeters compared to the global positioning errors of the helicopter and the relative large distance to obstacles of several meters. The small distance of the simulation screen without collimation requires a complete six degree of freedom tracking in order to mitigate simulation induced errors in the experiment. For this work, only HMDs are considered and no aircraft fixed conventional HUDs.

2.1.1.1 Head-Mounted Displays

The history of head-mounted displays goes back until the year 1618 with the earliest recorded description of a helmet-mounted sight, the *celatone*, by Galileo Galilei in order to conduct an accurate measure of longitude for ship navigation [57]. The first documented helmet-mounted sight with drawings is a patent by Albert Bacon Pratt from 1916 [139]; see Figure 2-1 a). The patent comprises a weapon for soldiers with a simple crosshair for visual aiming functionality. Thus, it is very close to current military systems in use, considering the aiming of a target. In 1965, Sutherland developed the idea of ‘The Ultimate Display’ [166] with one cathode ray tube (CRT) for each eye providing a stereoscopic display. It included a mechanical tracking system mounted on the ceiling and later an ultrasonic head position sensor [167]. In the 1970’s the development of airborne HMDs proceeded with a simple targeting imagery similar to the idea of Pratt, until the

advanced 3D-conformal cueing systems developed in recent years. Further historical developments can be found according to developments of Rockwell Collins [57], BAE [34] and the systems applied at the NASA [21]. Three optical design methods were reviewed by Li [107], in fact, off-axis design, freeform optical surface design and the holographic optical waveguide technology. Figure 2-1 b) shows a high-end HMD (TopOwl) system with visor projection, which provides a large FOV with a 40° fully overlapping binocular view. In contrast, Figure 2-1 c) shows a light-weight monocular state-of-the-art HMD (Q-Sight) system using the holographic waveguide technology. The latter technology provides adequate performance at lower cost and thus it may allow the use of such HMDs for civil operators in the future.

a) Albert Pratt [139] **b) TopOwl Thales [104]** **c) Q-Sight BAE [34]**

Figure 2-1: HMD technology evolution with selected examples

In addition to the optical see-through designs, video see-through devices may also be conceivable in the future. Video see-through designs require a real-world image captured by a camera, display processing and optional image manipulations to add synthetic content. With increasing computational power, a fast transformation of the video with a high resolution can provide similar results compared to an optical design. Video see-through devices can mitigate registration errors of the synthetic symbology added to the video images of the outside world cues. However, additional latencies of the video rendering must be low enough, failing this will result in a mismatch between vision and proprioception, which can lead to problems in controlling the rotorcraft. The two technologies have been compared in detail by Rolland et al. [147] [148]. Besides the fidelity of the real world and the system latency, the implementation of the occlusion effect is another important issue. This important monocular depth cue is explained further in chapter 2.2.1, and how it is implemented in the advanced visualization concept with an optical see-through device is described in chapter 3.

For the optical see-through devices, different ocularity configurations are currently in operation, in fact, a monocular display for one eye only, a biocular display providing equivalent images to both eyes and a binocular display with different images for each eye. While the monocular version is less complex and lower in weight [116], it is prone to binocular rivalry [180], the phenomenon when the pilot is not able to fuse the different images perceived by both eyes. The binocular display enables a stereoscopic representation adding this depth cue, which can be relevant at lower distances below 30 m. The latter is required for the integration of the HMD into the simulation environment without a collimated projection system, since most HMDs are designed to focus at

infinity with the optical lenses system. The projection system of helicopter simulator does usually not include a collimation system, because of the large vertical field-of-view required. Thus, the eye convergence and motion parallax needs to be adjusted through different images for each eye without changing the focal distance of the optical design.

In general, the performance of a HMD can be defined by the following important characteristics amongst others explained by Rash et al. [142]:

- Field-of-view
- Image quality, resolution and modulation transfer function (MTF)
- Exit pupil, eye box and eye relief
- Color, luminance, see-through transmission and contrast
- Weight, center of mass and volume

The field-of-view (FOV) can be defined as "the maximum angle of view that can be seen through the optical device" [142]. This can be in the shape of a rectangle with different horizontal and vertical FOV or a circular FOV in some devices. While humans can perceive an overall binocular FOV of 200° horizontally by 120° vertically [202], most HMDs are very limited in the FOV, ranging from very small angles (e.g. 23° x 17°) up to 80° x 40° provided for example by the JEDEYE of Elbit Systems [44]. Current HMDs in use have typically around 40° x 30° FOV, which is sufficiently for most tasks. Depending on the purpose of the applied HMD a very small FOV with only a few degrees would be sufficiently for targeting [142], while displaying imagery of the flight environment or providing peripheral cues for hover requires a larger FOV. The latter is also addressed in the scenario tasks of the experiment, because of the very limited FOV of the low-cost HMD applied with 23° x 17°. The image quality is mainly depending on the resolution, which is given by the covered FOV in degrees and the resolution of the image source in pixels. Thus, it should be defined in minutes of arc per pixel, where dissolving one minute of arc per pixel corresponds to the average visual acuity of a human (20/20 vision). Another metric used is the modulation transfer function (MTF) [107] [142], which describes the performance of the entire system as a function of spatial frequency. The latter is a measure of the details in a scene and the metric defines how the system degrades the image from the input to the output. The eye relief defines the space between the pilot's eye and the optical system, while the exit pupil or the eye box defines the positioning of the eye and the optical system in order to ensure that the pilot can see the entire FOV displayed by the system. Weight and center of mass are influencing the wearing comfort and thus are also important parameters, considering missions with a long duration. For operations in a highly illuminated environment, a bright image source is required to ensure the readability of the symbology. The see-through transmission of the combiners needs to be counterbalanced with the luminance of the display source and other optical elements, which are influencing the perceived brightness of the outside world, for instance, the rotorcraft canopy or a protective visor of the pilot. Cathode Ray Tubes (CRT) have been applied in most HMDs because of their high luminance. However, other emissive image sources achieve high luminance performance in recent years, e.g. the Organic Light Emitting Diode (OLED), which allow the use of color in addition. Almost all airborne HMDs are only monochrome so far, but augmented reality

devices from the consumer market and new technologies, for instance the holographic waveguide approach, are very promising in order to provide full color on airborne HMDs in the near future.

2.1.1.2 Head-Motion Tracking Systems

To display information at a geospatial or aircraft referenced location, while the pilot's head is moving, a highly accurate head-tracking is required to recalculate the position of the point of interest on the display. Table 2-1 shows well established head-tracking technologies [180].

Direct measurement	Self-contained	Remote sensing	Hybrid systems
Mechanical	Inertial	Electro-magnetic	Electro-m. + inertial
		Optical	Optical + inertial
		Acoustic	Acoustic + inertial

Table 2-1: Head-tracking technologies

Direct measurements with a mechanical linkage as implemented for the system used by Sutherland [167] are rarely used for head-motion tracking nowadays. Inertial sensors with accelerometers and angular rate sensors are very accurate, small and they provide a high update frequency (500 Hz or more). Their disadvantage of drift over time can be compensated with additional remote sensing technologies in hybrid systems. Optical and acoustic (usually ultrasonic) systems have usually a lower update frequency (less than 200 Hz), which results in a larger system latency without the combination through inertial sensors. Electro-magnetic trackers are preferred in the military field, since optical systems sometimes require light emitting markers on the pilot's head. However, the installation requires measurements of the magnetic field in the cockpit for high precision without interferences [109]. Ultrasonic systems may be disturbed by frequencies of the fast rotating engine turbines. Thus, the applied technology must be evaluated carefully and tested in the operational environment for the best performance result.

In general, the head-tracking technologies contribute only to a small amount of the total system latency (< 5–10 ms), because of the limited display update frequency of usually 60 Hz (16.67 ms) at the moment. Thus, higher update frequencies for the displays are desired to reduce the overall latency. Furthermore, the image sources from ranging or imaging sensors are even slower, which requires a decoupling of the sensation of the environment and the rendering of the scenery content on the display. In addition, numerous head-motion prediction methods are applied to reduce the system latency to a minimum for a very stable and accurate superposition of the synthetic imagery over the real world environment [23]. The Kalman Filter is a very common approach and is often used in hybrid tracking systems [124] in order to predict the head-motion a few milliseconds ahead of time for compensating the delay caused by the rendering and displaying process. Particle filters [1] or neural networks [58] [185] were also investigated to further improve the head-motion prediction. These prediction methods usually have the common characteristic that with an increasing interval of prediction, the tracking result leads to larger errors and thus less accuracy [124]. In order to achieve a sufficient superposition of the synthetic imagery and the real world, an angular dynamic accuracy of less than 0.5° (10 mrad) is adequate and less than 0.1° (2 mrad) is desired.

2.1.1.3 Helicopter Positioning Systems

The georeferenced information presented on the HMD requires a highly accurate global positioning and attitude determination for the global gaze direction and position, in addition to the head-motion tracking. If the attitude and heading reference system (AHRS) installed in the helicopter does not provide an accuracy of similar magnitude compared to the head-tracking system, additional inertial sensors must be installed. Ground based radio navigation systems, e.g. 'non-directional beacons' (NDB) with an 'automatic direction finder' (ADF) or 'very high frequency omnidirectional radio range' (VOR) system do not provide sufficient positioning accuracy area-wide. Instrument landing systems (ILS) provide very accurate position deviation references, but only at the airport infrastructure. The operative environment requires infrastructure independent positioning for unknown landing sites within rescue missions for example. Thus, the only technologies available at the moment are global navigation satellite systems. The performance of the Global Positioning System (GPS) achieves a worst case accuracy with a horizontal error of less than 7.8 m. However, in the latest analysis of the Federal Aviation Administration (FAA) with real-world measurements, the GPS accuracy had a horizontal error of less than 3.5 m at 95% confidence level and a vertical error of less than 4.7 m [11]. With ground based augmentation systems (GBAS) or satellite based augmentation systems (SBAS) even more accuracy can be obtained. While GBAS requires reference stations on the ground in order to provide differential GPS information, it is very accurate and could replace the ILS in the future. However, SBAS is independent of ground references. It uses geostationary satellites, which provide additional information in order to increase the accuracy and the reliability of the system. SBAS systems already in operation are the North American "Wide Area Augmentation System (WAAS)", the "European Geostationary Navigation Overlay System (EGNOS)", the Japanese "Multi-functional Satellite Augmentation System (MSAS) and the Indian "GPS Aided Geo Augmented Navigation (GAGAN)". The poor vertical accuracy of the GNSS can be further improved by the information of a radar altimeter. Moreover, the GNSS information can be fused with inertial measurement sensors by a Kalman Filter [141] in order to provide a highly accurate navigation system with a high update rate, since GPS runs currently at 1 –10 Hz and inertial navigation up to 1 kHz.

In low-altitude flight, the helicopter is usually a lot further away from the ground or from obstacles than the error of the augmented GNSS and thus the error in superposition of 3D-conformal content can be neglected. However, when hovering against a wind turbine or a ship deck, where the visual references or obstructions are very close, an even more accurate positioning system will be required. Hence, relative positioning systems are under development based on optical markers or radio frequency sensors, e.g. the *DeckFinder* [187] system of Airbus Defense and Space. The DeckFinder system works similar to the GNSS principle, but in a small scale. A ground segment provides radio frequency based range signals and the airborne segment can detect the signals and calculate the relative position to the ship deck. For frequently planned hover destinations, such a system can be very beneficial. However, for air rescue missions it is more difficult to apply without having an infrastructure to mount the ground segment. It could be installed at an ambulance or other ground vehicles. This would allow an accurate positioning in DVE, but requires ground vehicles on-site before the helicopter arrives.

2.1.2 Environmental Information Sources

The basis of 3D-conformal augmentation of the flight environment consists of database information and real-time sensor feedback for the visualization of synthetic scenery reference cues. Databases provide a wide-area information source with static terrain and obstacle data. However, databases need to be updated frequently. Even though, new built or installed obstacles might be missing. Furthermore, dynamic moving obstacles, e.g. other air traffic, cars and pedestrians, or temporarily installed obstacles, for instance, a construction crane cannot be considered in a database. Thus, sensors are required to detect missing components and to rectify terrain database inaccuracies in order to provide a reliable information source, when flying very close to those obstacles. This section explains database contents and their available resolution, followed by the performance of passive imaging and active range measuring sensors together with air traffic collision avoidance systems for completeness.

2.1.2.1 Terrain and Obstacle Databases

Synthetic world representations consist of basic terrain elevation data and aerial images. Even though, hundreds of geodetic reference systems exist from historical developments, the World Geodetic System 1984 (WGS 84) is a prevalent reference system and it is applied as standard in aerospace. It consists of a reference ellipsoid adapted to the earth's surface with latitude and longitude for localization. The available database resolution and accuracy has increased over the last decades. However, there might be regional differences, due to the increase of accuracy in land surveying, which is still an ongoing process. The U.S. Department of Defense has defined a performance specification of the Digital Terrain Elevation Data (DTED), in MIL-PRF-89020B [15]. Table 2-2 shows the three DTED levels currently defined in the MIL-standard.

DTED Level	Grid spacing [arc seconds]	Resolution [m]	Horizontal accuracy 90 % circular error [m]	Vertical accuracy 90 % linear error [m]
0	30 x 30	≈ 900	-	-
1	3 x 3	≈ 90	≤ 50	≤ 30
2	1 x 1	≈ 30	≤ 30	≤ 18

Table 2-2: DTED performance specification

The grid spacing is only valid for areas between 0° and 50° north and south latitude, since the resolution around the poles of the earth decreases. In Germany and other countries, resolutions of up to 1 m in elevation data is available. Figure 2-2 shows examples with different elevation database resolutions of the same area with a) DTED Level 1 of the Shuttle Radar Topography Mission (SRTM), b) a 5 m grid elevation of the digital terrain model and c) the highest resolution to date available from the Bavarian Land Surveying Authority with a 1 m resolution. For global high resolution data, two earth exploration satellites have been launched in 2007 and 2010, the TerraSAR-X and TanDEM-X as add-on for digital elevation measurements. Together they accomplish a resolution of 12 x 12 m with a vertical accuracy of 5 m [98]. With the local determined 1 m resolution, it is already possible to perceive man-made infrastructure, for instance, railways, streets and small pathways without additional aerial images on top of the elevation data.

Moreover, it should be distinguished between the Digital Terrain Model (DTM) data, which represents the bare ground surface without obstacles or vegetation and the Digital Surface Model (DSM) [101], shown in Figure 2-2 d). The DSM represents the visible surface including buildings and vegetation. Without a sufficient high resolution of the DSM or additional information, it is not possible to assign a single bump in the data to a certain object in the real world.

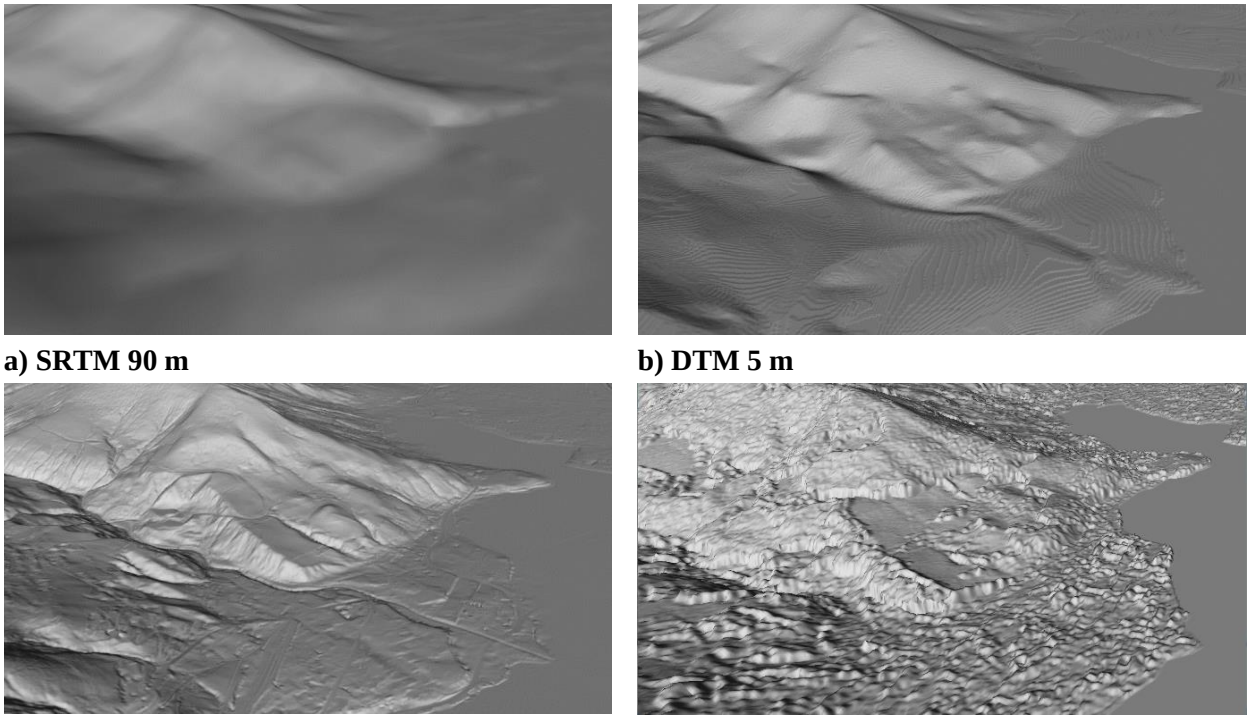

a) SRTM 90 m **b) DTM 5 m**

c) DTM 1 m **d) DSM 5 m**

Figure 2-2: Terrain elevation data with different resolution

In addition to the elevation data, aerial images or Digital Ortho Photos (DOP) provide colored textures of the terrain surface. These textures are currently not used for HMD applications in order to maintain the see-through capability or to allow the use of night vision goggles or forward looking infrared images instead. However, the DOP textures are used in flight simulation environments for the outside visible cues. The resolution of those DOPs has a great influence on the velocity and altitude perception of the pilot, especially during low-speed flight and hover [36] [75]. The drawback of high resolution DOPs is the increasing amount of data and its handling within the simulator. The highest resolution from the Bavarian Land Surveying Authority provided for this work contains 25 pixels per square meter (0.2 m/pixel). Figure 2-3 shows the difference of the high resolution DOP with 0.2 m/pixel on the left and a 1.0 m/pixel resolution on the right. With the higher resolution, much more details are discernable at the cost of 25 times more data to be processed in this case. Even higher resolutions are available in some cases at other land surveying institutions, usually with special purpose flight measurements for the region of interest.

Figure 2-3: Aerial images: left) DOP 0.2 m/pixel, right) DOP 1.0 m/pixel

Airborne Synthetic Aperture Radar (SAR) measurements provide usually a higher accuracy than the global elevation measurements with satellites. The first and last pulse responses can be used to distinguish between ground measurements and objects, for instance, buildings or vegetation. Figure 2-4 shows the first pulse measurements in form of a point cloud over the DTM with DOPs.

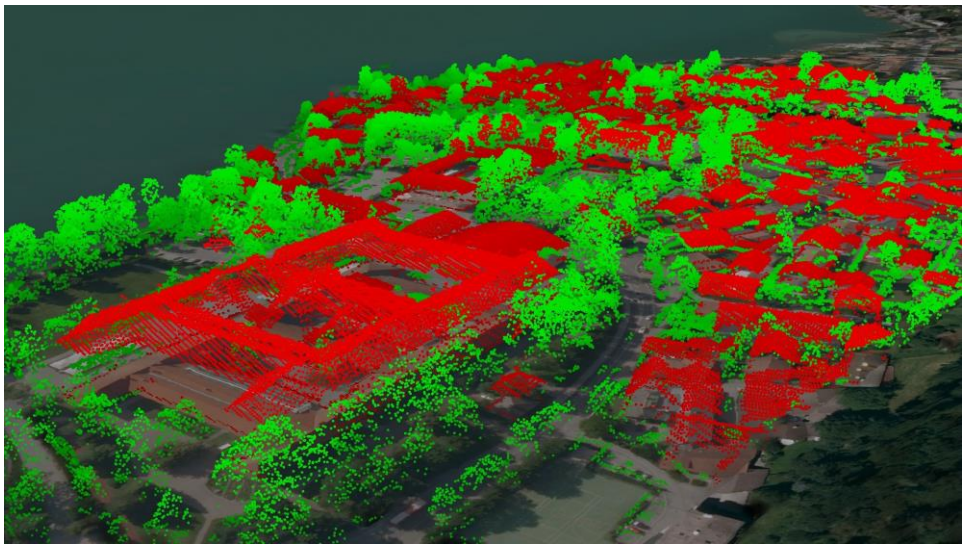

Figure 2-4: First pulse of synthetic aperture radar measurements

Instead of using such a large amount of data in form of a point cloud, static objects are stored in separate databases. Guidelines for the electronic obstacle mapping can be found in the ICAO documentation [12]. Forty obstacle types are defined together with an obstacle attribute definition. For this experiment only area-wide obstacle database information containing building data was applied with level-of-detail 2 (LOD 2 [125]). Figure 2-5 on the right shows LOD 2 buildings containing the architectural roof geometry compared to the simple LOD 1 block model on the left side. This LOD 2 representation can increase the fidelity of the obstacle perception when presenting them as wireframe. Additional surface textures provided with LOD 3 are not required for the see-through application up to the present.

Figure 2-5: Buildings: left) LOD 1, right) LOD 2

In addition to the obstacle data, information about the land utilization can be found in data bases. The transportation network with railways and streets is already stored in every automotive navigation system. This information is applied by Airbus in the synthetic vision representation on head-down displays [121], but it can also be used on the HMD for landmark navigation. The assignment of the vegetation to land areas and the classification of other regions could be used to find and rank proper landing sites, when knowing where forest, farmland or urban areas are located [132] [200].The information about larger water surfaces might be useful in combination with different sensors [162], since these surfaces often have specific characteristics in reflecting radio waves with certain wavelengths. Pilots also try to avoid those areas in DVE because of the little references available when flying over water. Figure 2-6 shows the ground classification with different land utilization. Even more attributes are stored in the data files, for instance, to distinguish between small pathways, streets and highways.

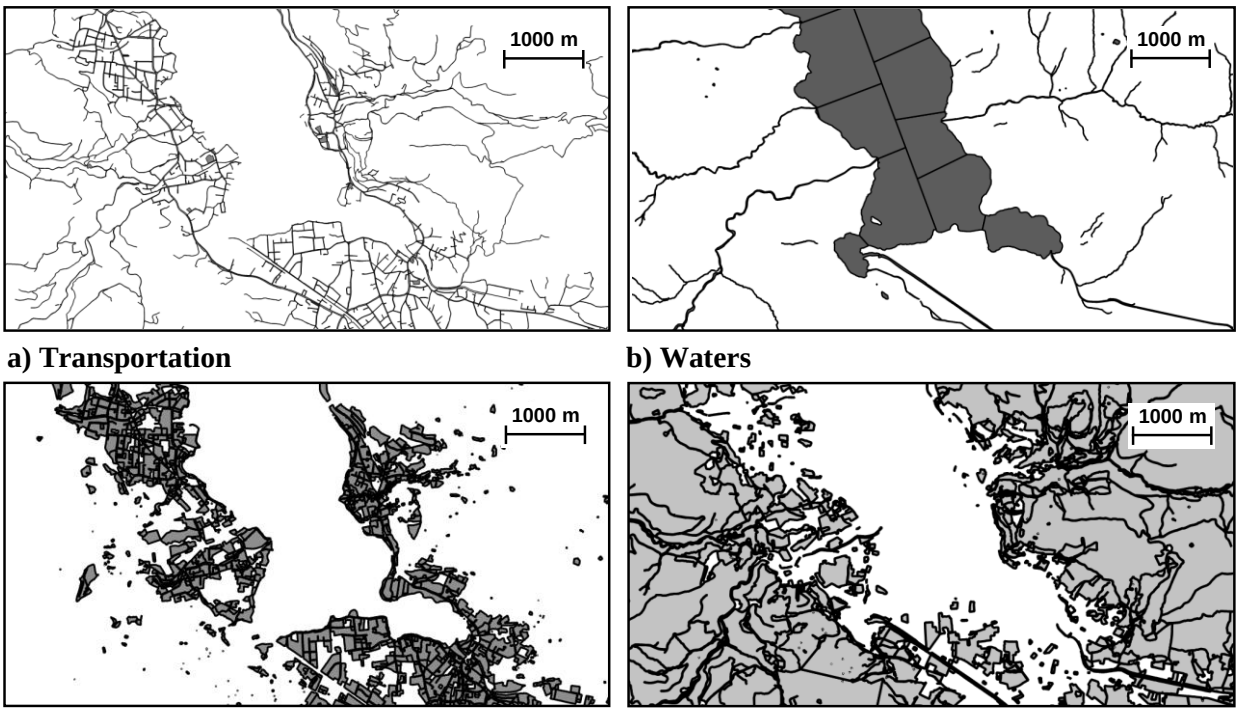

a) Transportation **b) Waters**

c) Urban areas **d) Vegetation**

Figure 2-6: Ground classes with effective land utilization data

2.1.2.2 Sensors for Real-Time Environmental Information

Two types of sensors exist for remote sensing of the flight environment, in fact active and passive technologies [12]. The latter captures electromagnetic information, which is originated from the sun and then reflected from the earth's surface, e.g. a camera in the visual spectrum, night vision goggles or a passive millimeter wave imaging system. In contrast, active sensors first illuminate the scene and then capture the reflected information from the ground or obstacles, e.g. a radar or a lidar sensor. Both technologies are considered for helicopter flight in DVE [63]. Figure 2-7 shows the attenuation of the atmosphere depending on the electromagnetic frequency for different weather conditions. In general, the attenuation decreases with longer wavelengths [140]. The red line shows that wavelengths in the visual spectrum are hindered in foggy conditions, while radar sensors with longer wavelengths (e.g. at 35 GHz) have a very good see-through capability.

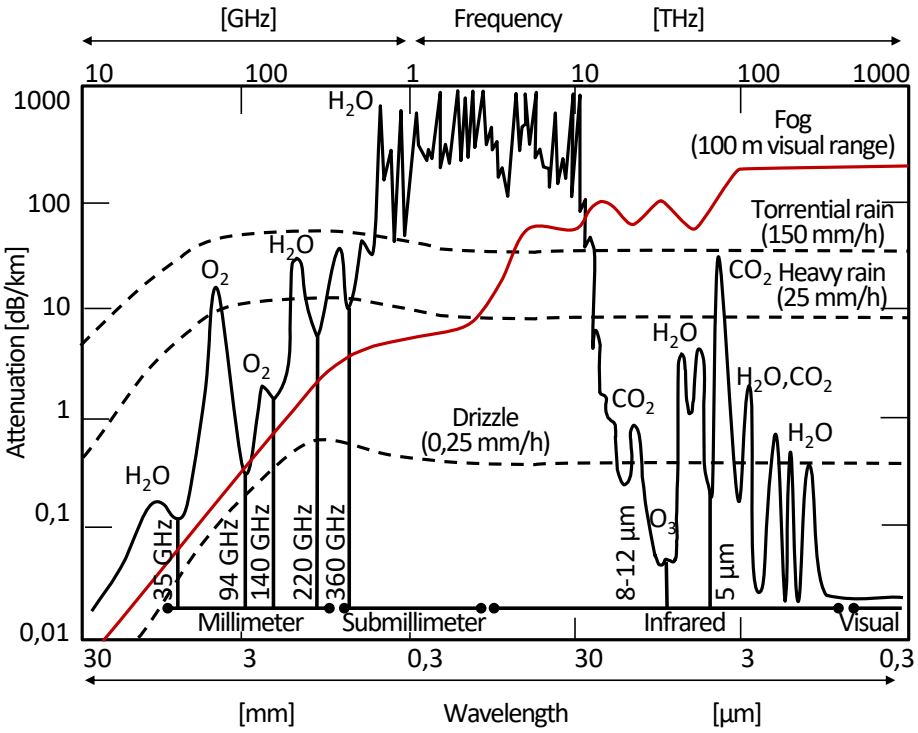

Figure 2-7: Attenuation of the atmosphere for different weather conditions depending on wavelength [63][140]

In the 1970's, the first vision aids used were night vision goggles, because of the requirement to expand the flight envelope for night operations in the military field. NVGs intensify the remaining radiation at night with a micro-channel plate and a photocathode in order to increase the amount of emitted photons [72]. The resolution of NVGs has improved over the last decades. For NVG-aided visual acuity assessments, again the resolution and the modulation transfer function are important and thus analyzed in Ref. [137]. A drawback remains still the limited FOV of about 40°. Figure 2-8 shows a typical NVG imagery with adverse halo effects, which are caused by incompatible cultural lightings [10]. Due to these limitations and the different appearances of clouds or fog, when looking through the NVGs, an appropriate training is required to avoid misinterpretations of the perceived environment [95] [173]. Full color mapping has been investigated to overcome the limitation of monochrome imagery, due to the applied photocathode

[176]. In addition, digital night vision goggles (DNVG) can effectively compete with analog goggles in recent years, which allows full-color imagery as well [69].

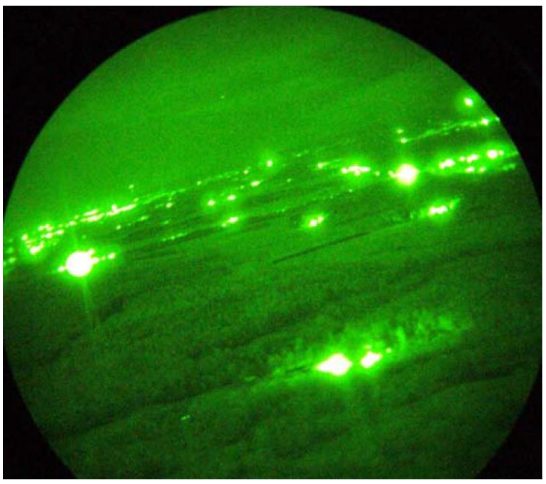

Figure 2-8: NVG imagery with incompatible cultural lighting [10]

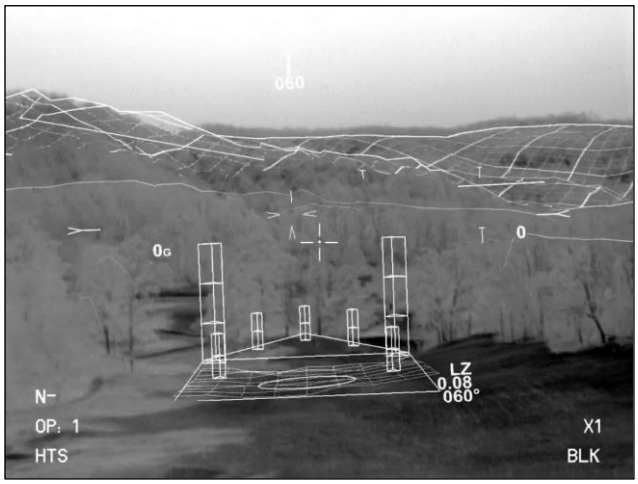

Figure 2-9: Infrared sensor imagery with 3D-conformal symbology [122]

Short after the entry of NVGs, thermal (infrared) technology became also available as airborne sensor imagery [143]. Forward looking infrared (FLIR) sensors visualize variances in temperature to identify objects in the darkness. Figure 2-9 shows an example of a FLIR imagery with superimposed 3D-conformal symbology elements. For the attack helicopter AH-64 Apache, the aviator night vision imaging system (ANVIS), which consists of image intensifying NVGs sensitive to both visible and near-infrared energy, has been compared to the integrated helmet and display sighting system (IHADSS) with a FLIR system and flight symbology cues [72]. The pilot evaluation demonstrated a preference of the NVGs considering wire detection and avoidance as well as for reconnaissance. In addition to the infrared imagery, which is already less damped by the atmosphere or fog than the visual spectrum, passive imaging sensor technology can really see through fog. It uses longer waves in the millimeter range, instead of micrometer waves (e.g. 8–12 µm). Figure 2-10 shows flight test results of a passive millimeter wave (PMMW) imaging sensor at 77 GHz [42]. The advantages of a PMMW system are the low attenuation and a relative high update rate compared to active sensor systems. The drawbacks of such a long wave sensor system are the limited resolution up to the present and a usually large aperture or antenna size.

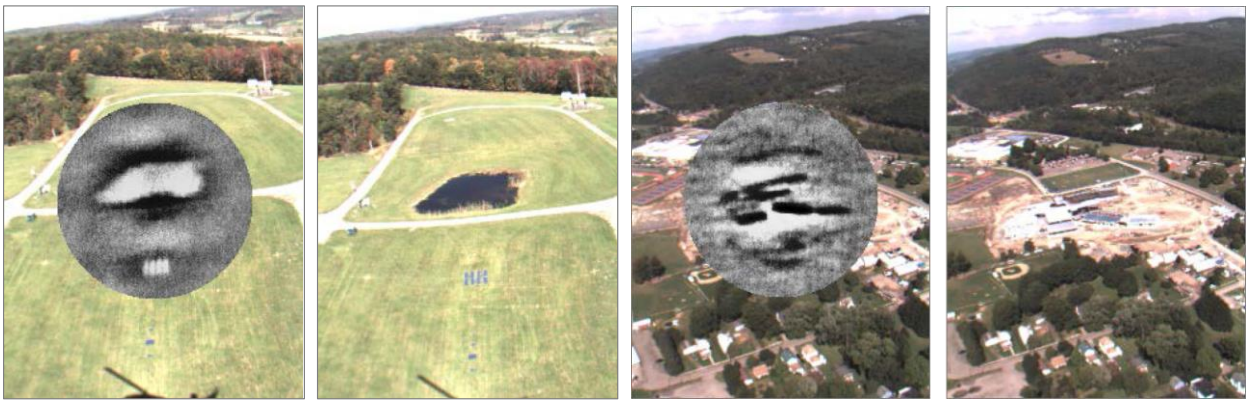

Figure 2-10: Flight test results of passive millimeter wave imaging system [42]

The active sensor systems applied for helicopter flight in DVE are radar (radio detection and ranging) and lidar (light detection and ranging) systems. Ladar (laser detection and ranging) is another acronym for the optical counterpart of radar, which uses for example a wavelength of 1.5 µm compared to radar with a frequency of for example 35 GHz [63]. The latter benefits again from the low attenuation in fog or dust cloud conditions, while the lidar system usually has a better range resolution. Both technologies have the advantage of providing additional range information compared to the passive imaging systems. However, they have a very low update rate of about 2 Hz for scanning the whole FOV of the sensor. Figure 2-11 shows the results of ladar range measurements. These measurements provide 3D point clouds and can be used to update inaccuracies of terrain database information sources in real-time or to detect static or dynamic moving obstacles. Terrain morphing algorithms have been developed to fuse DTED level 1 data with 94 GHz millimeter wave radar sensor information in the context of the Brownout Landing Aid System Technology (BLAST) project [169] [170] [172] [179].

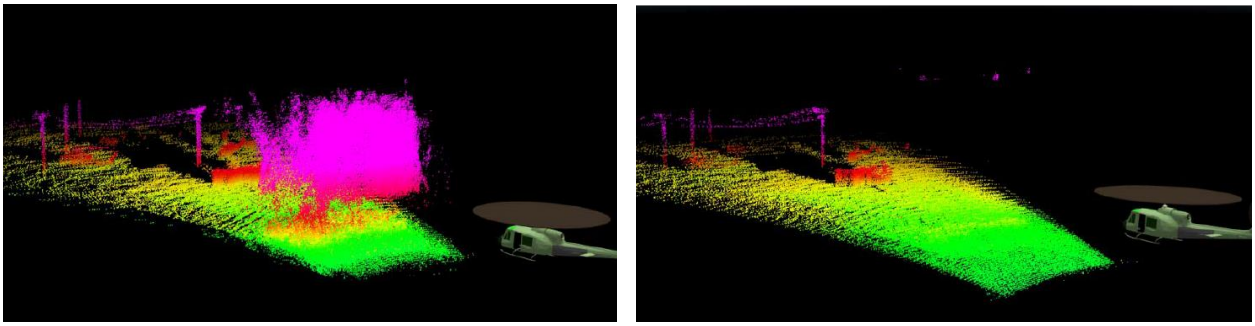

Figure 2-11: Point cloud data from range sensor, left) unfiltered, right) dust particles filtered out [163]

The ladar system returns also reflections from the dust cloud in front of the helicopter during approach and landing, due to the lower wavelength; see Figure 2-11 on the left. However, filtering methods have been developed to remove those undesired reflections for visualization [151] [163]; see Figure 2-11 on the right. In addition, algorithms have been developed to classify ground from lidar data in real-time to extract obstacles for separate visualization [49] [52]. Furthermore, non-classified lidar points can be clustered for improved visualization with less clutter for the pilot [50] [52].

Finally, air traffic can also be very hazardous in DVE for helicopters. Besides radar systems, which are independent surveillance systems used by air-traffic controllers, an aircraft can be equipped with radio transmitters and receivers, so-called transponders, to provide direct communication of position, identification, speed, intended flight direction or other characteristics of the aircraft [51] [52]. The Automatic-Dependent Surveillance Broadcast (ADS-B) is such a system, which provides necessary information about other aircraft. The FLARM system [157], similar to the ADS-B, was developed for light aircraft and general aviation, where the pilots fly predominantly according to VFR. Figure 2-12 shows a typical FLARM display, which indicates the direction and distance to prevent collisions. A similar visualization concept has been developed for the circumferential view of a rotorstrike alerting system (Figure 2-13), which is based on automotive radar sensors. Approaches to visualize the air-traffic in a see-through HMD with geometrical shapes, e.g. circles

or rectangles in order to highlight objects, have been developed by Lenhart [105] [106] and Eisenkeil et al. [51], see Figure 2-14.

Figure 2-12: FLARM – collision avoidance system [8]

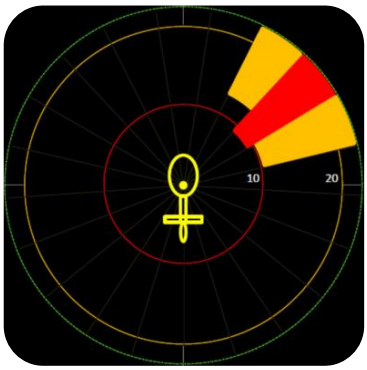

Figure 2-13: Rotorstrike alerting system [191]

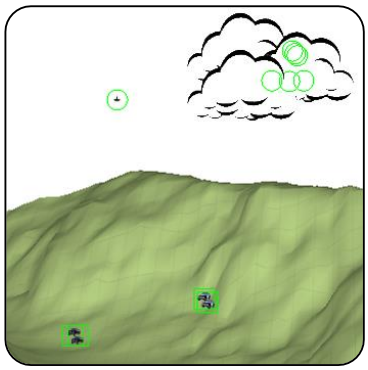

Figure 2-14: Traffic visualization with HMD [51]

For large aeroplanes (over 5.700 kg maximum take-off weight or more than 19 passengers) an airborne collision avoidance system is mandatory. The Traffic Alert and Collision Avoidance System (TCAS) is also based on the direct communication of aircraft with a transponder. In addition to just displaying other aircraft information, the TCAS provides instructions to resolve possible conflicts. More information about TCAS can be found in the Guide of Eurocontrol [4].

2.1.3 3D-Conformal State-of-the-Art Visualization Concepts

The final section of the available technologies for augmented vision demonstrates examples of how the environmental sources have been applied for visualization at the HMD in previous work. Two prevalent phases of flight have been considered, in fact the visualization of low-altitude flight guidance with obstacle avoidance and the visual cues for hover and landing.

2.1.3.1 Low Altitude Flight Guidance and Obstacle Avoidance Cues

Several approaches have been established to visualize terrain and obstacle information in order to prevent collisions. While terrain is usually presented in the form of a grid, contour lines or a combination of both (Figure 2-15), obstacle information can be pre-processed and displayed as symbols, whenever a classification is possible (Figure 2-15) [123] [135].

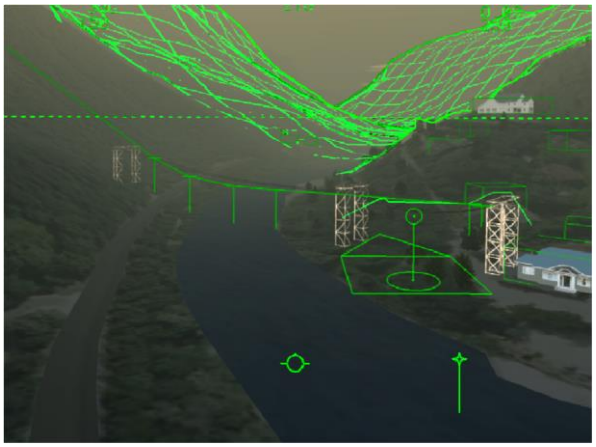

Figure 2-15: 3D-conformal terrain and obstacle visualization concept [17]

Figure 2-16: Symbology with wire and pole ladar imagery [150]

Alternatively, range measurements of a sensor can be shown directly if the resolution is high enough (Figure 2-16). Sensor measurements, which cannot be classified, can also be clustered and visualized [50] as a bounding box with wireframe; see Figure 2-15 on the right side. The terrain can be culled in the near-field in order to avoid cluttering at regions where the outside cues are still visible [121]. Comparisons of different obstacle visualization concepts have been conducted by the DLR. Figure 2-17 a) – c) shows examples of obstacle displays with variations in the transparency and the shape for representation [131]. The basic findings resulted in an advantage of the opaque and wireframe display over the thorned shape [89].

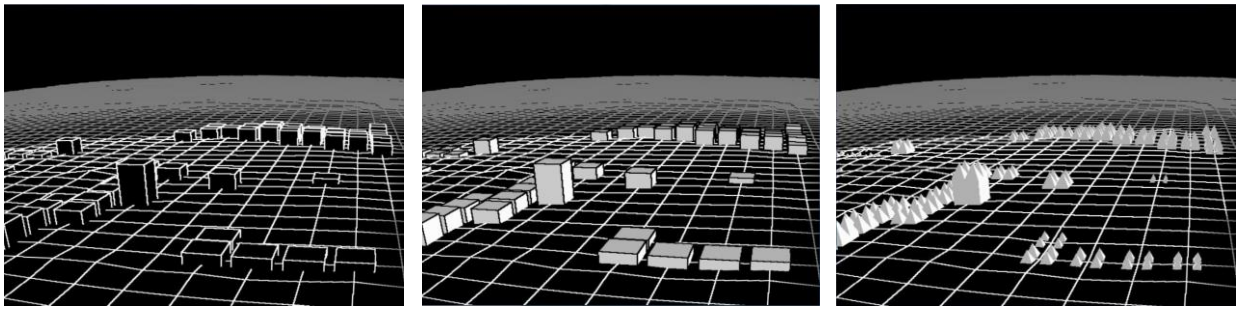

a) **Wireframe display** **b) Opaque display** **c) Thorned display**

Figure 2-17: Comparison of different obstacle visualizations [89]

Further discussion on the abstract symbolic representation of obstacles versus a photorealistic approach which shows the pilot lidar point cloud data directly is given by Voelschow et al. [186]. Latest flight test results with the SferiSense system of Airbus Defence and Space demonstrate the current performance of a photorealistic lidar sensor visualization; see Figure 2-18.

Figure 2-18: SferiSense results with a photorealistic representation of obstacles [186]

For flight guidance and navigation at low altitude, two remarkable concepts have been developed. The first is derived from fixed-wing head-up displays, mainly used for the final approach. The tunnel-in-the-sky (Figure 2-19) provides horizontal and vertical guidance to the landing site. It is useful for a very strict following of the target guidance. The second approach (Figure 2-20) considers navigational markers fixed to the ground surface, which provide horizontal guidance only [90] [91]. It demonstrated less susceptibility to the effect of attentional tunneling, compared to the tunnel-in-the-sky concept. More attention can be directed to the outside, searching for obstacles around the flight path or landing site with these markers in form of a triangle or an arrow-

head. Furthermore, the pilot can decide how strictly the horizontal path should be followed and how the vertical path should be selected.

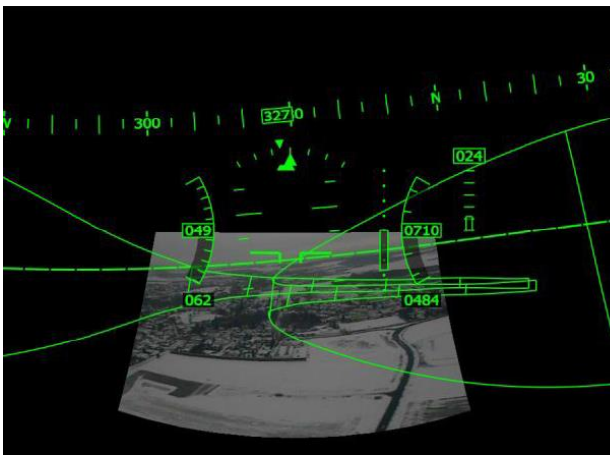

Figure 2-19: Tunnel display for landing approach [44]

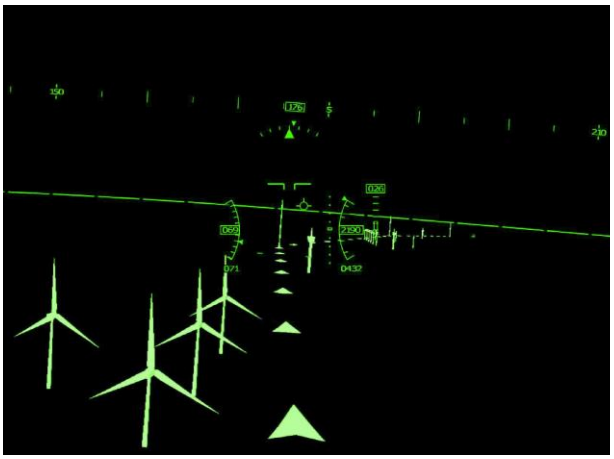

Figure 2-20: Flight path navigation markers with obstacle symbology [133]

In addition, two dimensional primary flight references are superimposed, as known from conventional head-up displays in fixed-wing aircraft, including speed, altitude, heading, attitude and other important flight parameters.

Integrated approaches of obstacle avoidance cues with flight guidance information considering flight path and speed resulted in the safety line concept [61] [160]; see Figure 2-21. The safety line is a completely abstract guidance information, which shows a minimum clearance above larger obstacles, which are detected by sensors. The pilot simply has to keep the flight vector above the line deemed to be safe.

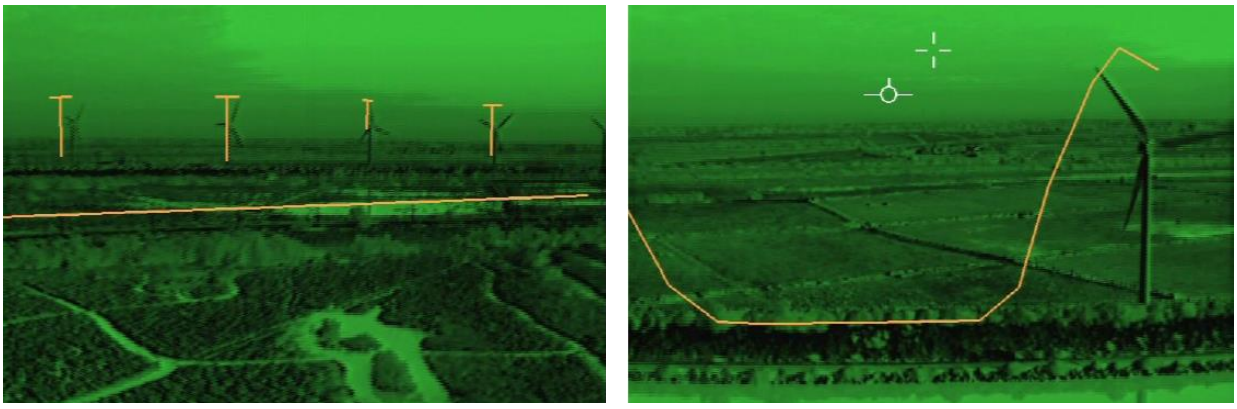

Figure 2-21: Safety line concept for obstacle avoidance [123]

2.1.3.2 Hover and Landing Reference Cues

To overcome the challenge of zero-visibility landings in brownout or whiteout, many symbology sets have been developed. They can be classified into the group of symbologies which contain a mix of two dimensional views (forward view and bird's eye view; see Figure 2-22) without requiring a head-tracking system, or they belong to the group of 3D-conformal landing zone cues superimposed by primary flight references, see Figure 2-23.

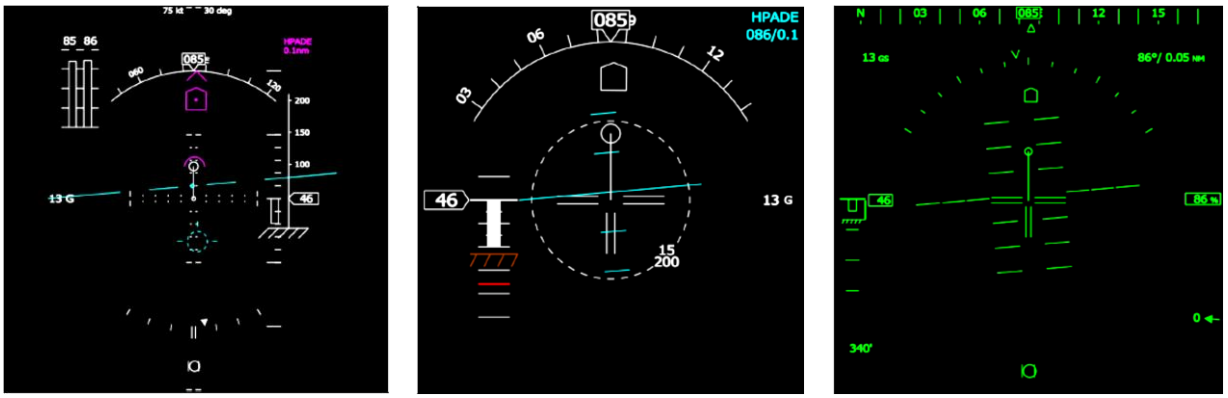

a) BOSS **b) DEVILA** **c) JEDEYE**

Figure 2-22: Different symbology sets for hover and landing [43]

Figure 2-22 shows the BrownOut Symbology System (BOSS), which was developed by the U.S. Army Aviation and Missile Research Development and Engineering Center (AMRDEC), and modified concepts based on BOSS. DEVILA was developed by former EADS, Germany and the JEDEYE concept was designed by Elbit Systems together with the DLR and with consultancy from the German Armed Forces [88]. The symbology sets were designed to assist the pilot in landing, when outside visual cues are lost, e.g. during brownout. In addition to the basic flight parameters, speed and acceleration cues are presented in order to indicate drift velocities just before landing. Inside a dust cloud, the pilot gets a wrong impression of self-motion and thus requires additional references to prevent accidents, for example a rollover during touch down. The DLR evaluated the above shown symbology sets [43]. Even though, pilots preferred the head-mounted displays, results showed no evidence that the performance of the pilots improved with the symbologies. They further believed that 2D concepts do not provide sufficient guidance quality due to the drawbacks of attentional tunneling, cluttering and differences in the optical flow between near and far domain. Thus, it has been concluded that head-tracked HMDs with a 3D-conformal visualization of flight guidance assistance together with obstacle hazards are a key technology for helicopter operations in DVE.

The 3D-conformal reference cues often contain a kind of landing zone representation with an indication of the desired landing position on the ground surface. Figure 2-23 shows examples of such implementations. The top left image shows the 2D BOSS extension with a 3D landing pad [150]. Another design, the Brownout Landing Aid System Technology (BLAST), has been developed for the same purpose by the U.S. Army Aeroflightdynamics Directorate (AFDD) together with BAE systems (Figure 2-23 b)) [179].

a) BOSS display with 3D landing pad [150]

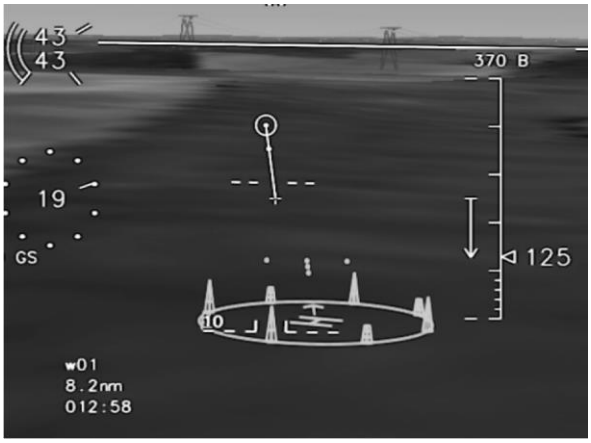

b) BLAST conformal landing symbology [169]

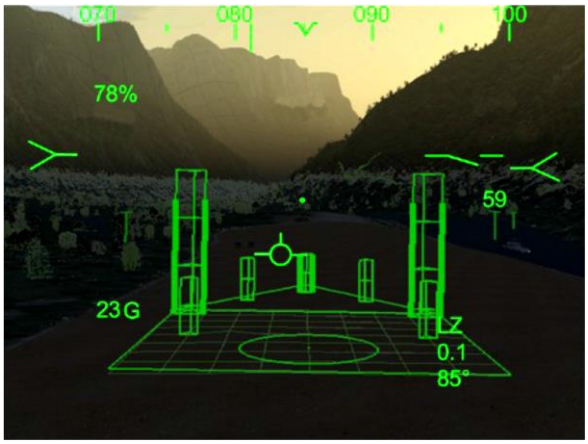

c) Airbus 3D-conformal landing zone [121]

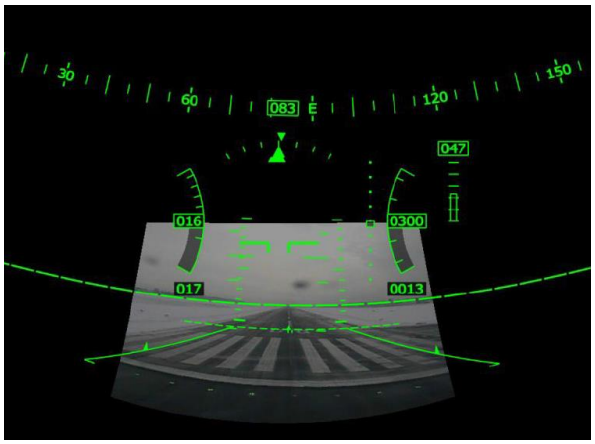

d) DLR landing display [44]

Figure 2-23: Examples of 3D-conformal reference cues for landing

The bottom row images show the 3D-conformal landing zone development of Airbus Defense and Space [121] and the reference cues of the landing concept designed by the DLR [44]. The BOSS and the Airbus design contain a grid in order to show additional surface properties of the terrain with high accuracy. Reference towers with height bars shall indicate the height above ground and they serve as fixed reference points for estimating self-motion, e.g. drift velocities. The DLR design deviates a bit more from the other approaches and presents an open rectangle on the ground with markers indicating the relative position. They used a height scale instead of towers and added additional lines for drift indication.

Furthermore, a few completely different approaches have been invented, which use peripheral symbology. Rogers et al. developed an attitude cueing for a wide field-of-view HMD containing rings, arranged in a cylindrical geometry around the helicopter [146]. The cylinder provides attitude cues and when approaching the ground, a relative motion of the rings indicate the rate of decent. The idea is based on the "Malcolm horizon" amongst others which provides an artificial horizon line throughout the whole cockpit, projected by a laser [112].

In addition to the landing concepts, Bachelder [24] [25] developed hover cues using a very limited field-of-view in contrast to the previous methods, which are based on the peripheral vision as well.

The design uses geospatial referenced synthetic cubes and rectangles connected with lines in order to provide hover cues with respect to the relative position of the helicopter, see Figure 2-24.

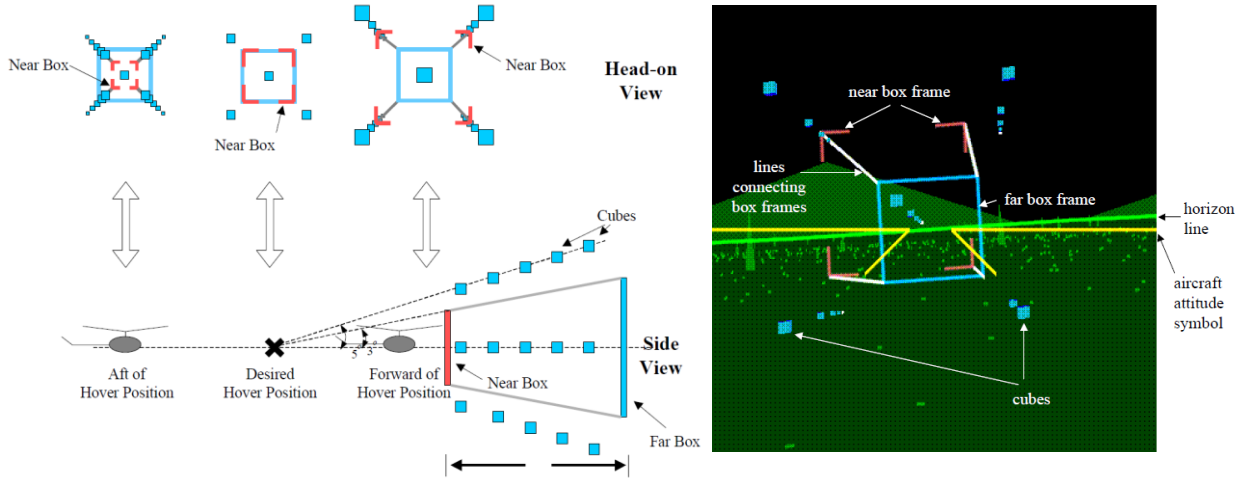

Figure 2-24: 3D-conformal references for hover with NVGs (Bachelder [25])

With the small FOV considered for this design, the longitudinal axis is more difficult to perceive with the same precision as the lateral and vertical axis. Thus, Bachelder investigated an artificial gain for the longitudinal reference cues to match a similar perception as for the other two axes. He showed evidence that an optimal gain set exists, which is sensitive to factors as vehicle dynamics, task demands and the flight environment.

In summary, chapter 2.1 demonstrates the complexity of a visual assistance system for helicopter flight in DVE with a HMD, and explores which technologies are required and available to date in order to support the pilot in a meaningful way. It shows examples of recent developments, but does not claim to describe all technologies exhaustively. In order to understand the mechanisms behind the display concepts the next chapter explains the relating theories.

2.2 Pilot Visual Perception and Control Strategy

The 3D-conformal visualization of flight references and scenery information requires a fundamental understanding of the human visual perception and the control strategies of the pilot for locomotion. This subchapter explains the background required in order to understand, to advance and to evaluate the evolving display concepts. Furthermore, pilot workload and situational awareness assessments are discussed, since they are a key factor for the overall performance. In addition, the problem of visual clutter is explained and design characteristics reducing this effect are discussed.

2.2.1 Visual Perception Theories

Two primary theory sets for visual perception exist in the field of psychology. Gibson [60] invented the ecological approach to visual perception, which believes that perception relies directly on the information of a stimulus [115]. In contrast, the constructionist viewpoint, based on the ideas of Helmholz [73], believes that perception builds upon knowledge and depends on experiences from interacting with the world around us [108]. According to Gregory [62], the

perception is a constructive process and requires a lot of hypotheses testing based on past experiences and accumulated knowledge. Hence, according to his theory, indirect perception depends on inference and higher-level cognition [196].

This work uses the ecological approach to explain some optical invariants that provide pilots with useful information, in addition to some classical mechanisms of depth perception. It is assumed that the environment the pilot is flying in degraded visual conditions, is not known. Thus, information from the optical array augmented by the synthetic vision system forms the basis for controlling the rotorcraft. Whether the perception is learned in the training phase of the experiment or if it is directly relying on the stimulus of the reflecting light on surfaces, is not in the scope of this work.

2.2.1.1 Optical Invariants of the External Environment

Gibson [60] identified several optical invariants, which represent environmental properties. The light rays received by the visual system have an invariant or unchanging relationship with the location and heading of the observer [196]. Changes in the optical array contain important information about the type of movement and can be used for the control of egomotion. A few of these invariants have been used already to some extent in previous concepts. The considered optical invariants are further explained by Wickens [196], in fact, splay, compression, optical flow, time-to-contact, edge rate and global optical flow. The angle between two receding lines (splay), together with the gradient of separation between horizontal lines (compression) provide information about height and distance. Figure 2-25 demonstrates those two effects. On the left, the observer perceives as being higher above the ground with the view downwards, while on the right, the observer is located closer to the ground looking forward. These cues are considered for example intentionally with the synthetic application of a regular terrain grid, representing the ground surface.

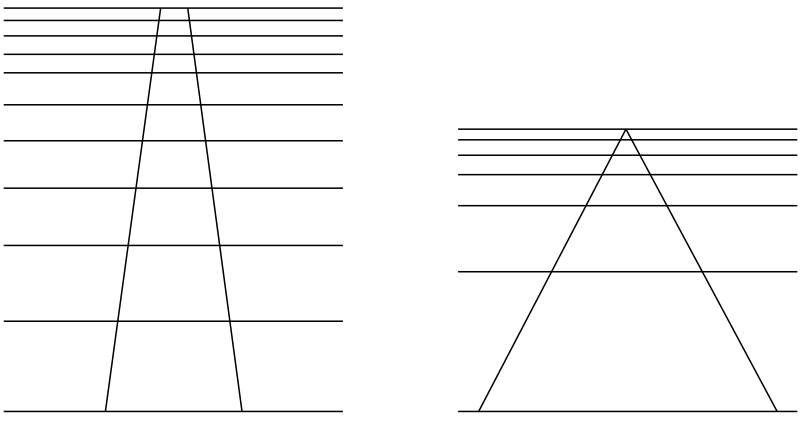

Figure 2-25: Perception of height and distance with splay and compression [196]

Another optical invariant is the optical flow field observed, when moving through the environment. It indicates the relative velocity of objects or points in the scenery. Figure 2-26 shows two examples of an optical flow field, a) while moving straight above the surface to the horizon and b) during a landing glide towards the runway. The point of expansion indicates the direction

of motion. From this point, all flow radiates and thus provides reference cues for the perception of heading. Furthermore, the relative rate of flow in the scenery provides information about the ground surface, e.g. a slope in the terrain surface.

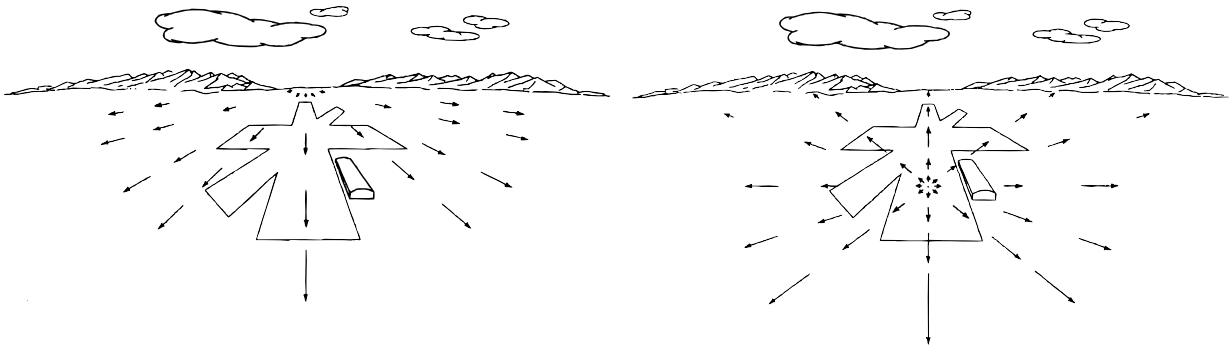

a) Focus of expansion on the horizon in a straight flight

b) Focus of expansion on the runway in a landing glide

Figure 2-26: The outflow of the optic array [60]

Global optical flow and edge rate both contribute to the perception of velocity. With more edges passing the observer, a faster velocity is perceived, compared to flying over sparse trees which merge into a dense forest, for example [196]. Global optical flow increases when flying closer to the ground and with higher velocities, which provides a general feedback about those two parameters. With the general rule of flying low and slow in degraded visual conditions, it can be assumed that the global optical flow field is also maintained constant in order to retain a certain amount of visual cues.

Finally, time-to-contact (TTC or tau (τ), Eq. (2-1)) defines the remaining time needed to close the distance to a certain object (x) under constant velocity, namely the closure rate ($\dot{x}$). If the flight direction is not pointing to the considered object or surface, time-to-passage (TTP) is used [85] [108]. Based on the optical flow field, it is assumed that τ can be perceived directly through the rate of change of the expansion of an object [196].

$$\tau(t) = \frac{x(t)}{\dot{x}(t)} \qquad \textbf{Eq. (2-1)}$$

Based on the work of Lee [102], Padfield investigated τ to close several motion gaps. In the final approach for example, the pilot has to decent and to reduce velocity in order to have zero height and velocity at touch-down. Padfield applied τ-coupling [103] to ensure that those motion gaps are closed simultaneously [129]. Furthermore, together with Clark [36] he proposed a usable flow region, where the pilots are perceiving the required optical flow and τ for obstacle avoidance in the geometrical relation of eye-heights (eh). They assume that this region is located between 12 and 15 eye-heights in front of the rotorcraft to maintain a minimum of 5 to 6 seconds ahead in order to consider a flight as safe. Moreover, they added a safety margin and linked the time-to-contact to the usable cue environment (UCE) classification, see Figure 2-27. Having an additional τ-margin, the visibility conditions can be rated to UCE 2 or even UCE 1.

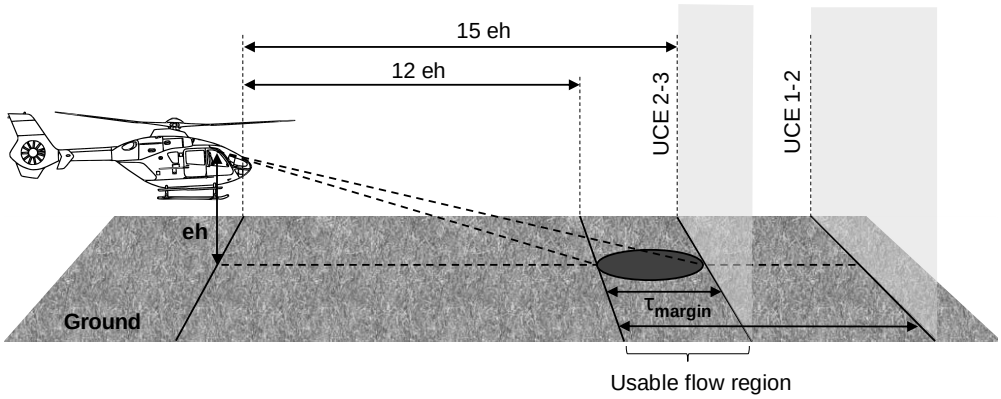

Figure 2-27: Usable optical flow region in eye-heights (adapted from [129])

In addition, Padfield et al. [36] [108] [128] investigated τ-guidance for the development of vision aids, based on a prospective flight guidance. They demonstrated that a constant rate of change of τ ($\dot{\tau} = c$) is applied by pilots to close the motion gaps during deceleration maneuvers. This resulted in a patent for a vehicle guidance system using τ either for automatic flight guidance or to provide guidance information to the pilot [82].

Two further interesting approaches applied an amplification of the optical invariants with synthetic cues placed in the external environment. The first concept is the hover cue design of Bachelder [24] explained in chapter 2.1.3.2 (Figure 2-24). He tried to compensate the reduced optical flow field available, due to the limited FOV. With artificial gains applied to the pretended fixed cubes in the environment, the observer perceives a faster motion in the longitudinal axis, in order to have an equal sensitivity compared to the other axes. However, the cubes are also moving synthetically for generating this illusion. This is a good example of the challenges which arise when relying on the optical flow field with a HMD applied. Focusing on the point of expansion provides only small rates of change. In this case, the peripheral vision perceives the larger amount of provided information. The limited FOV of most HMDs allows only to perceive a small portion of the optical flow, as compared to the possibilities of the human vision.

The second approach developed by Schmerwitz et al. [155] [156] aims to compensate drift velocities at helicopter landings in DVE. They added a moving line to the landing rectangle (Figure 2-23 d)) giving the pilot the impression of an amplified egomotion. In hover or landing, only little changes in the optical flow field occur. Thus, drift velocities are often perceived too late. The moving line or a tested motion pattern on the ground surface inside or outside the landing area introduces a synthetic optical flow in order to provide sufficient cues. Findings showed that it was beneficial for most pilots resulting in improved performance in the experiment, but it seems that the amplified motion will not be perceived subconsciously and requires specific training. In addition, it is difficult to determine the amount of amplification required.

The direct perception of the optical flow provides useful information, when a sufficient rate of change occurs. This occurs usually at closer distances, as can be seen in Figure 2-26. For longer distances, additional principles of depth perception become more important for interpreting depth, which are explained in the next section.

2.2.1.2 Mechanisms of Depth Perception

The basic mechanisms of human depth perception have been scientifically investigated in detail [78]. Two general sources of depth cues exist. On the one hand, effects originated from our visual system (observer-centered cues), and on the other hand, cues generated by the properties of an object in the world (object-centered cues) [196]. Observer-centered cues, which are more relevant at closer distances (< 30 m), are:

- **Binocular disparity:** Humans perceive slightly different images with each eye, due to the physical separation in space (stereopsis).
- **Accommodation:** A muscle must form the eye lens to receive a sharp image.
- **Convergence:** The two eyes must cross their line of sight to focus at closer points in space.

If the accommodation of the synthetic HMD image does not match the real-world distance, the pilot will perceive a blurred image either from the real-world or the synthetic display. A wrong convergence in a synthetic representation will result in perceived ghost- or double-images, because the observer cannot adjust the eyes to several distances simultaneously. In the real-world application, accommodation and convergence of the HMD are set to infinity, because the relevant information is located beyond 30 m. Without adding more depth layers to the HMD [96], accommodation and convergence cannot be used for providing depth cues. In this case, only stereopsis can contribute to depth perception, e.g. by filtering information to reduce visual clutter. In dome-projected simulators the focus to the screen is in the range of a few meters, thus the consideration of all those effects is required, see chapter 4.2.2.

In addition to the observer-centered cues, pictorial depth cues provide monocular references, which offers us advice on how to design 3D-conformal see-through scenery visualizations. The following list briefly explains selected pictorial depth cues from Refs. [24] [196]:

- **Linear perspective and texture gradient (relative density):** Similar to splay and compression of the optical invariants, Figure 2-28 a) shows the parallel lines of the road, which converge at farther distance. In addition, the markers of the center line of the road are more compressed when approaching the horizon.
- **Relative size:** Smaller objects appear farther away when compared to objects, which are physically similar in size, see Figure 2-28 b).
- **Height in the plane:** Viewing objects from above leads to a perception of larger distances, if objects are placed higher in the visual field, see Figure 2-28 c).
- **Aerial perspective:** Objects at farther distance tend to be vague or hazy, see Figure 2-28 d).
- **Occlusion (or interposition):** One object partially or completely obscures another object. The occluded object appears to be farther away, see Figure 2-28 e).
- **Motion parallax:** Moving objects at larger distances appear to have less relative motion than objects closer to the observer, see Figure 2-28 f).

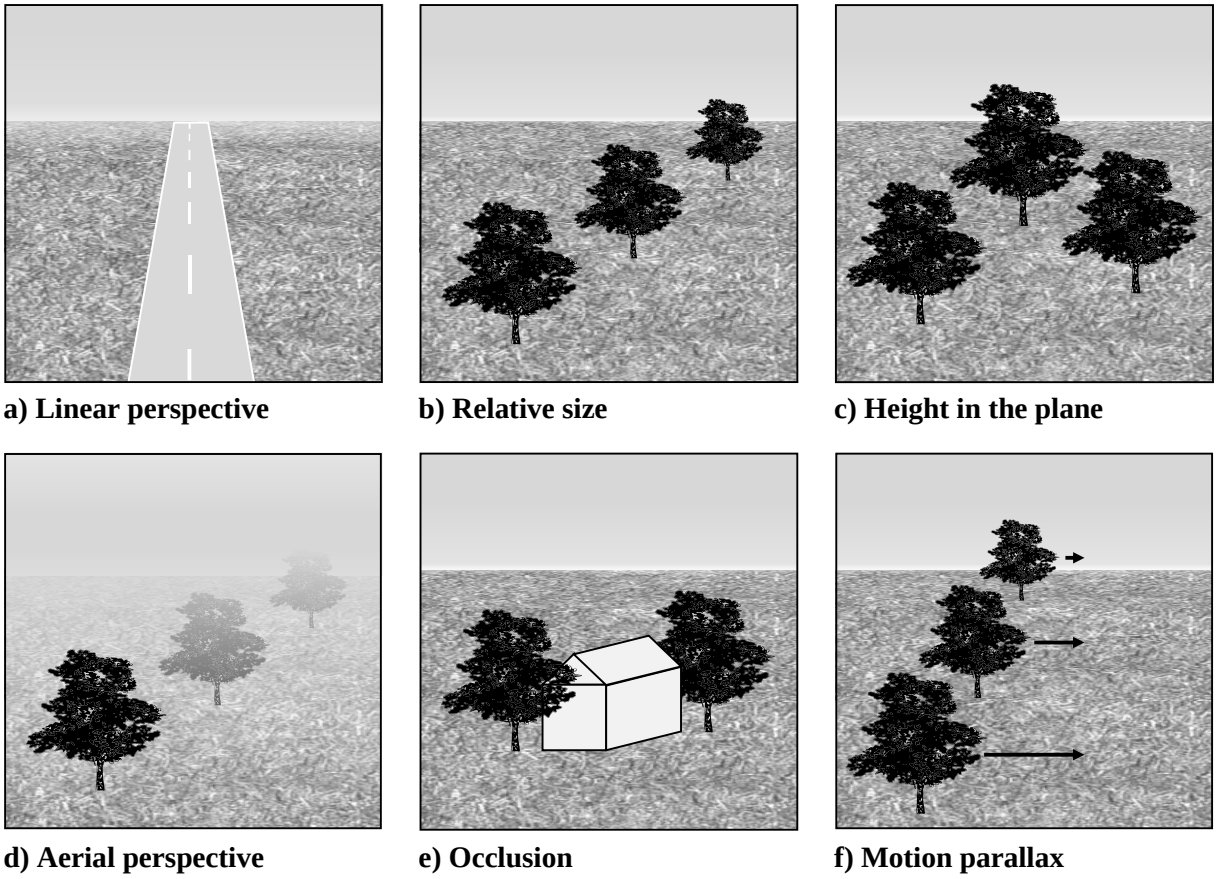

Figure 2-28: Selected monocular depth cues (adapted from [55])

Some depth cues have a varying effectiveness depending on the viewing distance, see Figure 2-29. While height in the plane and motion parallax have a larger impact at closer distances, aerial perspective contributes more to depth perception at larger distances. Occlusion, relative size and relative density are independent of the viewing distance.

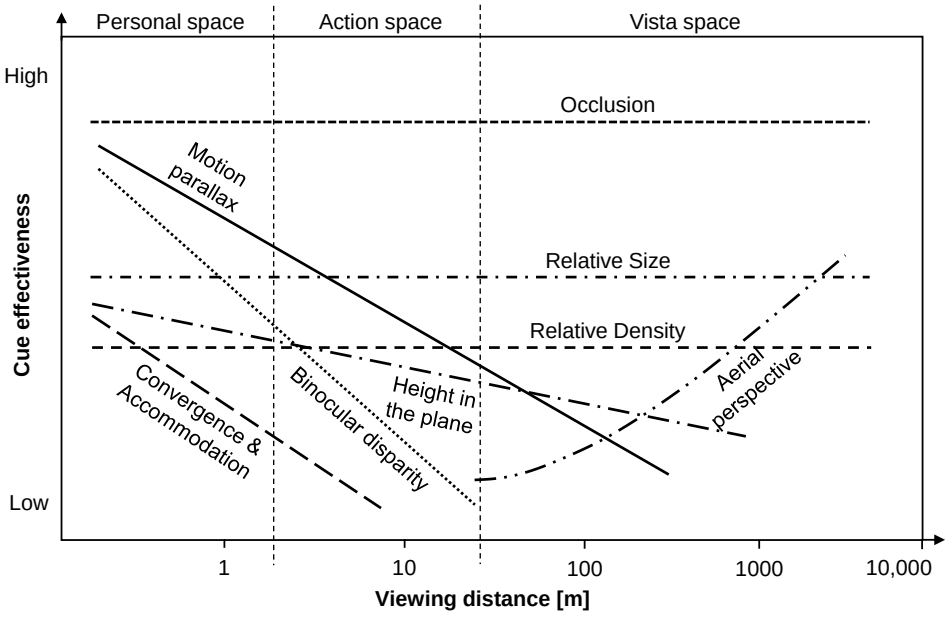

Figure 2-29: Effectiveness of various depth cues depending on the viewing distance [40] [196]

Research on depth perception indicates a dominance of three depth cues, in fact, motion parallax, stereopsis and occlusion [196]. Considering the relevant distance for the task of helicopter flying in DVE, stereopsis should be less relevant, but the cues of relative size and density might be interesting in addition to the relative motion and the occlusion effect.

2.2.1.3 Principle of Micro- and Macro-Texture

The external environment can be reconstructed synthetically with micro-textures and macro-textures, in order to provide sufficient optical flow [24] [36]. Macro-textures can be obstacles, like poles, trees or synthetic generated elements, e.g. the cubes in Figure 2-24 or the towers, placed at the landing zone concepts (Figure 2-22). In contrast, micro-textures represent either more detailed parts of a macrotexture, e.g. branches and leaves of a tree, or fine-grained textures of the surface. The motion pattern applied by Schmerwitz et al. [154] makes use of synthetic generated micro-texture cues in order to provide further drift indication. A more quantitative classification has been investigated by the research of QinetiQ funded by the Safety Regulation Group of the UK Civil Aviation Authority [13]. The research focused on how pilots use visual cues to fly helicopters. Image metrics were considered for analyzing available cues, for instance, smoothness, intensity, uniformity and density, which need further effort for validation.

Hoh discovered that micro-texture has a strong influence on the task of low speed flight and hover [75]. However, it is very difficult to use micro-textures in a see-through HMD, because the detailed textures increase the amount of occlusion of the real-world behind. Corwin et al. introduced the concept of emergent detail to add more texture details for terrain representation needed at lower altitudes [39]. This approach increases the information by placing rectangular tiles into a regular terrain grid, which compensates for the loss of required optical flow, but also increases the occlusion as well as potentially visual clutter. Therefore, most recent concepts try to avoid the use of micro-textures and rely more on macro-textures, although both provide important cues.

2.2.1.4 Visual Cue Rating and the Usable Cue Environment

In the aeronautical design standard about handling qualities requirements (ADS-33E-PRF [5]) the visual cue rating (VCR) is applied for determining the usable cue environment (UCE) in order to define the required control augmentation in DVE. Thus, the VCR is a widely used subjective rating of the available visual cues, in addition to the image analysis approaches mentioned before. The current VCR scale relies solely on the pilot's rating of the ability to perform aggressive and precise maneuvers, because Hoh found out that in the original version of the VCR scale, the pilots were not able to reliably rate the quality of the visual cues [77]. Even after rating a visual cue environment as adequate, pilots had problems when flying with these cues available. The rating considers now the control of the attitude (pitch, roll and yaw) and the translational rates (lateral, longitudinal and vertical) on a scale from 1 (good) to 5 (poor) [5]. Since, the VCR is relying on the maneuver precision and aggressiveness, all visual limitations are indirectly included, e.g. not only micro- and macro-textures, but also FOV and other limitations. In addition, Hoh assigned control augmentation methods with higher-level helicopter response types to the UCE [77], e.g. attitude command and translational rate command. Thus, the UCE ratings could be linked to the Cooper-Harper handling qualities rating (HQR) [38], which is another important rating scale used

in the ADS-33E-PRF, to assess aircraft characteristics and the demand on the pilot to fly it. Both, the HQR and VCR scale are depicted in the appendix A.1.

2.2.2 Pilot Control Behavior and Workload

The task of flying a helicopter can be subdivided into three main sub-tasks according to Padfield [127], in fact, stabilization, guidance and navigation. Stabilization is considered as the permanent task of attitude control, while guidance contains mid-term tasks, e.g. controlling the trajectory with altitude and course. The long-term task of navigation includes the task of determining the pathway from the starting point to the destination. This breakdown into subtasks allows the design of task-specific visual cues for the pilot. With regard on human performance, Rasmussen [144] has derived another three levels of human behavior:

- **Skill-based:** Direct sensory-motor performance without conscious control.
- **Rule-based:** Application of stored rules or sub-routines in a familiar situation.
- **Knowledge-based:** Unfamiliar situation for which no rule exists and a higher conceptual level is required.

The boundaries of these behavioral levels are not distinct and are depending on the attention of the person and the level of training. An example is the general rule for the pilots when flying in DVE, in fact to fly low and slow in order to remain sufficient visual cues and enough time to react for unknown occurrences. In addition, control augmentation systems have been developed to assist the pilot in DVE, especially for the task of stabilization. With higher level of rotorcraft response types applied, the control functions are changing the behavior of the helicopter to control directly the attitude or the translational rate, compared to the basic rate command. Thus, stabilization is not required by the pilot and attention can be focused on other tasks, e.g. to remain situation awareness and to search for obstacles. Figure 2-30 shows the attitude responses of several helicopter command types, following a cyclic control step input.

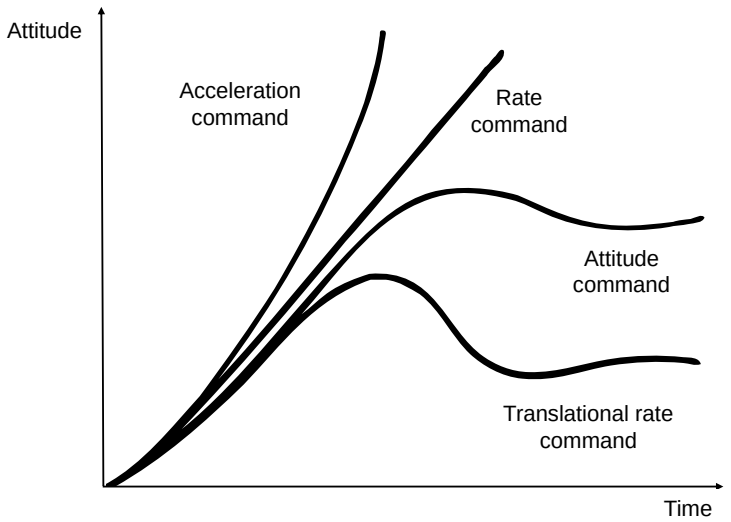

Figure 2-30: Attitude response based on a cyclic control step input [127]

The additional stability reduces the workload of the pilot, but also decreases the agility and maneuverability of the helicopter [127]. An acceleration command would have the highest agility, but it would be very difficult for the pilot to control the helicopter over a longer period of time. In order to support the pilot in DVE, visual augmentation is added for maintaining situation awareness, e.g. detection of obstacles in the surrounding environment. Figure 2-31 shows the information flow with control and visual augmentation applied. The rotorcraft contains the main functionalities and information sources from the available technologies discussed previously. The degraded visual environment provides the residual information cues augmented by the visual assistance system, which generates missing information synthetically on the HMD. The control augmentation in this case does only control the reference value of the pilot. It could also provide reference values to the pilot, for example if haptic cues are considered with active control inceptors.

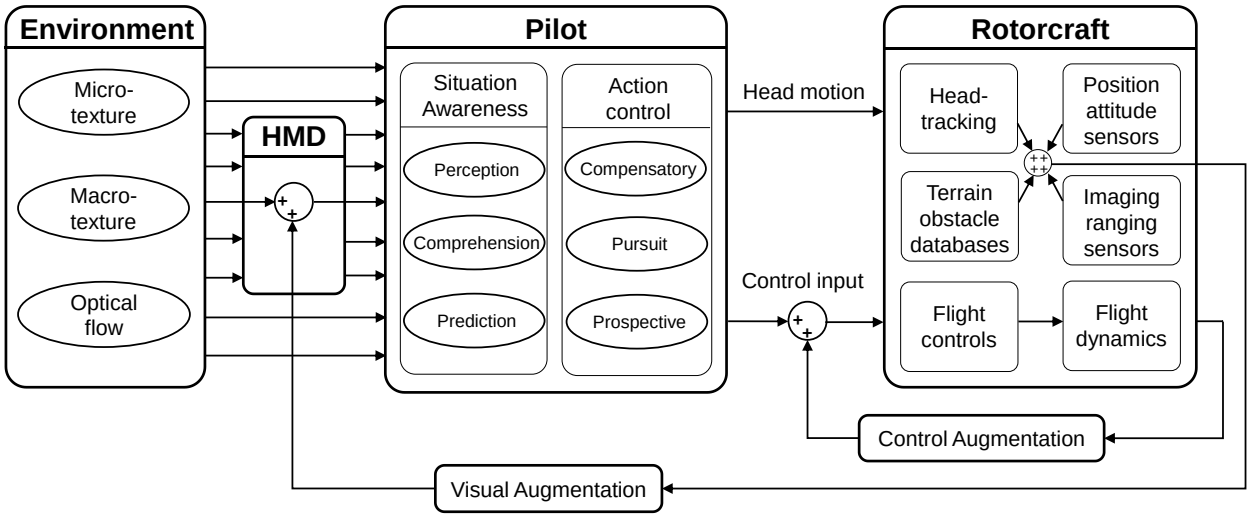

Figure 2-31: Information flow with control and visual assistance

Finally, the pilot runs several internal processes to maintain enough situation awareness and to derive the desired action with control inputs. Those behavioral processes are further explained in the next subsections, together with the workload in order to describe the required mental resources.

2.2.2.1 Human Control Behavior

The control behavior of the pilot depends on the amount and kind of information available. Three basic control mechanisms including their corresponding information presented are:

- **Compensatory**: The error of a parameter to be tracked is displayed, e.g. deviation to the localizer or the glide slope.
- **Pursuit**: A command value is displayed, e.g. a flight director, which should be followed.
- **Prospective (or preview)**: The whole course or trend of the parameter to be tracked is displayed, e.g. a tunnel-in-the-sky, which provides a preview of the flight path.

In addition, the pilots can not only perceive the future trajectory to be flown with a prospective display, they can also anticipate the future state of the helicopter due to their experience. However, the prediction of this is mentally demanding and therefore, predictive displays have been

developed [68] [158]. A flight path predictor symbol has been implemented together with a tunnel-in-the-sky in order to show the pilot the position of the helicopter a few seconds ahead. Current 3D-conformal display concepts are mainly based on prospective information, which allow the pilot to anticipate the future position of the helicopter in the obstacle scenery. Some approaches apply predictive contents, e.g. the safety line [123] calculates the minimum flight path altitude for passing the obstacles, or other concepts calculate the predicted level of danger with a risk factor indication, e.g. the obstacle presentation starts blinking when it has been predicted as a high risk [84]. In addition, Kahana et al. investigated an altitude predictor – flight path marker (AP-FPM) in order to provide vertical guidance only. The pilot is then able to freely choose the correct path in the obstacle scenery.

Independent of the control behavior of the pilot, controlling the rotorcraft takes a certain amount of workload. The less effort it takes, the more resources can be spent on achieving situational awareness.

2.2.2.2 Situational Awareness

One of the objectives of this work is to achieve a high level of situational awareness with the visual augmentation system applied in order to avoid any kind of collision. Hoh demonstrated that improved handling qualities, especially stabilization for low-speed and hover, have a direct and positive impact on pilot workload and situational awareness [77]. There exist more than 25 different definitions of situation awareness [32]. In general, situation awareness can be broken down into awareness of the surrounding environment, the mission's goals, the aircraft systems and human resources including crew member activities [32]. In this work, the spatial awareness of the surrounding environment with the rotorcraft position, attitude and velocity is of primary interest. There is one descriptive model of situational awareness, which has gained a wide acceptance by experts in the field. The model developed by Endsley serves as a common ground for discussion without the claim to be exhaustive [53].

In Endsley's model situation awareness is divided into three levels:

Level 1: Perception of the elements in the environment

Level 2: Comprehension of the current situation

Level 3: Projection of future status

The first level mainly reflects the basic visual sensing in order to gather information, which has been described in the previous chapter already. Looking into the second level, the elements perceived in level one are synthesized in order to obtain a comprehensive and holistic picture of the environment. The third level represents the projection of the current state into the future, involving knowledge and comprehension of the situation in order to make the right decisions and take correct actions. The ecological approach to visual perception assumes that basic egomotion does not require comprehension and knowledge. However, other environmental information may require the construct of those higher levels, e.g. a classification of the obstacle hazard in order to derive alternative actions.

The cognitive processes to assess the required situational awareness are the limiting factors. Attention and working memory are two very important human properties affecting situational awareness. The following list shows a selection of typical phenomena from Endsley [54], which can degrade situational awareness, the so called SA demons:

- **Attentional tunneling:** Fixation on specific elements of information, while becoming blinded to other elements.
- **Workload, anxiety, fatigue or other stressors:** Psychological and physical stressors can negatively affect information gathering and they can reduce an already limited working memory.
- **Data overload:** If there are more auditory or visual cues than can be processed, situational awareness may contain significant gaps when forming a mental picture.
- **Misplaced salience:** Salience can be used to promote situational awareness, but if used inappropriately, it can hinder situation awareness.
- **Out-of-the-loop syndrome:** Automation can push the user out-of-the-loop, resulting in lower situational awareness, e.g. wrong mode awareness.

Davison and Wickens investigated the effects of rotorcraft hazard cueing on pilot attention and trust in the cueing system in case of reduced reliability [41]. Highlighting hazards produced an negative attention cost effect, in which uncued targets were less likely to be detected. On the other hand, the experiment with twenty four pilots showed clear benefits of providing pilot hazard awareness. However, the pilot must know the reliability of the system or its possible failures in order to appropriately adapt his trust to the system. While the latter experiment displayed the hazard cueing on a map, the experiments of Knabl [93] including eighteen pilots applied the cueing on a wide FOV HMD in a conformal manner with similar results on the uncued target detection.

Finally, measuring pilot situational awareness is complex and difficult. Several methods have been developed for direct measurement and are further explained by Salmon et al. [149]. In a freeze probe technique, the situation is frozen and all displays and screens are blanked. Then, the pilot has to recall the current situation based on a set of prepared questions at the time of the freeze. The most popular technique is the Situation Awareness Global Assessment Technique (SAGAT) based on the construct of Endsley. Further methods are self-rating and observer-rating techniques. The Situation Awareness Rating Technique (SART) is such a post-trial subjective approach, where the pilots have to rate each dimension on a scale from one (low) to seven (high) after the task. The experiment of this work used performance measures of the task in order to indirectly determine the situational awareness of the pilot, in addition to subjective self-ratings of the pilot workload. For example, the time margin for obstacle detection and avoidance as well as lateral distances to hazards in the flight path are considered to determine the performance under different visual conditions. Freeze and real-time probes were assumed to have adverse effects on the evaluation of the considered control strategy of the pilots and thus have been discarded for this experiment.

2.2.2.3 Pilot Workload

Establishing sufficient situation awareness and maintaining control of the helicopter both requires mental resources of the pilots and contributes to their workload. Blanken et al. and Hoh worked on reducing pilot workload by control augmentation. Figure 2-32 shows an interesting example of the control activity of two pilots during a hover task with three different rotorcraft response types, in fact, rate command (RC), attitude command / attitude hold (ACAH) and translational rate command (TRC).

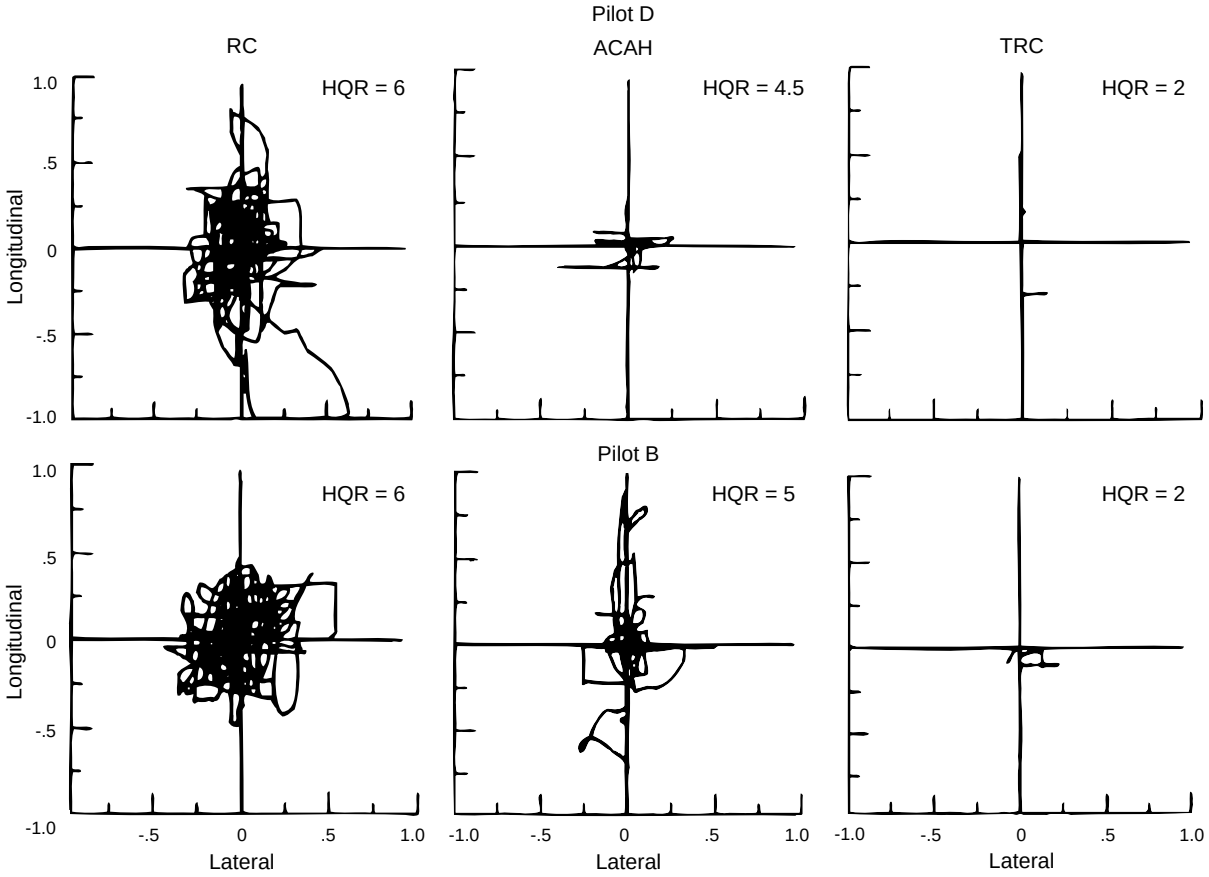

Figure 2-32: Cyclic control activity during hover task [31]

The results demonstrated that much more effort was required by the pilot to hold the position with the conventional RC compared to the ACAH and TRC, which was also reflected by the higher handling qualities rating. According to Hoh [77], hovering an unaugmented helicopter in DVE requires at least 70 % of the pilot's workload capacity, which leaves only 30 % for maintaining situational awareness. While control augmentation is a suitable mean for low-speed and hover with advanced stabilization, visual augmentation is required to reduce workload for maintaining situational awareness in order to prevent obstacle collisions.

Besides behavioral measurements, the Task Load Index (TLX) [70] approach of the NASA is applied for subjective ratings of the pilot workload. It is an easy to use multi-dimensional scale to obtain the workload immediately after performing the task and has proven to be reasonable and reliably sensitive to experimental conditions [71]. The six dimensions, in fact, mental demand, physical demand, temporal demand, effort, performance and frustration are rated between low and

high and can be weighted for the task applied. The dimension definitions are described in the appendix A.1.

In addition to behavioral and subjective measures, secondary tasks are often applied to determine pilot workload [84] [93] [197]. The better this concurrent secondary task is performed, the more capacities are assumed to be available. Poor performance on the secondary task indicates a high workload on the primary task. The drawback of applying secondary tasks is the possibility to also influence the performance of the primary task. Hence, the approach was not applied in the experiment of this work.

2.2.3 Visual Clutter within 3D-Conformal Display Concepts

Display clutter is a term for the undesired effect of pilot confusion through displayed information or increased search time to gather necessary information rather than enabling the pilot to accomplish the required task successfully and safely [183]. Most quantitative investigations regarding display clutter evaluate the displayed content, in which clutter depends on the number of objects, the density or proximity of several objects, the size of objects, the saliency and contrast or the structuring of entities [83] [86] [196]. In addition, also subjective measures with pilots are adopted to derive better guidance for designing displays [83] [86]. The see-through application with a HMD further requires to not only consider the displayed content, but also the remaining cues from the real world background. Thus, the term ‘visual clutter’ might be a suitable alternative to ‘display clutter’. 3D-conformal visualization approaches were found to mitigate clutter [91] and to have lower scanning cost [194] compared to conventional two dimensional presentations, because of the one-to-one relation of the superimposed objects with the outside world [199]. The display design process is basically a trade-off between the information needed and the display clutter [9] [44], in what de-clutter is the goal to allow faster information perception and thus to reduce pilot workload. However, reducing the amount of displayed pixels alone does not automatically result in lower clutter cost, as has been found by Knabl et al. [89] with three obstacle variants tested (Figure 2-17). The opaque display type was found to produce less clutter than the wireframe type. Even though, the opaque display induced more occlusion of the outside view, the wireframe variant was difficult to be distinguished from the terrain grid. Thus, useful design properties for decluttering are briefly explained in the next subsection.

2.2.3.1 Design Properties Reducing Visual Clutter

Designing 3D-conformal display concepts should consider at first the principles of visual perception, for instance, depth perception cues and the optical flow. In addition, decluttering strategies can be applied to structure the content and to reduce the amount of occlusion of the real world and other displayed symbology.

Frames of reference

Conformal visualization displays allow to place objects and symbols in different frames of reference, compared to non-head-tracked HMDs. Information for primary flight states is usually still located in the head-fixed frame of reference, while terrain and obstacle content is assigned to the geospatial referenced frame. In addition, attitude information has been fixed to the aircraft

frame, for instance the roll scale, the aircraft axis symbol and the heading tape [44]. Placing the attitude indicator in the forward projected longitudinal helicopter axis avoids mental rotation between the attitude indicated at the display and the attitude perceived from the environment. The cost of mental rotations with respect to the frame of reference are further discussed by Wickens [196]. Moreover, hybrid concepts, which partially fix a symbol to more than one frame of reference are technically feasible. Doehler et al. [44] for example implemented the heading tape rotating with the outside horizon. Thus, it indicates not only the current heading, but also serves as an artificial horizon reference. However, with the limited FOV of most HMDs, such a heading tape can quickly disappear in conjunction with larger head movements, if it is only geospatial referenced. To solve this issue, the heading tape can be horizontally aligned and also fixed to the pitch of the pilot's head in the hybrid approach. Hence, it always remains visible within the available FOV and simultaneously assists in heading and roll attitude perception.

Color coding

While past and present HMDs in airborne applications are still monochrome, full color HMDs become more and more available and are therefore considered in this work. Without color, differences in visualization had to be realized through variations of brightness or by other means to increase saliency (e.g. flashing [84]). The pilots request color HMDs [90], because color is a suitable mean to distinguish between different groups of separate information, in addition to the application of different frames of reference. The terrain visualization with a regular grid or with contour lines contributes tremendously to visual clutter. The drawn lines are distributed over the whole display and are dynamically moving depending on the pilot's head motion. Therefore, elements presented in the head-fixed frame of reference will inevitably cross and thus occlude elements in the geospatial frame of reference. However, with different colors for terrain and primary flight state parameters, it is much easier to distinguish between the symbol elements and terrain lines. Thus, color-coding supports the differentiation between the frames of reference. According to most recommendations, color should be used very carefully and only where it is necessary and cannot be realized by other means, e.g. different shapes of symbols [59] [111]. Moreover, it is recommended to apply a very limited number of colors for already categorized and structured information. Care should also be taken in a see-through display application, where some colors are not usable under certain conditions, e.g. white during whiteout or yellow in brownout conditions. Further design consideration for the color coding of display content can be found by Wickens et al. [196].

Concept of information blending

The see-through display application requires a detailed consideration of what can be occluded by the displayed content without adverse effects. Two occlusion effects should be regarded therefore:

- **Real-world occlusion:** Displayed content shall not obscure important visible features in the real-world view.
- **Symbology occlusion:** Displayed content shall not mask other important display content unintentionally.

Near-field objects are often still visible in DVE, although in a reduced visual range. Thus, a continuous fade-out can be applied to blend out or to cull the terrain visualization in the foreground up to the remaining visual range [121]. This results in a smooth transition from the still visible cues in the outside world to the synthetic cues provided on the HMD. Thus, the pilot experiences an augmentation of the real-world environment only where outside visual cues are degraded. A double source of information from real-world and synthetic augmentation is avoided and it is assumed that the pilots are less confused, especially if the conformity is not perfect, due to the errors of the positioning and head-tracking system. Since the visible range cannot be detected automatically by an airborne sensor yet, the pilot has to set this distance manually, either continuously or with discrete decluttering modes.

The second type of occlusion originates from the dynamic content in the geospatial frame of reference. Presenting two dimensional information in the head-fixed coordinate frame can cause an overlap or interferences with the terrain and obstacle information displayed in the background. To ensure readability of the numerical parameters, an area around these symbols should be rendered semi-transparent. With this approach, primary rotorcraft state parameters can also be prioritized above scenery content. Examples will be given in chapter 3, which further explains the development of the advanced display concepts.

2.2.3.2 Determining Visual Clutter

Direct measuring of visual clutter is very difficult in the see-through HMD domain, due to the many contributing factors. Besides performance measurements, Kaber et al. [83] examined subjective measures with pilots in order to identify semantic pairs used for describing clutter on a HUD, resulting in “redundant / orthogonal”, “monochromatic / colorful”, “salient / not salient”, “safe / unsafe”, and “dense / sparse”. Furthermore, they developed a pixel analyzer tool to determine the active illuminated pixels, and thus the occlusion of the real-world with displayed content [86]. Kaber et al. were able to analyze screenshots of recorded videos in a follow-up process to evaluate the amount of occlusion, which contributes to display clutter. This idea has been developed further in order to determine the occlusion in real-time for this work, see chapter 3.3.

2.3 Summary

The available technologies demonstrate the complexity required for 3D-conformal visualizations within a see-through HMD in order to assist the pilot in DVE. Very accurate positioning and head-tracking systems are required for an acceptable scene-linking of the synthetic content over the real-world background. The performance of head-mounted displays has increased tremendously over the last decades. Emerging low-cost systems, which provide full-color already, will enable the usage of HMDs for civil applications. Databases are growing and the precision and resolution are increasing in order to provide fundamental information for the presentation of 3D-conformal scenery content. In addition, sensors are required to detect obstacles, which are not available in databases. The sensor technologies need further developmental effort for providing reliable and high resolution data.

Based on the available maturity of these technologies, several 3D-conformal display design concepts have been introduced by previous publications. Evidence for an optimal obstacle representation on the HMD for low-altitude flight or visual cues for a precise hover maneuver in DVE has not been demonstrated so far. However, those first display designs served as a starting point for the development of enhanced HMD cues in this work. In addition, the theoretical background enabled performance enhancements through a better understanding of the pilot perception and behavior. Knowledge about optical invariants and depth cues provided fundamental guidelines for designing meaningful display concepts. Finally, visual clutter has been addressed in order to find solutions, which are able to decrease this adverse effect and thus reduce pilot workload. Design properties with a high potential to mitigate visual clutter were explained. These properties were applied as design principles in the development process of the advanced display concepts in this work. The development of two new display designs for low-altitude flight and hover based on the background presented in this chapter is further explained in the next chapter.

3 Development of Advanced Display Concepts

The objective of this work is to evaluate not only the latest display concepts, but also to assess combinations of approaches satisfying the needs of the pilot according to the visual perception theories. In order to demonstrate the behavior of the pilot, two tasks have been selected, in fact, low-altitude flight for determining the obstacle avoidance reactions and hovering for observing the stabilization performance in DVE. Thus, two novel display designs were developed for these tasks on the basis of previous work. Furthermore, the methodology of measuring the active illuminated pixels was advanced and applied as a valuable engineering tool for further improvements. Hence, the amount of occlusion of the real-world image with displayed content could be determined in real-time and it was used to reduce visual clutter in early stages of the development process. The piloting task of stabilization, flight guidance and obstacle avoidance is described first.

3.1 Piloting Task Analysis and Requirements

The emphasis of this work is on the primary task of flying the helicopter. Thus, secondary tasks were not considered so far, for instance, rotorcraft system monitoring, mission planning tasks and automation tasks. Those tasks can be conducted before take-off or during less demanding flight phases, e.g. the IFR cruise flight to the accident site in a rescue mission. Multi-crew concepts with crew coordination were also not yet considered in the conducted experiment. In NVG operations for instance, the copilot frequently reports important flight state parameters to the pilot, e.g. speed and altitude in order to assist the pilot in command. Using the NVG with a limited FOV the pilot usually has difficulties to take a look into the cockpit to check out the head-down instrumentation and to shift between the near and far domain. The HMD design aimed to provide sufficient information making another crew member unnecessary, even though another set of eyes is always beneficial considering safety issues. The primary task of flying contains stabilization, guidance and navigation tasks. However, detection and identification of obstacles for a collision-free flight path is not only a constraint, but rather another primary task for maintaining sufficient situational awareness especially in DVE. Thus, the first part of the experiment considered the obstacle detection and avoidance with guidance of the helicopter through the scenery at low altitude. While the second part focused on stabilization of the rotorcraft in hovering with the respectively developed display concepts. Table 3-1 shows the minimum required information for the primary tasks of flying the helicopter together with examples from conventional 2D head-down instrumentation and existing 3D head-up approaches. The assignment of the information parameters required by the pilot to the implemented visualization entities, enabled an identification of redundant elements on the display. Thus, unnecessary information could be eliminated or redundant information could be purposefully applied in order to increase the probability of correct perception. Nevertheless, the low-altitude flight in unknown terrain and obstacle scenery required further information for the obstacle avoidance task.

Primary flying task	Required parameters	2D examples	3D examples
Stabilization	Pitch angle / rate, Roll angle / rate	Attitude indicator: pitch ladder, artificial horizon, aircraft symbol	World aligned horizon, Landing zone reference symbols (e.g. towers)
Guidance	Airspeed / rate, Ground speed, Vertical speed, Barometric altitude, Radar altitude / rate, Heading / rate	Primary flight display: airspeed tape, altitude tape, vertical speed bar, digital ground speed, radar altimeter, heading tape	Optical-flow-field from terrain and obstacles, Tunnel-in-the-sky
Navigation	Position, Course, Waypoints	Horizontal situation indicator or navigation display, Digital moving map	Ground referenced flight path markers and waypoints, Landmarks (terrain and obstacles)

Table 3-1: Required information for the primary flying tasks with examples

3.1.1 Obstacle Avoidance Task

Three different low-altitude flight conditions are typically regarded, see Figure 3-1. Low-level is considered as flying above the obstacle scenery, while contour flight implies following the elevation profile of the ground and the obstacles. The lowest flying strategy is the nap-of-the-earth (NOE) flight around obstacles, using them as camouflage in the military field. However, also in civil missions the pilot has to fly very close to the ground and obstacles in such situations, when searching for a suitable landing site during the final approach.

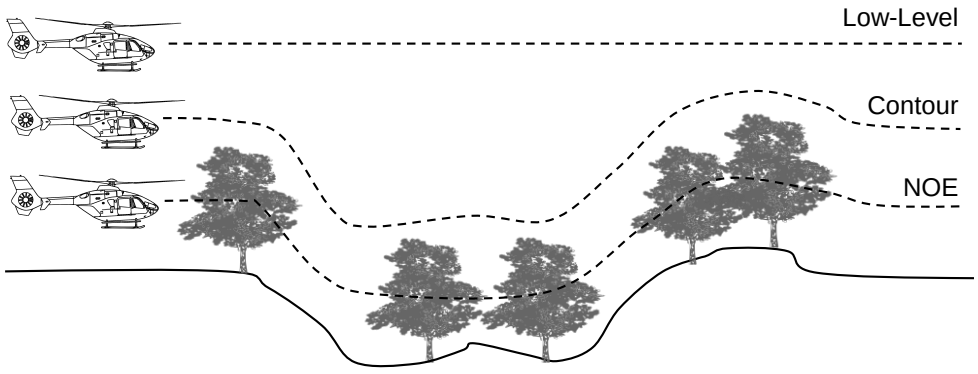

Figure 3-1: Three categories of low-altitude rotorcraft flight [30]

In general, static and dynamic obstacles must be considered. Database and sensor information is indispensable during degraded visual conditions in order to provide the required information for collision avoidance. Table 3-2 summarizes example solutions using these information sources, as described already in chapter 2.1.

Collision avoidance task	Required parameters	2D examples	3D examples
Static obstacles	Terrain, Object types (buildings, poles, wires, trees…), Airspaces	Digital moving map, Helicopter terrain awareness and warning system with colored terrain elevation	Synthetic terrain visualization (grid, contour lines, opaque), Obstacles from databases, Unclassified obstacles from sensor information, Safety line
Dynamic obstacles	Air-traffic, Ground-traffic	Horizontal situation indicator or navigation display with TCAS or ADS-B	Highlighted traffic symbols, Additional ADS-B information fixed to the aircraft, Unclassified vehicles from sensor information

Table 3-2: Required information for the collision avoidance task with examples

According to the ecological approach based on the optical-flow-field, information around the usable region of 12 to 15 eye-heights in front of the helicopter is most important in order to allow the pilot to predict the future flight trajectory without collisions. The list does not claim to be exhaustive, since individual mission tasks may require additional flight guidance and obstacle parameters. Up to the present, only static obstacles were considered in the conducted experiment of this work. However, dynamic obstacles could be included in further investigations.

3.1.2 Hover Task and Stabilization

The hover task had the highest demands on stabilization in this simulation experiment. Besides attitude control, the pilot had to compensate position errors and required additional cues for the sensation of drift velocities. Without movement, the optical-flow vectors disappear and the pilot perceives deviations from the target position too late. Close to the ground, micro-textures provide the most sensitive cues, but are lost in DVE. Hovering out-of-ground, e.g. for a hoisting operation against a wind turbine, precludes optical-flow information from micro-textures over the whole FOV. Thus, the pilot can only use the wind turbine itself as a reference, making this task a very difficult and demanding challenge without control and visual augmentation methods, even under good visual conditions. In addition to the attitude information, the pilot requires sufficient cues to determine the position deviations and drift indications through acceleration or velocity cues.

3.2 Sense and Avoid Display Concept

Two general approaches can be applied for designing an obstacle avoidance display. Presenting information either with abstract guidance symbologies (e.g. safety line) or by a synthetic replacement of the real-world picture. The latter provides visual cues in the same manner as the pilot would perceive in good visual environments. Thus, it was assumed that the pilot must not

change the control behavior. Hence, due to that unchanged control behavior, it was anticipated that the high amount of occlusion with a synthetic terrain and obstacle representation is worth the cost of visual clutter, at least in very low visibility conditions. In addition, environmental situation awareness can be improved, if the presented information is reliable. Figure 3-2 shows the resulting display concept with flight guidance plus sense and avoid (FGSA) information. It contained 2D and 3D-conformal flight guidance symbology together with 3D-conformal terrain and obstacle representations, considering the requirements listed above.

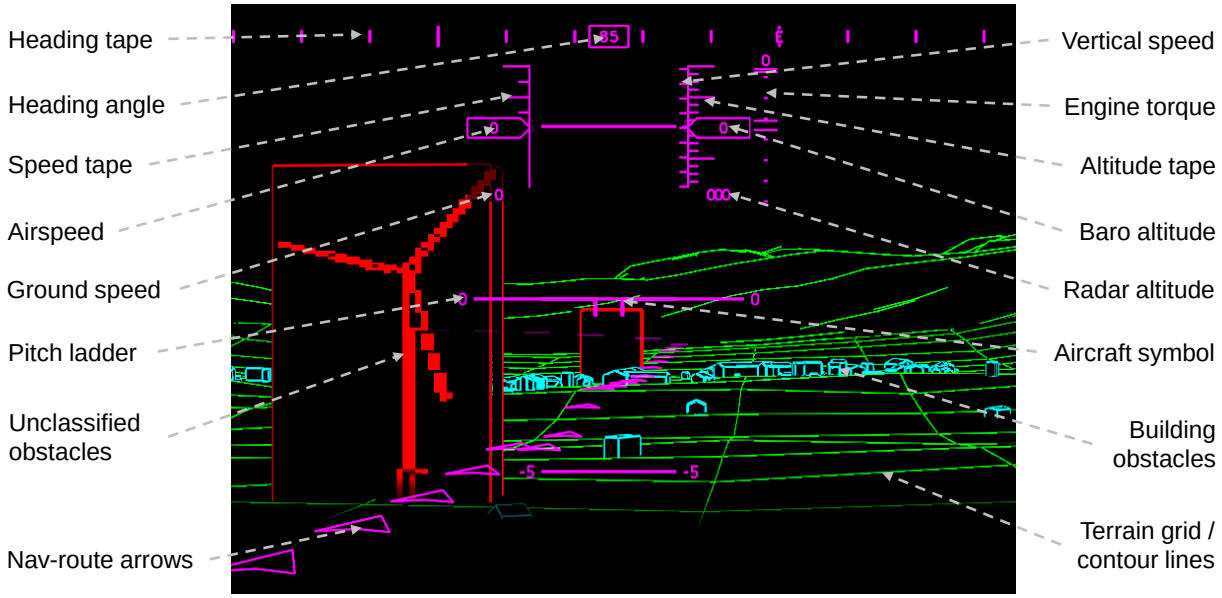

Figure 3-2: Flight Guidance plus Sense and Avoid (FGSA) display concept

Everything shown here in black conforms to transparency on the HMD. The details are further explained in the next subsections together with the applied design properties to address the visual perception mechanisms of the pilot.

3.2.1 2D-Primary Flight Display Information

The two dimensional primary rotorcraft state information was located head-fixed, except of the attitude indicator, which was aircraft-fixed. The information was grouped together in a conventional “T-Arrangement”, as known from many primary flight displays, but inverted with the heading-tape on top. The parameters displayed shown in Figure 3-2 are:

- Airspeed and speed tape
- Ground speed
- Vertical speed bar
- Barometric altitude and altitude tape
- Radar altitude
- Heading and rotating heading tape
- Engine torque with limit indications

The whole arrangement was shifted to the top region of the display within the limited FOV. In fixed-wing fighter aircraft, this was done for air-to-ground missions in order to reduce the

occlusion of the important lower part of the display for this case. It was shifted to the bottom for the same reason in air-to-air missions [59]. The low-altitude flight task requires also a more unobscured view downwards, thus the less important free space at the top region was appropriate for rotorcraft state information.

Moreover, some areas of the two dimensional symbology were rendered with a black background in order to ensure transparency on the HMD and thus provided increased readability for the pilot. Figure 3-3 shows the important numerical parameters that had a complete black background, in fact, airspeed, altitude and heading. Other parts were rendered only with a certain amount of transparency in the background (e.g. 70 %, depicted by the grey background rectangles in Figure 3-3). Thus, scenery information in the background was not occluded completely by this procedure. Only the brightness of this background data was reduced. Applying this information blending concept aimed to support the pilot in reading the primary state information and it increased the effect of grouping similar information. Thus, visual clutter could be mitigated.

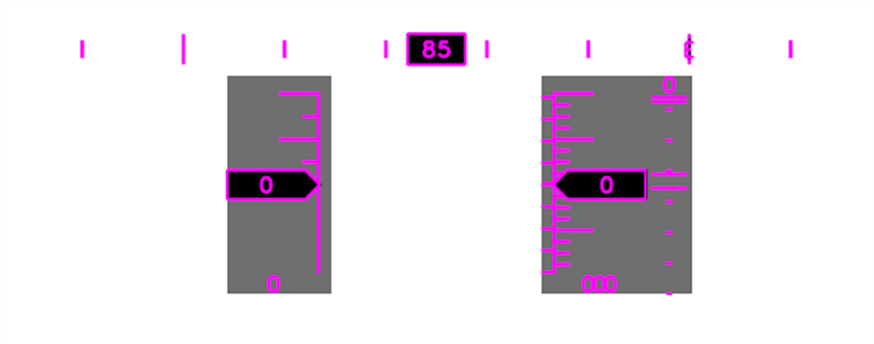

Figure 3-3: Two dimensional primary flight state information with background transparency

Furthermore, the heading tape rotated in alignment with the horizon, and the attitude indicator was fixed to the longitudinal extension of the rotorcraft in order to mitigate the cost of mental rotations [196] and to increase visual conformity [44], even though the information was presented in two dimensions only.

The rapid prototyping of the 2D symbology was implemented with the software toolbox 2Indicate. 2Indicate was developed by the German Aerospace Center (DLR) for flexible visualization of technical user displays [3].

3.2.2 3D-Conformal Flight Guidance Information

Navigation assistance head-up was provided by markers in the form of triangles or arrowheads (Figure 3-4 d)), referenced to the ground surface according to Knabl et al. [90] [91]. These navigational markers allow horizontal guidance and demonstrated less susceptibility to the effect of attentional tunneling, compared to the conventional tunnel-in-the-sky concept (Figure 3-4 a)). Thus, more attention can be spent looking outside, searching for obstacles around the flight path or the landing site. Furthermore, a precise tracking of the path, as it is required for an ILS approach, was not necessary. Moreover, an obstacle free flight path usually cannot be guaranteed during the planning phase, when database information is the only source of obstacles. However, with a real-time update through sensor information, which can provide a reliable obstacle-free flight path, a

precise tracking can become important. Moreover, vertical guidance information is often not available at unknown landing sites without additional infrastructure. Thus, the navigational markers on the ground were applied for the obstacle avoidance task in low altitude.

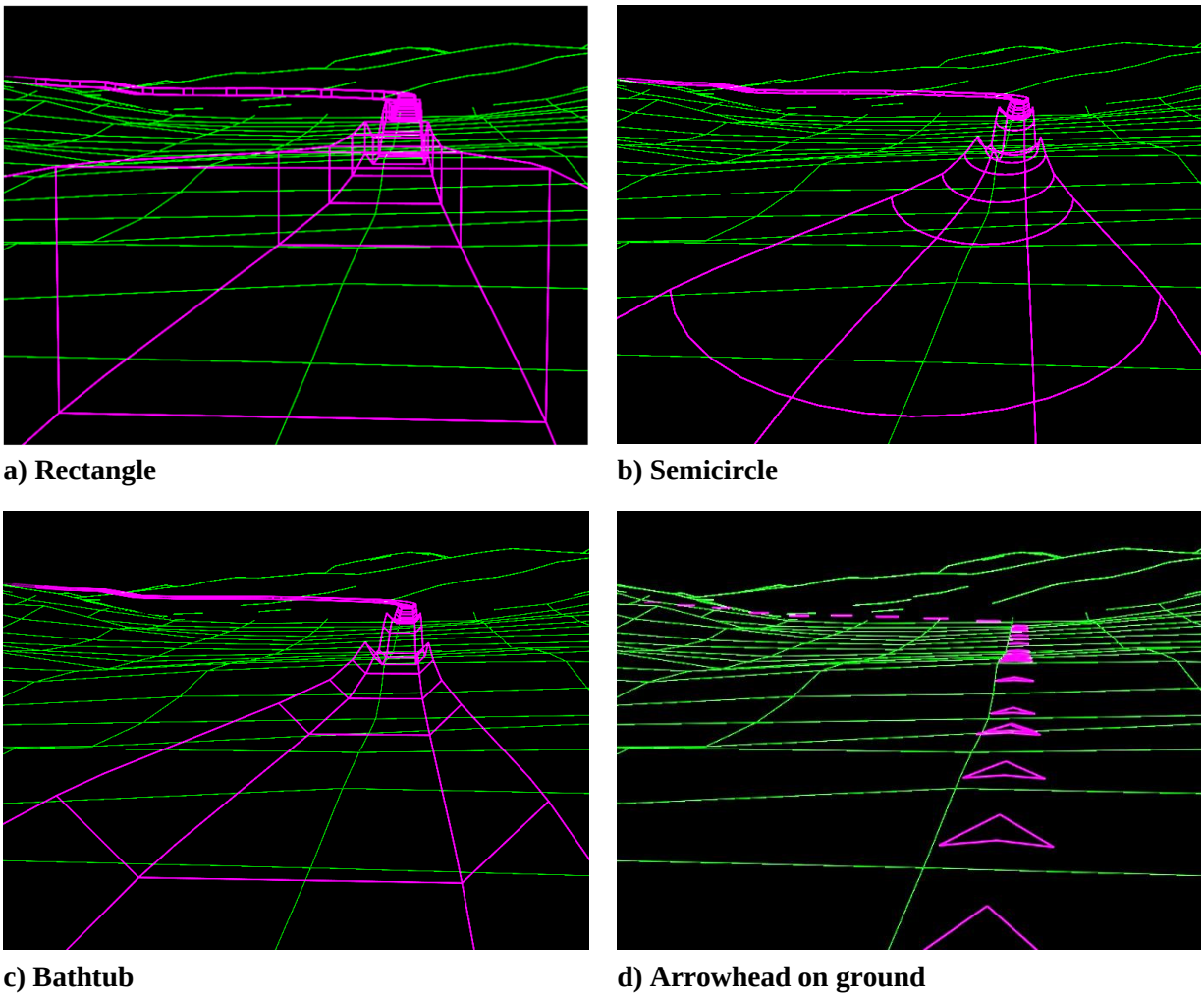

a) Rectangle **b) Semicircle**

c) Bathtub **d) Arrowhead on ground**

Figure 3-4: Examples of 3D-conformal pathways for navigation

Figure 3-4 b) and c) show different designs of a reduced highway-in-the-sky concept providing horizontal and vertical guidance. They use a semicircle or a bathtub geometry without a top cover in order to guide the pilot less strictly. The bathtub variant was applied for the approach of the hover task against a wind turbine in the second part of the experiment. Without vertical guidance, it would have been impossible for the pilots to find the wind turbine in DVE. Furthermore, ground visibility was lost due to the relatively high winching area at the wind turbine.

Moreover, the connecting lines between the bathtub frames were removed in some previous designs. In addition, flight state parameter information was displayed directly referenced onto the pathway-elements in order to avoid shifting the attention between the near- and far-domain. The distortion of the scene-linked numerical information and latencies, due to the head-tracking system, can cause difficulties in perception, as has been found by Schmerwitz et al. [152]. Thus, the approach was not included for this work.

3.2.3 3D-Conformal Terrain and Obstacle Visualization

The synthetic reconstruction of the environment aimed to provide collision avoidance information in addition to cues, which generate an optical-flow-field to perceive velocity, altitude and spatial orientation. Corwin et al. [39] investigated quite a lot of different synthetic terrain representations, including expansion gradient lines, points, ridgelines, meshes, rectangular tiles and turning orthogonal lines, with the regular grid and contour lines being the most promising solutions. The regular grid (Figure 3-5 left) provides depth cues of splay (linear perspective) and compression. The drawback of this approach is the high density of lines at farther distances, especially in flat terrain. This effect adversely contributes to the occlusion of the remaining background. The contour lines (Figure 3-5 right) are less prone to this effect. The static image with contour lines is more difficult to interpret, but when dynamic motion is present, the edge rate contributes to velocity and altitude perception, just as with the grid representation.

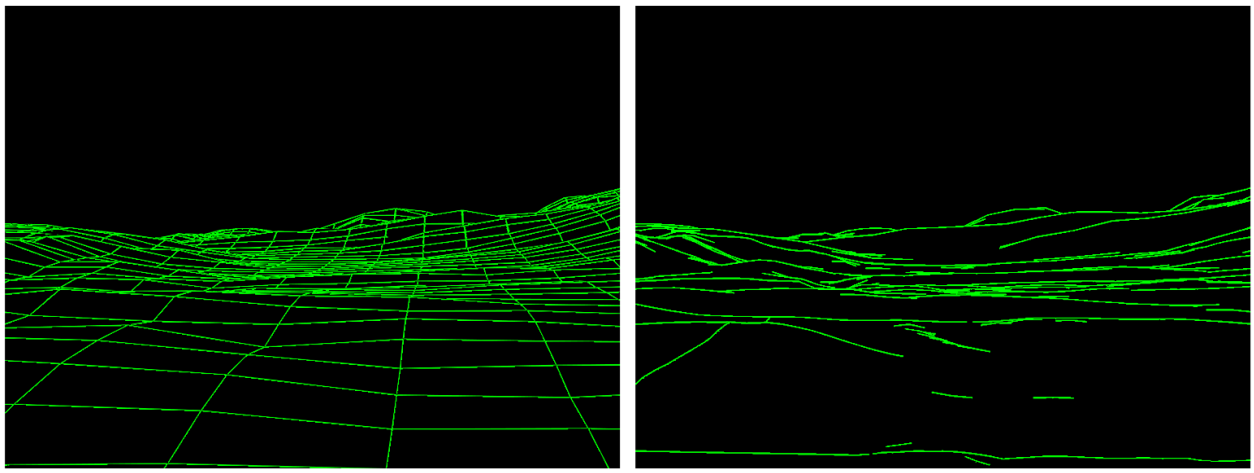

Figure 3-5: Terrain visualization, left) regular grid and right) contour lines

The advanced display concept combined both approaches in order to benefit from the advantages and to avoid the drawbacks. Thus, the regular grid was used in the foreground, while the contour lines were used in the background, as shown in Figure 3-2.

Additionally, a few implementation issues must be considered. According to the depth cue principle of occlusion, hidden lines by the surface must be removed. This can be accomplished by drawing the terrain elevation as a black surface just before the lines are added (Hidden Surface Removal [39]). The second issue concerns the resolution of the elevation data and the resolution of the mesh representation. For instance, the applied grid resolution in this experiment was set to 100 m for the low-altitude flight task. If the highest resolution in elevation data of 1 m would be applied with the lines following the terrain surface, a bumpy representation would be the result, which diminishes the effect of the aforementioned linear depth cues, see Figure 3-6. Whilst it looks regular over flat surfaces, it gets more and more bumpy over rough and hilly ground. In contrast, maintaining the regularity of the mesh results in a reduced resolution of the terrain elevation.

In order to retain the beneficial effect of the depth cues with the regular grid, the consequences of losing resolution were accepted for this concept. When the highest points in the elevation data are used for generating the mesh, a certain safety margin is then artificially added. To account for the

highest resolution during the landing, additional high-resolution grids were added at the landing zone area, as mentioned already in chapter 2.1.3.

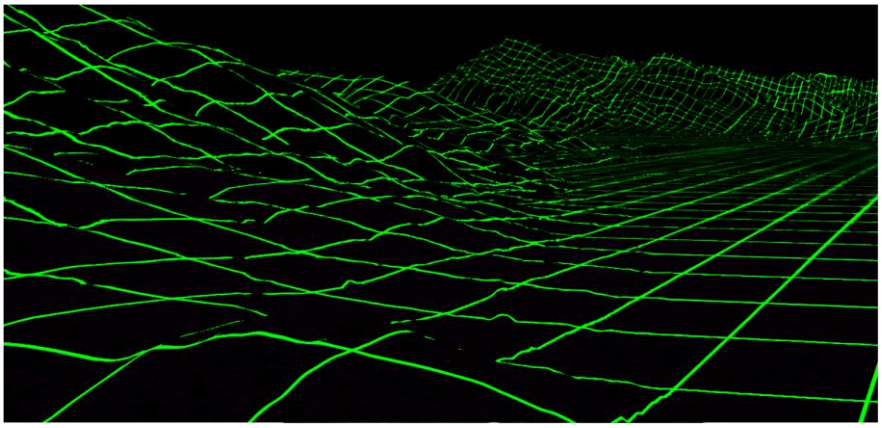

Figure 3-6: Terrain representation with a 100 m grid and a 1 m resolution in elevation

Obstacle representation was divided into two general categories, either from the database or detected by a range sensor. Database obstacles considered in this work were buildings with LOD2, including architectural geometries. A wireframe was implemented to include all details of the buildings with relatively low occlusion (Figure 3-7 right). The hidden lines of the buildings and the terrain surface must be removed in this case also in order to comply with the principles of depth perception and to reduce visual clutter [131].

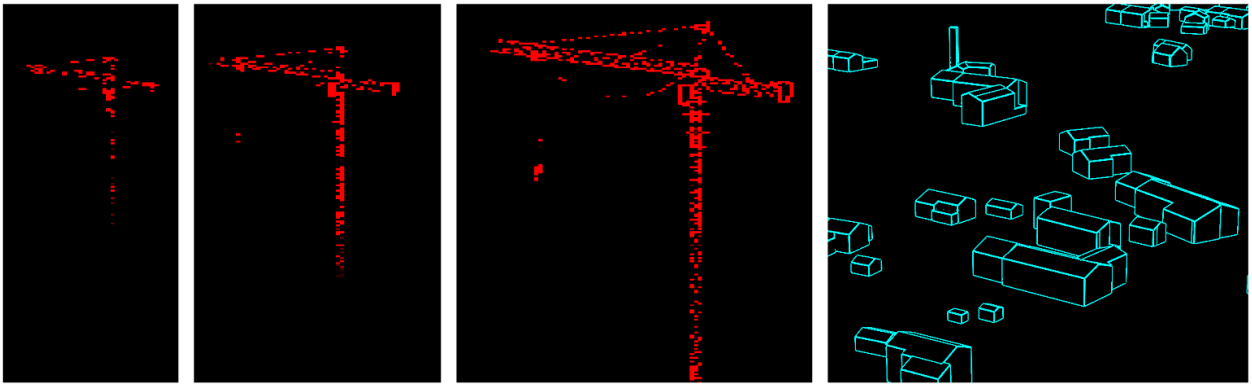

Figure 3-7: Obstacle visualization of sensory and database information
left) point cloud imagery at varying distances, right) wireframe of LOD2 buildings

The second obstacle category represented the sensory information, which contains a 3D-point cloud in the case of a range measuring sensor. The point cloud data can be filtered with classified obstacle and terrain information from databases as demonstrated by Eisenkeil et al. [49]. This approach enables a separate visualization of the remaining unclassified range measurement points for a better differentiation from classified obstacles and from the terrain. For this work, the visual result only was modeled, but not the whole physical behavior of the sensor. However, the modeling was conform to the physical behavior by using the depth buffer of the rendered obstacles, which represents a range map of the obstacle content. A Sobel edge detection filter was applied in order to determine the contours of the obstacles. The Sobel operator approximates the gradient of the image intensity at each pixel [198]. In addition, the resolution of the depth map was reduced in order to simulate the lower resolution of the range sensor compared to the resolution of the HMD.

The left three images shown in Figure 3-7 demonstrate the results of the sensor simulation at varying distances of 425 m, 300 m and 175 m respectively from left to right. At large distances, the pilot could detect an obstacle, but the classification was nearly impossible. Coming closer allowed further identification of the construction crane by providing additional information to the pilot, which enabled, for example, the detection of the hook and the cables. For a further reduction of the occlusion, a second display variant of these sensor detected obstacles was applied, which has just used a rectangular bounding box with a wireframe visualization around the objects. All obstacles appeared at 1.500 m of visual range to simulate the range measurement limit of the sensor. Moreover, detailed obstacle information at farther distances was not required by the pilot and would only contribute to visual clutter. FOV limitations of the sensor or latencies from an alternative moving sensor platform have not been considered in the experiment so far.

The 3D-conformal display content was implemented using the open source libraries of OpenSceneGraph (OSG). The approach of using scene graphs enabled a rapid implementation and adaptation of terrain and obstacles visualization concepts for testing different prototypes early in the development process. More details about the possibilities and limitations with the scene graph implementation can be found by Peinecke [134].

3.2.4 Applied Design Principles

A reduced perception of visual clutter was achieved by applying several design principles as described in the concept above or in the theoretical framework (chapter 2.2.3.1). This subchapter recapitulates the display design properties and links them to the theoretical ideas behind the concept.

3.2.4.1 Color Coding

Different frames of reference were applied, in fact, head-fixed, aircraft-fixed and geospatial referenced, in order to minimize the required attention shift for information capturing. This approach has been supported by using different colors in order to structure and to separate the different display elements. Therefore, the visualization concept contained four elementary colors to aid in decluttering the large amount of information available, i.e. the complementary colors of magenta / green and cyan / red. They were assigned as follows:

- Magenta: All synthetic guidance and navigation symbols
- Green: Terrain visualization
- Cyan: Known obstacles from database
- Red: Unclassified obstacles from sensor information

With the applied colors, it was easier for the pilot to distinguish between the head-fixed primary rotorcraft information and the terrain lines. Furthermore, the flight path markers could be discerned from the ground surface. Unclassified obstacles were considered as most hazardous and thus were colored in red, while the database obstacles were treated similar to the terrain database with less saliency between cyan and green.

3.2.4.2 Principles of Depth Perception

In addition, several depth cues were provided by the 3D-conformal content, for instance, linear perspective and texture gradient with the regular terrain grid, relative size and density through the obstacles and occlusion by removing not visible lines of the terrain and building visualization. Moreover, the effect of motion parallax was also present, as long as the rotorcraft was moving with a certain velocity in low altitude. Thus, for the low-altitude flight task this depth cue was automatically available, but for the hover task, other means were required, see chapter 3.4.

3.2.4.3 Concept of Information Blending

Occlusion is one of the most important depth cues in a see-through display, since it has to be considered twice, once within the displayed content and secondly for the interaction with the real-world background. In order to avoid confusions of the pilot between these considerations, the synthetic image and the real-world image, all synthetic lines hidden by real obstacles must be culled according to the principle of occlusion to maintain a correct depth perception. This approach was introduced by Muensterer et al. [121] for culling the terrain representation in the near-field and was adapted for this work in order to consider the obstacles as well. Thus, the region around each obstacle must be rendered black to achieve this effect. Figure 3-8 shows the effect of culling or blending out near-field information from the synthetic display to achieve that the pilot clearly recognizes obstacles as early as possible in the remaining real-world environment.

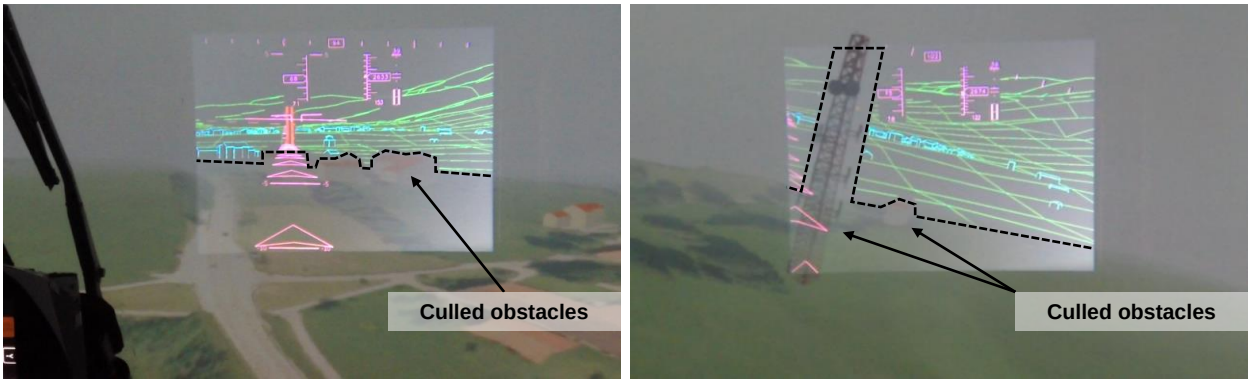

Figure 3-8: Culling of the near-field terrain and obstacle visualization

Without removing those active illuminated pixels, the green terrain lines would continue through the cell tower presented on the right image of Figure 3-8. These lines would then occlude the cell tower, leading to a wrong depth perception. Furthermore, the obstacle visualization was removed at closer distances together with the terrain lines in order to avoid confusion, caused by two different information sources, the synthetic and real-world image. With this information blending principle applied, obstacles were indirectly highlighted without drawing any active illuminated pixels. Information was only presented at regions, where no usable cues were available because of the degraded visibility conditions. However, as mentioned in the theoretical background chapter before, this approach requires information about the visual range or a manual setting by the pilot in order to adjust for the amount of information blended out. Since the effect of occlusion has such an important impact on depth perception, the display concept has been further analyzed according to the amount of active illuminated pixels in the next section.

3.3 Analyzing the Active Illuminated Pixel Ratio

The display design described above already included different variants of terrain-surface and obstacle visualizations. The design has been iteratively improved by the results of analyzing the active illuminated pixel ratio. All terrain and obstacle display variants result in a different amount of active illuminated pixels, depending on the dynamic head motion and thus line-of-sight or the distance to the ground and to the obstacles. The aim was to reduce the occlusion of the outside world view and thus the amount of active drawn pixels in order to declutter the display. The method of Kaber et al. [83] and Kim et al. [86] to determine the ratio of active pixels in static and dynamic images of different head-up display configurations has been improved in this work using a novel implementation to measure the ratio of active pixels in real-time. Hence, the amount of occlusion by the displayed content was directly available in the application to be used for active adjustments of the visualization, in addition to evaluations of the display design. The challenge in this context was the time demanding pixel analyzing process. Even with a moderate resolution of the applied HMD of 800 x 600 pixels and a framerate of 60 Hz, 28.8 million pixels must be processed per second. To achieve this in real-time, an OpenGL (Open Graphics Library) Shader has been implemented for the HMD render application to determine the ratio between the colored pixels and the total amount of display pixels in real-time. With a fragment shader (pixel shader) each pixel can be analyzed directly in the OpenGL rendering pipeline and does not require a complete new post-process. Only basic operations (atomic counters) were used to determine the number of magenta, green, cyan and red pixels. With the applied color-coding in the display design concept, each color can be directly linked to the corresponding content. The concept of information blending resulted in different brightness levels at some display regions. Thus, only pixels above a minimum threshold were counted in order to distinguish them from black rendered pixels.

3.3.1 Active Pixel Ratio Comparison

Figure 3-9 shows four examples of the active illuminated pixel ratios, recorded over a period of 180 seconds for the same flight scenario with different visual ranges respectively. The flight guidance symbology in magenta maintained a very constant level, because mainly the navigation path arrows and the rotorcraft-fixed attitude indicator have changed over time. A similar and nearly constant low amount of active drawn pixels was determined for the building representation from the database in cyan, since an area of medium population density was simulated. The major contribution to the total active pixel ratio occurred from the terrain visualization. Higher occlusion values arose temporarily only by the imagery visualization of the obstacles applied for this scenario, when approaching them very close at lower visual ranges, see Figure 3-9 a) with peak values above 6 %. The active pixel ratios of the green terrain and red obstacle representation decreased with higher visual ranges, because of the near-field fading applied. Even though, the display design (Figure 3-2) seems to have a high degree of active pixels, the mean value of occlusion remained below 4 %, with peaks lower than 12 %. Moreover, these values appear even smaller if the total human FOV is regarded. The limited FOV of the applied HMD of 23 x 17 degrees covers only less than 2 % of the human FOV of about 200 x 120 degrees [24]. However, it must be noted that the display covers mainly the foveal view and partially the near-peripheral FOV and thus the most important part of the human vision system.

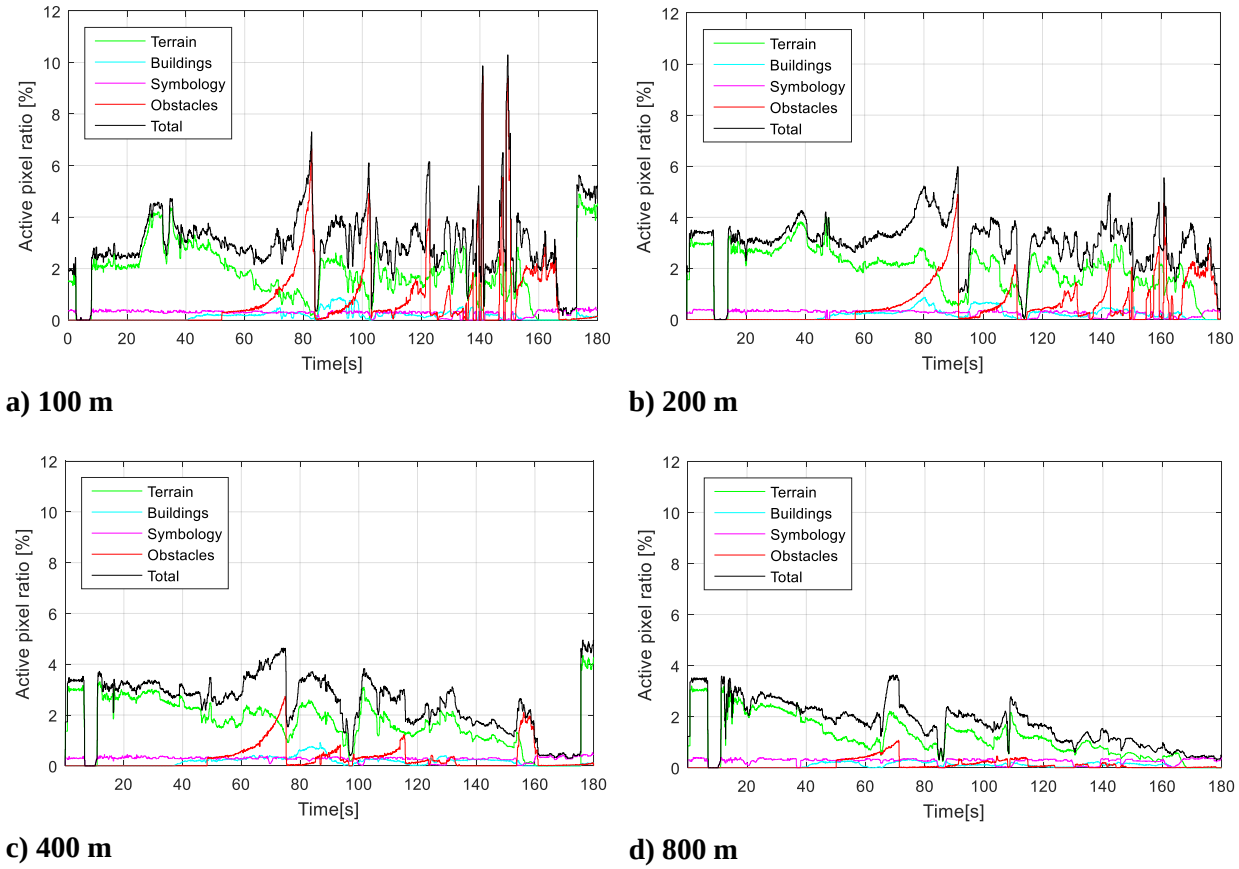

Figure 3-9: Active illuminated pixel ratio depending on visual range

With the real-time measurements of the active pixel ratio, different terrain and obstacle visualization variants can be compared by considering their contribution to the overall occlusion. Figure 3-10 indicates the mean active pixel ratios over an equal period of time subdivided into the four color-coded information groups for different visual ranges and for two different terrain representations, in fact, contour lines (cl) and a regular grid (rg). Although the differences were small, the contour lines (left bars with blue border) required less active pixels, compared to the regular terrain grid with 100 m mesh size (right bars with orange border). The overall percentage value decreased with increasing visibility for both configurations, as expected, due to the applied near-field culling. The flight dynamics and head-motion data were reused from a recorded flight simulation in order to ensure equal conditions for the comparison with regard on the viewing direction and thus visual content.

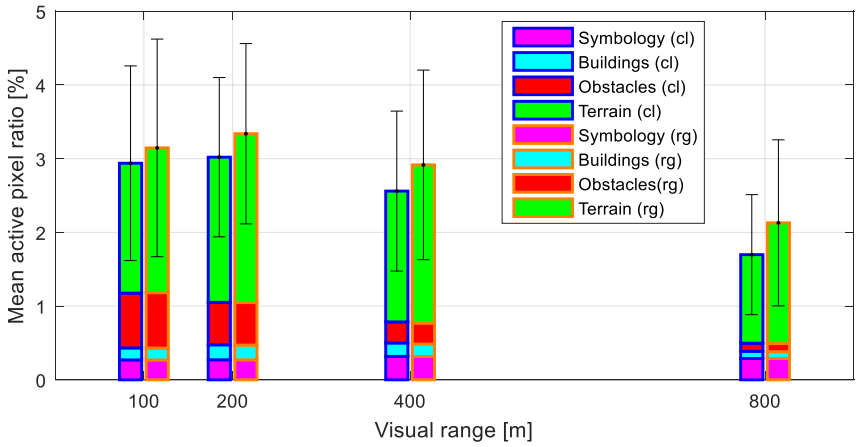

Figure 3-10: Mean active pixel ratio depending on the visual range and the terrain representation with contour lines (cl) and regular grid (rg)

3.3.2 Active Pixel Ratio Utilization

The information about the active illuminated pixel ratio can be used at several different levels in order to reduce visual clutter [183] in future developments:

1) **Engineering tool:** As a mean for engineers to gain knowledge by determining the sources of occlusion and to derive improved concepts.
2) **Development of guidelines:** Definition of desired and adequate threshold values for the maximum occlusion in 3D-conformal display designs.
3) **Adaptive information control:** Using the real-time information for automatic adjustments.

For engineers, the knowledge about the sources contributing to the occlusion can be very useful for deriving improved display designs. For this work, as a result from the active pixel ratio measurements above, the two terrain concepts were combined in order to benefit from the advantages of both, the depth cues from the regular grid and the lower occlusion of the contour lines. In addition, the increase of the mean active pixel ratio of the obstacle visualization at lower visual ranges (Figure 3-10) could be reduced. Similarly, a combination of the imagery visualization of the point cloud data of the sensor and a bounding box representation, which uses only a wireframe, was applied. The analysis of the data showed, that the increase of active pixels resulted from the peaks with the imagery visualization at closer distances to the obstacles, see Figure 3-9 a) and b). Due to the high saliency with the red color, the attention of the pilot was focused on those obstacles during the avoidance maneuver. Changing the visualization from the imagery visualization to the wireframe depiction at closer distances mitigated this effect. Figure 3-11 shows the differences in the contribution to the active pixel ratio between the three variants, in fact, imagery visualization, wireframe and a combination of both. With a smooth transition between the two variants, the peaks at 100 m and 200 m of visual range could be mitigated, while the pilot could still benefit from the imagery cues at farther distances. The imagery visualization was assumed to provide more overall situational awareness by enabling the pilot to identify the obstacles, in addition to the localization.

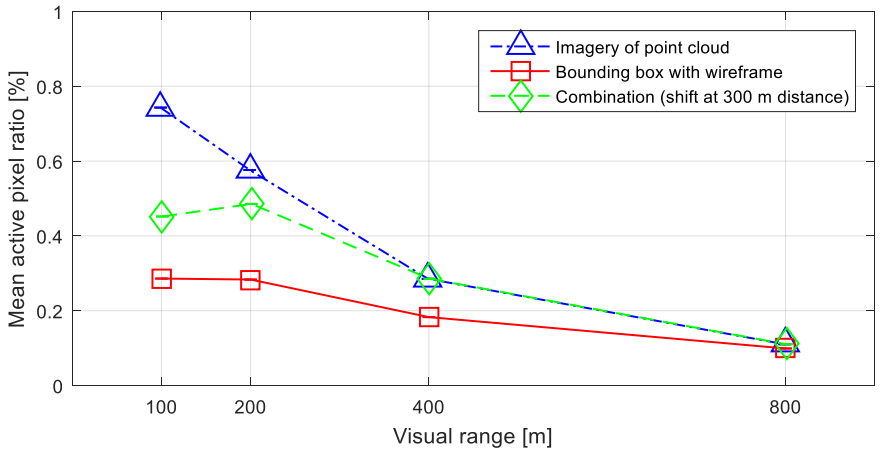

Figure 3-11: Mean active pixel ratio – part of the unclassified obstacle representation

Although, the development of guidelines and the adaptive information control require more data analysis and further evaluations before they can be applied, they might be very interesting in reducing visual clutter. The active pixel ratio information available in real-time could be used in order to dynamically change the level of automation and to relieve the pilot in adjusting the displayed content, e.g. for controlling the near-field culling. Moreover, in conjunction with the adaptive automation concepts of Melzer [117], the amount of occlusion could be controlled by real-time psycho-physiological measures, which are able to determine the state and the workload of the pilot.

3.4 Precision Hover Display Concept

In contrast to the obstacle avoidance display specified before, the hover display required completely different visual cues. Stabilization and precise positioning became more important, while the pilot still needed to look out for approaching obstacles in DVE. Compared to the landing zone solutions from previous work, this concept concentrated only on the hover task, for instance, to precisely maintain position and to minimize drift velocities. Even though, some of the implemented elements may also assist in landing, the transition to hover has not been considered yet. This section begins with the explanation of the hover mission task element of the ADS-33E-PRF as a basis for the derivation of the HMD reference cues. Afterwards, the 3D-conformal concept and the 2D-extension are specified.

3.4.1 ADS-33E-PRF Hover Mission Task Element

In general, the mission task elements (MTE) of the ADS-33E-PRF were developed for evaluating the rotorcraft handling qualities through precisely defined flight test maneuvers. These maneuver tasks have been successfully applied in real flights as well as in simulation experiments. In this work, the suggested reference elements for the hover task were converted into a synthetic and symbolic design for usage on the HMD. Basically, the hover course consists of hover boards at 150 feet distance to the hover point. Furthermore, at the half distance to the hover board, a reference symbol is placed in order to allow the pilot to generate a line-of-sight relationship, see

Figure 3-12. Thus, the pilot observes the reference sphere moving within the rectangles on the hover board, which indicate the desired and adequate performance ranges.

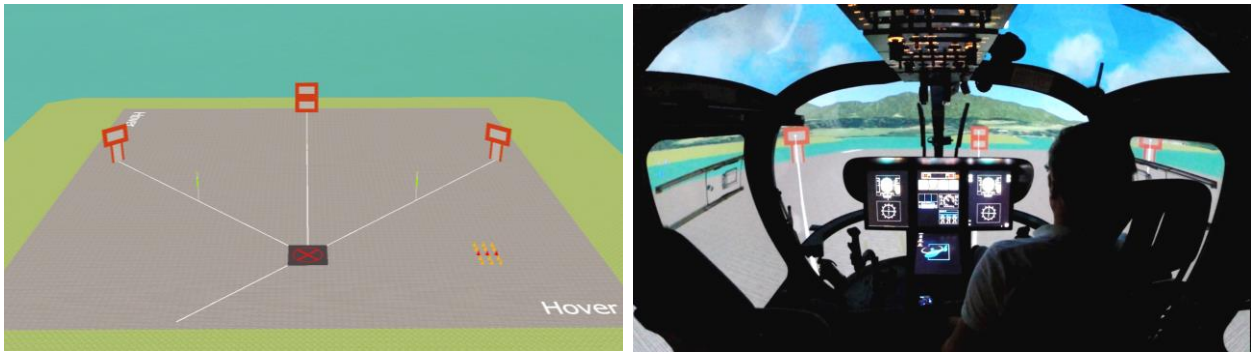

Figure 3-12: Hover Mission Task Element of ADS-33E-PRF

The hover boards provide similar static references as the 3D-conformal towers or cones in the landing zone concepts (chapter 2.1.3.2), but with the line-of-sight relationship, they provide additional cues for a precise hovering. It was hypothesized that the hover MTE reference cues provide suitable macro-textures for a precise hover maneuver without micro-textures and with a limited FOV available by the HMD.

3.4.2 3D-Conformal Concept for Hover

Figure 3-13 shows the synthetic cues converted from the hover MTE together with the line-of-sight relationship from the virtual eye-point over the reference symbols to the hover boards. The small spheres, usually mounted on a pole, were placed onto a line for a simple representation. In addition, a high resolution grid was placed over the obstacles and the ground in order to indicate the slope and the obstacles around the hover position. Small cones were placed at a segment of the circle around the hover boards at five degree intervals for providing sufficient heading references.

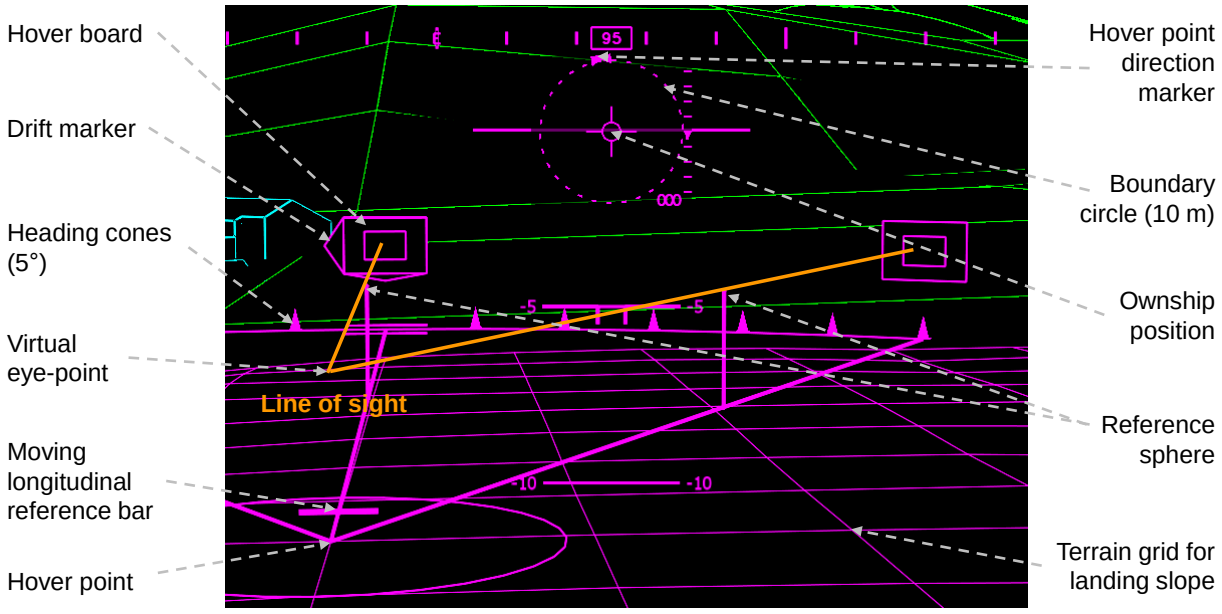

Figure 3-13: Precision Hover Symbology (PHS) display concept

According to the proposed hover MTE of the ADS-33E-PRF, the line-of-sight relationship is not horizontally aligned, instead it is slanted downwards in order to allow a perception of the vertical

plus the longitudinal positioning. Without sufficient micro-textures available, it was not possible to distinguish between those two drift directions, e.g. upward and forward. Thus, additional hover boards were placed to the left and right at 30 degrees. Pilots can use these additional hover boards in order to cross-check whether they are in a correct longitudinal position or not. Such a cross-check requires large head-movements, which can lead to more drift. A longitudinal reference bar was included in order to provide the required cues without the need to move the head. This reference bar was fixed to the rotorcraft and moved forward until it reached the segment of the hover board circle, which then indicated the correct longitudinal position. The hover board itself provided only lateral and vertical reference cues.

Regardless of which 3D-conformal reference elements are used within the small FOV of the HMD in the forward direction, they raise the potential problem of differentially perceived sensitivity between the longitudinal and transverse axes [25]. Thus, synthetic display gains were identified and applied by Bachelder [24] in order to enhance the perception of the longitudinal position error. Even though, an optimal gain set appears to exist, it should depend on the rotorcraft dynamics, the task demands and the flight environment [25]. In order to avoid this dependency, reference cues were sought for this work, which are independent of those factors. Figure 3-13 shows the 2D-extension added therefore, indicating the horizontal position with a co-planar representation of a birds-eye-view. It indicated the own position relative to the hover target position.

In addition, drift velocities were indicated by swelling triangles attached to the hover boards. Since the optical flow field disappears nearly completely in a precise hover maneuver, the pilot requires additional information in order to predict the future dynamics of the helicopter including disturbances. For large transport helicopters, acceleration cues were usually provided (Figure 2-22) in order to compensate the drift before it even occurs. The acceleration cues for small helicopters can be very shaky, due to the lower mass inertia. Thus, the velocity has been indicated directly in order to indicate the drift in a smooth way. The swelling triangles showed the actual direction of the drift velocity of the helicopter and not a command value for drift compensation in the opposite direction. The latter can lead to misinterpretations depending on the current position.

3.4.3 2D Extension for Horizontal Positioning

To solve the problem of indicating the longitudinal position error with the constraint of having a very limited FOV when using the HMD, a co-planar two dimensional view from above was added. The 2D-hover display contained the own position of the helicopter, a dashed circle indicating the area around the helicopter with a radius of 10 m and the target hover position moving relatively to the own position. Figure 3-14 demonstrates different states of the display concept. At farther distances, e.g. during the approach, only a marker was shown at the boundary circle, indicating the direction of the desired hover position only, but no distance yet. The target hover position symbol, consisting of a dashed cross with the character “H” in the middle, was scaled according to the relative height of the helicopter in comparison to the target height. Thus, the symbol appeared smaller at higher positions and larger at lower positions, as it would appear when looking downwards. At the accurate position, the aircraft symbol and the hover point symbol coincided.

The airspeed and the barometric altitude were removed in the head-fixed view, since they do not provide useful information for the hover task. The radar altitude and a vertical speed bar with a higher sensitivity compared to the normal flight were retained. The location was maintained at the upper part of the display in order to enable the perception of both, the 3D-conformal cues and the 2D view from above, without the need of extensive eye movements.

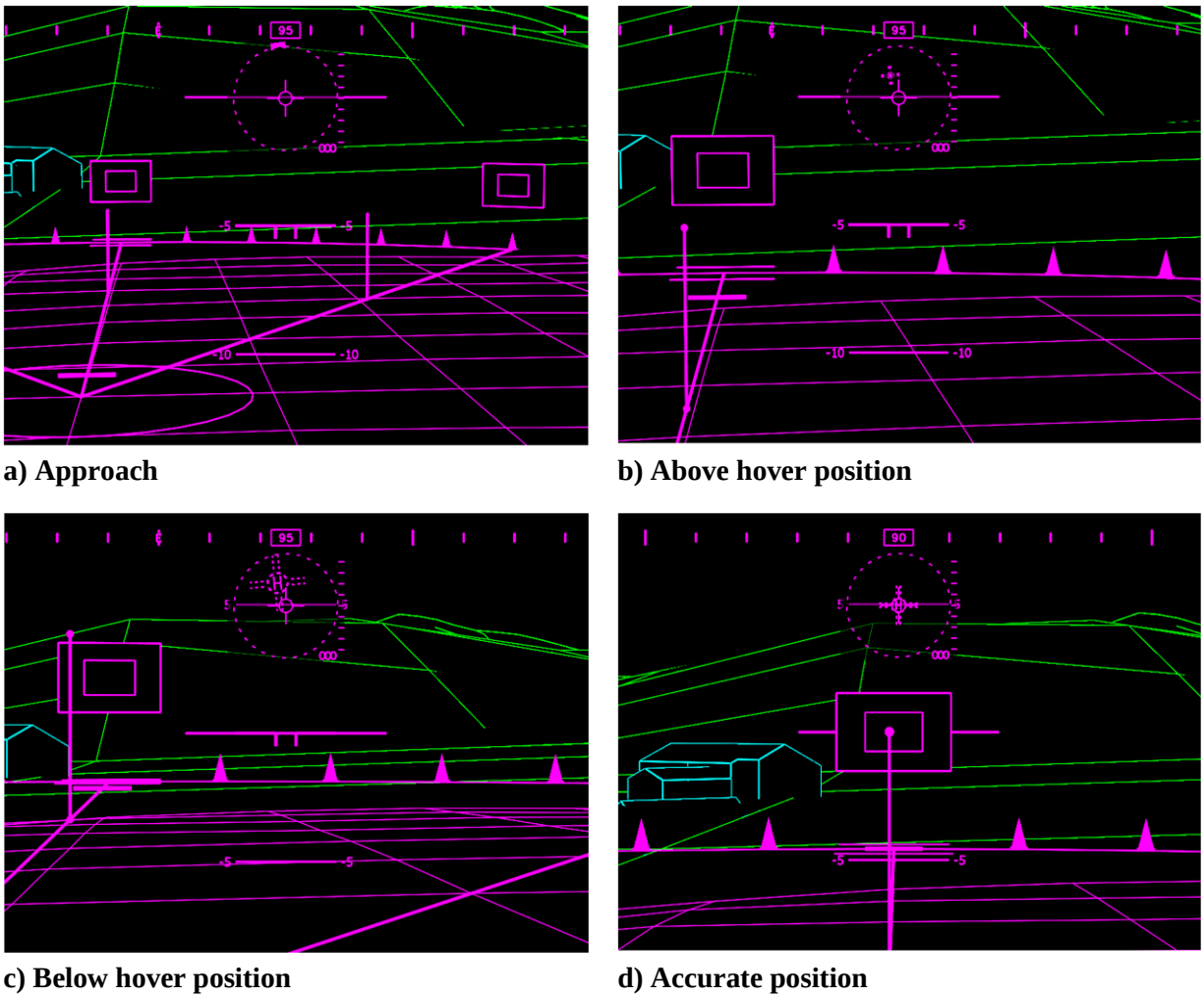

a) Approach **b) Above hover position**

c) Below hover position **d) Accurate position**

Figure 3-14: PHS concept with different viewing positions

3.5 Summary and Discussion

This work allows an in-depth evaluation of 3D-conformal display content because two completely different tasks were selected. While the sense and avoid display concept addresses the low-altitude flight with hazardous obstacles, the hover display shall enable precise hovering without further control augmentation in DVE. The 3D-conformal content can partially replace the lost cues from the surrounding environment and it is possible to add further obstacles as well as stabilization and navigation cues. However, both display concepts are not completely 3D-conformal and they contain additional two dimensional parts for meaningful extensions. In the development process, several design principles according to the visual perception theories have been considered and transferred into the design, for instance, depth cues, frames of reference, color-coding and information blending. Furthermore, the analyzing technique of the active illuminated pixels was

advanced, in order to determine the amount of occlusion of the real-world by the synthetic cues. Easy accessible information about the active pixel ratio has already allowed significant improvements to the display design. It further enables future advancements and comparisons of other display designs with regard to the amount of occlusion. Even adaptive automatic control of the displayed content is conceivably with the data available in real-time. The developed display designs may look overloaded, but with the decluttering design principles considered, they have the potential to reduce the workload of the pilot. Moreover, they include a high degree of 3D-conformal content for the desired evaluation in this work, which is further depicted in the next chapters.

4 Design of the Pilot-In-The-Loop Simulation Experiment

To evaluate these highly sophisticated human-machine interface concepts developed in chapter 3, piloted flight simulation trials have been conducted with the Rotorcraft Simulation Environment (ROSIE) at the Institute of Helicopter Technology. This chapter describes the entire experiment, including the hardware facilities. It starts with an explanation of the basic simulator characteristics, followed by modifications and extensions for an enhanced simulation of the 3D-conformal HMD content, which have been developed especially for this work with the aim to enhance simulation fidelity. With the dynamic eye-point implementation for the image generator of the outside visual cues, the registration error of the synthetic HMD image against the dome projection system has been minimized. These errors are induced by simulators and are not present in the real world application. Therefore, they could distort the result of the laboratory experiment adversely without compensation. After a discussion on the hardware performance, the methodology of this experiment is explained with the description of the experimental procedure, containing the selection of the participating pilots, the task sequences and the ratings conducted by the participating pilot. Finally, the training tasks and more importantly, the developed scenario designs for the two display concepts together with the main hypotheses are described.

In general, compared to training simulators, flight simulators being used for research are often not certified according to the specification (‘CS-FSTD (H)’ [6]) of regulation authorities. Thus simulation fidelity varies greatly between different studies at different facilities. Thus, a detailed description of the applied flight simulation environment is essential for comparison of similar experiments.

4.1 Rotorcraft Simulation Environment

The Rotorcraft Simulation Environment is a fixed-base simulator with a six channel dome projection system and a high level of flexibility for research purposes [182]. Figure 4-1 shows the MBB Bo105 cockpit applied for this experiment together with the visual projection system. The simulation environment can be structured into three main parts:

- The rotorcraft flight dynamics and simulation control
- The image generator with the six channel projection system for the outside visual cues
- The cockpit environment with the human-machine interaction systems

These subsystems provide the basic functionality for simulating helicopter flights in degraded visual conditions in a safe laboratory environment and thus are described in more detail within the next subsection.

Figure 4-1: Rotorcraft Simulation Environment (Side View)

4.1.1 Main System Description of ROSIE

The core simulation software consists of a Matlab/Simulink development environment, which handles all data input/output of the cockpit and the image generator. Moreover, it serves as a data concentrator unit and enables the data recording with a high sampling rate (100 Hz). The flight dynamics model GENSIM [81] is integrated as external S-function block into the Simulink model. For the simulation experiment, the in-flight validated dynamics model of a H135 of Airbus Helicopters is simulated. Characteristic rotorcraft phenomena, e.g. ground effect and pitch up responses at higher velocities are considered. All environmental conditions, e.g. positioning of the rotorcraft in the world and weather settings, can be controlled within this Simulink environment as well as the initial rotorcraft state parameters, like take-off weight and center of gravity.

The six channel projection system for the outside visual cues provides a large horizontal field-of-view of 200 degrees and vertically -50/+30 degrees. Especially the field-of-view downwards is very important when simulating visual ranges below 800 m to ensure enough ground visibility. Therefore, the cueing system matches perfectly the needs of the simulation experiment. Each projector has a resolution of 1920 pixels x 1200 pixels, which provides a resolution of about three minutes of arc per pixel depending on the field-of-view of each individual projector. For the distortion correction and the blending of the single projector images to one homogeneous image, an auto-calibration system with two cameras and LED-markers embedded in the screen is installed. The image generator software is also based on OpenSceneGraph (OSG) using the high resolution elevation data and aerial images described already in chapter 2.1.2.1. The Common Image Generator Interface (CIGI) is used for communication with the Simulink environment and the synchronization of all channels is achieved with a software solution developed at the Institute. Weather animation, e.g. clouds, rain, night and day conditions are realized by commercial software libraries for OSG. To ensure equal visibility conditions for all participating pilots, fog was applied to simulate the degraded visual environment.

The MBB Bo105 cockpit provides a perfect platform to simulate small and medium sized helicopters. The standard analog instruments have been replaced by a generic glass cockpit configuration. Figure 4-2 shows the basic two dimensional head-down instrumentation, which has been implemented with “2Indicate”, a script based tool developed by the German Aerospace Center (DLR). For navigation assistance, a commercial off-the-shelf digital moving map has been installed, which is depicted in Figure 4-3.

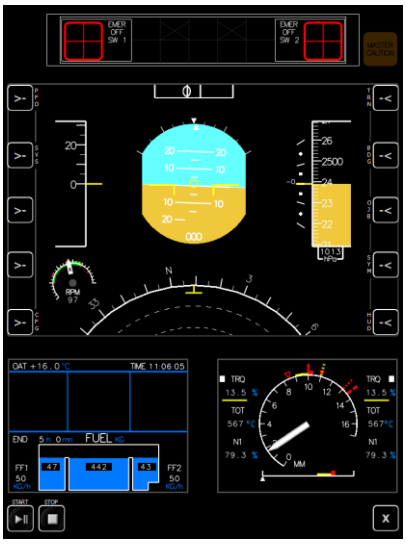

Figure 4-2: Flight instrumentation

Figure 4-3: Digital moving map (Sky-Map)

Figure 4-4: Seat shaker

Even without having a full motion platform, it is possible to provide feedback about the load factor by simulating the vibrations induced by the main rotor. Therefore, a seat shaker has been installed at the rear side of the pilot seat, see Figure 4-4. The system is capable of producing oscillations from 5 Hz to 200 Hz and thus it is perfectly suited to simulate the vibration induced by the rotor harmonics with an amplitude depending on the load factor.

The sound system generated noise from the main rotor through ordinary stereo speakers. Acoustic warnings were intentionally not applied in this experiment, making sure that the results of this work are solely based on the visual information available for the pilot.

The original Bo105 flight control sticks and pedals were retained together with its mechanic artificial force feedback and the cyclic trim actuators to ensure an authentic control feeling. The basic beep-trim functionality with a four-way-switch has been extended by a follow-up trim function, in which the actuators automatically drive the cyclic stick to the current trim position as long as the pilot pushes the follow-up trim button. The collective lever features a friction brake, which can be adjusted by the pilot individually.

Finally, Figure 4-5 shows the hardware architecture of ROSIE containing the subsystems described above. The “SIM-Host” computes the rotorcraft flight and system dynamics, while the instructor/operator station (IOS) controls the simulation environment. The Image Generator (IG) workstations render the visual scene for the projection system. The basic cockpit configuration contains two workstations (HMI 1 and HMI 2) for the input signal processing and for displaying

the required instrumentation. The system communication is implemented through Ethernet and the User Datagram Protocol (UDP).

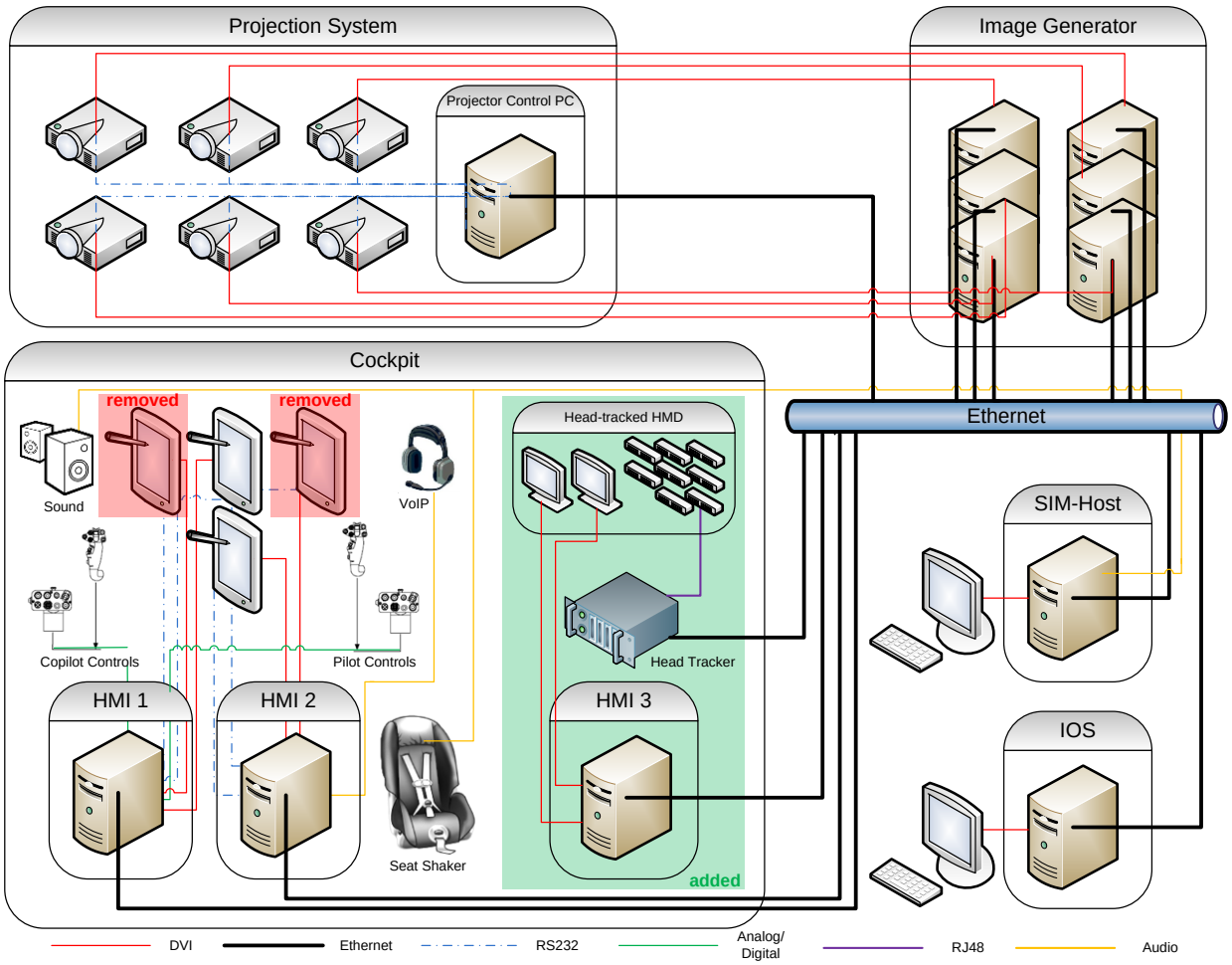

Figure 4-5: Hardware architecture of ROSIE

Additionally, the hardware architecture diagram highlights the extension of ROSIE for this work with a head-mounted display and a head-tracking system operated by a third workstation (HMI 3). It also indicates the modification of the instrumentation concept with only two head-down displays, which is further explained in the following chapter.

4.1.2 System Tailoring of the Cockpit Environment

During most critical flight phases, e.g. low-altitude flight, approach and landing, the pilot requires an unobscured view downwards to detect obstacles and to locate a suitable landing site in unfamiliar terrain. With the 3D-conformal content, the pilot can get the necessary information through the HMD, but current cockpit designs occlude partially the area of interest with large head-down displays, see Figure 4-6. Consequently, the left and right displays have been removed and only the central displays have been retained (Figure 4-7), which show all the necessary information including a moving map for navigation. In order to develop a reliable product, a system safety analysis must be performed, which is worthwhile to be considered in future research. However, this study focuses on the human-machine-interface design and not on the reliability of the displays.

Figure 4-6: Cockpit: 4 display configuration

Figure 4-7: Cockpit: 2 display configuration

The principle of an unobscured head-down view has also been investigated in the aviation research project "HELIcopter Situation Awareness fuer eXtreme Missionsanforderungen (HELI-X)" [94] [145], funded by the German Federal Ministry for Economic Affairs and Energy. In HELI-X a semi-transparent head-down display system has been developed and evaluated. It aimed to enable the capability to see through the important area of interest during critical flight phases, which is usually obscured through conventional head-down displays. The German Aerospace Center further invented the concept of a complete virtual aircraft-fixed cockpit instrumentation [45] [56] [110]. Thereby, traditional head-down instruments, e.g. a primary flight display, a navigation display or even a digital knee-board were implemented on the HMD to be shown in near-field areas, in addition to the far-field 3D-conformal symbology. Thus, conventional head-down displays would be obsolete and they would not obscure important regions in the forward or downward field-of-view. These ideas demonstrate the effort, which has been undertaken to remove conventional head-down displays for operations in DVE. They aim to maintain the information required by the pilot at the same area in the near-field, while using different mediums.

4.1.3 Simulation Fidelity

The rating of the overall simulation fidelity is an additional research topic and goes beyond the requirements specified by the certification authorities (CS-FSTD (H) [6]). Especially for research applications, it is desired to have a high level of simulation fidelity, because this can strongly influence the results of an experiment. Moreover, for a comparison of different experiments conducted at different simulation facilities, it would be of interest to know the rating of the simulation fidelity. Thus, the University of Liverpool has developed a simulation fidelity rating (SFR) scale together with the National Research Council of Canada (NRC) [136] [192] [193], based on the Cooper Harper Handling Qualities Rating Scale [38]. Furthermore, to rate the simulation fidelity, handling qualities of simulations and real flights can be compared with regard to the given task, but this requires tremendous efforts. The Mission Task Elements (MTE) of the Aeronautical Design Standard ADS-33E-PRF [5] can serve as simplified tasks for such ratings [27]. Armstrong analyzed the overall simulation fidelity through an adaptive pilot model and the τ-guidance strategy from the visual flow theory [20]. To gain the subjective impressions of the participating pilots about the simulation fidelity of ROSIE, a few simplified ratings have been added to the general questionnaire at the end of the simulation experiment. The three basic subsystems of ROSIE have been evaluated, i.e. the visual cueing system, the flight dynamics

simulation and the flight control inceptors together with the reduced instrumentation panel concept, see Table 4-1 showing the mean rating score (M) and standard deviations (SD).

Questionnaire item		M (SD)
The outside visual cues were adequate	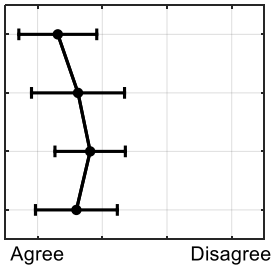	1.3 (0.6)
The flight dynamics simulation was adequate		1.6 (0.7)
The flight controls were adequate (e.g. control forces)		1.8 (0.5)
The cockpit concept with the reduced head-down instrumentation complemented the HMD concept		1.6 (0.6)

Table 4-1: General questions about ROSIE

The rating was based on a four point Likert scale (1: Agree; 2: Rather agree; 3: Rather disagree; 4: Disagree). It can be concluded, that the overall simulation fidelity was accepted to be adequate for the given tasks, especially the visual cueing system being the most important part regarding the coupling of 3D-conformal HMD content. The flight dynamics simulation was also rated appropriate, while the flight controls could benefit from some upgrades, like a full control loading system to optimize the force feedback. A trim-release function was also missing, which could have influenced the rating. However, no pilot had problems with adapting to the flight controls for the given tasks and the performance was rated to be adequate. Moreover, the cockpit concept with the reduced head-down instrumentation received also very positive feedback, even though no direct comparison with a conventional display configuration has been conducted.

4.2 Head-Mounted Display Integration with Dynamic Registration

The used head-mounted display defined some performance limits, for instance the available field-of-view or color. Thus, the physical characteristics are specified and the performance is validated with regard on the tracking accuracy and latencies. Furthermore, the integration of the HMD into the multi-channel dome projection system of ROSIE with a dynamic eye-point in the image generator is explained. This novel approach has been derived from existing implementations of faceted displays [33]. Moreover, it has been compared to an alternative approach [28], which induces artificial errors in the visualization with offset angles added to the line-of-sight in order to compensate for registration errors against the dome projection.

4.2.1 LCD29 HMD and IS900 Head-Tracking System

The applied low-cost LCD29 HMD of Trivisio, see Figure 4-8, is a binocular see-through HMD with modified combiners (30 % reflection / 70 % transmittance). Thus, it provided an improved see-through capability in the simulation environment with a reduced brightness compared to the real world. It consists of two full color liquid crystal displays (LCD), each with a resolution of 800 x 600 pixels and a field-of-view of 23° horizontally and 17° vertically. Two separate DVI input interfaces enable the generation of two different images for a stereoscopic presentation and a dynamic vergence adjustment. The latter was required because of the difference in eye

accommodation distance of the screen with a radius of 2.5 m and the fixed eye accommodation distance of the HMD, which was defined by the manufacturer to 1.58 m. Furthermore, the distance to the screen varies between 2.0 m and 3.0 m, due to the offset of the pilot eye-point with 0.35 m to the right side in the cockpit and the translational and rotational head motion.

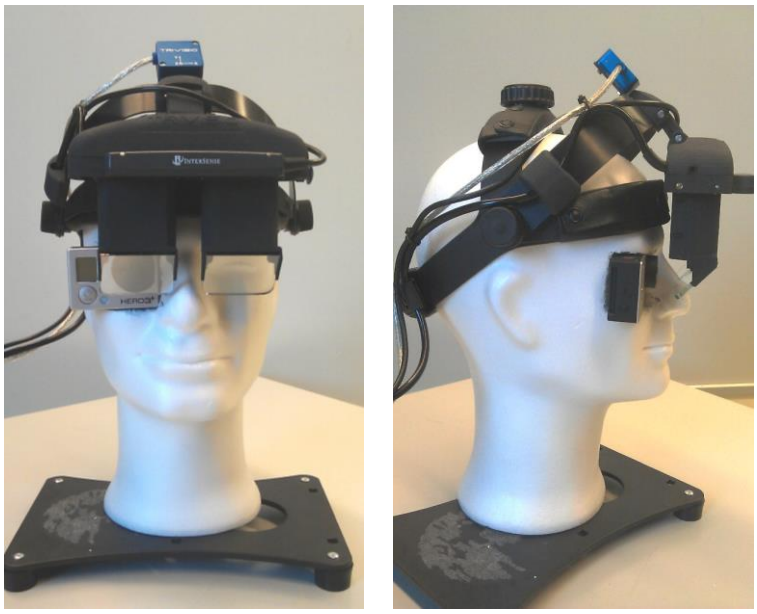

Figure 4-8: LCD29 HMD of Trivisio

The decision to use the LCD29 HMD in this study was further confirmed by the great advantage of the unhindered view sideways and downwards of the combiners. Compared to many other augmented reality devices, the LCD29 HMD enabled an unobstructed view of the head-down instruments and the peripheral field of vision.

The installed InterSense IS900 six degree-of-freedom (DOF) hybrid inertial-ultrasonic head-tracking system has the advantage of being without electromagnetic interferences. It consists of a very fast inertial tracking and ultrasonic sensors. Thus, the drift in acceleration measurements can be compensated by the positioning through the ultrasonic sensors. This results in an update frequency of 180 Hz. Jitter and latencies are further reduced through factory in-built Kalman Filters. The static accuracy, according to the data sheet, can reach 2.0 – 3.0 mm translational with a resolution of 0.75 mm and a rotational accuracy of 0.25° in pitch and roll as well as 0.5° in yaw with a resolution of 0.05°. Eight ultrasonic emitters have been installed into the cockpit of ROSIE, which have been exactly surveyed with a total station theodolite to achieve the above listed accuracy in positioning. Two microphones are installed in a small beam together with the inertial sensors, which can be attached to the HMD. The constellation of the eight ultrasonic emitters has been designed to ensure that always sufficient emitters are in the line-of-sight with the head-mounted microphones, while they are not blocked through the flight controls or the instruments. Thus, the whole field-of-view of the outside projection system was covered for the pilot seating area.

4.2.2 Dynamic Registration Against the Multi-Channel Projection System

A collimated projection system is usually preferred in a simulator when using an optical see-through HMD to avoid problems with eye accommodation and convergence. Since collimated visual cueing systems do not provide the required large vertical field-of-view yet, rotorcraft flight simulators are equipped with a dome projected system. Consequently, the light rays are not received by the pilot in parallel. This section briefly summarizes the main findings from the author [181] regarding the eye accommodation, the dynamic vergence and the compensation of motion parallax required to minimize simulation induced optical errors and to improve the fidelity of this experiment. A dynamic eye-point implementation in a multi-channel projection system with a spherical screen to compensate the motion parallax dependent on the head-tracking system has not been published elsewhere before.

4.2.2.1 Eye Accommodation and Dynamic Vergence

Different focal distances of the augmented HMD image and the virtual background projection can lead to a blurred perception of one of the information sources or to perceived ghost images [33]. Ghost or double image perception is a result of an error in vergence, i.e. the angle between both eyes can only be adjusted to one focal plane. A blurred vision is perceived when the monocular eye accommodation cannot be adjusted adequately, because of a too large distance between the two focal planes. Figure 4-9 shows errors in convergence and divergence, due to the varying distance of the viewer to the screen, depending on the head position and viewing direction.

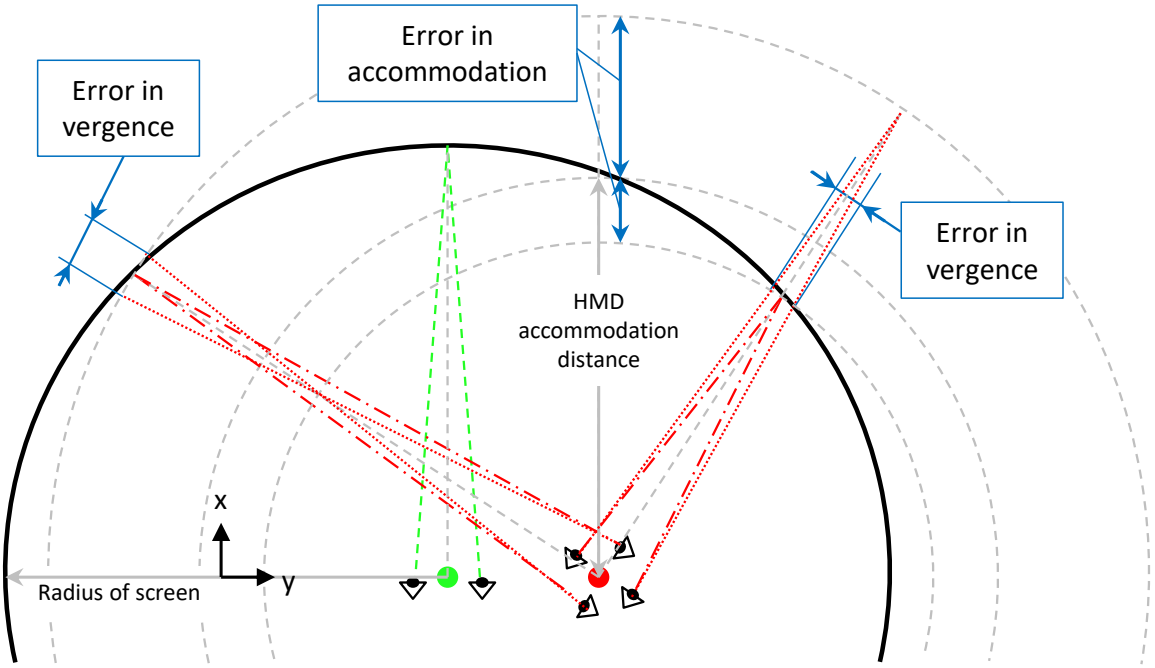

Figure 4-9: Two dimensional example of the mismatch in eye accommodation and binocular vergence of different eye-point positions and viewing directions

While monocular eye accommodation is fixed by the optical lens system, binocular vergence is adjusted through rendering different perspectives for each eye separately to avoid ghost images. The recommended tolerances for the difference in the focal planes of +/- 0.3 D [74] [118] are

maintained with the applied HMD and the screen of ROSIE. The focal deviation would also be in an adequate range of +/- 0.5 D for an HMD with an eye accommodation set to infinity, see Table 4-2.

Accommodation Distance x [m]	**Optical Power P [D]**	**Deviation ΔP [D]** (HMD f = 1.58 m, P = 0.633)	**Deviation ΔP [D]** (HMD f = infinity, P = 0.0)
2.0	0.5	-0.133	0.5
3.0	0.333	-0.3	0.333

Table 4-2: Deviation of optical power for two different HMD accommodation distances

The offset angle for a dynamic compensation of the vergence depending on the screen distance, which is determined by the head-tracking position, can be calculated with Eq. (4-1). The interpupillary distance (IPD) is assumed to be 65 mm for the average male person.

$$offset(x) = \arctan\left(\frac{\frac{IPD}{2}}{x}\right) - arctan\left(\frac{\frac{IPD}{2}}{HMD\ focus}\right) \qquad \textbf{Eq. (4-1)}$$

With a given HMD focus of 1.58 m and a dynamic distance of the eye position to the screen, ranging from x = [2.0 m … 3.0 m], the offset angle to compensate the perspective of each eye varies between 4.3 mrad and 9.7 mrad. Thus, without compensating the vergence error, the maximum tolerances for horizontal binocular alignment of 3 mrad [118] cannot be achieved. Consequently, a dynamic vergence adjustment has been implemented to avoid problems of double images or somatic effects, e.g. eye strain, for the duration of the experiment.

4.2.2.2 Motion Parallax

The depth cue of motion parallax is only present through the "motion" of the helicopter dynamics in flight simulators without collimated projection systems. In highly dynamic maneuvers, additional depth cues through small head movements can be neglected, but in hover state, they might be very valuable. Figure 4-10 demonstrates a static shift of the PEP from the center of the screen to the right of y_{PEP} = 0.35 m. With a screen radius of r_{SCREEN} = 2.5 m, the resulting optical flow field leads to a wrong yaw perception of $\beta = \arctan(y_{PEP} / r_{SCREEN}) \approx 8°$ without adjusting the perspective (frustum) and the distortion of the projection. Furthermore, moving the displays, which are firmly mounted on the head, cause a shift or displacement of the overlaid image onto the outside simulation screen [130]. Although, the head motion around the design eye-point is very limited to approximately +/- 0.15 m, the result is a significant error of up to +/- 3.43° between the IG and the HMD representation of scene-linked obstacles without compensation.

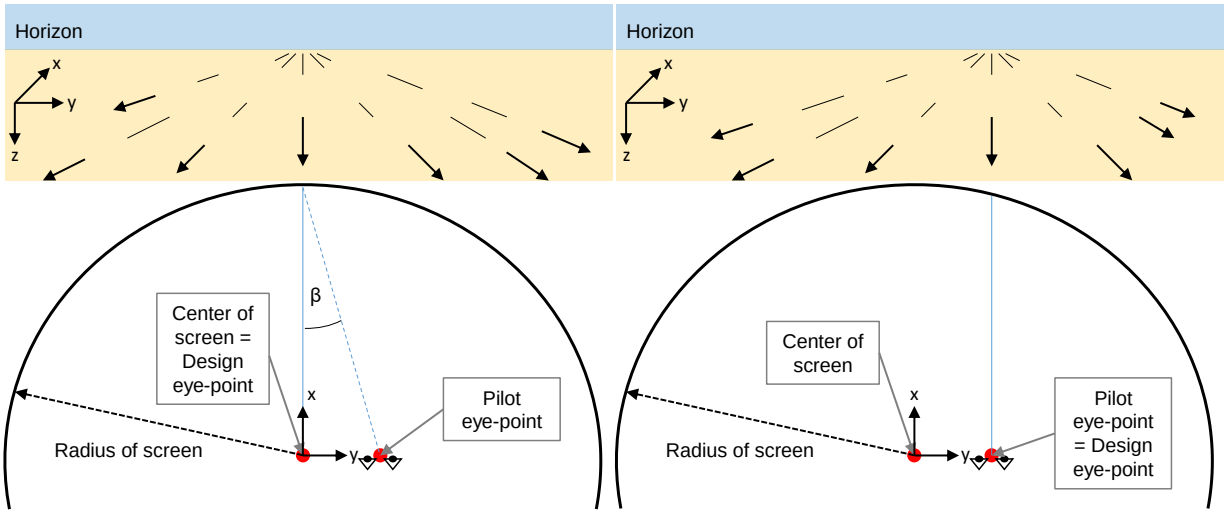

Figure 4-10: Shift of the optical flow field with respect to the design eye-point

The simulation induced errors are one order of magnitude larger than errors, which result from positioning systems in the real helicopter application, for instance a global navigation satellite system (GNSS). Although the inaccuracy of the GNSS is larger than the head movement of the pilot, the distance to the outside obstacles in the real world flight is usually much larger (> 25 m) than the distance to the screen in the simulator (2.5 m). For situations where obstacles are very close and the piloting task is a precise hover maneuver against a wind turbine or a ship deck, very accurate positioning systems are under development, e.g. DeckFinder of Airbus Defence and Space [187]. For this experiment, such real world positioning errors have not been simulated. However, the much larger effect of relative head motion in the simulator dome has been accounted for. Without the dynamic correction of these simulation errors, objective performance and subjective pilot ratings could have been affected negatively in the experiment.

Two approaches for compensating the image displacement due to small head movements have been investigated. The first one adapts the HMD images to the outside dome projection by adding offset angles for pitch and yaw to the true viewing direction of the pilot, as it has been applied by Beechey et al. [28]. Indeed this leads to an artificial error in the perception of the optical flow field, but it generates the same error at the HMD, as it is returned by the outside dome projection. Hence, both representations coincide. In case of a dual pilot simulation or if it is not practical to modify the image generator of the simulator, this is a reasonable solution. The second approach does not only compensate the HMD image displacement, it further increases the overall simulation fidelity by adjusting the outside dome projection according to the dynamic eye-point position of the pilot. Thus, errors in the perception of the optical flow field are not present anymore. Therefore, the solution with a dynamic eye-point in the projection system of the simulator is applied for this experiment. The implementation requires a recalculation of the perspective of each projector channel in every rendered frame. Moreover, the viewing position must be updated with respect to the translational head motion feedback from the tracking system. The dynamic perspective calculation has been adapted from the instruction of Kooima [97] for the multi-channel projection system. The changing asymmetric perspective of the projection onto the spherical screen requires a recalculation of the distortion in each channel based on the calibrated three dimensional distortion grid points at the screen (blue points in Figure 4-11). For each channel 30 x 20 = 600

points are calculated with basic vector analysis and are then updated in every frame. In Figure 4-11 the green points represent the distortion grid in two dimensional coordinates (uv-warped) with respect to the center of the screen (y = 0.0) and the red points are distorted with respect to the PEP (y = 0.35).

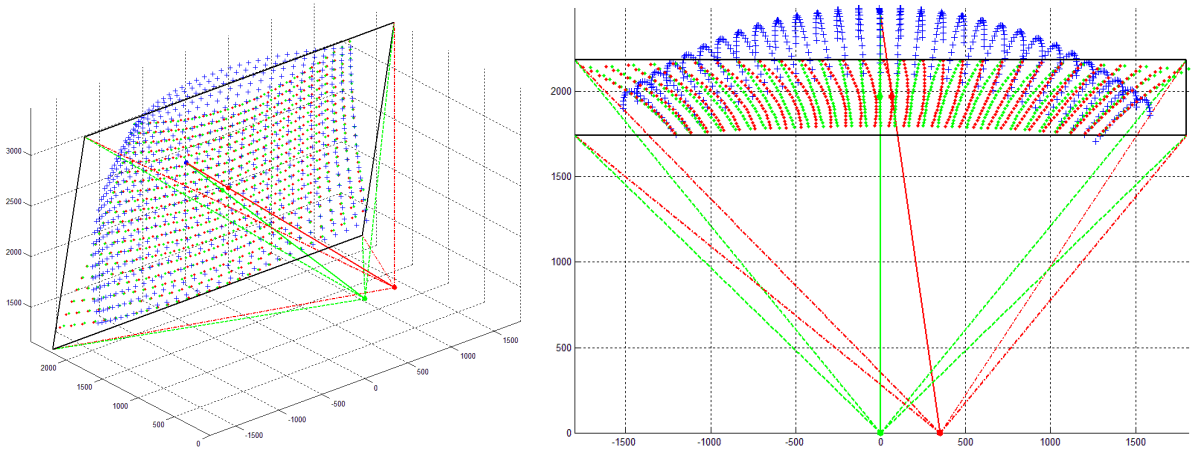

Figure 4-11: Distortion grid variation of two different eye-points

The blending of the intersection areas does not require an update in each cycle. Further details about the implementation can be found in the publication by Viertler et al. [181].

4.2.3 Performance Validation of the Head-Mounted Display

The performance of the HMD was evaluated quantitatively to some extent with theoretical analyses and video recordings and qualitatively with pilot questionnaires. The resolution of the low-cost HMD is 1.5 – 1.8 times higher compared to the resolution of the image generator of ROSIE in minutes of arc per pixel (arcmin/pixel) because of the large difference in the covered FOV, see Table 4-3. Thus, the viewer can hardly distinguish the difference when it comes to resolutions of the same magnitude. A person with average visual acuity can dissolve a spatial pattern with a visual angle of one minute of arc per pixel [19] [46]. For flight simulation, a projection system with human visual acuity is already possible and has been implemented for human vision studies [19]. However, this is not required for flight simulation training devices, see CS-FSTD(H) [6].

	Horizontal / Vertical Resolution (pixel)	Horizontal / Vertical FOV (degree)	Horizontal / Vertical (arcmin/pixel)
IG-Channel (mean value)	1920 / 1200	84 / 61.3	2.625 / 3.067
HMD (each eye)	800 / 600	23 / 17	1.725 / 1.700

Table 4-3: Resolution comparison of the HMD with the Image Generator of ROSIE

The delay between the augmented HMD image and the virtual outside cues in the simulation environment differs from the problem in real world, because the image generation in the simulation

environment contains a certain transport delay considering the visual response on the helicopter flight dynamics after a control or head motion input of the pilot, see Figure 4-12.

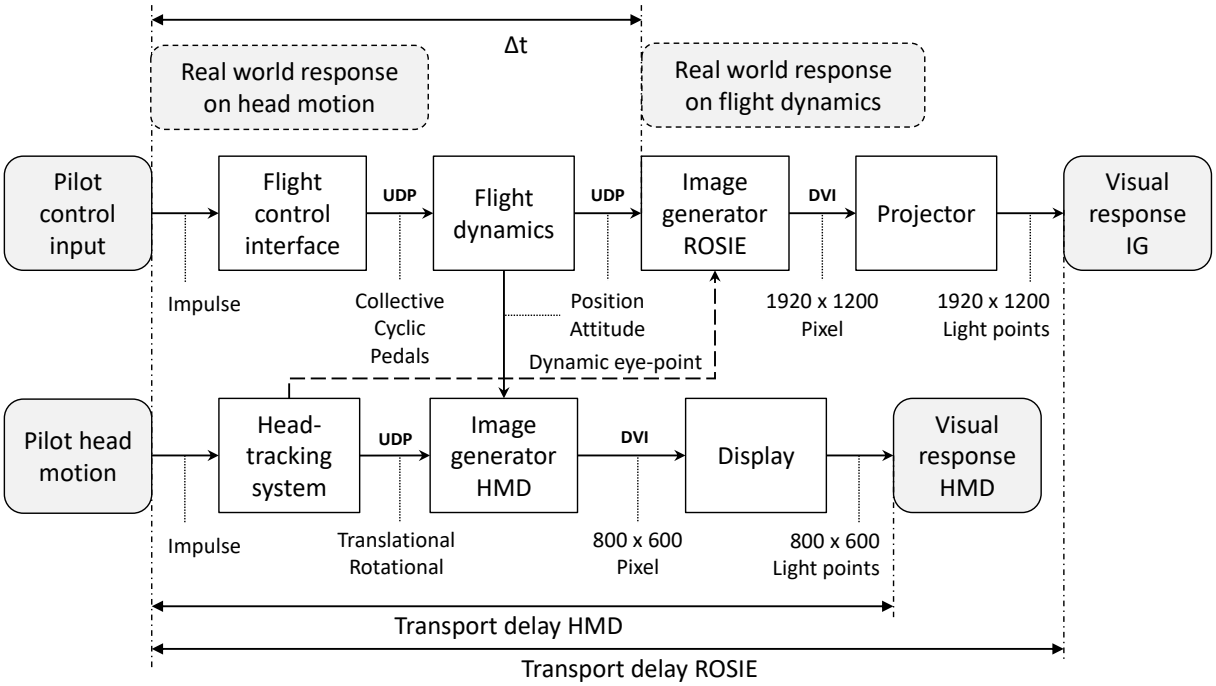

Figure 4-12: Transport delay of ROSIE and HMD compared to real world responses

The transport delay can be minimized with an asynchronous process communication. For ROSIE, the total transport delay results in a range between 36.67 ms and 56.67 ms with an assumed refresh rate of the projectors of one frame, i.e. 16.67 ms at 60 Hz [182]. The head-tracking for the HMD requires a lower delay to ensure a 3D-conformal representation without too many disturbances. Thus, predictor algorithms are more important for compensating the delay from head motion responses, since latencies in the range of 6 ms to 20 ms can be detected by the pilot [168]. The IS900 with 180 Hz update frequency provides a factory built-in Kalman Filter to compensate the delay from the rendering process and the display refreshing. With these methods applied, the system latency can be decreased below 20 ms, a minimum performance value recommended by Bailey et al. [26]. The delay and the minimization of the registration errors with the dynamic eye-point in the image generator has been validated with a high-speed (120 Hz) and high-resolution (1920 x 1080 pixel) compact action camera. Figure 4-8 shows the camera mounting in a styrofoam head. This approach allows a validation in the final application of the experiment and thus, it ensures an adequate performance.

With the compensation of the geometrical registration mismatches, the remaining errors result from dynamic positioning inaccuracies of the head-tracking system and the calibration process. Tests have shown that the registration quality can be improved by a short recalibration of the rotational parameters after each start-up process of the tracking system. Therefore, a quick boresight alignment procedure has been implemented. Two cross-hairs were shown to the pilot, one in the outside dome projection in a rotorcraft-fixed frame of reference and the other one on the HMD in a head-fixed frame of reference, see Figure 4-13.

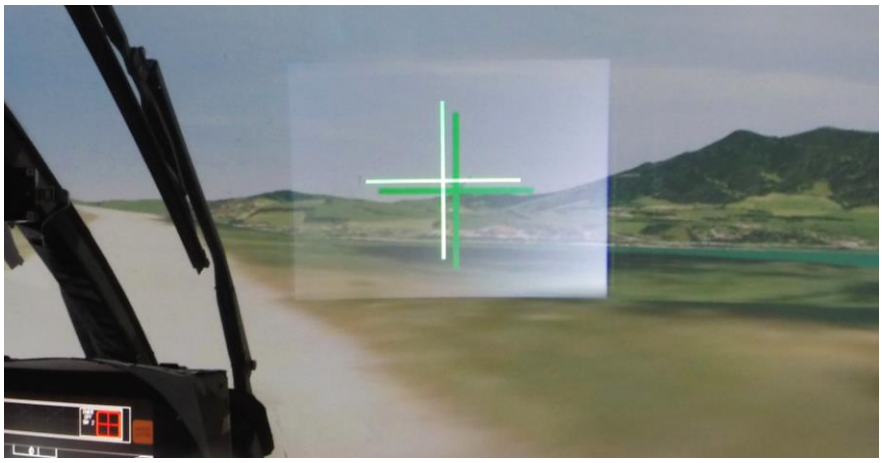

Figure 4-13: Boresight calibration procedure with two cross-hairs

In the next step, the pilot had to coincide both cross-hairs and reset the angular parameters. With this procedure, a quick and accurate alignment (< 0.5°) was achievable, as demonstrated in [22]. To minimize inaccuracies through head sway during the procedure, a method for fine adjustment has been implemented to account for that drawback. After the quick boresight resetting, the pilot was able to use the four-way-switch at the collective stick to move the cross-hair on the HMD, which was then located in the rotorcraft-fixed frame of reference also. Thus, the influence of head sway was eliminated.

To obtain pilot feedback about the HMD performance, four questions including the main advantages and drawbacks of the low-cost HMD system have been added to the subjective rating at the end of the experiment and are listed in Table 4-4 together with the mean rating score (M) and standard deviations (SD).

Questionnaire item		**M (SD)**
The wearing comfort of the HMD was good	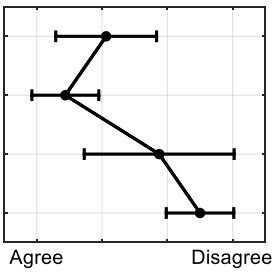	2.1 (0.8)
The limited field-of-view was no problem for me		1.4 (0.5)
The brightness in the background was disturbing		2.9 (1.1)
The HMD restricted my remaining view (head-down)		3.5 (0.5)

Table 4-4: Subjective pilot evaluation of selected HMD characteristics

The rating was again based on a four point Likert scale (1: Agree; 2: Rather agree; 3: Rather disagree; 4: Disagree). The results show that the wearing comfort of the HMD was rated as adequate for the simulation experiment. A few pilots struggled with the missing mass balance, since the weight of the optical system (320 g) was located at the front side and no helmet was used. Instead, a flexible headband with a mechanism for adjusting the mounting to an arbitrary head size was applied to fit the HMD for all participants. The limited FOV of the HMD was not a problem for the participating pilots. However, most of the pilots had no possibility of comparison through previous experience with other HMDs, equipped with a larger FOV. The remaining brightness at the background of the HMD because of the LCD technology, did not disturb the majority of pilots.

After a short period of flying with the system in the simulator, the illumination of the transparent area was usually no longer noticed. Finally, the view of the pilots around the active illuminated area of the HMD has not been restricted by the combiners nor other parts of the optical system. This is a great advantage of the LCD29 HMD. In summary, the performance of the applied HMD provided a suitable system and the developed integration methods improved the simulation fidelity for the experiment on augmented vision.

4.3 Experimental Simulation Methodology

The experimental methodology described in this chapter provides the framework of the experiment, besides the applied hardware described already in the last two subchapters. It contains a summary of the biographical background and the experience of the participating pilots. Simulation data recordings and the subjective ratings are described and the reasons why they have been selected are explained. Furthermore, the time schedule of the experimental procedure is depicted and the simulator training phase is explained, including the task practicing. Finally, this chapter defines the scenarios and the piloting tasks for the evaluation of the two display concepts regarding sensation and avoidance of obstacles in low-altitude flight and a precise visual hover assistance in degraded visual conditions below 800 m visibility. In this context, the main investigated hypotheses will be explained together with the independent and dependent variables for statistical analysis.

4.3.1 Participating Pilots

In the final development phase of the experiment, a test pilot of the WTD 61 (German Federal Armed Forces, Technical Center for Aircraft and Aeronautical Equipment) evaluated the display concepts and provided valuable feedback for improvements on the design and the procedure of the experiment. In particular, recommendations have been given to change the drift indication at the hover display concept, to avoid reflections of the head-down instrumentation at the optical system of the HMD and how to handle the subjective ratings in the simulator cockpit. After the realization of the improvements, sixteen pilots participated in the experiment with an average age of 47 years (SD = 11). Most of the pilots were from civil operators, six from air rescue providers (ADAC: 3, DRF: 3), five from the police (German Federal Police Force: 2, Bavarian Police PHuStBy: 3), three form commercial operators (Helicopter Travel Munich HTM: 2; IABG: 1) and two military pilots from the WTD 61. They had an average flight time experience of 4538 (SD = 3634) hours and eight of the pilots held an instrument rating. Pilots experienced in handling small twin-engine helicopters with similar flight dynamics to an EC135 from Airbus Helicopters were recruited, to minimize the time for adoption to the simulator. Except of one pilot who had experience with single-engine helicopters (AS350) only, all other pilots had type ratings for an EC135, EC145 or the predecessor types of a Bo105 and Bk117 respectively, amongst others. Nine pilots had practical experience with Night Vision Goggles (NVG) and four of them had prior experience with HMDs, either in real flight (NH90) or various HMD types in simulation. All pilots reported that they encountered DVE situations in visibility conditions below 800 m, while flying VFR.

4.3.2 Measurements, Ratings and Questionnaires

For quantitative evaluation of the results, all important input and flight state parameters have been recorded with a frame rate of 100 Hz, e.g. helicopter position, attitude, velocity, accelerations, angular rates, the primary control axis input, buttons and switches input and head motion, together with display settings and visibility conditions. In addition, all flight sessions have been recorded with a camera, which was mounted behind the pilot to obtain the outside view and the control and head motions of the pilot at the same time. Using the camera, the communication between the pilot and the instructor has been recorded as well. The HMD view was simultaneously rendered for the instructor, who was sitting behind the pilot to verify correct settings and viewing conditions. The HMD view can be reproduced with the recorded flight and head motion data after the simulation, if required.

In addition, subjective ratings have been conducted by the pilots, to identify correlations between the objective results from data recordings and the subjective pilot opinions. Furthermore, with display specific questionnaires, feedback about visualization characteristics have been collected, which could not be measured by other means in the experiment. For the low-altitude sense and avoid scenarios the NASA Task Load Index (NASA-TLX) [70] has been applied, because it is a well-accepted rating for workload assessment [71]. On a scale from 0 to 100 in gradation steps of five, six categories are assessed: mental demand, physical demand, temporal demand, performance, effort and frustration. Because the demanding categories or dimensions regarding the sense and avoid task have not been known, the generic NASA-TLX has been identified as an appropriate mean.

The second scenario of a precision hover task was derived from the hover mission task element of the ADS-33E-PRF [5]. The task is more related to the stabilization of the rotorcraft, where the pilot has to close the open-loop between the visual references and the control inputs. Thus, the Cooper-Harper Handling Qualities Rating (HQR) [38] of the ADS-33E-PRF was applied. For the latter, the pilot has to rate the demand required to fulfill the task on a scale from 1 to 10. The rating one specifies that the pilot compensation is not a factor influencing the the desired performance and the rating ten represents partial loss of control during the task. In the experiment nothing has been changed on the flight controls or flight dynamics of the rotorcraft. The response type was always a simple rate command with an active stability augmentation system (SAS), but without any higher level autopilot functions or control response types. Therefore, the HQR was used to rate the different visual cues under which the hover task had to be performed, instead of rating the rotorcraft dynamic characteristics and response types. With no changes applied to the flight controls, the differences in the results rely solely on the changes of the visibility condition and the visual assistance by the HMD. For that reason, audio warnings were also deactivated.

For a more detailed differentiation according to the changing visual cue conditions the Visual Cue Rating (VCR) has been conducted as well. Here, the pilot had to assess the attitudes (pitch, roll and yaw) and the translational rates (lateral-longitudinal, vertical) for stabilization effectiveness on a scale from 1 to 5, e.g. possible aggressiveness and precision of the maneuver under the given circumstances. Rating one is assigned to a good precision and aggressive corrections, while with rating five, the pilot can only achieve gentle corrections and consistent precision is not attainable

[5]. These standardized ratings (NASA-TLX, HQR and VCR) were conducted on a writing board directly after each run in the cockpit.

After each session, ratings with tailored questionnaires for the individual display concepts were performed. The first one about the sense and avoid display concept addressed the usability and the acceptance of the 3D-conformal visualization characteristics, as well as the 2D flight guidance presentation. Moreover, feedback about the color-coding and the concept of information blending has been assessed. The second questionnaire focused on the 3D-conformal visualization for hover assistance with the hover board references, the drift velocity indication and the co-planar extension of the 2D horizontal hover display. Finally, a last questionnaire with general questions about the HMD, ROSIE, perceived simulation sickness and feedback about the simulation study has been conducted.

4.3.3 Experimental Procedure

For each pilot the entire test day took approximately eight and a half hours to complete. The schedule of test program is shown in Table 4-5.

Test program		Timeline
Briefing	• Motivation, display concepts, task explanation • Biographical questionnaire • Visual acuity test	09:00 – 10:00
Training session	• Simulator handling (flight dynamics and controls) • Practicing HMD concepts and scenario tasks • Familiarization with ratings (TLX, HQR, VCR)	10:00 – 12:00
	Lunch break	12:00 – 13:00
Scenario block I	• Sensation and avoidance of obstacles (NASA-TLX) • Adjustment of near-field blending (NASA-TLX) • Questionnaire I	13:00 – 15:00
	Coffee Break	15:00 – 15:30
Scenario block II	• Precision hover with reduced FOV (HQR, VCR) • Precision hover with HMD (HQR, VCR) • Questionnaire II	15:30 – 17:00
Debriefing	• Questionnaire III • Feedback and comments	17:00 – 17:30

Table 4-5: Test program of the experiment

During the comprehensive briefing in the morning, the pilots received information regarding the background and the motivation of this work. The display concepts have been explained theoretically and the piloting tasks have been described. Afterwards, the pilots completed a biographical questionnaire and conducted a short visual acuity test to ensure 20/20 vision. Except

of one pilot, all pilots achieved at least the desired visual acuity or better. However, further readability tests with the HMD later on demonstrated enough eyesight capability for all pilots in the experiment. Using optical aids together with the HMD, e.g. contact lenses or eyeglasses, was no problem. The remaining time of about two hours in the morning was used for training purposes. It started with a basic simulator training to enable the pilot to adopt his control behavior to the handling qualities of the simulator. This training session was followed by practicing the desired tasks with the HMD visualization concepts. After lunch, the first scenario block about the low-altitude flight including obstacle avoidance has been conducted. The second scenario block with the precise hover maneuver tasks started after a thirty minute coffee break. Since the hover scenarios were assumed to be the most demanding tasks, they were placed at the end of the day, so that the other tasks would not be influenced negatively due to the exhaustion of the participants. Finally, the day was closed with the final questionnaire and feedback about the visualization concepts. Checklists were used by the instructor to ensure proper simulation settings and compliance with this procedure. The checklists were an important mean to control the varying sequences of the conditions during the first scenario block for each pilot, which were applied in order to mitigate further training effects. The training session and the two scenario blocks containing the developed scenario designs are explained in more detail within the next subsections.

4.3.4 Simulator Training and Task Practicing Phase

Training of the simulator handling and the visualization concepts with the HMD was very important. Every simulator is slightly different to another and compared to the real flight conditions the fidelity differs even more. Thus, the pilots had to adopt their control behavior to the flight dynamics and the flight controls simulated with ROSIE. To mitigate influencing effects on the final results, a well-developed training about flying with focus on the outside visual cues was required for this experiment. This thorough training ensured that the pilots would react properly in case of an obstacle avoidance maneuver with very limited reaction time, due to the bad visibility conditions. Furthermore, the workload of the basic simulator handling was minimized to provide enough workload capacity for the new HMD concepts. This was important, because most of the pilots had no experience with a HMD before. Familiarization with both this new technology and the display concepts was the second important part of the training session. Since the experimental time was very limited, the available two hours of training were not enough to mitigate further training effects during the scenario sessions completely. However, the 3D-conformal visualization concepts were designed to be very intuitive for the pilots. Thus, it was anticipated that less training is required compared to two dimensional concepts currently being used by military operators. Finally, after the training session, the pilots performed very well and no more uncertainties have been observed by the instructor. Table 4-6 shows the detailed training plan for each pilot, starting with the basic simulator training (T.1 – T.5) without HMD, followed by the HMD concept familiarization (T.6 – T.10) after a short break.

Task ID	Task Description	Visibility (m)	Duration (min)
T.1	Cruise flight (take-off, cruise, landing)	25.000	10
T.2	Hover MTE	25.000	5-10
T.3	Slalom MTE	25.000	5-10
T.4	Pirouette MTE	25.000	5-10
T.5	Slalom MTE in DVE	400	5-10
-	Break	-	5-10
T.6	HMD calibration check	800	5-10
T.7	Sense and avoid scenario (FG)	800	5-10
T.8	Sense and avoid scenario (FGSA) NASA-TLX training	200	10-15
T.9	Visible distance adjustment	100 – 800	10
T.10	Precision hover task in ground effect, HQR and VCR training	800	10- 15

Table 4-6: Agenda of training session

4.3.4.1 Basic Simulator Training

The basic simulator training started with a cruise flight (T.1) in the area close to the Alps in south Germany, where the following scenarios were located as well. The level of difficulty has been increased step by step with scenario specific mission task elements. Thus, after practicing the first hover maneuvers (T.2), the pilots had to fly the slalom test course (T.3), see the example runs of the first pilot from varying directions in Figure 4-14. This element partially reflects the lateral collision avoidance maneuvers in the low-altitude flight task later.

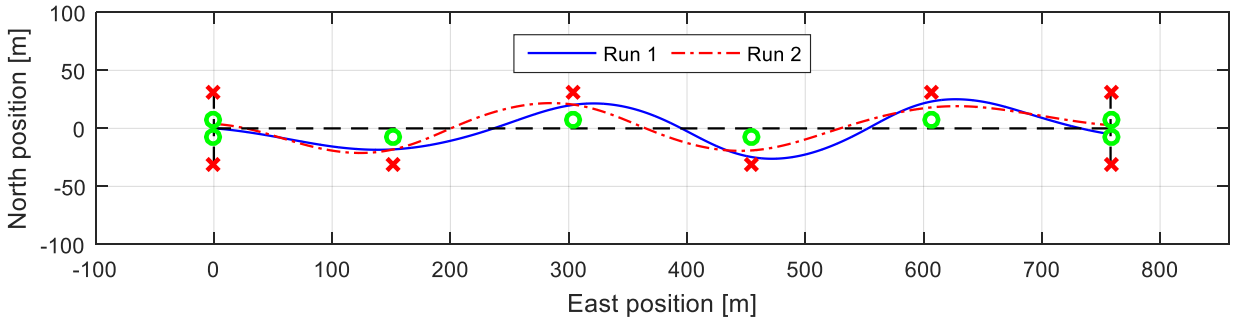

Figure 4-14: Two example runs of the slalom mission task element from both sides

To increase maneuver complexity even further, the pilots had to fly the pirouette mission task element (T.4), in which control input coordination of all four control axis is very demanding, while flying the circle with focus on the point at the center, see Figure 4-15. It was no priority, that the pilots were able to achieve the desired or adequate results, which are requested in the ADS-33E-PRF, nor were time limitations postulated.

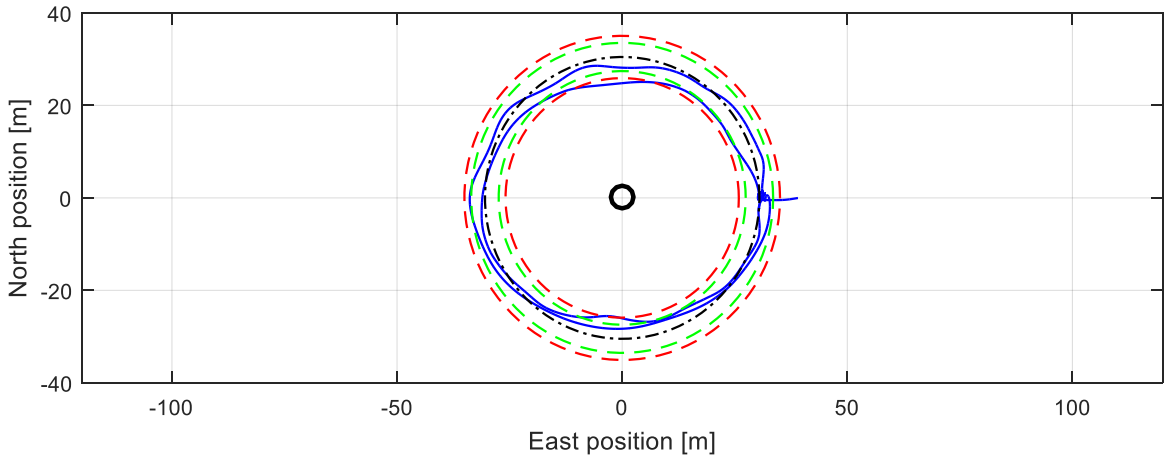

Figure 4-15: Example runs of the pirouette mission task element

The MTE test courses aimed to serve only as a training environment for improving the skills of the pilot in the simulator, while reducing workload for the primary task of flying the helicopter. The basic simulator training was finalized with the first flights in degraded visual conditions of 400 m (T.5), while flying the slalom task, before heading to the first HMD trials.

4.3.4.2 Display Concept and Task Practicing

First of all, the fitting of the HMD with the adjustable headbands had to be checked by the pilot to ensure proper wearing, readability and head-tracking alignment (T.6). This procedure was conducted in two stages. Figure 4-16 on the left shows the first part, in which the pilot had to verify that a magenta colored frame covering the whole FOV can be seen completely. Furthermore, combinations of alphanumeric characters and numbers in different colors and sizes were placed at the corners in order to prove legibility. This procedure ensured a correct fitting of the HMD and readability of all symbology by the pilots.

Figure 4-16: Verification of correct HMD fitting through the pilot

While for the first part, the displayed content was presented in the head-fixed frame of reference, the second part presented a green rectangle in the aircraft-fixed frame of reference, see Figure 4-16 on the right side. The pilot had to check whether the green synthetic rectangle remains between a smaller and a larger magenta colored rectangle presented in the outside dome projection. This approach verified that the alignment accuracy has been achieved within certain tolerance limits. If this was not the case, the pilot had to apply the short boresight calibration procedure described in chapter 4.2.3. This verification method was conducted every time when the pilot put on the HMD.

After the fitting of the HMD, the pilots familiarized themselves with the display concepts and they were practicing the tasks planned for the afternoon sessions, which are explained in more detail in the following subsections. For the sense and avoid task, two display variants were applied, see Figure 4-17. The basic display included only the magenta colored flight guidance (FG) symbology, which consists of the two dimensional primary flight references together with the 3D-conformal flight path markers and the rotorcraft-fixed attitude indicator. Without that minimum amount of information presented head-up, it would not have been possible to fly the scenario tasks at visual ranges below 200 m. For the second display variant, additionally all terrain and obstacle visualizations, as outlined in chapter 3.2 were applied in order to sense obstacles and to avoid collisions (FGSA).

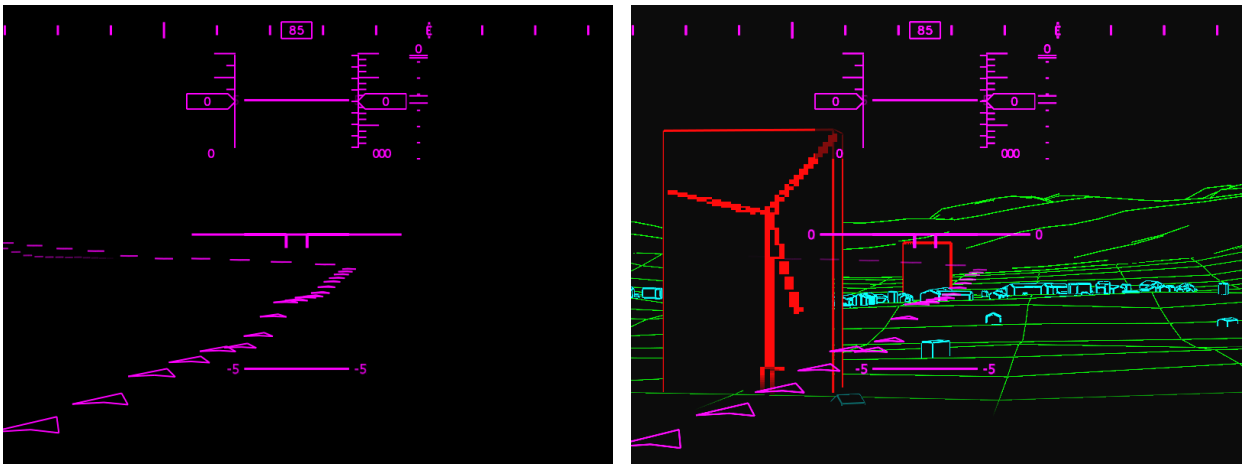

Figure 4-17: Basic (left) and advanced (right) display variants for collision avoidance

Pilots started with practicing the basic display variant (T.7), followed by the advanced display variant (T.8) including more information and reduced visibility. At this point, the NASA-TLX was also conducted for training purposes. The additional task of adjusting the near-field culling (T.9) was practiced afterwards as well, while flying in the obstacle scenery. The training session was completed by practicing the hover display concept (T.10), followed by the familiarization with the handling qualities (HQR) and visual cue rating (VCR).

4.3.5 Sense and Avoid Scenario Design and Piloting Task

The scenario block I of the simulation experiment is intended to demonstrate the control behavior of the pilots in DVE below 800 m visual range. Thus, the following question arises: how is the control strategy of the pilots and their perceived safety influenced by the advanced display concept, which helps the pilots to detect obstacles at a safe distance? Currently, only air rescue, police or military pilots are allowed to fly below 800 m of visual range under exceptional circumstances in Germany. This is possible due to their extensive training, but maintaining safety is still a key challenge. However, the perception of the height-above-ground and the current velocity with the synthetic terrain and obstacle visualization is still difficult without having micro-textures or sufficient outside visual cues. So, the question is to what extent the “low and slow” flying strategy will be influenced by the advanced display concept. Moreover, can the workload of the pilot be reduced with more information presented on the HMD? Does the perceived safety by the pilot improve with 3D-conformal content of the scenery? Is the large amount of active illuminated

pixels disturbing the pilot when scanning the outside visual cues? Are the pilots able to adjust the near-field culling to the changing visibility and workload conditions accurately enough? Is there a quantitative measure for the increase in perceived safety of the pilots?

To answer above mentioned research questions, a low-altitude contour flight scenario with collision avoidance maneuvers has been developed. It was mainly derived from the mission task elements of the ADS-33E-PRF [5] and the work of Gary Clark [36] at the University of Liverpool. Even though, the mission task elements are intended to be used in good and degraded visual conditions, they do not reflect the problem of flying close to ground and obstacles in DVE in a sufficient manner. Clark broke down the collision avoidance maneuver and developed three new task elements intended to serve as a suitable expansion. He investigated the pilot behavior for a turn, climb and stopping maneuver at visual ranges of 80 m, 240 m, 480 m and 720 m. Furthermore, for the implementation of a suitable flight guidance strategy including sensors to measure the obstacle environment, his next idea was a low-altitude flight scenario in a valley with numerous trees the pilot has to avoid. This idea based on the work of Lam [100], who simulated automatic rotorcraft nap-of-the-earth flights with 2D-range maps. In general, a trade-off between laboratory conditions, which are suitable for data evaluation and the fidelity of real world flight scenarios must be made. On the one hand, the experiment must be reproducible to allow a comparison with previous and future research results. On the other hand, a certain level of difficulty and complexity of the task is required to reflect the real world conditions sufficiently. Consequently, a low altitude contour flight scenario, in which the pilots are forced to fly in the obstacle scenery, has been designed. Thus, the pilots had to fly a kind of slalom around the obstacles, but in a more realistic scenery with unknown objects, compared to the mission task element of the ADS-33E-PRF with very predictable visual references. This enables an evaluation of the higher-level control strategy of the pilot in addition to the performance, which results from the handling qualities including visual aids. The details of the task are described in the following subsections.

4.3.5.1 Piloting Task for Sensation and Avoidance of Obstacles

The low-altitude contour flight scenario implemented was located at a small area around the lake “Tegernsee” close to the Alps in south Germany. The region provides different kinds of geologic features, like mountains, hills, rivers, creeks, lakes and man-made infrastructure and obstacles, like villages, streets, railways and power lines. Thus, the pilot was confronted with a realistic environment with regard to helicopter emergency medical services and bad visibility conditions through fog. The pilots had to follow the given flight path of about six kilometers shown in Figure 4-18, as close as possible, while they had to avoid collisions with obstacles. The obstructions were placed directly into the flight path to provoke collisions without timely avoidance maneuvers conducted by the pilot.

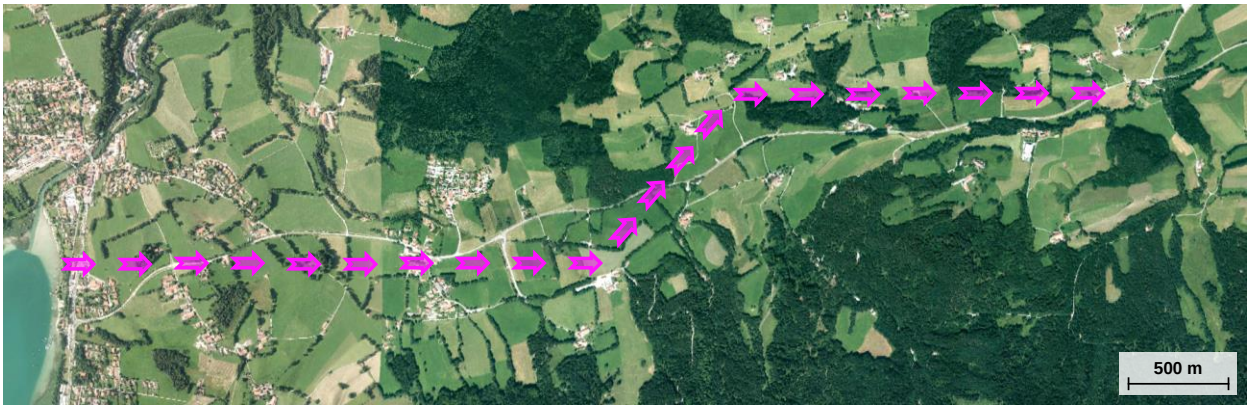

Figure 4-18: Sense and avoid scenario flight path

The pilots were told to avoid the obstacles, if possible with a lateral maneuver, otherwise with a vertical maneuver, e.g. in the case of a power line. For the latter, the pilots where free in their decision if they go above or underneath the power line, wherever they felt more safe. Usually, pilots flew above the power line, but in cases with 100 m visibility the risk of losing the ground visibility was very high, so that they preferred to fly beneath the power lines. However, depending on their training, some pilots will never fly below the power lines. Instead, they apply procedures, in which they fly over the pole between the power lines and maintain visual contact with the pole during the complete maneuver, i.e. they have to turn around the yaw-axis during the maneuver to keep the pole as a visual reference in case of ground references are lost. Figure 4-19 shows the used obstacles, which have been simulated to be detected by the sensors, compared to the level-of-detail 2 (LOD) buildings, which are available in the area-wide database. In addition, these obstacles are tall enough (> 100 feet) to assure collisions without any avoidance reaction. After the avoidance maneuver the pilots were asked to return and continue to stay on the track. Two heading changes were included to validate if the pilots were able to follow the track accurately with the presented flight path markers for navigation.

Figure 4-19: Obstacles to provoke collision avoidance maneuvers (Wind turbine WT, cell tower CT, construction crane CC, power line PL)

Each pilot had to fly the test course eight times in counterbalanced sequence. Half of the pilots started with the basic display variant (FG) and flew the four different visibility conditions of 100 m, 200 m, 400 m and 800 m. Afterwards, they flew another four runs with the advanced display variant (FGSA) and the same visibility conditions again. The other half of the pilots started with the FGSA concept followed by the FG variant to mitigate effects through the scenario

sequence or to make them visible, in case they have a significant influence. Furthermore, the visibility conditions were applied in counterbalanced sequence for each pilot. All test runs contained four obstacles for every visibility condition. To avoid memorization of the obstacle location and the order of the obstacles, the positions on the flight path were slightly changed and the sequence of the obstacle type was varied across the investigated visibility conditions. However, the flight path was identical for all conditions in order to allow for better comparison between the test runs.

A further primary task for the pilots was to adjust the velocity and height above ground depending on the outside visibility conditions, in order to conduct a safe flight through the obstacle scenery. Compared to experiments with specified reference velocities and altitudes (e.g. 60 kts +/- 10 kts and 50 feet height at a visibility level of 0.25 mile (≈ 400 m) [61]), this pilot-defined velocity and height control enables conclusions about their perceived safety. In addition, the pilots were told that they can rely on the visual assistance system and that no completely unexpected events were included in the scenario. The pilots did not know where and when an obstacle would occur during the test run, but they were aware that obstacles could appear at any time, as they would expect in the real world flights as well. Interesting results regarding completely unexpected events in this context can be found in the work of Knabl [93]. Besides adjusting the velocity, the pilots should maintain the height above ground with a target value of 100 feet to stay within the obstacle scenery, whenever visibility conditions permitted it. The test course contained a certain height profile, as can be seen in the lower part of Figure 4-20.

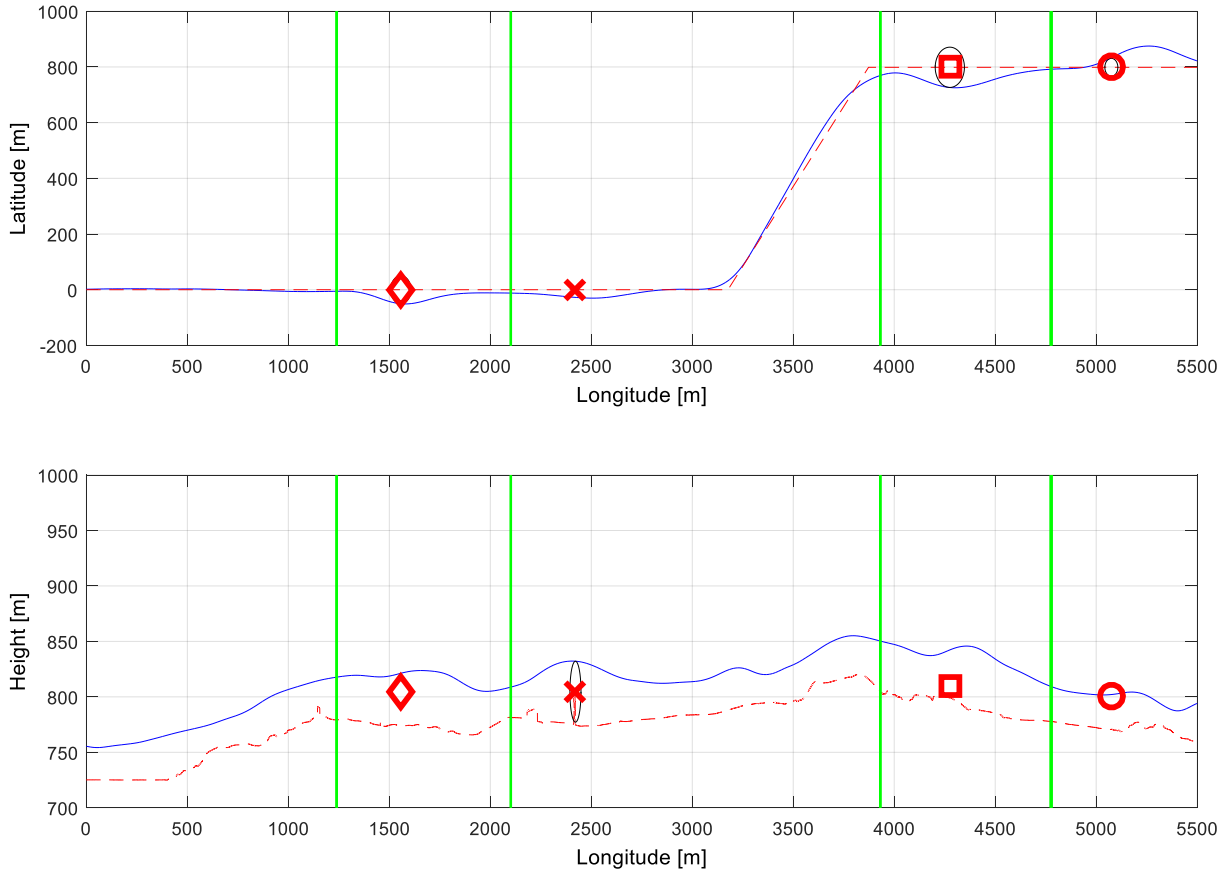

Figure 4-20: Example of one sense and avoid test run

At lower visual ranges, the pilots had to reduce the height above ground to maintain ground visibility. Figure 4-20 shows the horizontal and vertical flight profile of the task together with an example trial run of one pilot with avoidance maneuvers around the red marked obstacles. While the initiation of an avoidance maneuver can be determined through the flight path deviation together with the control input of the pilot, the point in time of the first detection of an obstacle by the pilot cannot be determined through the control behavior. Thus, the pilots had the secondary task to trigger each obstacle detection with a switch on the collective lever, when they perceived a specific obstacle in the flight path for the first time, either through the visual support with the HMD or in the outside visual cues. Figure 4-20 demonstrates these triggered moments in time with the green vertical lines.

The detailed schedule of the scenario block I is listed in Table 4-7. The two sessions with four runs of different visual ranges for each display variant were followed by two additional subtasks. For the latter, the fog and thus, the visual range changed dynamically. The pilots had to track the changes in the visibility conditions and had to readjust the near-field culling and the amount of displayed information on the HMD. The subtask is explained in more detail in chapter 4.3.5.3. At the beginning, two different patterns of how the fog is changing dynamically have been considered. However, due to the tough time schedule of the experiment, the second trial has been excluded. The session has been completed with the first questionnaire about the sense and avoid display concept.

Task ID	Task Description	Visibility (m)	Duration (min)
SA.11-14	4 x Sense and avoid scenario (FG)	100 - 800	45
-	Break	-	5-10
SA.15-18	4 x Sense and avoid scenario (FGSA)	100 - 800	45
SA.19	Visible distance adjustment – Pattern 1	100 - 800	10
SA.20	Visible distance adjustment – Pattern 2 (later skipped)	100 - 400	10
-	Questionnaire I	-	10-15

Table 4-7: Program of scenario block I

4.3.5.2 Dependent Variables for the Sense and Avoid Scenario

The scenario design included two independent variables (treatments), in fact visibility with four conditions and display type with two variants. The dependent variables (measurements) recorded are listed in Table 4-8. The main considered flight parameters were the velocity and the height above ground. For the obstacle avoidance maneuvers the particular distances for detection, avoidance and the minimum distance when passing the obstacles were determined and evaluated. In addition, the workload of the pilot in each condition was assessed by the subjective NASA-TLX. For the additional subtask, a descriptive analysis was conducted for the display adjustment through the pilot. The tailored questionnaire at the end of block one considered the subjective

rating of the pilots about display elements, which could not be measured objectively in this experiment so far.

	Group of dependent variables	Parameter classification
Objective measurements	Flight performance	Velocity Height above ground
	Obstacle avoidance	Minimum distance to obstacles Detection distance to obstacles Avoidance maneuver distance to obstacles (in meter, eye-heights and time-to-contact)
	Display adjustment (subtask only)	Visual range
Subjective ratings	Workload (NASA-TLX)	Mental demand, physical demand, temporal demand, performance, effort and frustration
	Sense and Avoid questionnaire	3D-conformal terrain visualization, 3D-conformal obstacle visualization, flight guidance parameters and general aspects

Table 4-8: Dependent variables of the scenario block I

4.3.5.3 Subtask Scenario of Near-Field Culling

The controllability of the amount of information displayed on the HMD with the near-field culling, enables an augmentation of the degraded visual environment, without showing information at regions, where the outside cues are still visible and thus reduces visual clutter. Since there is no airborne sensor available with the capability to detect the visual range reliably at the moment, the adjustment of that near-field culling function can only be performed by the pilot. This subtask aimed to evaluate if pilots were capable to adjust the near-field blending to the outside visual conditions. Thus, the pilots had to fly the previous test course again. Additionally, they had to adjust the near-field culling manually with a switch at the collective lever to the perceived outside visual range, which was changing dynamically for this task, see Figure 4-21.

Figure 4-21: Near-field culling adjustment with a switch at the collective stick

A small preliminary study with five students has been conducted previously to the piloted experiment in order to demonstrate whether this manual adjustment is practicable. For this small experiment the task of flying has been removed and the students (no pilots) perceived a recorded flight simulation, in which their only task was to adjust the near-field culling. This was done without any further information about the visibility distance and the participants could perform the adjustment in a continuous setting. The degraded visual conditions have been generated with simulated fog at varying distances. The profile of the changing visibility can be seen in Figure 4-22 with the black curve representing the image generator reference. Furthermore, the average result of the students is depicted together with the standard deviation at certain points in time. The weather changes very quickly at some points [$\Delta t = 10$ s], while it switches slowly at other moments [$\Delta t = 30$ s] in order to make it more difficult to be recognized. The results from the preliminary experiment showed an overall good tracking performance with a mean standard deviation of 87 m without any additional tasks. At lower distances the students achieved more accurate results than at higher distances. They required more time to recognize that the visible conditions have improved (see larger deviations from the reference with increased variances 60 s – 120 s and 270 s – 330 s), compared to situations where the visual range decreased. Here, the students responded quickly and with high precision (120 s – 150 s and 340 s – 350 s). This case was more critical, because if not adjusted adequately, important information was neither visualized on the HMD, nor was it visible through the outside cues. Whereas in the other cases, where the students responded with a delay, the information was visible at both sources. However, this potentially increased problems in perception due to visual clutter.

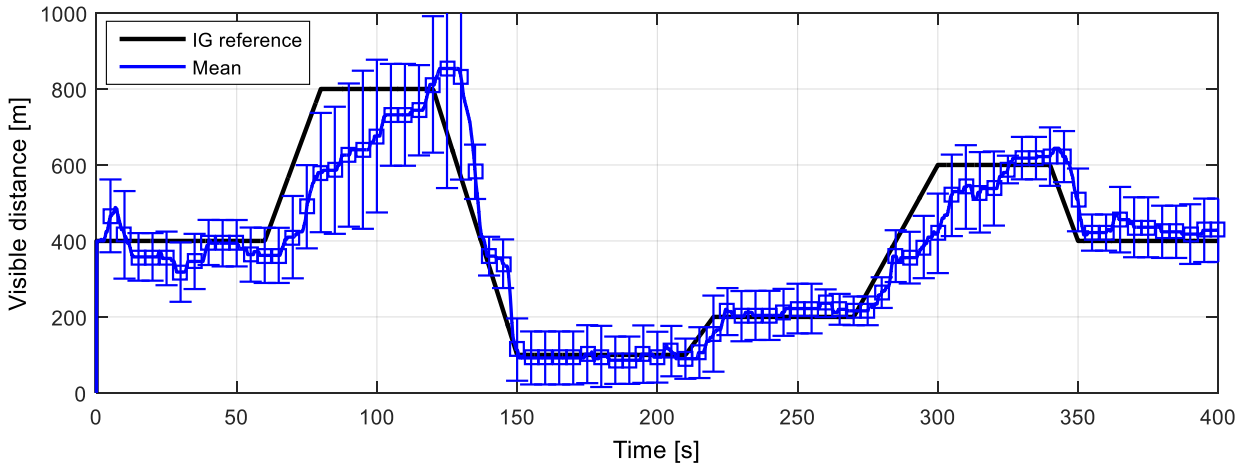

Figure 4-22: Mean visible distance setting of the students (N = 5) according to the simulated image generator (IG) reference [183]

The piloted experiment further investigated if pilots were able to achieve similar results, even with a higher workload during manual flight.

4.3.6 Precision Hover Scenario Design and Piloting Task

The intention of the scenario block II was to evaluate the second challenging task of hover with the assistance of visual references under different degraded visual conditions. The research questions concentrated on the achievable hover performance of the pilots with these 3D-conformal hover board references derived from the hover mission task element of the ADS-33E-PRF. The

following questions were of particular interest: How crucial are the limitations of the low-cost HMD with regard to the limited FOV according to previous findings from literature? Is a manual flight still possible in severe visual conditions without high-level control assistance in case of a failure?

The task for the pilots was identical regardless of the circumstances. They had to capture the hover position, stabilize the rotorcraft and then they had to maintain the position precisely for two minutes. The approach to the hover position and the time for stabilization were not evaluated, due to the frequently changing conditions and the fact that not all of the conditions could be practiced during the training session. Thus, the pilots got a couple of minutes in every run to familiarize themselves with the environmental conditions. To observe differences with respect to the visual references, no higher-level control response types (attitude command / attitude hold, translational rate command or hover hold) were simulated, besides the basic stability augmentation system of the H135. Table 4-9 shows the sequence of tasks in this scenario block. It started and ended with a reference hover task at the basic hover mission task element presented at the outside visual cues. This enabled an observation of training effects during the test runs. The pilots wore the HMD, but it was deactivated and no display support was provided. The first reference flight was followed by two trials with reduced FOV and no HMD assistance for an independent examination of the FOV effect. Afterwards, the HMD hover visualization concept was tested with three different visibility conditions in ground effect over a field with limited micro-textures. The aerial images used provided a resolution of 25 pixel per square meter. Finally, to increase the difficulty, the display concept was tested for a hover task against a wind turbine, although it has not been designed for this task. The session was closed by a subjective questionnaire about the display characteristics.

Task ID	Task Description	Visibility (m)	Duration (min)
PHS.21	Hover MTE reference	800	8
PHS.22	Hover MTE 40° x 30° FOV	800	8
PHS.23	Hover MTE 23° x 17° FOV	800	8
PHS.24 – 26	Precision hover in ground-effect	800, 100, 25	25
-	Break	-	10
PHS.27 – 29	Precision hover out of ground-effect	800, 400, 100	30
PHS.30	Hover MTE reference	800	5
-	Questionnaire II	-	10

Table 4-9: Agenda of scenario block II

4.3.6.1 Hover Task with Reduced Field-of-View

The FOV of the pilot was restricted to a medium sector of 40° x 30° at first, which represents the performance of most high-end military HMDs or the restriction of Night Vision Goggles (NVG). Secondly, the FOV was further restricted to the small FOV of 23° x 17° provided by the applied low-cost HMD. To achieve these restrictions in the FOV of the pilot, numerous approaches can be found in literature. A very simple method has been described by Clark in [36] by using blinkers

like those in a horse race. A set of laboratory glasses were masked to reduce the lateral FOV. The drawback is, that because of the differences between the pupillary distances of the test pilots, the masking must be conducted for every pilot individually. Furthermore, this method can only consider the area of binocular vision, but there is still a remaining monocular area at the lateral edges. In [79], Jennings et al. used a similar approach with masked glasses to reduce the FOV for testing NVGs. They considered the problem of binocular vision by masking each eye separately, instead of just using blinkers. Hoh [75] varied the FOV by masking the helicopter canopy with cutouts made in blackout curtain material attached to the cockpit windows. The current experiment is limited to the simulator and thus the head-tracking information can be used together with a simple functionally extension of the image generator to simulate the reduced FOV in the outside dome projection with arbitrarily geometries and without the need to make individually adjustments for each pilot, see Figure 4-23. Thus, experimental time has been saved without requiring the adjustment and validation of the FOV configurations.

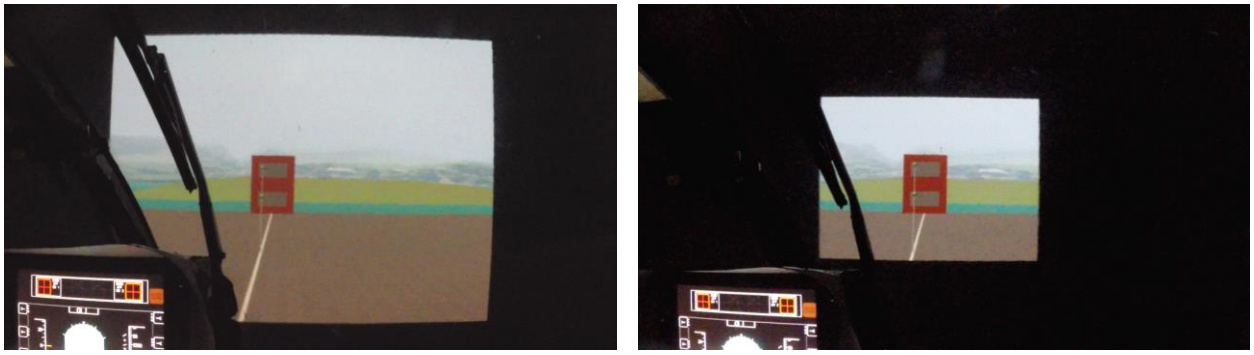

Figure 4-23: Hover task with reduced FOV, left: 40° x 30° and right: 23° x 17°

With this additional functionality implemented, the pilot perceived the outside cues, limited to the defined FOV, while the rest of the FOV was darkened depending on the line-of-sight. For these tasks, the pilot wore the HMD with deactivated displays but active head-tracking system.

4.3.6.2 Hover Task with Precision Hover Assistance

The actual evaluation of the display concept with hover references was tested under two main conditions, in-ground effect and out-of-ground effect while hovering against a wind turbine. The first task was to hover close to the ground at twelve feet eye-height, i.e. the helicopter landing skid was about six feet above ground. At these very close distances to the ground, only a minimum of micro-texture references were retained with the aerial images applied. Three different visibility conditions have been tested. It started with 800 m of visual range, where the pilot still perceived macro-textures in form of buildings and terrain contours in the background. Afterwards, the visibility was reduced to 100 m followed by a reduction of 25 m. With this reduction in visual range, the macro-textures in the outside cues were decreased as well as the remaining micro-textures in the peripheral vision of the pilot from the near-field, see Figure 4-24 on the left side. Consequently, the pilots had to rely on the synthetic HMD references more and more.

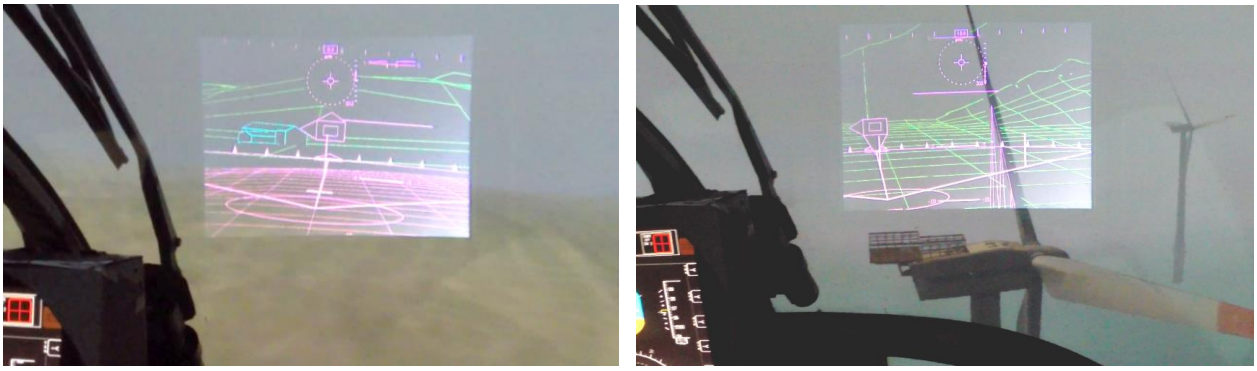

Figure 4-24: Precision hover task in ground effect (left) and against a wind turbine (right)

The second task series increased the level of difficulty by reducing the visual cues even further. The optical flow was reduced to a minimum, due to the large distance to the ground of 285 feet, while hovering against a wind turbine. The latter was placed in the middle of a lake with no micro-textures, see Figure 4-24 on the right, so that the only visual references were perceived from the wind turbine itself and the synthetic HMD cues. The test runs started again with 800 m of visual range followed by 400 m, where the ground was still visible. The last condition of 100 m visibility was comparable to fly according to visual flight rules (VFR) under instrument meteorological conditions (IMC). The test runs started on ground at the bank of the lake close to the wind turbine. A highway-in-the-sky was applied to assist the pilots in finding and approaching the wind turbine, see Figure 4-25.

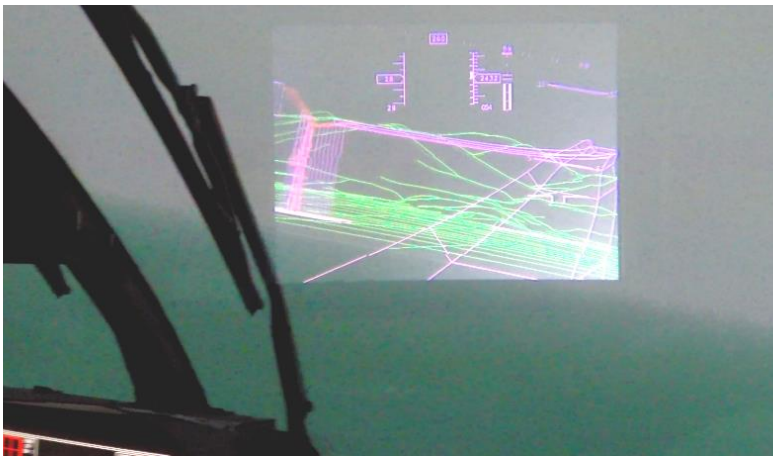

Figure 4-25: Highway-in-the-sky in bathtub style for wind turbine approach

It was left to the pilots, which reference they used to accomplish the task. According to their preferences, they could use the station of the wind turbine as reference, the synthetic hover boards or a combination of both. The task was not trained in the morning session and thus the pilots obtained a certain amount of time to figure out their best practice before starting the two minutes of measurement.

4.3.6.3 Measurements for the Hover Tasks

For the hover tasks the main parameters that have been considered for the evaluation are the horizontal and vertical precision in maintaining the hover position and the corresponding control inputs of the pilots. In addition, subjective ratings have been gathered for comparisons with the objective results. Table 4-10 lists all parameters relevant for the evaluation.

	Group of measurements	Parameter classification
Objective measures	Flight performance and pilot behavior	Horizontal, vertical hover precision and heading (RMSE) Cyclic control input (RMSE) Head motion (RMSE)
Subjective ratings	Handling Qualities (HQR)	Rating of visual conditions instead of different control characteristics (Rating: 1 – 10)
	Visual Cue Rating (VCR)	Detailed rating of visual conditions (visibility including hover references)
	Hover questionnaire	3D-conformal hover boards, 3D-conformal drift indication, 2D horizontal position indication

Table 4-10: Measurements of the scenario block II

4.4 Summary

The Rotorcraft Simulation Environment has demonstrated to be a perfect mean to achieve laboratory conditions with a very high level of simulation fidelity in a safe environment. The latter is inevitable for very low visibility conditions in order to mitigate the risk of the pilots. Even a safety pilot, knowing all obstacles in the surrounding environment would struggle to ensure enough safety for real flight tests. Thus, flight simulation is an important mean for demonstrating the system performance including pilot behavior before going into flight tests as a next step. Furthermore, the advanced HMD integration with the dynamic adaption of the outside multi-channel projection system with respect to the head-tracked eye position mitigated simulation induced errors and thus increased the simulation fidelity even further. The sixteen participating pilots enabled a statistical analysis showing differences between the display types and visibility conditions. The experiment did not attempt to show differences between different groups of the pilots, for instance, the influence of pilot experience (flight hours) or the age of the pilots. For this purpose, a larger number of pilots would be required. A sophisticated training has been established for the experiment and the novel display concepts in order to mitigate training effects as much as possible. The new scenario designs for this experiment enabled not only to reveal the performance of the visual augmentation assistance, they also allowed to get insight into the general pilot behavior during low-visibility contour flight. Furthermore, the stabilization task in hover addressed the limitations of the visual augmentation methods in contrast to the benefits in obstacle detection and collision avoidance.

5 Results and Discussion on the Flight Simulation Experiment

The results of the experiment are presented and discussed for each scenario individually in this chapter before a concluding discussion is given on both sub-tasks. The findings of the low-altitude sense-and-avoid scenario are described first. These results are followed by the performance evaluation of the hover tasks under different visibility conditions. Subjective ratings complement the objective pilot behavior measurements for both tasks.

5.1 Sense and Avoid Scenario Results

The evaluation of the low-altitude flight scenario focuses on the research questions mentioned in chapter 4.3.5 and proves the expectations about the pilot behavior, when flying in low-visibility conditions (Figure 1-5). For instance, to what extent can the advanced display concept (FGSA) assist the pilot in order to compensate the effect of flying "low and slow" compared to the basic display type (FG)? How does the display variant affect the obstacle avoidance maneuvers with regard to the absolute distance and time-to-contact? Additionally, the pilot workload has been measured to indicate whether the large amount of 3D-conformal information contributes to pilot confusion and visual clutter, or if it is able to reduce the pilot's cognitive load. The discussion on these results further highlights some invariants in the pilots' control behavior, for instance, a minimum time-to-contact for reactions on unexpected events or an unchanged control of velocity in eye-heights, because of the invariant optical flow region used by the pilots. The main results have been previously published by the author in [184].

Statistical data analysis was conducted by using MATLAB and repeated measures analysis of variance (ANOVAs) with post-hoc Bonferroni corrections for multiple comparisons. The four visibility conditions of 100 m, 200 m, 400 m and 800 m and the two display types, in fact, FG and FGSA resulted in a 4 x 2 ANOVA, where each pilot flew all eight different conditions. Greenhouse-Geisser correction was adopted for sphericity violations and an alpha level of .05 was applied for significance. Furthermore, all data was presented as mean (M) and standard deviation (SD).

5.1.1 Velocity and Height Control

The velocity control of the pilots was expected to be constantly reduced at lower visibility conditions with the basic flight guidance display (FG). In contrast, differences were expected with higher velocities using the advanced sense and avoid display (FGSA). Figure 5-1 shows the mean velocity adjustments of all sixteen pilots with standard deviations for all conditions. The velocity control revealed a strong main effect of the visibility, $F(1.23, 18.39) = 125.18$, $p < .001$, $\eta_p^2 = .89$, and also of the display type, $F(1, 15) = 21.92$, $p < .001$, $\eta_p^2 = .59$. In general, velocity adaption decreased at lower visibility conditions for both display types. With the advanced FGSA concept, higher velocities were achieved with significant differences at the visual ranges of 100 m, 200 m,

and 400 m. At 800 m of visual range, no significant difference was found as expected, since the advantage of the terrain and obstacle visualization was not absolutely necessary during moderate or better visibility conditions. This can be verified by the significant interaction effect of visibility and display type, $F(1.23, 18.39) = 6.40$, $p = .004$, $\eta_p^2 = .30$.

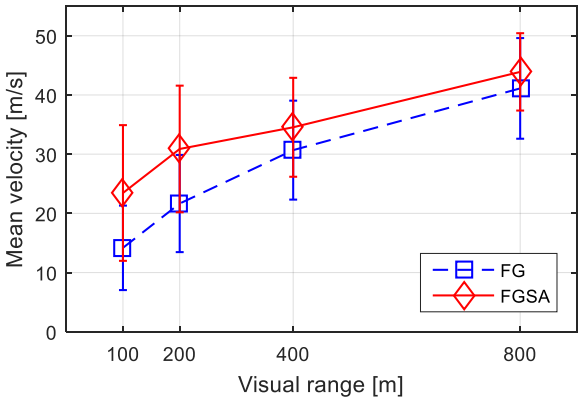

Figure 5-1: Velocity control results [184]

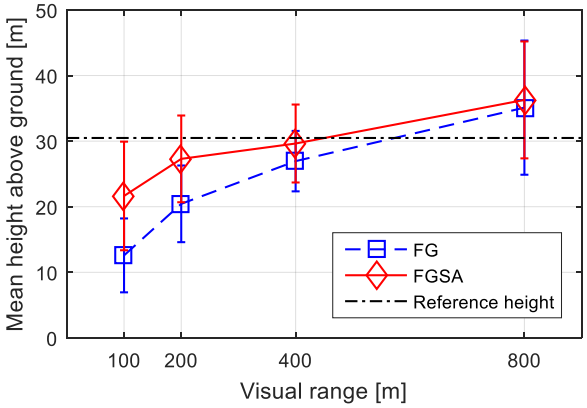

Figure 5-2: Height control results [184]

The pilots were able to fly with a moderate velocity of around 40 m/s (≈ 80 knots) at 800 m of visual range with both display types. While they had to reduce the speed below 15 m/s (≈ 30 knots) at 100 m of visibility with the FG display type, they were able to fly 65 % faster with the FGSA display at the lowest visibility range of the experiment. Table 5-1 lists detailed mean values with standard deviations for all conditions together with p-values for the significance of the differences between the display types.

Visibility	FG (SD)	FGSA (SD)	p-value
100 m	14.18 (7.14)	23.44 (11.46)	.000
200 m	21.66 (8.23)	30.88 (10.70)	.000
400 m	30.68 (8.36)	34.54 (8.36)	.041
800 m	41.11 (8.50)	43.90 (6.53)	.176

Table 5-1: Mean velocity control [m/s]

Similar results were obtained for the control of the height above ground, see Figure 5-2. Both main effects were again significant, the visibility $F(0.99, 14.87) = 29.75$, $p < .001$, $\eta_p^2 = .66$, the display type $F(1, 15) = 23.86$, $p < .001$, $\eta_p^2 = .61$ and the interaction $F(0.99, 14.87) = 5.73$, $p = .005$, $\eta_p^2 = .28$. Multi-comparisons of the individual cases showed significant differences between the display variants at the two lower visibility conditions of 100 m and 200 m. The pilots could not maintain the 100 feet (≈ 30 m) reference height at 100 m of visual range with both display types, due to the missing ground visibility. With 800 m of visual range, the pilots also struggled to track the reference height. They tried to stay outside the obstacle scenery, because their intuition caused them to reduce the risk of potential collisions. Thus, they flew higher in moderate or better visual conditions (800 m), because they could see the obstacles far in advance. In addition, the result of higher altitude control at the lower visibility conditions demonstrates that the terrain and obstacle presentation in the FGSA display helped the pilots to maintain sufficient visual references, even with very limited ground visibility available. Table 5-2 lists the detailed height above ground

results for each condition with p-values for significance of the differences between the display types.

Visibility	FG (SD)	FGSA (SD)	p-value
100 m	12.58 (5.63)	21.64 (8.28)	.000
200 m	20.44 (5.84)	27.29 (6.61)	.001
400 m	26.95 (4.61)	29.64 (5.94)	.065
800 m	35.10 (10.23)	36.28 (8.91)	.532

Table 5-2: Mean height above ground [m]

Even tough, no significant results regarding differences between the pilots were expected with a sample size of sixteen pilots, the velocity control behavior has been analyzed considering the age of the pilots, their experience with respect to the total amount of flight hours and the group of pilots holding an instrument flight rating (IFR) compared to pilots flying according to visual flight rules (VFR) only. In addition, the influence of the display type sequence has been analyzed, looking at the fact if the pilots started with the FG display or the FGSA display. Besides the group of IFR versus the group of VFR pilots, no significant differences could be observed. The interaction of the display type with the between subject factor IFR/VFR resulted in a marginal significant effect $F(1, 14) = 4.64$, $p = .049$, $\eta_p^2 = .25$. Figure 5-3 shows the differences in pilot velocity control behavior between IFR and VFR pilots.

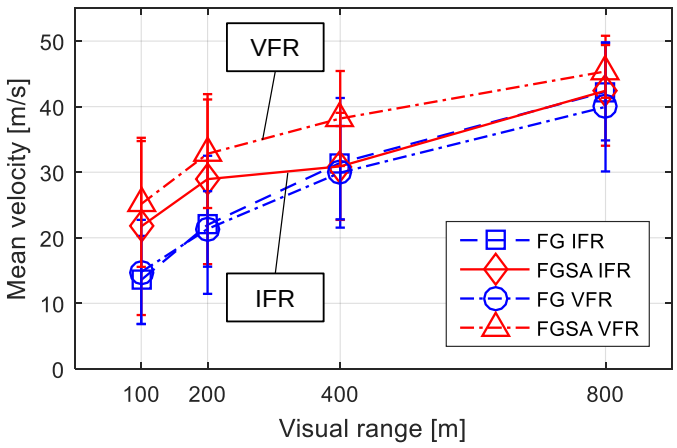

Figure 5-3: Comparison of velocity results between IFR and VFR pilots

Both groups adjusted the velocity nearly identical with the FG display type. The IFR pilots showed only differences with the FGSA display type at the lower visibility conditions of 100 m and 200 m. They flew with a similar velocity with the FGSA display at 400 m and 800 m. Reason for that could be that the IFR pilots were more familiar with severely degraded visual conditions as they frequently fly under zero-visibility conditions according to the instrument flight rules. In addition, they learned to rely on the instruments in such conditions. In case of further visual degradation, they could initiate a climb and switch over to the instrument flight procedure. In contrast, the VFR pilots relied solely on what they could see and the available visual cues. Thus, they flew faster with the additional information of the FGSA display during all visibility conditions compared to the basic FG display.

5.1.2 Obstacle Avoidance Maneuvers

The minimum clearance to the obstacles after the avoidance maneuvers have been conducted by the pilots show a similar trend as the results from velocity and height control evaluation. Figure 5-4 shows the results of these minimum distances from the lateral avoidance maneuvers. The pilots came closer to the obstacles at 100 m and 200 m of visual range, due to the limited time margin to initiate an avoidance maneuver with the FG display type. With the FGSA variant, they could maintain a constant average lateral clearance of around 65 m. All main effects and the interaction were again significant, in fact, the visibility $F(2.20, 32.98) = 14.73$, $p < .001$, $\eta_p^2 = .50$, the display type $F(1, 15) = 32.36$, $p < .001$, $\eta_p^2 = .68$ and the interaction $F(2.20, 32.98) = 10.89$, $p < .001$, $\eta_p^2 = .42$.

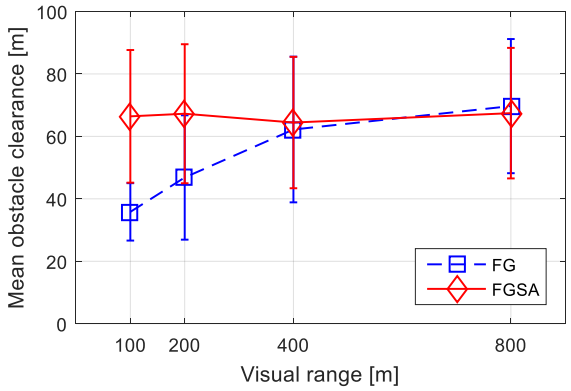

Figure 5-4: Minimum lateral distance to obstacles [184]

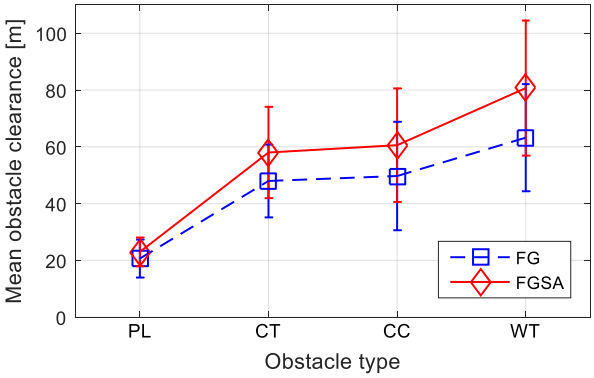

Figure 5-5: Minimum distance dependent on obstacle type

Table 5-3 shows the mean values with standard deviations of the minimum lateral clearance to the obstacles, again with p-values for significance of the differences between the two display variants.

Visibility	FG (SD)	FGSA (SD)	p-value
100 m	35.83 (9.19)	66.42 (21.24)	.000
200 m	46.84 (19.91)	67.26 (22.26)	.000
400 m	62.21 (23.33)	64.44 (21.04)	.666
800 m	69.70 (21.48)	67.44 (20.90)	.577

Table 5-3: Minimum lateral distance to obstacles [m]

Figure 5-5 shows the mean minimum obstacle clearance depending on the obstacle type over all visibility conditions, in fact, the power line (PL), the cell tower (CT), the construction crane (CC) and the wind turbine (WT). The vertical avoidance maneuver resulted in a very low clearance of around 20 m and with no significant difference between the two display types, because of the limited space when pilots crossed the power line underneath. The largest minimum distances were obtained for the wind turbine. A reason therefor could be that the wind turbine was the largest obstacle and the pilots expected a higher risk from the potentially rotating blades, even though, they were static in the scenario.

Figure 5-6 shows the results of the two events at which the pilots detected and triggered (DT) the obstacles in the flight path, and when they initiated the required avoidance maneuver (AV). With the FG display type, the visibility range was the limit for detecting the obstacles in the outside view, shown by the blue dashed line and the circle markers. While the pilots were able to detect the obstacles with the saliency in the FGSA display before they appeared in the real outside view at a distance of around 1,000 m, marked with red circles in the figure. It should be mentioned again that the obstacle appearance was set to 1,500 m in the FGSA display, due to sensor limitations and to reduce the amount of information in order to declutter the display. This early detection of obstacles in the flight path provided additional time for the pilot to judge the environmental situation and to derive the best action.

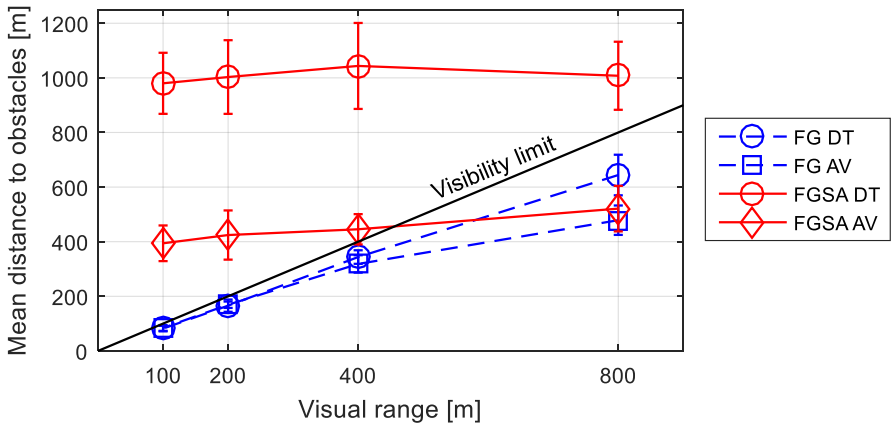

Figure 5-6: Distance of obstacle detection (DT) and avoidance (AV) [184]

The distance at which the pilots initiated the obstacle avoidance maneuver (AV) was even more interesting, because it provided an indication of the safety margin the pilots decided to maintain. For the FG display type, the limiting factor was again the visual range. An immediate reaction was required by the pilots at the lower visibility conditions (100 m, 200 m and 400 m) in order to avoid collisions, marked by the blue rectangles in Figure 5-6. In some cases at 100 m of visual range, the pilots first responded with a control input, before they were able to trigger the obstacle detection. In contrast, with the FGSA display type, the pilots were able to initiate the avoidance maneuver much earlier at safe distances between 400 m and 500 m. They reacted to the obstacles based on the FGSA information before they could actually perceive the obstacles in the outside view. Thus, very strong significant effects were obtained for the visibility $F(1.80, 27.03) = 137.55$, $p < .001$, $\eta_p^2 = .90$, the display type $F(1, 15) = 260.49$, $p < .001$, $\eta_p^2 = .95$ and the interaction $F(1.80, 27.03) = 40.20$, $p < .001$, $\eta_p^2 = .73$. At 800 m of visual range, again, no significant differences between the two display types were found for the initiation of the obstacle avoidance maneuvers. Table 5-4 shows the detailed results for both display types together with the p-values for the significance of the differences between FG and FGSA. While the detection of obstacles was triggered by the pilot, the start of the avoidance maneuver had to be determined manually by analysis of the pilot control input and flight path deviation. If an avoidance maneuver could not be defined clearly, only the results of the remaining obstacles were taken into account for comparison. This procedure was also applied for the detection event, when pilots failed to trigger an obstacle and the analysis of the video recordings could not reveal whether the perception of the obstacle

was really missed, or a pilot trigger was simply absent. Missing trigger events from the pilots occurred only during visual ranges of 100 m and 200 m, due to the higher workload.

Visibility	FG (SD)	FGSA (SD)	p-value
100 m	84.10 (10.54)	394.14 (65.31)	.000
200 m	169.12 (11.70)	424.36 (90.10)	.000
400 m	318.52 (31.83)	445.46 (55.46)	.000
800 m	478.73 (53.85)	521.07 (83.41)	.098

Table 5-4: Distance to obstacles at the initiation of the avoidance maneuver (AV) [m]

Furthermore, determining the exact initiation point of the obstacle avoidance maneuvers is difficult and a time-consuming task. To improve this process, recent techniques considering time-frequency representations (TFR) of the pilot control activity [177] have been investigated. While these analyzing methods have shown unique insight into handling qualities evaluation [178], continued research is suggested to obtain distinct results for determining the initiation of an obstacle avoidance maneuver [184]. For the experiment conducted, the time-frequency representation (e.g. spectrogram of a short-time Fourier transform of the control input signal) did not reveal satisfying results. Further results on the obstacle avoidance maneuvers and the flight path tracking accuracy are provided in the appendix A.2. A root-mean-square error of the flight path deviation has not been evaluated, because most departures from the flight path were intentionally caused by the obstacle avoidance maneuvers. However, the figures provide additional qualitative impressions about all 128 test runs.

5.1.3 Pilot Workload

The pilot workload has been assessed by subjective ratings of the NASA Task Load Index (TLX). Figure 5-7 shows the results of the eight conditions, which indicate a strong significant influence of the visibility $F(1.29, 19.27) = 47.06$, $p < .001$, $\eta_p^2 = .76$.

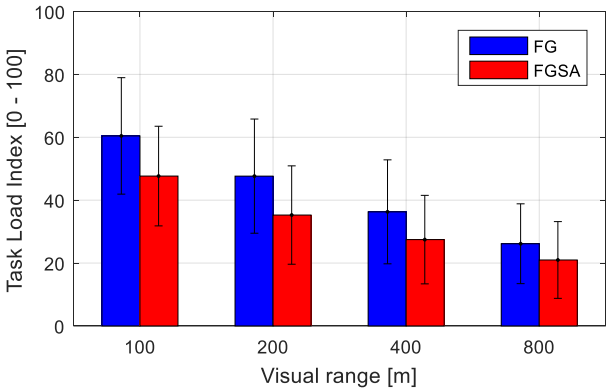

Figure 5-7: Workload results (NASA-TLX) [184]

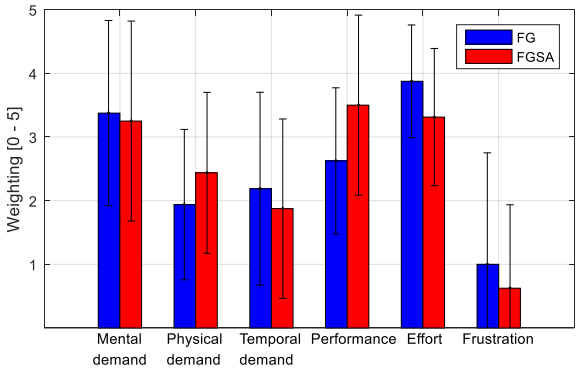

Figure 5-8: Task-Load-Index weighting

The TLX and thus pilot workload increased as the visibility range decreased for both display types. However, for all visibility conditions tested, the workload was rated significantly lower with the FGSA display variant, $F(1, 15) = 18.99$, $p < .001$, $\eta_p^2 = .56$. In addition, the interaction of both main effects was also significant, although less distinct, $F(1.29, 19.27) = 3.28$, $p = .037$, $\eta_p^2 = .18$.

Table 5-5 presents the corresponding mean TLX-values with standard deviations together with the p-values for the significance of the differences between the two display types. With the additional information for the pilots presented on the FGSA display, the workload was reduced about 25 % compared to the basic FG display.

Visibility	FG (SD)	FGSA (SD)	p-value
100 m	60.44 (18.52)	46.67 (15.84)	.001
200 m	47.65 (18.16)	35.27 (15.64)	.001
400 m	36.29 (16.53)	27.46 (14.07)	.012
800 m	26.15 (12.69)	20.98 (12.20)	.008

Table 5-5: Pilot workload (NASA-TLX) [0 – 100]

A weighting of the six NASA-TLX dimensions has been conducted directly after the four runs for each display type respectively. Figure 5-8 shows these weighting results for both display types. Since the task for the pilots did not change and the amount of information on the display was the only modification applied, the weighting results did not differ very much. Only the physical demand ($p = .041$) and performance ($p = .034$) weighting resulted in slightly, but significant differences. However, the results demonstrate the subjective evaluation of the pilots about the relevance of each TLX dimension for the low-altitude task in DVE. Effort, mental demand and performance were weighted higher than physical demand, temporal demand and frustration, which was less relevant. In addition, Figure 5-9 and Figure 5-10 demonstrate the TLX rating results on the main effect display type and visibility respectively. Thus, Figure 5-9 represents the differences between the FG and FGSA variant as mean over all visibility conditions. Similarly, Figure 5-10 shows the results of all six TLX dimensions for the four visibility conditions independently of the display type.

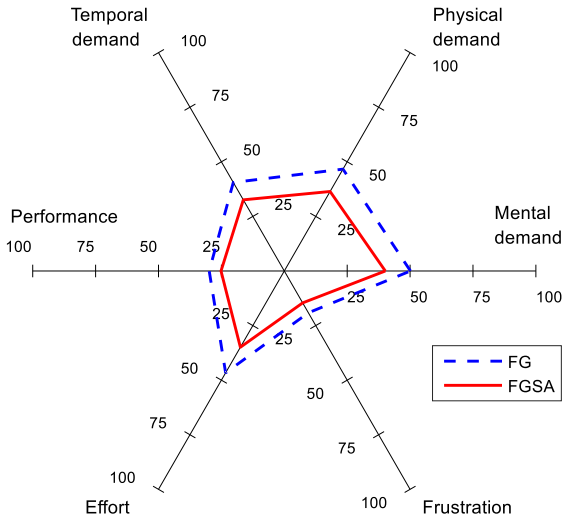

Figure 5-9: Workload results on main effect display type [184]

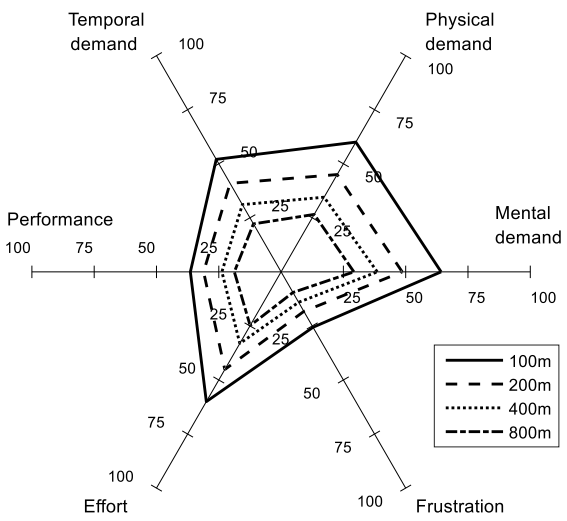

Figure 5-10: Workload results on main effect visibility [184]

Both figures show that the results of the two main effects are consistent across all six TLX dimensions. The categories mental demand, physical demand and effort were rated with the

highest scores, followed by the temporal demand and the pilot's evaluation of their own performance. The frustration level was very low in general, since all pilots were able to complete the scenarios successfully without obstacle collisions.

5.1.4 Manual Adjustment of the Visual Range

The subtask scenario of culling the near-field information in order to reduce visual clutter has been conducted again with the professional pilots. Figure 5-11 shows the results of the pilots compared to the outside visual reference distance and the student trials in a dynamic changing visual environment.

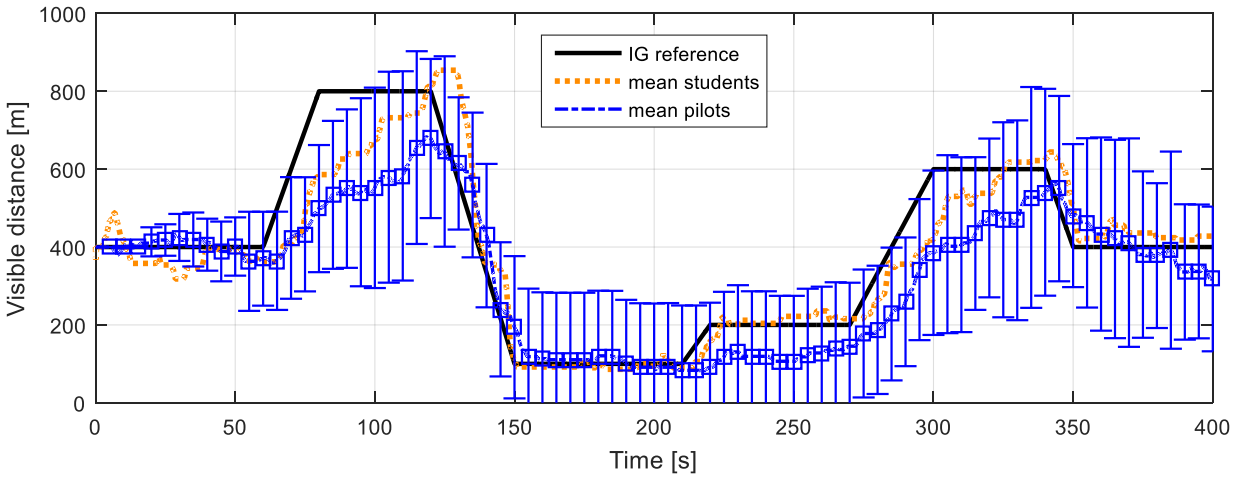

Figure 5-11: Mean visible distance setting of the pilots (N = 15) compared to the simulated image generator (IG) reference and the student trials (N = 5)

While the task of flying was removed for the students, the pilots had to fly the helicopter manually to increase the workload. Only fifteen pilots participated in this subtask scenario. In general, the pilots were able to adjust the visual range, but they could not achieve the same accuracy as of the student trials. The variances in setting the distance were also very large. However, the results show a similar trend. The pilots required a longer period of time to realize improvements of the outside visual conditions (60 s – 120 s and 270 s – 330 s) compared to the quick and precise adjustments made in the opposite case when the visibility degraded (120 s – 150 s and 340 s – 350 s). The pilots did not respond to the small change of the visible distance from 100 m to 200 m (210 s – 270 s) at all. The critical case again occurs when the visibility degrades and the near-field culling is not adjusted. Then, required information is neither presented in the HMD, nor is it visible in the outside cues. Here, the pilots responded quickly and precisely as the students did before. The slow adjustment of the near-field culling in case of visibility improvements is less critical. Important information is still visible in both the HMD and the outside view. However, it is suggested to further investigate the potential negative effects of visual clutter, caused by wrong or imprecise visual range adjustments. Additionally, the development of a sensor, capable of measuring the visual range, would relieve the pilot in this task.

5.1.5 Discussion on the Sense and Avoid Task

Based on the results of velocity and height control of the pilots and the obstacle avoidance maneuvers described previously, this section discusses the findings in general and compares them with previous work from literature, as previously presented by the author in [184].

5.1.5.1 Time-to-Contact

The time margin available for the pilots to react to obstacles or to make decisions on obstacle avoidance maneuvers is very important and provides an indication for flight safety. The time-to-contact (TTC) to the obstacles at the beginning of the avoidance maneuver reveals the time the pilots tried to retain and thus it represents this safety margin. For deceleration maneuvers, Padfield [128] demonstrated a constant $\dot{\tau}$-guidance strategy applied by the pilots, in which τ represents the time-to-contact. However, the obstacle avoidance maneuvers, which contain a turn or a climb differ from the acceleration maneuver and τ-guidance could not be verified for these maneuvers so far. The experiment of this work focused on the specific point in time, when the pilots initiated the obstacle avoidance maneuver, instead of continuously tracking the τ-motion until the obstacle has been passed. Figure 5-12 shows the TTC with constant velocity of both display types regarding the distance to the obstacles and to the fog (visible limit) when the avoidance maneuver was initiated.

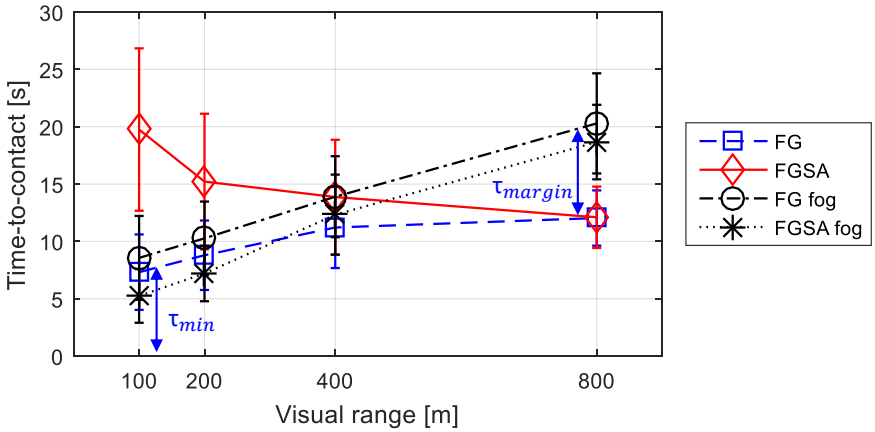

Figure 5-12: Time-to-contact to obstacles and fog [184]

The TTC to the obstacles represents the available time to react to the obstacles, which are placed into the flight path, while the TTC to the wall of fog represents the available time to react to the remaining outside cues, i.e. the cues visible despite the fog. For the TTC to the obstacles the main effect display type resulted in significant differences $F(1, 15) = 43.36$, $p < .001$, $\eta_p^2 = .74$, while the main effect visibility $F(0.97, 14.54) = 1.93$, $p = .16$, $\eta_p^2 = .11$ did not result in significant differences due to the high level of interaction with decreasing visibility $F(0.97, 14.54) = 46.28$, $p < .001$, $\eta_p^2 = .76$. Table 5-6 shows the detailed results of the TTC to the obstacles with mean and standard deviation together with the p-values for the significance of the differences between the two display types.

Visibility	FG (SD)	FGSA (SD)	p-value
100 m	7.32 (3.29)	19.76 (7.08)	.000
200 m	8.79 (3.03)	15.22 (5.91)	.000
400 m	11.22 (3.54)	13.87 (4.99)	.005
800 m	12.04 (2.41)	12.10 (2.68)	.925

Table 5-6: Time-to-contact to obstacles [s]

Under moderate visual conditions (800 m), the pilots initiated the avoidance maneuver 12 seconds ahead to the obstacles with both display types. At that point, they had 18 seconds with the FGSA display and 20 seconds with the FG display type as a time-to-contact limit for the remaining outside cues up to the distance of fog. With the FG display variant, the pilots reduced this buffer almost consistently to at least 7 to 8 seconds with decreasing visibility. With the FGSA display type, they flew faster and thus reduced the TTC to the fog even further, down to around 5 to 6 seconds. However, regarding the obstacle itself, the TTC increased with the FGSA display type at the lower visibility conditions. It appears that not all pilots trusted the visual assistance completely and it seemed as if they did not want to rely solely on the visual assistance system. The increasing variances with the FGSA display type under decreasing visibility indicate the increase in uncertainty of the pilots. Moreover, their confidence might have been affected by the short amount of training time available, although they were told to assume that the system is reliable for this experiment. Consequently, the pilots acted conservatively and maintained a minimum safety margin with respect to the remaining outside cues and to completely unexpected events, which could not be detected by a sensor supported visual assistance system.

These findings are consistent with those of Clark in [36]. In his experiment, the test pilot retained a minimum TTC (τ_{min}) of between 5 and 8 seconds in degraded visual conditions with a limited optical flow field available. Furthermore, an additional time margin (τ_{margin}) to the minimum time required for conducting the maneuver was determined and related to the Usable Cue Environment (UCE) of the ADS-33E-PRF. According to this derived classification, the visibility condition of 800 m in the current experiment can be related to good visual conditions (UCE 1) with more than 7 seconds of time margin available. The 400 m of visual range would correspond to the boundary between moderate (UCE 2) and severe degraded visual conditions (UCE 3) with 3 seconds of time margin for the FG display type, as expected. However, the results presented so far demonstrate that with the FGSA display this time margin can be influenced positively, as long as the obstacle information can be detected and indicated on the HMD. The minimum time for conducting the maneuvers explains to some extent the reduction in velocity control at lower visibility conditions (Figure 5-1), since most pilots tried to retain that minimum time to react to unexpected events, for instance to obstacles, which could not be highlighted on the HMD. Considering the anticipated hypothesis at the beginning of this work (Figure 1-5), the pilots flew faster with the additional information about the environmental situation displayed with the FGSA variant. However, the pilots also reduced the velocity as visibility decreased in order to retain a safe flight with the minimum time margin of 5 to 6 seconds, which was also concluded by Padfield in [129].

5.1.5.2 Invariable Distance and Velocity in Eye-heights

The discussion about time-to-contact does not explain the increasing period of TTC to the obstacles as visibility decreased using the FGSA display type. Considering the hypothesis of Padfield [129], the pilots require information from the usable optical flow region (see Figure 2-27), which is located between 12 and 15 eye-heights in front of the helicopter. Figure 5-13 shows the results of the mean distance to the obstacles in eye-heights at the onset point of the avoidance maneuver. The large differences between the FG and FGSA display variant at lower visibility conditions resulted in a significant main effect of the display type $F(1, 15) = 74.79$, $p < .001$, $\eta_p^2 = .83$, and the interaction between the visibility and the display type $F(1.07, 16.07) = 23.23$, $p < .001$, $\eta_p^2 = .61$, but not on the visibility effect $F(1.07, 16.07) = 2.40$, $p = .133$, $\eta_p^2 = .14$.

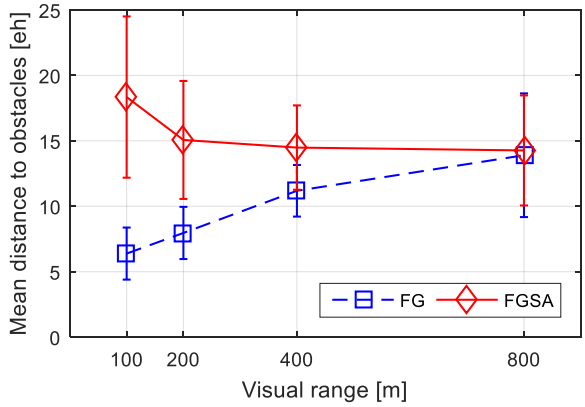

Figure 5-13: Distance to obstacles at the avoidance maneuver in eye-heights [184]

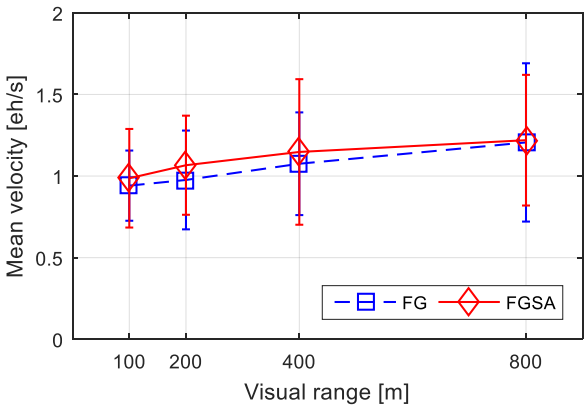

Figure 5-14: Velocity control in eye-heights per second [184]

Table 5-7 shows the corresponding mean values with standard deviations for the distance to the obstacles in eye-heights (eh) together with the p-values for the significance of the differences between the two display types.

Visibility	FG (SD)	FGSA (SD)	p-value
100 m	6.39 (1.99)	18.35 (6.16)	.000
200 m	7.96 (1.99)	15.07 (4.51)	.000
400 m	11.19 (1.97)	14.49 (3.22)	.002
800 m	13.90 (4.73)	14.27 (4.21)	.701

Table 5-7: Distance in eye-heights [eh] to the obstacles

The results show that the pilots were able to maintain a mean distance to the obstacles of 14 to 15 eye-heights with the FGSA display, except in the case of 100 m visibility. At the visual range of 800 m no significant differences between the two display variants were observed. However, with the FG display type, the distance to the obstacles in eye-heights decreased as visibility decreased. Since the pilots could not react to the obstacles at larger distances in the low visibility conditions without further information displayed on the HMD, they could only maintain this constant distance in eye-heights by further reducing the height above ground. However, they already flew as low as possible with about 10 m to 20 m within the visual ranges of 100 m and 200 m. Thus, one reason

why they did not maintain the constant distance in eye-heights could be that they were not able to further decrease the height above ground. However, it is assumed that they responded to the usable flow region of around 15 eye-heights as long as they could retain enough τ_{margin}. With a reduced time margin due to visibility constraints, the distance, height, and velocity were also reduced.

Another interesting parameter observed was the velocity in eye-heights per second (eh/s), which demonstrated invariant pilot behavior. Even though adjusted velocity and height showed significant differences in the absolute values for both display types (see Figure 5-1 and Figure 5-2), the velocity in eye-heights per second (eh/s) did not result in significant differences for the main effect display type $F(1, 15) = 2.60$, $p = .128$, $\eta_p^2 = .15$ (see Figure 5-14), nor did the interaction with the visibility result in significant differences $F(1.38, 20.74) = 0.38$, $p = .683$, $\eta_p^2 = .02$. Only the main effect visibility showed slight differences with lower velocities (in eh/s) as visibility decreased $F(1.38, 20.74) = 7.87$, $p = .003$, $\eta_p^2 = .34$. Table 5-8 shows the individual results for each visibility condition tested with the p-values for differences between the display types.

Visibility	FG (SD)	FGSA (SD)	p-value
100 m	0.94 (0.22)	0.99 (0.30)	.427
200 m	0.98 (0.30)	1.07 (0.30)	.192
400 m	1.08 (0.31)	1.15 (0.45)	.135
800 m	1.21 (0.48)	1.22 (0.40)	.829

Table 5-8: Velocity control in eye-heights per second [eh/s]

An interesting comparison was found by Kaiser et al. [85] with the average person's normal walking speed of around 1.5 m/s. The normal walking speed results in about one eye-height per second or slightly above when moving through the environment. Thus, it is assumed that the pilots simultaneously control velocity and height to perceive a constant amount of image velocity or optical flow with velocities between 0.9 eh/s and 1.3 eh/s. They tried to maintain this amount of information as they experienced the optical flow when walking or moving through the environment. Even though this effect is slightly influenced by the visibility conditions, it is independent of the display type used. Similar results with velocities ranging from 0.9 eh/s to 1.4 eh/s were obtained by Clark [36] for the stopping maneuver in visual ranges between 80 m and 720 m. His results differed for the climbing and turning maneuver with velocities of around 2.5 eh/s. However, he found out that the velocity in eye-heights per second was strongly influenced by the amount of micro-texture available to the pilot. This could be a reason for this deviation, but also for the general reduction of velocity in eye-heights as visibility decreased in the current experiment.

5.1.5.3 Head Motion

The small FOV of the low-cost HMD of 23° x 17° led to the assumption that the pilot's head motion could increase with the degradation of the outside visibility. Moreover, the required head motion for searching obstacles without the synthetic visualization in the FGSA display type could have led to an increase of head motion using the FG display type. Figure 5-15 shows the root-mean-square error (RMSE) of the head motion yaw angle and Figure 5-16 shows the RMSE of the

head motion pitch angle. These head movements are necessary for scanning the environment, while the roll attitude is of minor importance. Both assumptions mentioned above could not be observed for the yaw head motion in the experiment with the resulting main effect of the visibility $F(0.91, 13.72) = 0.27$, $p = .680$, $\eta_p^2 = .02$, and the display type $F(1, 15) = 0.30$, $p = .589$, $\eta_p^2 = .02$. Additionally, the interaction did also not show a significant effect $F(0.91, 13.72) = 0.08$, $p = .913$, $\eta_p^2 = .01$.

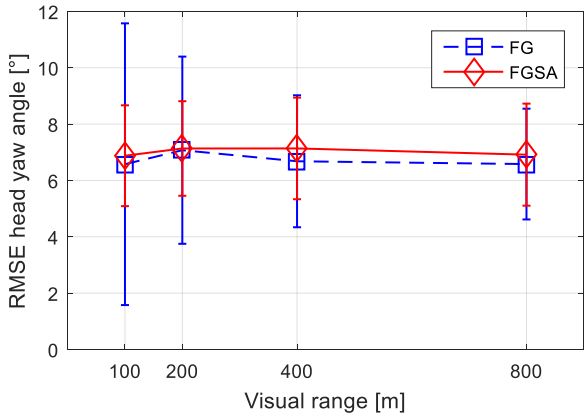

Figure 5-15: Head motion – yaw angle

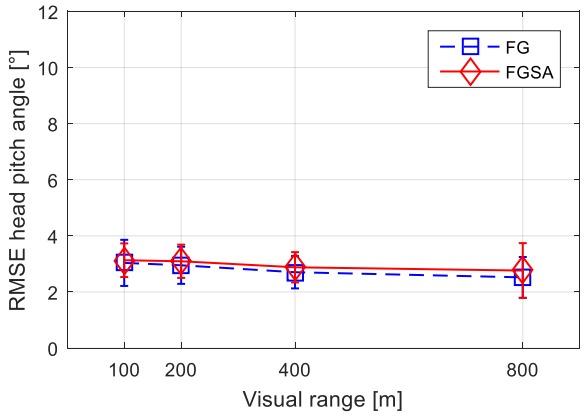

Figure 5-16: Head motion – pitch angle

Table 5-9 and Table 5-10 show the mean results of the yaw and pitch RMSE respectively, with the p-values for the significance of the differences between the two display types. The only difference that could be observed with the yaw angle between the display types was the increasing standard deviation of the FG type with the two lower visibility conditions of 200 m and 100 m. The general uncertainty of the pilots during these situations could be a reason for the variances between the pilots, since most pilots are not very familiar with such low visibility conditions or usually try to avoid them.

Visibility	FG (SD)	FGSA (SD)	p-value
100 m	6.58 (5.00)	6.88 (1.79)	.769
200 m	7.07 (3.32)	7.13 (1.68)	.943
400 m	6.68 (2.34)	7.14 (1.80)	.392
800 m	6.58 (1.97)	6.92 (1.81)	.292

Table 5-9: RMSE head motion – yaw angle [°]

The RMSE of the pitch head motion showed indeed a significant, although very slight increase of head motion with decreasing visual ranges $F(1.49, 22.33) = 4.34$, $p = .021$, $\eta_p^2 = .22$. Moreover, the main effect of the display type was also significant $F(1, 15) = 6.73$, $p = .020$, $\eta_p^2 = .31$, while the interaction between the two main effects was not significant $F(1.49, 22.33) = 0.10$, $p = .883$, $\eta_p^2 = .01$. Contrary to the assumption above, the RMSE of the pitch angle was even higher with the FGSA display type than with the FG variant. However, the overall magnitude of the pitch motion was very low compared to the yaw motion. Thus, the small differences, which are not significant according to the individual comparisons (see Table 5-10), do not allow to derive a meaningful conclusion.

Visibility	FG (SD)	FGSA (SD)	p-value
100 m	3.04 (0.82)	3.13 (0.60)	.584
200 m	2.95 (0.66)	3.09 (0.59)	.335
400 m	2.70 (0.58)	2.88 (0.54)	.266
800 m	2.52 (0.73)	2.76 (0.98)	.328

Table 5-10: RMSE head motion – pitch angle [°]

In summary, no considerable differences in the amount of head motion depending on the visibility and between the display types could be observed during the low-altitude scenario.

5.1.5.4 Subjective Pilot Evaluations

Further subjective pilot feedback was collected in addition to the evaluated pilot workload and the objective flight parameters. The questionnaire focused on the less tangible factors, for instance, the situational awareness, the attention allocation, the occlusion of the outside view or if some parts of the display concept were confusing for the pilot rather than providing useful assistance. The rating was based on a four point Likert scale (1: Agree; 2: Rather agree; 3: Rather disagree; 4: Disagree). The questionnaire began with the evaluation of the 3D-conformal terrain and obstacle representation, followed by a few questions about the flight guidance parameter visualization. Finally, the design principles of color-coding and information culling were addressed.

The 3D-conformal terrain representation in general was rated as being intuitive and comprehensible and it increased the pilot's situational awareness and their spatial orientation. Table 5-11 shows the rating results with mean values and standard deviation for the query.

The 3D-conformal terrain visualization ...	**M (SD)**
… was intuitive and comprehensible in general	1.2 (0.4)
… increased situational awareness	1.1 (0.3)
… increased spatial orientation	1.3 (0.5)
… enabled an assessment of distance to ground	2.4 (0.8)
… enabled an assessment of velocity	2.3 (0.6)
… demanded too much attention	3.4 (0.6)
… occluded important information in the outside view	3.3 (0.6)
… was confusing	3.9 (0.3)
… was disturbing	3.8 (0.4)
… hindered me to perceive other data on the HMD	3.5 (0.5)

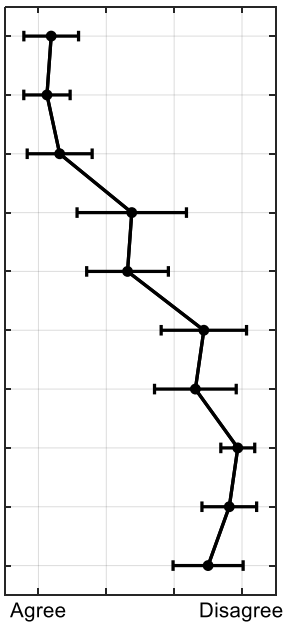

Table 5-11: Subjective pilot evaluation of the 3D-conformal terrain representation

The statements of the pilots differed in the feasibility to assess the distance to ground as well as the velocity by using the combination of the regular terrain grid and contour lines. The missing micro-textures could be a reason for the difficulties several pilots experienced when they tried to sufficiently assess these parameters. One pilot stated that the simulator itself could have caused these difficulties. In addition, the attentional demand was not too high and the displayed data did not occlude important information in the outside view. Moreover, the terrain visualization was neither confusing the pilots, nor was it disturbing. Perception of other data displayed on the HMD was not hindered by the terrain representation by using the information blending concept with background transparency for the flight guidance data.

Table 5-12 shows similar feedback about the 3D-conformal obstacle visualization compared to the terrain representation discussed above. The obstacle visualization was also intuitive and comprehensible in general. It increased the pilot's situational awareness, while attentional demand was not overloading the mental resources of the pilot. The synthetic obstacle representation did not occlude important information in the outside view, as expected, since the active illuminated pixel contribution is much lower than the amount caused by the terrain data (see chapter 3.3). Thus, the perception of other data on the HMD was also not hindered by the obstacle depiction.

The 3D-conformal obstacle visualization ...		**M (SD)**
… was intuitive and comprehensible in general	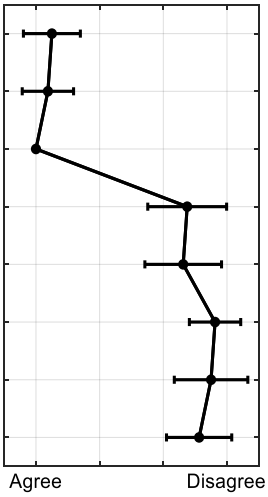	1.3 (0.4)
… increased situational awareness		1.2 (0.4)
… enabled timely detection of obstacles		1.0 (0.0)
… demanded too much attention		3.4 (0.6)
… occluded important information in the outside view		3.3 (0.6)
… was confusing		3.8 (0.4)
… was disturbing		3.8 (0.6)
… hindered me to perceive other data on the HMD		3.6 (0.5)

Table 5-12: Subjective pilot evaluation of the 3D-conformal obstacle representation

The obstacle visualization was neither confusing nor was it disturbing the pilots. Furthermore, all sixteen pilots completely agreed with the benefit of a timely detection of hazardous obstacles in the flight path.

The navigation markers are not yet available in helicopters operated currently. Since they are still in a research state, feedback on these triangles or arrow-heads on the ground was collected (see Table 5-13). The results show that the navigation markers did not confuse most of the pilots and sufficiently supported them in the given navigation task. Moreover, the arrow-heads were clearly visible during the visibility conditions tested. However, one pilot stated that in very low-altitude and hilly terrain the markers were a bit confusing, while another pilot was able to use the perception of the varying geometry of the triangles to determine the height above ground. The

geometry of the navigation markers is changing, due to different perspectives depending on the height above ground. Two pilots stated, that their attention fixation was very high with the markers, especially below the visual range of 400 m. Potential solutions for this problem could be the reduction of the brightness of the marker or a greater distance between the arrow-heads, which reduces the overall number of used markers. Even though the navigation markers were used in combination with the digital moving map head-down, which additionally showed the reference flight path, two pilots stated that they did not use the map nor was it required for the task at all.

The navigation markers on ground ...		**M (SD)**
… supported me in the navigation task	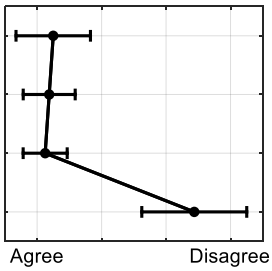	1.3 (0.6)
… were sufficient for the given task		1.2 (0.4)
… were clearly visible		1.1 (0.3)
… were confusing		3.4 (0.8)

Table 5-13: Subjective pilot evaluation of the navigation markers on ground

In general, the pilots were primarily using the HMD for the task and did not pay much attention to the head-down instrumentation. Nevertheless, further research will be needed to address the combination of head-down and head-mounted information perception.

Two aspects about the 2D flight guidance symbology were addressed in the questionnaire, because of the interaction with the 3D-conformal scenery content, in fact, the ability to easily perceive the data and the position on the display (see Table 5-14). Most pilots agreed with an easy readability and they were able to distinguish the 2D symbology from the 3D-conformal terrain and obstacle representation. Both design principles the color-coding and the information blending concept helped the pilot to achieve these capabilities. However, two pilots mentioned that the saliency of speed and radar altitude indication should be increased to improve the readability.

The 2D flight guidance parameters ...		**M (SD)**
… were always readably	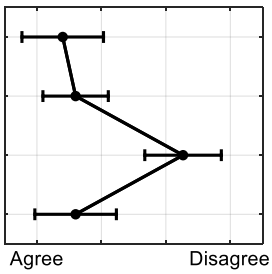	1.4 (0.6)
… at the top enabled unhindered obstacle detection		1.6 (0.5)
… would have been preferred at the center position		3.3 (0.6)
… were distinguishable from the 3D-conformal content		1.6 (0.6)

Table 5-14: Subjective pilot evaluation of the 2D flight guidance parameters

In addition, most pilots agreed with the positive effect of placing the 2D symbology at the upper part of the display in order to have an unhindered view for obstacle detection. Thus, they would not prefer the 2D symbology placed at the center of the display, although this condition has not been individually tested.

Feedback about the color-coding confirmed the useful support for the ability to clearly distinguish between displayed content (e.g. terrain, obstacles and flight guidance parameters) and for an easy perception of individual items located in different frames of reference (see Table 5-15). Most pilots agreed that the use of color resulted in an increased situational awareness, due to the easy and clear differentiation between the different display contents.

The color implementation ...		**M (SD)**
… facilitated the perception of individual items	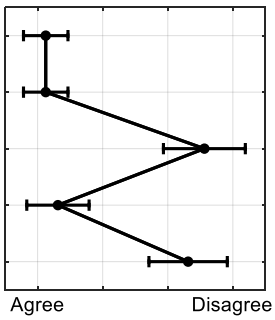	1.1 (0.3)
… increased situational awareness		1.1 (0.3)
… was too colorful		3.6 (0.6)
… enabled a clear differentiation of displayed content		1.3 (0.5)
… could consist of more colors		3.3 (0.6)

Table 5-15: Subjective pilot evaluation of the color implementation

The majority of the pilots agreed that the four complementary colors used in this experiment were not too colorful, but according to their opinion, the design does not need further colors. These findings are consistent with the recommendations from literature to use color only when there is no other way to code the information and when it has been shown to provide a benefit in performance [59].

Furthermore, the near-field culling of scenery content was evaluated by the pilots (see Table 5-16). In general, most pilots rated this functionality as very helpful and most of them consciously recognized the effect. After practicing the manual adjustment of the visual range, this additional task was completely feasible for most of the pilots. The near-field culling supported the pilots in detecting important objects in the real outside view and it was not disturbing, even under suboptimal adjustment, as one pilot stated.

The near-field culling of information ...		**M (SD)**
… I could consciously recognize	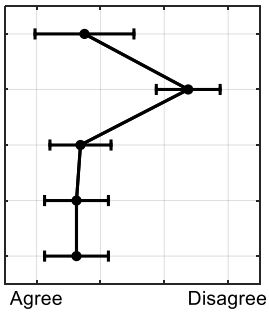	1.8 (0.8)
… was disturbing		3.4 (0.5)
… assisted me in detecting objects in the outside view		1.7 (0.5)
… was very helpful in general		1.6 (0.5)
… was feasible to be adjusted to the visual range		1.6 (0.5)

Table 5-16: Subjective pilot evaluation of the near-field culling

Finally, the pilots were asked to evaluate if hazardous situations occurred during the low-altitude scenarios and how often this happened (see Table 5-17). The rating was based on scale with five increments from ‘always’ to ‘never’. With the support of the HMD, they rarely experienced

disorientation. Moreover, the large amount of presented information on the HMD rarely hindered the pilots to detect hazardous obstacles in the outside view, nor did the pilots experience problems when they shifted their attention between the synthetic and the real-world cues.

Did you experience moments when ...		**M (SD)**
… you were disoriented despite the HMD support?	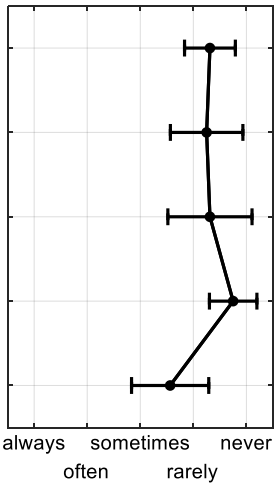	4.3 (0.5)
… you had problems in shifting attention between synthetic and real-world information?		4.3 (0.7)
… the large amount of information hindered you to detect obstacles in the outside view?		4.3 (0.8)
… you felt unsafe at visual ranges above 400 m?		4.8 (0.4)
… you felt unsafe at visual ranges below 400 m?		3.6 (0.7)

Table 5-17: Subjective pilot evaluation of hazardous situations

Almost all pilots felt never unsafe with a visibility above 400 m. However, below 400 m visual range, the number of unsafe situations increased a little bit. One pilot commented that with the FGSA display type in general, the subjective safety feeling was considerably higher than without the obstacle data.

5.2 Precision Hover Scenario Results

The evaluation of the precision hover tasks focuses on performance limitations of the HMD concept as known from literature [75], in fact, field-of-view limitations and missing micro-textures in DVE for rotorcraft stabilization tasks. Besides subjective handling qualities and visual cue ratings, objective pilot behavior, for instance, the control input and head motion, were compared with the resulting hover performance. Three main environmental conditions were investigated, each with three different visibility conditions. The pilots started with a successively decreasing FOV, while hovering at the standard mission task element (MTE) displayed in the outside view. Thus, the influence of the FOV limitation could be determined independently of other effects. These tasks were followed by testing the mission task element references transformed into the HMD visualization concept, namely three times with different visual ranges in ground effect and three times against a wind turbine. The reduction of visibility in the hover task enabled an observation of the influence of missing micro-textures, which are still visible from ground textures in the outside view.

Statistical data analysis was again conducted by using a repeated measures of variance with post-hoc Bonferroni corrections for multiple comparisons. The variation of the different visual hover task conditions was the only independent variable in this scenario. Besides the nine visibility conditions explained above, a tenth hover task was flown as a reference in order to observe any

training effects during the experiment. Greenhouse-Geisser correction was again applied for sphericity violations and an alpha level of .05 was adopted for significance. Only fifteen pilots participated in this part of the experiment, since one pilot could not continue the experiment after experiencing severe spatial disorientation in the first part. Moreover, due to the tight time schedule a few hover task conditions had to be skipped for some pilots. The number of participants for every condition is marked in the comparison section.

5.2.1 Individual Pilot Behavior and Performance in Precise Hovering

Before the root-mean-square errors (RMSE) of the dependent variables are considered with mean and standard deviation of all participants, the absolute values of the raw data measurements are briefly discussed. Figure 5-17 shows an example of one pilot's cyclic control input over ninety seconds of stabilization during the hover task. The first row shows the hover task control input without HMD by using the standard hover mission task element references presented in the outside view. The pilots started with the total FOV of the simulator (200° x 80°), followed by the limitation with a restricted FOV of 40° x 30° and 23° x 17°. The bottom row of Figure 5-17 and the following figures show the results of the HMD visualization concept while hovering in ground effect in twelve feet eye-height with different visual ranges (800 m, 100 m and 25 m). The individual graphs show the control input deflection around the cyclic trim positions (lateral: 54.6 % and longitudinal: 32.3 %) during hover in ground effect. The graphs show a range of +/- 10 % of the overall stick deflection to improve the visibility of differences. This should be kept in mind, when the results presented here are compared to the results from literature (Figure 2-32).

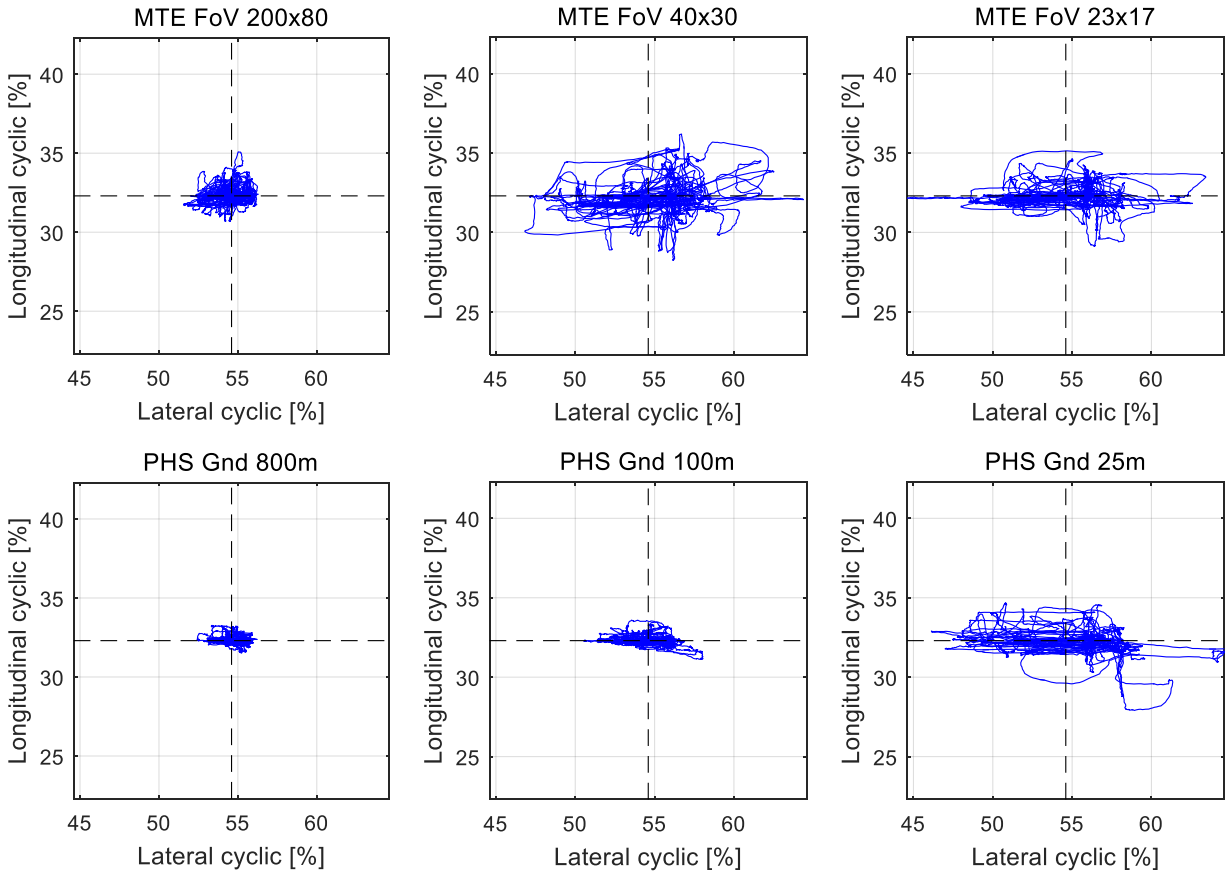

Figure 5-17: Example of one pilot's cyclic control input during the hover tasks

A lateral cyclic input of 0 % corresponds to the maximum left position of the cyclic stick, while 100 % stick deflection corresponds to the maximum right position. In the longitudinal axis, the 0 % corresponds to the maximum backward position and 100 % reflects the maximum forward position. Figure 5-17 shows a very low control activity in the reference condition with the total FOV available (MTE FoV 200x80) and the two better visibility conditions (PHS Gnd 800 m and PHS Gnd 100 m) using the synthetic precision hover symbology on the HMD. The other three conditions show a higher control activity in both axis, but especially the lateral cyclic control input increased extraordinarily.

Similar results were obtained for the horizontal position accuracy depending on the visibility conditions. Figure 5-18 shows the corresponding horizontal positioning results to the above described cyclic control inputs of the same pilot. The small black rectangles show the desired (+/- 3 ft. ≈ 1 m) and adequate (+/- 6 ft. ≈ 2 m) performance boundaries according to the ADS-33E-PRF [5] for the hover mission task element. The reference condition (MTE FoV 200x80) resulted in the best performance in positioning accuracy for this pilot, again followed by the two precision hover symbology conditions with 100 m and 800 m of visual range, besides the one drift backwards in the latter case. The other three conditions resulted in a worse hover precision, not even close to the adequate performance range.

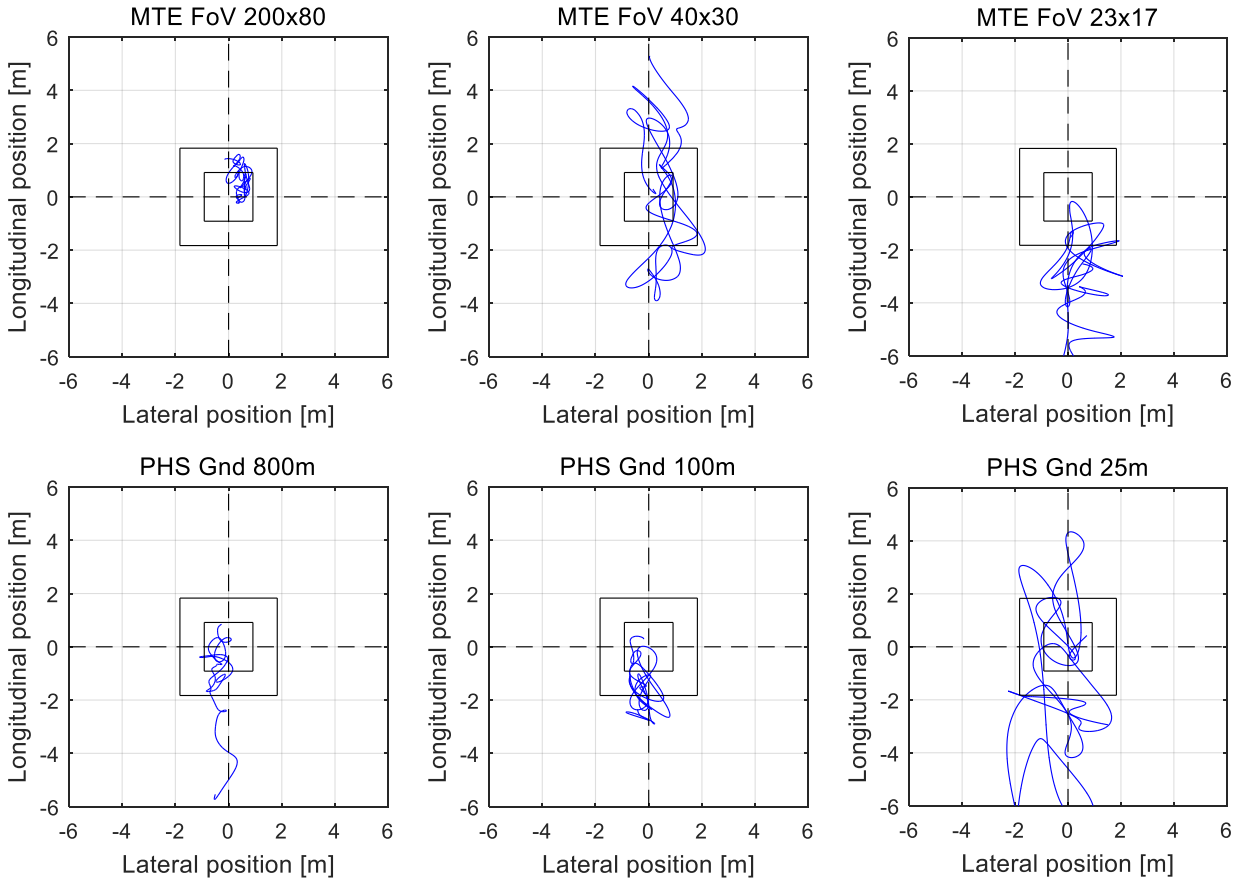

Figure 5-18: Example of one pilot's horizontal positioning accuracy during the hover tasks

What becomes particularly apparent is the relation between the control activity and accuracy in horizontal positioning. With the limited visibility conditions by FOV limitations or missing micro-textures, the control activity increased and position accuracy decreased. However, the lateral

position accuracy was better than the longitudinal performance, due to the higher lateral cyclic control activity (see Figure 5-17). The lower longitudinal increase of cyclic control activity indicates that the pilot was not able to sufficiently detect the longitudinal position error. This phenomena of differences in the perception of the longitudinal and lateral axis based on the FOV limitation was investigated by Bachelder [24]. He further examined artificial gains between the visualization of longitudinal and lateral positioning references to eliminate this effect. In the design concept of this work, the poor perception of longitudinal position was tried to be mitigated by adding the two-dimensional co-planar view, which shows the horizontal position as a view from above and the additional longitudinal marker, which moves along the axis in front of the helicopter. For visual ranges of 800 m and 100 m the results show an adequate mitigation. However, the case of 25 m of visual range with nearly no micro-textures from the remaining ground visibility resulted in a similar degradation of the performance than with the FOV limitations.

In addition to the horizontal position accuracy, Figure 5-19 shows the vertical position accuracy around the reference height of 12 ft. (≈ 3.6 m) over the ninety seconds. The dotted line represents the desired performance (+/- 2 ft. ≈ 0.6 m) and the continuous black line represents the adequate performance (+/- 4 ft. ≈ 1.2 m) according to the ADS-33E-PRF hover mission task element definition.

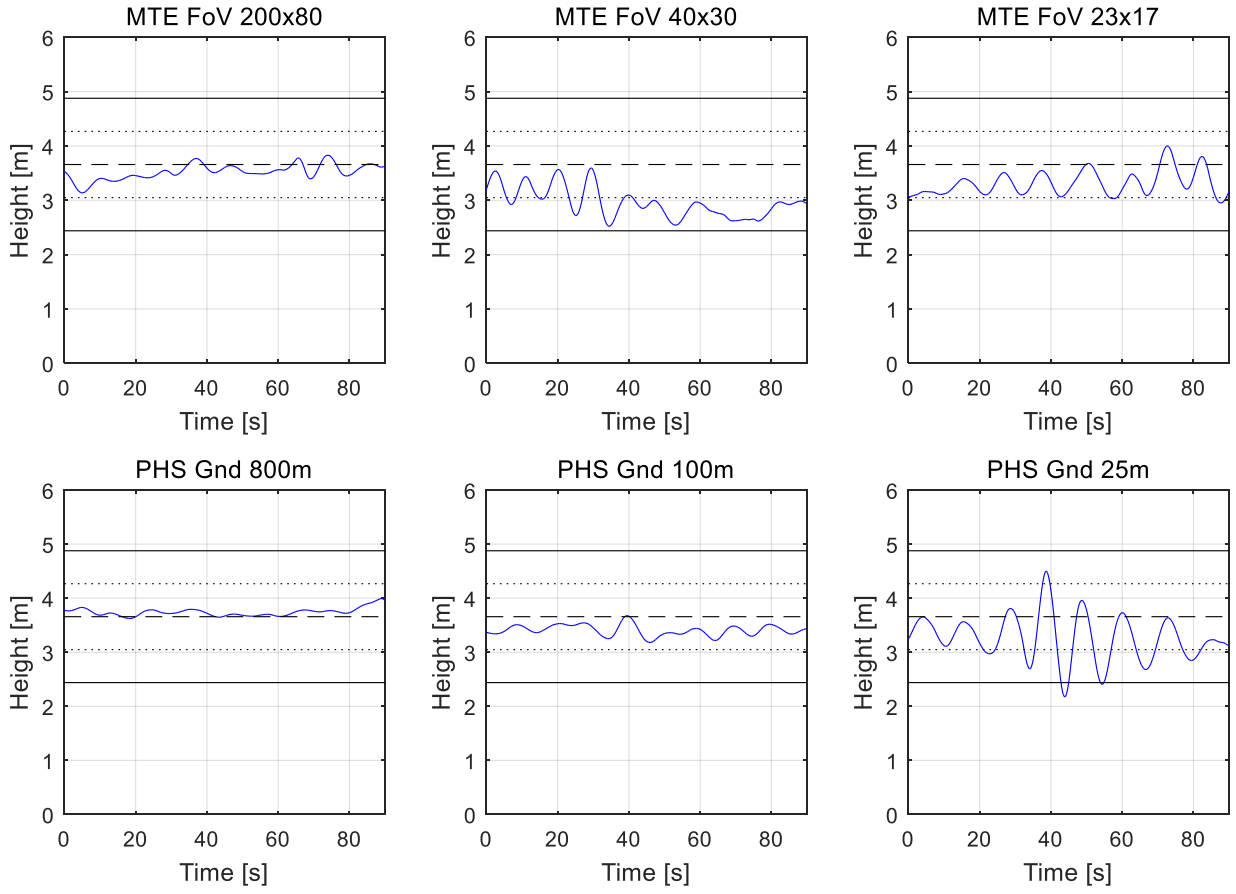

Figure 5-19: Example of one pilot's vertical positioning accuracy during the hover tasks

With the MTE reference condition and when the pilot used the HMD with 800 m and 100 m visual range, he achieved a vertical accuracy within the desired performance limitations. Considering the other three conditions, the pilot was mostly able to maintain the height within the adequate

performance boundaries. However, in these cases a low frequency oscillation in the vertical position can be observed during some time sections.

Figure 5-20 shows further position accuracy results with the heading deviation during the ninety seconds in hover of the same sample. The dotted line represents again the desired (+/- 5°) boundaries and the continuous black line the adequate (+/-10°) limitations. The performance in the heading hold accuracy was similar to the vertical position accuracy for this pilot in terms of the desired and adequate performance limits.

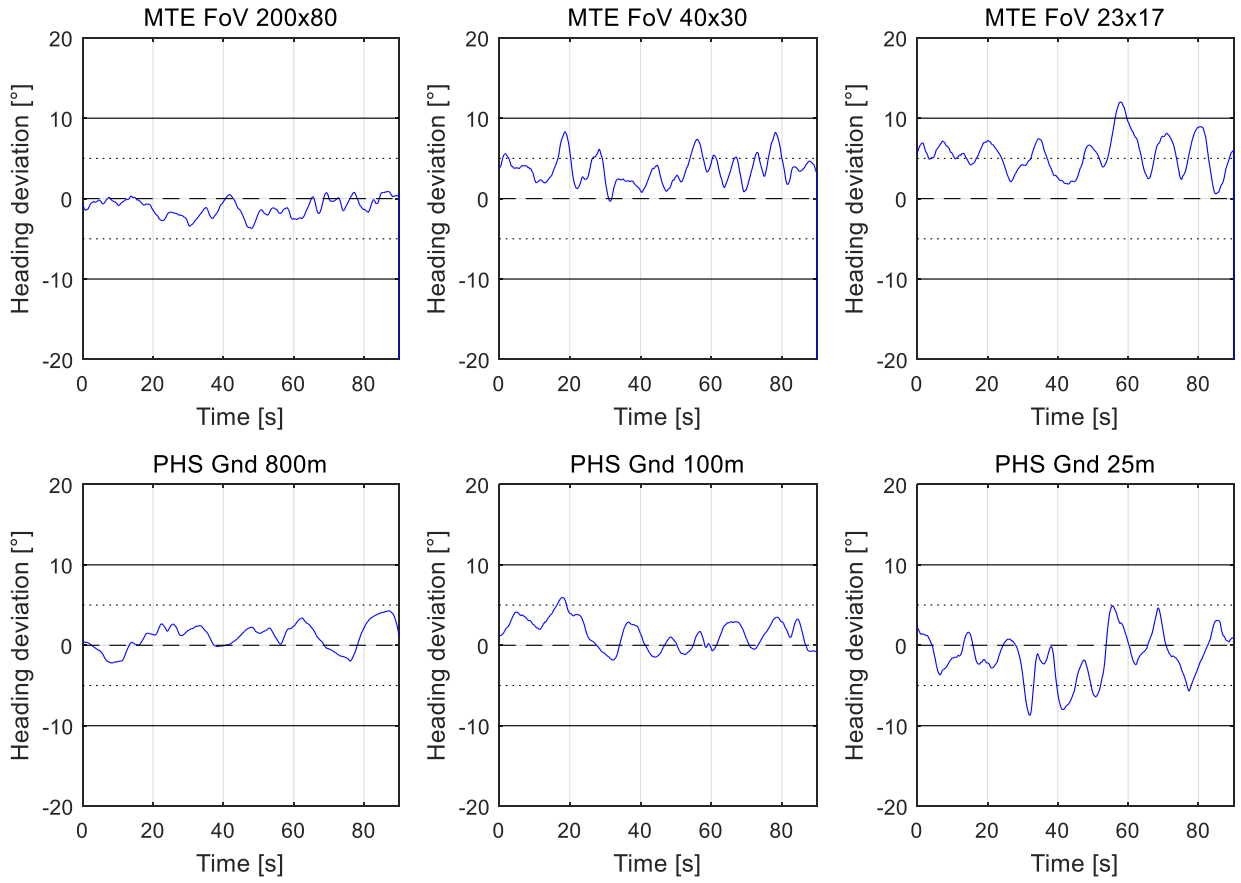

Figure 5-20: Example of one pilot's heading deviation during the hover tasks

Finally, the individual head motion results for the hover task, especially for the yaw axis, indicated that the pilots mainly focused their attention to the hover board in forward direction with a few head-turns to the hover boards at +/- 45° to the left and right. In general, head slewing (yaw) was again the dominant axis in the overall head motion. Figure 5-21 shows the head motion deviation to the left and to the right. With the standard hover mission task element using only the outside cues, the pilots required these views to the left and to the right to perceive information about the longitudinal position error. With the precision hover symbology, some pilots also used these hover boards on the side, but in addition they could rely on the 2D horizontal position extension displayed on the HMD. The increasing peaks in the standard MTE design (see top row of Figure 5-21) demonstrate that with a lower FOV the pilots had to turn their head much more. While with the FOV limitations the peaks reached 40° or more, the view to the right was only about 10° with the total FOV available for the pilot in the example.

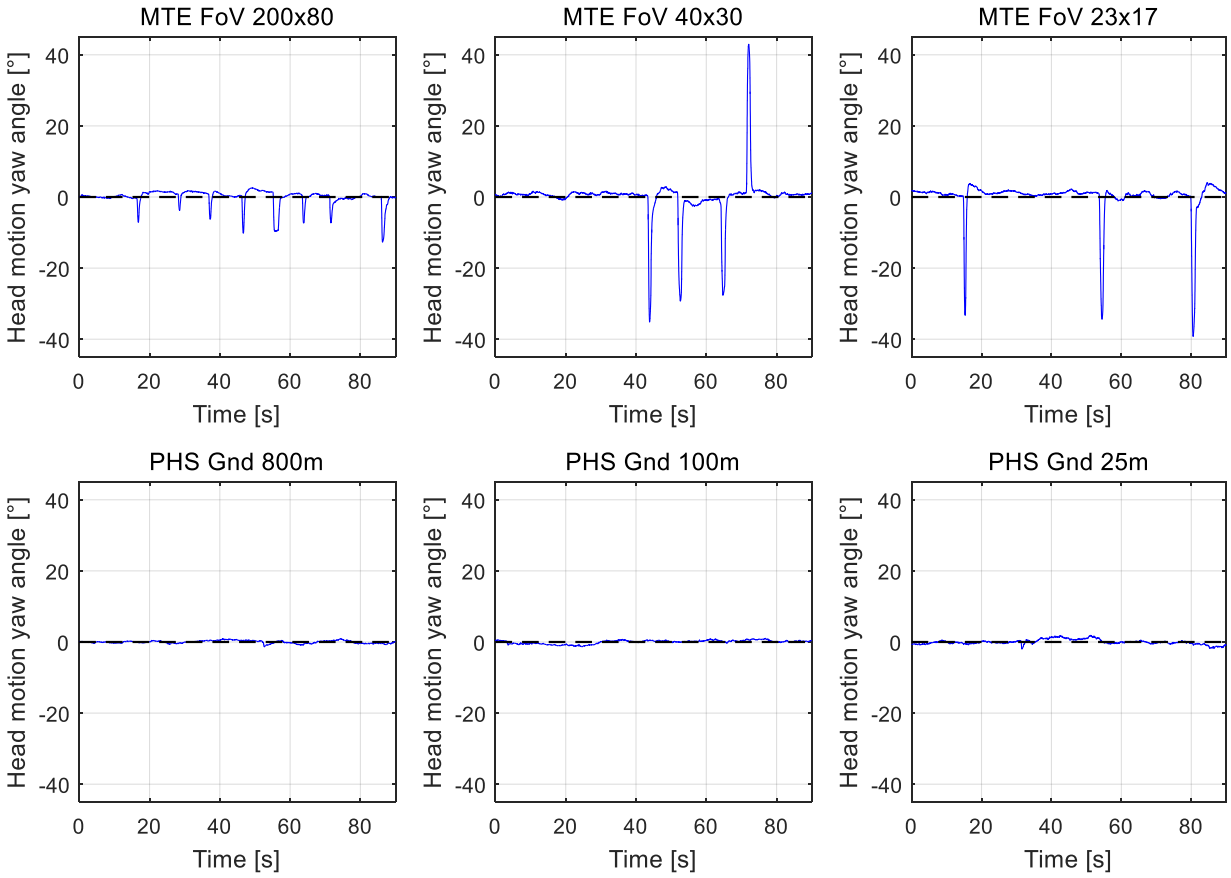

Figure 5-21: Example of one pilot's head motion about the yaw axis during the hover tasks

5.2.2 Comparison of Pilot Behavior in Precise Hovering

The individual results of one pilot shown above represented only one data set of the whole sample, but they already demonstrated a few common trends. This section presents the mean and standard deviation of the root-mean-square error (RMSE) of the above evaluated parameters for all participating pilots, in fact, the cyclic control input, the accuracy in positioning and the head motion. The pilots flew up to ten tasks in the sequence presented from left to right in Figure 5-22. After the first nine runs consisting of the standard MTE, the precision hover symbology in ground effect and against a wind turbine, another reference hover task with the standard MTE was conducted to observe any training effects. The number of participating pilots is given in the labels of the x-axis in each graph. The task of hovering against the wind turbine with 400 m visual range was excluded in the analysis of variances, because of the low number of available data sets (N = 10). Moreover, this case did not provide further important results, since the 800 m and 100 m visibility conditions were still considered. Thus, at least twelve complete data sets could be used for comparison.

In general, the performance of the three hover tasks against the wind turbine was worse compared to the other runs, due to the difficulty of this condition. Thus, the visibility degradation to 400 m and 100 m was applied for the wind turbine compared to the hover task in ground effect with only 100 m and 25 m. Hence, the pilots were still able to complete the task, although not with satisfactory performance. However, all pilots were able to conduct an adequate approach with the highway-in-the-sky, even without having trained this particular feature at all. With 100 m of

visibility and an altitude of nearly 300 ft. the pilots had to fly the approach in zero visibility. Thus, this last hover task was the most difficult one of the whole experiment.

The root-mean-square error (RMSE) of the longitudinal cyclic input resulted in a significant main effect between the nine tasks $F(4.28, 47.13) = 15.53$, $p < .001$, $\eta_p^2 = .59$, especially with differences between the wind turbine (WT) tasks and the remaining tasks (see Figure 5-22). The wind turbine task with 400 m visibility was excluded due to the small sample size.

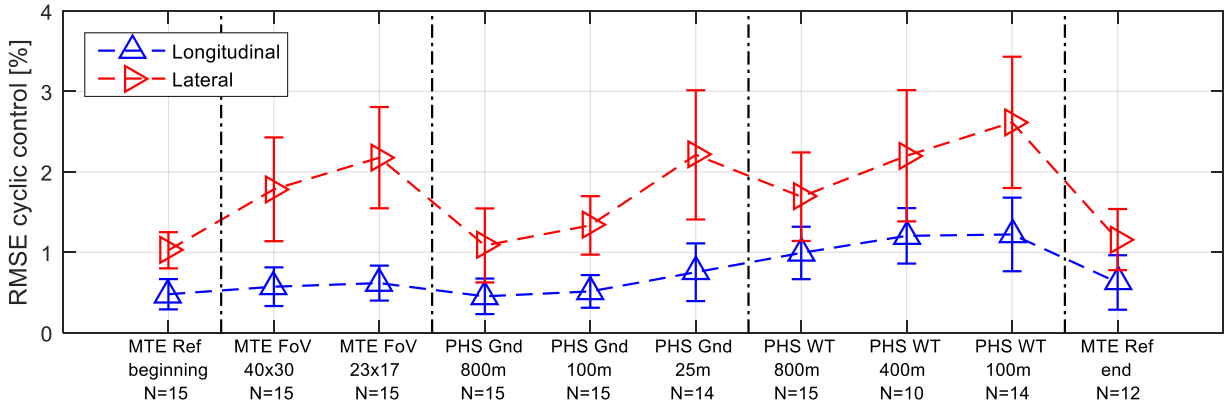

Figure 5-22: Cyclic control input results for all hover tasks

The individual p-values are given in Table 5-18 with respect to the MTE reference task at the beginning, which serves as a baseline for further comparison. In addition, the RMSE of the lateral cyclic input resulted also in significant differences between the tasks $F(3.82, 42.07) = 21.32$, $p < .001$, $\eta_p^2 = .66$. Significant differences for the lateral control axis were observed during the wind turbine conditions, the PHS task close to the ground with the worst visibility case of 25 m and for the MTE task with the smallest FOV of 23° x 17°. The medium FOV condition with 40° x 30° showed differences with a trend to be also significant.

Task	Longitudinal (SD)	p-value	Lateral (SD)	p-value
MTE Ref beginning	0.48 (0.19)	Reference	1.03 (0.22)	Reference
MTE FoV 40x30	0.57 (0.24)	1	1.78 (0.65)	.075
MTE FoV 23x17	0.62 (0.22)	1	2.18 (0.63)	.002
PHS Gnd 800 m	0.45 (0.22)	1	1.09 (0.46)	1
PHS Gnd 100 m	0.51 (0.20)	1	1.33 (0.36)	.664
PHS Gnd 25 m	0.75 (0.36)	.317	2.21 (0.80)	.008
PHS WT 800 m	0.99 (0.33)	.001	1.69 (0.55)	.042
PHS WT 400 m	1.20 (0.34)	Excluded	2.20 (0.82)	Excluded
PHS WT 100 m	1.22 (0.46)	.000	2.62 (0.82)	.000
MTE Ref end	0.63 (0.34)	1	1.16 (0.38)	1

Table 5-18: Cyclic control input results with mean (SD) [%] and p-values w.r.t the MTE Ref.

The mean horizontal position error confirms the trend shown already by the individual example that the precision in the lateral position is higher due to the higher control activity in the roll axis

compared to the precision in the longitudinal position with lower control activity in the pitch axis (see Figure 5-23). Both deviations in the horizontal position were significant between the flown tasks, the longitudinal RMSE from the reference hover position $F(3.25, 35.78) = 12.47$, $p < .001$, $\eta_p^2 = .53$, and the lateral RMSE $F(2.76, 30.38) = 9.00$, $p < .001$, $\eta_p^2 = .45$.

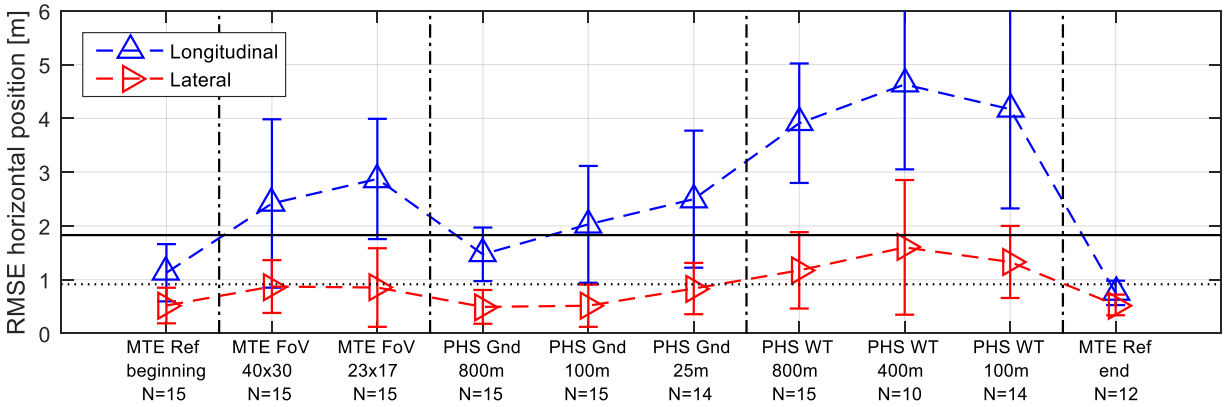

Figure 5-23: Horizontal position results for all hover tasks

Table 5-19 summarizes again the individual mean values for the position error together with the p-values for significant differences between the reference MTE at the beginning and the respective task. Differences could be observed for the longitudinal position error with the wind turbine conditions and the largest FOV reduction (23° x 17°) during the standard MTE condition. However, the 25 m visual range condition with the HMD symbology has already shown a trend towards a worse longitudinal position accuracy. Furthermore, the lateral position error resulted in significant degradation for the latter condition, although the mean magnitude was still within the desired performance limitation. The lateral position error for the wind turbine conditions resulted in an adequate performance, due to the larger effort in the lateral cyclic control activity. An adequate performance in the longitudinal axis was only achieved during the MTE reference tasks and with the 800 m visual range using the HMD symbology.

Task	Longitudinal (SD)	p-value	Lateral (SD)	p-value
MTE Ref beginning	1.13 (0.53)	Reference	0.52 (0.33)	Reference
MTE FoV 40x30	2.42 (1.57)	1	0.87 (0.49)	.332
MTE FoV 23x17	2.87 (1.12)	.021	0.85 (0.73)	1
PHS Gnd 800 m	1.47 (0.50)	1	0.49 (0.31)	1
PHS Gnd 100 m	2.03 (1.09)	.825	0.52 (0.39)	1
PHS Gnd 25 m	2.49 (1.27)	.078	0.83 (0.48)	.023
PHS WT 800 m	3.91 (1.11)	.000	1.17 (0.71)	.071
PHS WT 400 m	4.63 (1.58)	Excluded	1.60 (1.25)	Excluded
PHS WT 100 m	4.17 (1.85)	.016	1.33 (0.67)	.008
MTE Ref end	0.75 (0.23)	.498	0.53 (0.19)	1

Table 5-19: Horizontal position error with mean (SD) [m] and p-values w.r.t the MTE Ref.

The vertical position error was very small for all tasks in ground effect and it was within the desired performance boundaries (see Figure 5-24). Significant differences between the tasks were observed $F(2.85, 31.30) = 28.11$, $p < .001$, $\eta_p^2 = .72$, because of the poor performance during the wind turbine tasks (WT800m: $p = .001$ and WT100m: $p < .001$).

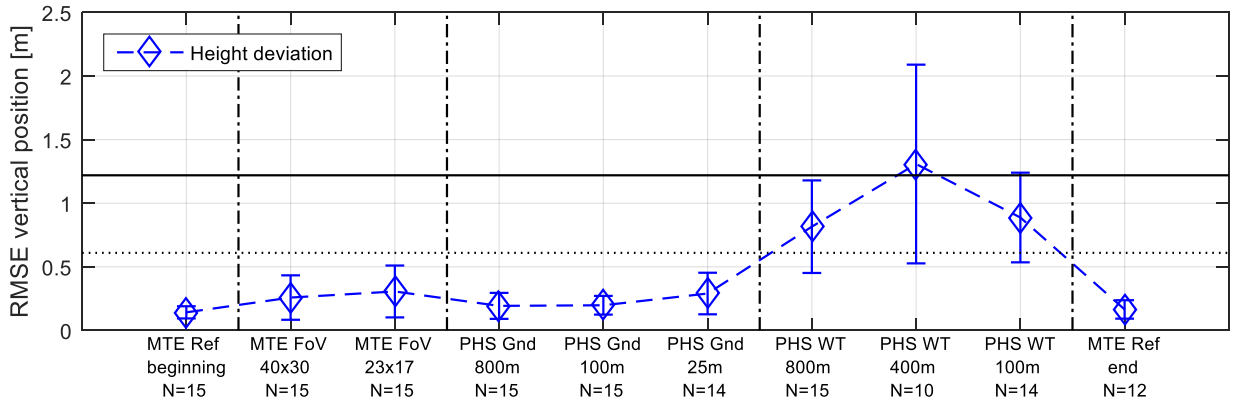

Figure 5-24: Vertical position results for all hover tasks

In addition, the heading deviation showed only marginal differences between the tasks $F(1.68, 18.45) = 6.03$, $p = .013$, $\eta_p^2 = .35$. The mean values stayed within the adequate performance limitation. Furthermore, with the HMD symbology close to the ground, the pilots achieved the desired performance, but no significant differences to the MTE reference task were measured.

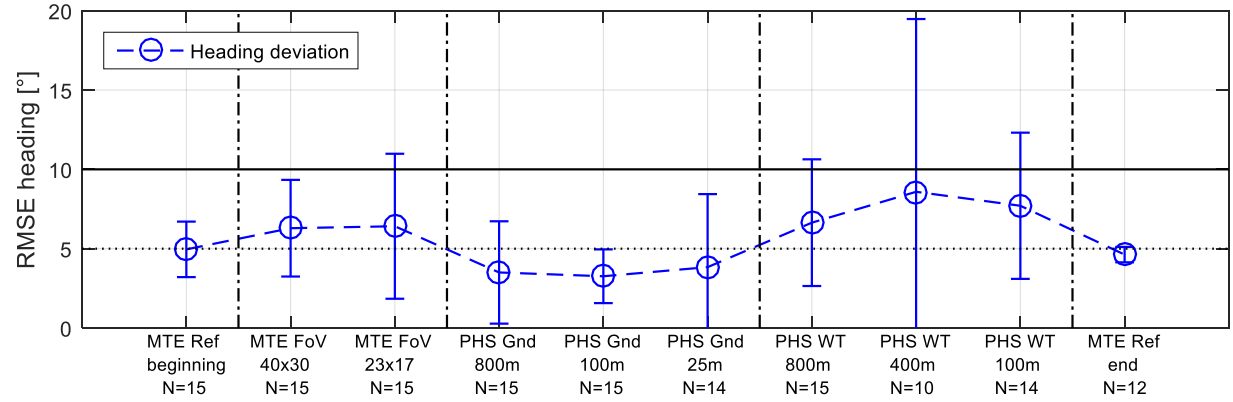

Figure 5-25: Heading deviation results for all hover tasks

In general, head motion showed similar results compared to the low-altitude sense and avoid tasks considering the higher amount of motion around the yaw axis compared to the pitch axis. Despite the fact that both axis resulted in significant differences between the tasks, a smaller effect was observed for the pitch axis $F(1.40, 15.42) = 4.51$, $p = .039$, $\eta_p^2 = .29$, than for the yaw axis $F(2.74, 30.18) = 7.85$, $p < .001$, $\eta_p^2 = .42$. Both standard MTE hover tasks with FOV limitations resulted in significant more head motion, due to the fact that the pilots required head movements to the left and to the right in order to perceive the longitudinal position error. With the HMD symbology, these head movements were no longer necessary.

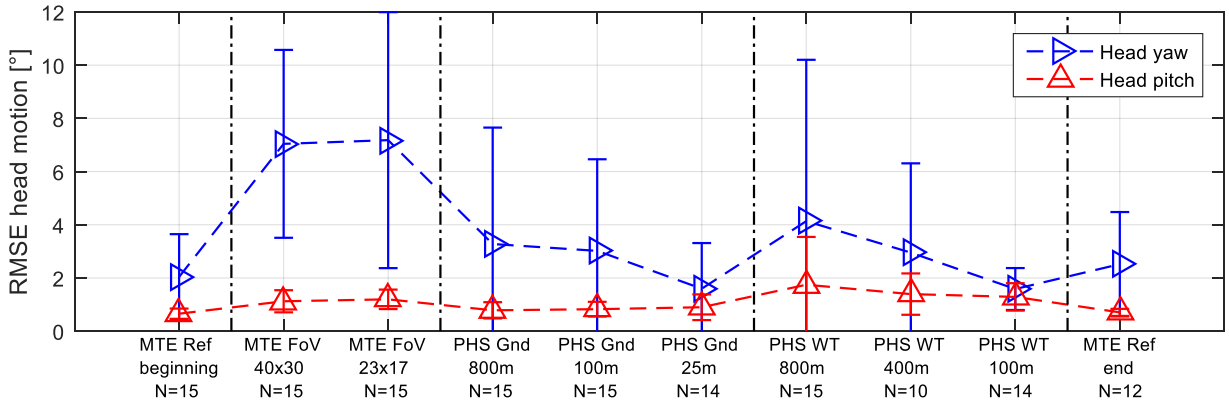

Figure 5-26: Head motion results for all hover tasks

The large standard deviation of the yaw head motion during the first wind turbine task was a result of the limited training for these conditions. During the first run, the pilots had to figure out their personal strategy of how to combine the HMD symbology with the rotor blade of the wind turbine located to their right hand side, which served as the only outside reference. Table 5-20 shows the corresponding mean values together with the p-values from the multi-comparison of each task with the reference MTE.

Task	Head yaw (SD)	p-value	Head pitch (SD)	p-value
MTE Ref beginning	2.04 (1.61)	Reference	0.66 (0.19)	Reference
MTE FoV 40x30	7.04 (3.53)	.002	1.12 (0.42)	.010
MTE FoV 23x17	7.18 (4.81)	.026	1.20 (0.37)	.001
PHS Gnd 800 m	3.28 (4.38)	1	0.78 (0.31)	1
PHS Gnd 100 m	3.02 (3.44)	1	0.83 (0.28)	.642
PHS Gnd 25 m	1.60 (1.72)	1	0.90 (0.48)	1
PHS WT 800 m	4.14 (6.07)	1	1.75 (1.80)	.983
PHS WT 400 m	2.95 (3.36)	Excluded	1.39 (0.78)	Excluded
PHS WT 100 m	1.58 (0.79)	1	1.29 (0.51)	.014
MTE Ref end	2.52 (1.96)	1	0.71 (0.13)	1

Table 5-20: RMSE of pilot head motion with mean (SD) [°] and p-values w.r.t the MTE Ref.

5.2.3 Handling Qualities and Visual Cue Ratings

Two standardized rating scales were evaluated as explained in chapter 4.3.2, in fact the Cooper Harper Handling Qualities Rating (HQR) and the Visual Cue Rating (VCR), both are defined in the ADS-33E-PRF [5]. The HQR addresses the demands on the pilot in the particular task, while the VCR considers the feasible precision with the visual cues available, in fact, the outside view plus the HMD symbology.

Figure 5-27 shows the mean HQR results for all hover tasks. The ratings 1 (excellent) to 8.5 (major deficiencies) can be assigned to three main handling quality levels. Ratings above 8.5 signify that the demand on the pilot was too high and the rotorcraft was not controllable. The two standard

MTE reference tasks reached the limit between ‘level 1’ and ‘level 2’. It should be noted that with the Bo105 controls and a simple rate command response type, level 1 handling qualities are very difficult to achieve. Thus, the similar rating for the HMD symbology with 800 m and 100 m visual range was a very positive result, since the reference cues for these hover tasks were presented only completely virtually on the HMD. The remaining hover conditions resulted in significant differences compared to the MTE reference $F(3.74, 41.18) = 27.38$, $p < .001$, $\eta_p^2 = .71$, with worse ratings in the level 2 and level 3 region. Except of the last wind turbine condition with 100 m visual range, which was almost not controllable, all other tasks were still feasible for the pilots.

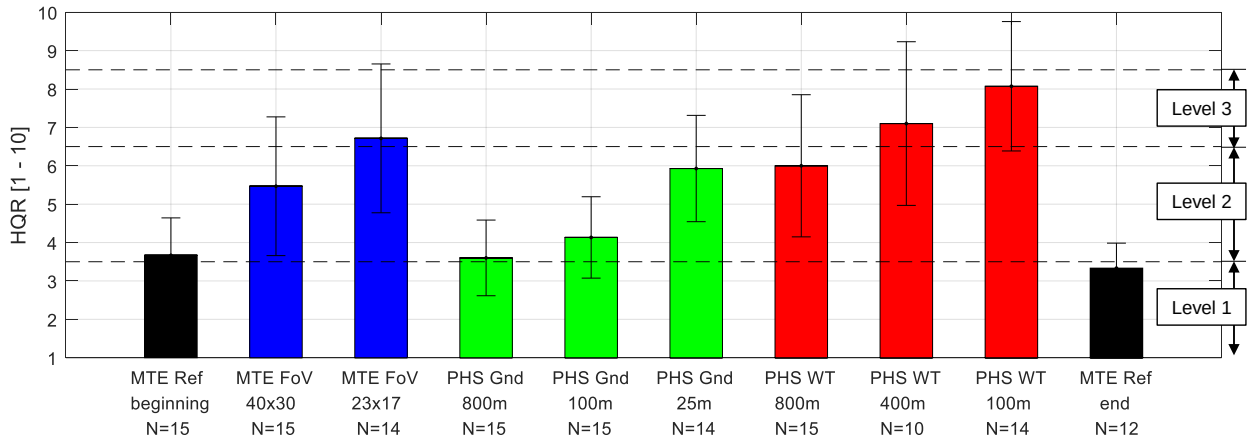

Figure 5-27: HQR results for all hover conditions tested

In addition, Figure 5-28 shows the translational rate VCR results compared to the attitude VCR results together with the assigned usable cue environment according to the ADS-33E-PRF definition.

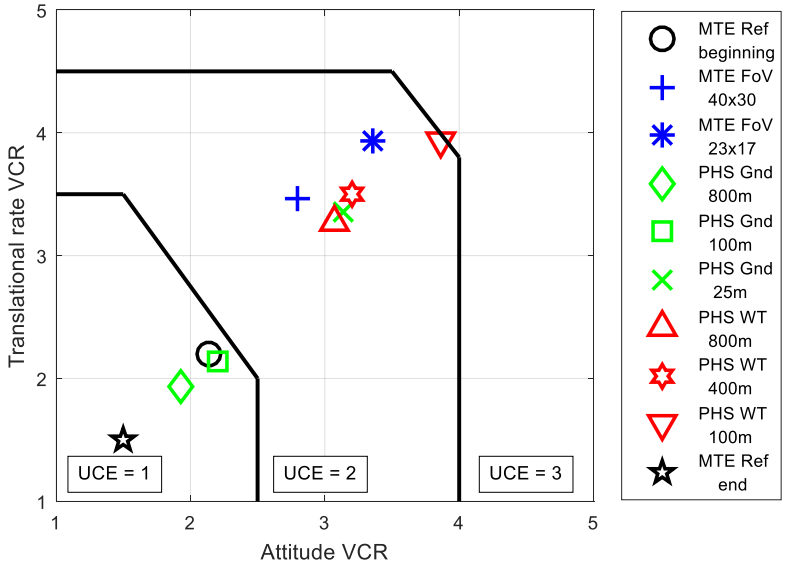

Figure 5-28: Usable Cue Environment (UCE) for all hover conditions tested

Similar to the HQR results, the standard reference MTEs and the two first HMD trials close to the ground (800 m and 100 m) were rated very well as to the precise control of the translational rate and the attitude. The remaining tasks were rated between fair and poor with the last wind turbine condition (100 m) being the worst case and thus it was rated on the boundary between UCE 2 and

UCE 3. In summary, both ratings verified the results from the measured pilot behavior with control input activity and the accuracy in positioning.

5.2.4 Discussion on the Precision Hover Task

There was no significant training effect observed between the first MTE reference hover and the last MTE reference at the end of this session considering the cyclic control input, the accuracy in position or the head motion. However, the visual cue rating showed better results for the last reference MTE, which indicates that the pilots rated the last hover as being easy to conduct with high precision. Thus, even if fatigue influenced the pilots already during the final tasks, the amount of training during all hover tasks reduced their effort and enabled a high level of performance at the end.

Further subjective pilot feedback was collected about the usability of the individual visualization parts, in fact the 3D-conformal hover boards, the attached drift velocity indication and the 2D horizontal situation extension. The rating was based on a four point Likert scale (1: Agree; 2: Rather agree; 3: Rather disagree; 4: Disagree). All three display functions for assisting in precise hover maneuvers were rated by the pilots as intuitive and as comprehensible in general and the pilots did not find them confusing (see Table 5-21 – Table 5-23). Moreover, most pilots agreed with an increase of their accuracy in positioning and spatial orientation by using the 3D-conformal hover board. It did not occlude other important information in the outside view and it provided useful assistance in combination with sufficient ground visibility. The opinions of the pilots differed about the question if the hover board enabled a precise hover. While the pilots tended to agree with the DVE conditions in general, they were uncertain about difficult tasks, for instance, the wind turbine scenario tested.

The 3D-conformal visualization with hover board ...		**M (SD)**
… was intuitive and comprehensible in general	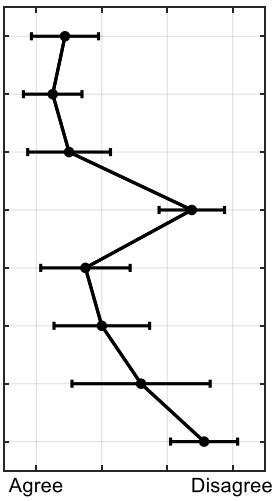	1.4 (0.5)
… increased the accuracy in positioning		1.3 (0.4)
… increased spatial orientation		1.5 (0.6)
… occluded important information in the outside view		3.4 (0.5)
… provided assistance with sufficient ground visibility		1.8 (0.7)
… enabled a precise hover in DVE		2.0 (0.7)
… enabled a precise hover in difficult conditions		2.6 (1.1)
… was confusing		3.6 (0.5)

Table 5-21: Subjective pilot evaluation of the 3D-conformal hover references

The novel approach of indicating the drift velocity was accepted very well by most of the pilots. It allowed the pilots to predict the future positions of the helicopter and usefully complemented the hover board according to their feedback (see Table 5-22). Even though the longitudinal drift

velocity was indicated superimposed on the ground, the saliency was not sufficient and together with the limited FOV of the HMD, it was not sufficiently supporting the pilots in the longitudinal direction. Moreover, the dynamically changing triangles attached to the hover boards did not disturb the majority of pilots.

The 3D-conformal drift velocity indication ...		**M (SD)**
… was intuitive and comprehensible in general	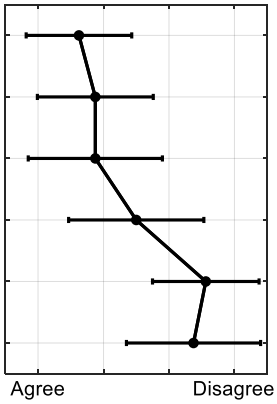	1.6 (0.8)
… facilitated a prediction of future positions		1.9 (0.9)
… usefully complemented the hover board		1.9 (1.0)
… provided support for longitudinal positioning		2.5 (1.0)
… was confusing		3.6 (0.8)
… was disturbing		3.4 (1.0)

Table 5-22: Subjective pilot evaluation of the drift velocity indication

Finally, all pilots agreed with the benefit of the 2D horizontal situation indication to increase the accuracy in positioning (see Table 5-23). It was necessary for the pilots to compensate the longitudinal drift. Even though most pilots focused on the 3D-conformal hover board, all of them shifted their attention to the 2D extension at regular intervals. Moreover, the horizontal situation indication placed at the top region of the display did not disturb the pilots. However, two pilots commented that sometimes the 2D symbology still partially occluded the 3D-conformal hover boards.

The 2D hover symbology extension ...		**M (SD)**
… was intuitive and comprehensible in general	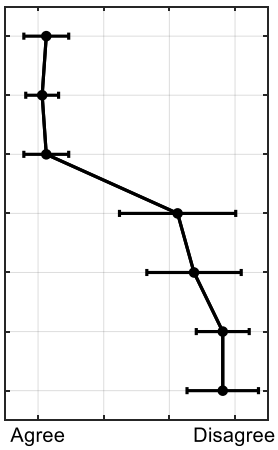	1.1 (0.3)
… increased the accuracy in positioning		1.1 (0.3)
… provided support for horizontal positioning		1.1 (0.3)
… occluded important information in the outside view		3.1 (0.9)
… was less considered, because of the hover board		3.4 (0.7)
… was confusing		3.8 (0.4)
… was disturbing		3.8 (0.5)

Table 5-23: Subjective pilot evaluation of the 2D hover symbology extension

Two pilots explicitly mentioned that more training would have been necessary to better handle the hover symbology. Another pilot commented that the hover symbology would be very good in combination with an automatic flight control system (AFCS) as backup, but even without an AFCS it was very helpful.

In summary, the results of the hover tasks showed that for the task of stabilization in hover, the visual symbology on the HMD alone was not enough support for all DVE conditions and for the extremely difficult condition against the wind turbine. However, the results also demonstrated that the hover symbology provided sufficient cues for a precise hover in DVE as long as a minimum amount of micro-textures was still available in the outside view. The pilots achieved precise hover maneuvers even with the very small FOV of 23° x 17° using the HMD compared to the results of Hoh with 38° x 23° FOV [75]. Nevertheless, both separately tested FOV limitations (40° x 30° and 23° x 17°) showed performance degradations. The main drawback, which resulted from the FOV limitation, was the perception and the control of the longitudinal position. The approach of Bachelder [24] to apply artificial gains between the longitudinal and lateral reference cues in order to mitigate this effect, is difficult to adopt for arbitrarily pilots with different control aggressiveness. An automatic flight control system in combination with the tested hover symbology seems to be a suitable solution for all conditions. Thus, a combination of control augmentation and visual augmentation is worthwhile to be tested in future experiments to improve the hover performance in DVE and in other difficult operations.

5.3 Summary and Discussion

The results of the obstacle avoidance task in low altitude and low visibility proved the great benefit of the HMD symbology. The pilots were able to fly faster and higher in visibility ranges below 800 m using the enhanced HMD assistance. Moreover, the workload was lower and the pilots maintained a minimum time-to-contact for completely unexpected events, which could appear in the remaining outside view. The results also demonstrated that the amount of head motion did not increase in spite of the limited FOV of the HMD. In addition, no difference between the display types was found relating to the pilot control of the velocity in eye-heights per second. This invariant but simultaneous control of velocity and height indicates that the pilots maintained a sufficient amount of visual cues obtained by the optical flow. Moreover, the pilots were able to manually adjust the visual range, but this task required further mental resources in order to control the amount of culled terrain and obstacle data. Thus, an additional sensor, capable of detecting the visual range and automatically controlling the required amount if displayed information, would be very beneficial.

In contrast, the task of stabilization during the hover maneuver showed some limitations of the HMD symbology. Even though the approach of using the hover board reference from the ADS-33E-PRF in the HMD worked in good and moderate visibility conditions, it could not sufficiently assist the pilots in severe degraded visibility conditions alone. The macro-textures in the precision hover symbology with the hover boards were not able to replace the required micro-textures in the peripheral field of vision (e.g. during the 25 m visibility condition). However, it is assumed that the 3D-conformal visual cues in combination with a control augmentation system could increase the performance for stabilization tasks. With a larger FOV in the HMD, an amplified pattern motion as introduced by Schmerwitz et al. [156] may provide additional visual references in the peripheral vision to account for the micro-texture problem.

Table 5-24 shows the pilot feedback on whether they wish to have the display concepts tested in visual ranges above and below 800 m. The results of the rating show that most pilots desired the visual augmentation concepts in visibilities below 800 m with a bit more emphasis on the obstacle display compared to the hover symbology. Above 800 m visual range, the pilots still desire the obstacle display, although it might be reasonable to reduce the amount of displayed information. The hover display was less relevant in visibility conditions above 800 m and thus was not desired. However, a few pilots commented that this might be also very beneficial at night or over low textured ground (e.g. water and snow).

The visualization concept for …		**M (SD)**
… low-altitude is desired below 800 m	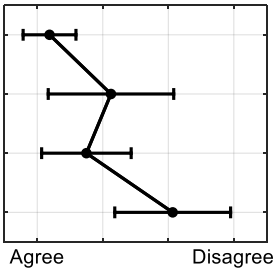	1.2 (0.4)
… low-altitude is also desired above 800 m		2.1 (1.0)
… hover is desired below 800 m		1.8 (0.7)
… hover is also desired above 800 m		3.1 (0.9)

Table 5-24: General questions about the instrumentation concepts

After the entire simulation experiment, a brief and tailored simulation sickness questionnaire was conducted (see Table 5-25). Most pilots were only very slightly affected by the symptoms of headache, dizziness, nausea, neck pain and general discomfort or had no symptoms at all. However, the results show that eye strain increased very slightly during the day using the HMD in the simulation environment. Fatigue was also noticed by the pilots, although only a slight amount. This was probably caused by the high effort and the required concentration to fulfill all the tasks.

How much did each symptom affect you?		**M (SD)**
… Fatigue	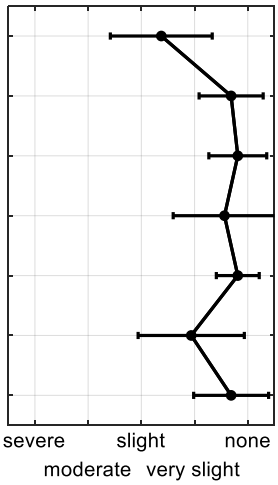	3.4 (1.0)
… Headache		4.7 (0.6)
… Dizziness		4.8 (0.5)
… Nausea		4.6 (1.0)
… Neck pain		4.8 (0.4)
… Eye strain		3.9 (1.0)
… General discomfort		4.7 (0.7)

Table 5-25: Subjective pilot evaluation of simulation sickness

One pilot commented that the new display concept required some additional effort for familiarization with the system. However, after the short training it required only marginally more effort than an ordinary helicopter flight.

6 Conclusions and Recommendations

The main motivation of this work was to define and investigate visual augmentation systems for rotorcraft pilots in degraded visual environments. These pilot assistance systems with a head-mounted display have the potential to increase flight safety in low-visibility conditions below 800 m, but quantitative results were almost not available. Thus, two representative flight tasks were selected and tested to gain knowledge about the pilot behavior in severe degraded visual conditions with enhanced 3D-conformal display concepts applied. The first task considered obstacle avoidance maneuvers during low-altitude contour flight, while the second task focused on the rotorcraft stabilization during the hover task. A flight simulation experiment with up to sixteen professional pilots from air rescue, police, commercial and military operators was conducted to obtain results on pilot workload, pilot control behavior and obstacle avoidance maneuvers amongst others.

Enhanced display concepts for the two considered tasks were derived, based on the visual perception theories and the current state-of-the-art technologies for visual augmentation explained in chapter 2. Several design principles, in particular, color-coding, different frames of reference, depth cues and the intended culling of information were applied to reduce visual clutter. A novel approach for measuring the active illuminated pixels on the HMD was developed and used to determine the actual perceived occlusion by the synthetic display content. Design improvements were derived using this kind of information. Moreover, a couple of potential future applications were also briefly discussed.

The cockpit of the rotorcraft simulation environment at the Institute of Helicopter Technology was fitted with a tailored head-down instrumentation for the application using the HMD system. Moreover, with the dynamic eye-point in the dome projection, an advanced and novel integration method was developed to reduce simulation induced errors and to increase the overall simulation fidelity. For the evaluation of the obstacle avoidance display concept, a new low-altitude contour flight scenario was developed. It enabled not only the comparison of different display variants, but also the observation of the pilot behavior at different visual ranges. The results of the experiment led to the following conclusions, beginning with the obstacle avoidance task.

Experimental findings: Low-altitude flight in DVE

- The fundamental control strategy of the pilots, based on the subjective perception of image velocity or optical flow, was not influenced by the display type. A similar control of the velocity in eye-heights was observed for both display types.
- Visibility had a significant influence on velocity and height control. However, the obstacle avoidance maneuvers were not negatively affected when using the advanced display concept with obstacle data.

- The workload of the pilots was significantly lower with the advanced display variant for all visibility conditions tested, even though the pilots had to process a lot more synthetic information.
- Neither the limited FOV of the HMD, nor the degraded visibility conditions resulted in a higher amount of head-motion.
- The absolute velocity and height-above-ground control was higher at lower visibility conditions using the advanced display type. In addition, the temporal margin to the obstacles increased when more time was available due to the early detection of those obstacles.
- The pilots maintained a minimum time-to-contact, depending on the remaining outside cues. Thus, a lower boundary of five to six seconds for completely unexpected events was observed.
- The pilots were consequently balancing flight safety (minimum time-to-contact) and flight envelope expansion (higher velocity and height), depending on the visual cues available.

The results of the low-altitude obstacle avoidance scenario demonstrated that the 3D-conformal terrain and obstacle representation is worth the potential cost of visual clutter at low visibility conditions. Furthermore, the pilots desired to have such an assistance in visual ranges below 800 m and partially in better visual conditions as well.

Further conclusions can be drawn from the hover task.

Experimental findings: Stabilization and hover task in DVE

- The hover task showed more control activity in the lateral cyclic than in the longitudinal direction. However, the pilots performed the task with a higher precision in the lateral position than in the longitudinal position. This was due to the better lateral drift perception than in the longitudinal axis.
- The degraded longitudinal drift perception was caused by FOV limitations and the reduced micro-textures in low visibilities.
- The macro-textures applied with the 3D-conformal hover boards and the two-dimensional co-planar horizontal situation extension enabled a precise hover, as long as sufficient peripheral vision was available (visibility > 100 m close to the ground).
- Head-motion activity was not higher using the HMD symbology than without the assistance.
- The subjective demand on the pilots was not higher using the HMD symbology. However, the visual augmentation could not compensate the missing outside cues completely. Severe degraded visual conditions or difficult task conditions still caused higher demands on the pilots.

In general, while the 3D-conformal symbology showed a great benefit for the low-altitude obstacle avoidance task, the rotorcraft stabilization task in hover demonstrated also the limitations of the low-cost HMD with the display concept tested. However, the 3D-conformal hover symbology was well accepted by the pilots and it provided useful assistance, even with the very limited amount of training during the experiment.

Recommendations for future work

The results of this work allow to derive important recommendations for future display designs:

- A 3D-conformal display design to sense and avoid obstacles should augment the remaining outside visual cues instead of replacing the outside view completely with synthetic content to avoid any pilot confusion. This mitigates any problems caused when the pilot's attention is shifted between the synthetic and the real world representation.
- The use of color-coding is strongly recommended to support the perception of display content presented in different frames of reference.
- The display limitations (small FOV) in hover could potentially be overcome with high-level control augmentation methods currently available in the upcoming helicopter generation. Hence, for the stabilization task, other means are just as important as the visual perception.

Moreover, findings from the applied methodology lead to recommendations for future experimental designs:

- Even though hover and low-altitude flight are challenging tasks for a fixed-base simulator, the simulation fidelity was high enough for the scenarios developed. For landing tasks, locally even higher texture resolutions are recommended.
- The observation of velocity and height control during the obstacle avoidance task enabled valuable measurements for the evaluation of the pilot performance depending on their perceived safety. Differences over a broad range of visibilities could be determined compared to experiments with specified target velocities and heights. Thus, the approach is also recommended for further comparisons of display variants related to DVE tasks.
- With focus on the rating of visual augmentation methods, only the handling qualities rating or the visual cue rating might be necessary for the hover task, since both provided a similar feedback.

Finally, a number of issues have been raised throughout this study, which are of interest for further investigation. The real-time measurement of the active illuminated pixel ratio to determine the amount of occlusion by the displayed content was so far only used to compare different display concepts. Following up on the briefly discussed idea of applying these measurements for automatic display adjustments can lead to further design improvements in the future. The experiment conducted intentionally focused on visual augmentation methods, since the visual cues provide the

most important contribution to solve the problem of rotorcraft pilots flying in DVE. However, the results also verified that the HMD technology with visual cues alone was not sufficiently supporting the pilots during all DVE flight tasks. Thus, further research is needed, which also considers control augmentation, audio and haptic feedback in a multi-modal analysis. In addition, multi-crew concepts and the necessary training should be investigated in such a multi-sensory cockpit environment. Even though the reliability of the visual augmentation technology has not been addressed in this work, a safety margin for the reliability of the human perception has been identified. Further investigations on the safety of the overall system are important to increase the maturity of this technology and to achieve airworthiness certification in the future.

References

[1] Ababsa, F., Didier, J. Y., Mallem, M., and Roussel, D., "Head Motion Prediction in Augmented Reality Systems Using Monte Carlo Particle Filters," Proc. of the 13th International Conference on Artificial Reality and Telexistence ICAT, Tokyo, Japan, December 2003.

[2] Ahollinger, F., "24-Stunden-Betrieb: Nachtflug und Allwettertauglichkeit als Voraussetzung einer primAIRen Notfallrettung," Symposium Proceedings of the Research Project PrimAIR, Fachhochschule Koeln, Berlin Pro Buisness, 2014.

[3] Anon., "2Indicate – The Instrument Development Tool," Product brochure v2.0, SEA Science & Engineering Applications Datentechnik GmbH, Troisdorf, Germany, undated.

[4] Anon., "ACAS Guide – Airborne Collision Avoidance Systems," Eurocontrol, December 2015.

[5] Anon., "Aeronautical Design Standard Performance Specification Handling Qualities Requirements for Military Rotorcraft," ADS-33E-PRF, United States Army Aviation and Missile Command, Aviation Engineering Directorate, Alabama, 2000.

[6] Anon., "Certification Specification for Helicopter Flight Simulation Training Devices CS-FSTD(H) Initial Issue," European Aviation Safety Agency (EASA), 2012.

[7] Anon., "Demonstration zum Thema UAV-Einsatz in Bayern (DemUEB)," Abschlussbericht der Arbeitspakete WP2200/2600, EADS Cassidian, July 2013.

[8] Anon., "External FLARM / PowerFLARM Display V4 Manual," www.swiss-bat.ch, ABOBA Elektronik, December 2013.

[9] Anon., "Final Report of NIAG SG167 on Helicopter Operations at low Altitude Degraded Visual Environment (DVE)," NIAG-D(2013)0014, NATO Industrial Advisory Group, July 2013.

[10] Anon., "Flight Testing of Night Vision Systems in Rotorcraft," RTO-AG-SCI-089, AC/323(SCI-089)TP/89, NATO, July 2007.

[11] Anon., "Global Positioning System (GPS) Standard Positioning Service (SPS) Performance Analysis Report," Report #86, FAA GPS Product Team, submitted by William J. Hughes Technical Center, July 2014.

[12] Anon., "Guidelines for Electronic Terrain, Obstacle and Aerodrome Mapping Information," Doc 9881, International Civil Aviation Organization (ICAO), undated.

[13] Anon., "Helicopter Flight in Degraded Visual Conditions," PAPER 2007/03, Safety Regulation Group, UK Civil Aviation Authority, 2007.

[14] Anon., “Human Engineering Considerations for Implementing Enhanced Synthetic Vision Systems in Vertical Flight Capable Platforms,” SAE ARP6023, Aerospace Recommended Practicep, September 2013.

[15] Anon., “Performance Specification Digital Terrain Elevation Data (DTED),” MIL-PRF-89020B, Department of Defense, May 2000.

[16] Anon., “Rotary-Wind Brownout Mitigation: Technologies and Training,” TR-HFM-162, RTO/NATO, 2012.

[17] Anon., “Solving the problem of flying in DVE for helicopter pilots: Brown-out, white-out or zero-light conditions,” White paper, Airbus Defense and Space, 2014.

[18] Anon., “Special Investigation Report on Emergency Medical Services Operations,” NTSB/SIR-06/01, PB2006-917001, 2006.

[19] Archdeacon, J. L., Iwai, N., and Sweet, B.T., “Designing and Developing an Image Generator for the Operational Based Vision Assessment Simulator,” Proc. of AIAA Modeling and Simulation Technologies Conference, Minneapolis, Minnesota, 2012.

[20] Armstrong, R. A., “Simulation Fidelity through an Adaptive Pilot Model,” PhD Thesis, University of Liverpool, 2009.

[21] Arthur III, J. J., Bailey, R. E., Williams, S. P., Prinzel III, L. J., Shelton, K. J., Jones, D. R., and Houston, V., “A review of head-worn display research at NASA Langley Research Center,” Proc. of SPIE Vol. 9470, Display Technologies and Applications for Defense, Security, and Avionics IX; and Head- and Helmet-Mounted Displays XX, 2015.

[22] Axholt, M., Peterson, S. D., and Ellis, S. R., “Visual Alignment Precision in Optical See-Through AR Displays: Implications for Potential Accuracy,” Proc. of the ACM/IEEE Virtual Reality International Conference, 2009.

[23] Azuma, R., and Bishop, G., “A Frequency-Domain Analysis of Head-Motion Prediction,” Proc. of the 22nd annual conference on computer graphics and interactive techniques, ACM, 1995.

[24] Bachelder, E. N., “Perception-Based Synthetic Cueing for Night-Vision Device Rotorcraft Hover Operations,” PhD Thesis, Massachusetts Institute of Technology, September 2000.

[25] Bachelder, E. N., McRuer, D., and Hansman, R. J., “Experimental Study of 3-D Synthetic Cues on Rotorcraft Hover Performance,” AIAA Atmospheric Flight Mechanics Conference, Monterey, California, August 2002.

[26] Bailey, R. E., Arthur III, J. J., Williams, S. P., and Kramer, L. J., “Latency in Visionic Systems: Test Methods and Requirements,” NATO-RTO-HFM-125, Toward Recommended Methods for Testing and Evaluation of EV and E/SV Based Visionic Devices, 2006.

[27] Beard, S. D., Reardon, S. E., Tobias, E. L., and Aponso, B. L., “Simulation System Fidelity Assessment at the Vertical Motion Simulator,” American Helicopter Society 69th Annual Forum, Phoenix, Arizona, 2013.

[28] Beechey, R., Lagace, G., Ruckel, P., Nigus, S., and Sammur, N., “Development of the AH-1Z Full Flight Simulator for the US Marine Corps,” American Helicopter Society 67th Annual Forum, Virginia Beach, USA, 2011.

[29] Benes, R., “An Integrated Three Dimensional Audio Display for the Rotorcraft Pilots's Associate,” Proceedings of the American Helicopter Society 54th Annual Forum, May 1998.

[30] Bhanu, B., Das, S., Roberts, B., and Duncan, D., “A System for Obstacle Detction During Rotorcraft Low Altitude Flight,” IEEE Transactions on Aerospace and Electronic Systems, Vol. 32, No. 3, pp. 875–897, July 1996.

[31] Blanken, C. L., Hart, D. C., and Hoh, R. H., “Helicopter Control Response Types for Hover and Low-Speed Near-Earth Tasks in Degraded Visual Conditions,” American Helicopter Society 47th Annual Forum, Phoenix, Arizona, 1991.

[32] Breton, R., and Rousseau, R., “Situation Awareness: A Review of the Concept and its Measurement,” DRDC Valcartier TR-2001-220, Defence Research and Development Canada – Valcartier, February 2003.

[33] Browne, M. P., Moffitt, K., Winterbottom, M., Williams, L., and Sepanski, J., “Mitigating Visual Anomalies for Binocular HMDs Integrated with Faceted Simulators,” Proc. of Interservice/Industry Training, Simulation, and Education Conference (I/ITSEC), Paper No. 11114, 2011.

[34] Cameron, A., “In the Blink of an Eye; Head Mounted Displays Development within BAE Systems,” Proc. of SPIE Vol. 9470, Display Technologies and Applications for Defense, Security, and Avionics IX; and Head- and Helmet-Mounted Displays XX, 2015.

[35] Church, P., “Realising EGNOS benefits in HEMS operations,” AirRescue Magazine, Vol. 2, 2012.

[36] Clark, G., “Helicoper Handling Qualities in Degraded Visual Environments,” PhD Thesis University of Liverpool, 2007.

[37] Clarkson, G. J. N., “The Development and Evaluation of Day Night All Weather Systems for Fixed and Rotary Wing Aircraft – A UK Perspective,” RTO-MP-HFM-141 (KN2), NATO, 2007.

[38] Cooper, G. E., and Harper, R. P., “The Use of Pilot Rating in the Evaluation of Aircraft Handling Qualities,” NASA TN D-5153, Ames Research Center and Cornell Aeronautical Laboratory, Washington D. C., 1969.

[39] Corwin, B., Whillock, R., and Groat, J., "Synthetic Terrain Imagery for Helmet-mounted Display," Volume 1, WL-TR-95-3025, Flight Dynamics Directorate, Wright Patterson AFB, November 1995.

[40] Cutting, J. E., and Vishton, P. M., "Perceiving layout and knowing distances: The integration, relative potency, and contextual use of different information about depth," In W. Epstein & S. Rogers (eds.) *Handbook of perception and cognition, Vol. 5, Perception of space and motion,* pp. 69–117, Academic Press, San Diego, CA, 1995.

[41] Davison, H. J., and Wickens, C. D., "Rotorcraft Hazard Cueing: The Effects on Attention and Trust," Presented at the 11th International Smposium on Aviation Psychology, Columbos, OH: The Ohio State University, 2001.

[42] Dillon, T. E., Schuetz, C. A., Martin, R. D., Mackrides, D. G., Shi, S., Yao, P., Schreve, K., Harrity, C., and Prather, D. W., "Passive, real-time millimeter wave imaging for degraded visual environmnet mitigation," Proc. of SPIE Vol. 9471, Degraded Visual Environments: Enhanced, Synthetic, and, External Vision Solutions, Baltimore, USA, 2015.

[43] Doehler, H.-U., Knabl, P., Schmerwitz, S., Eger, T., and Klein, O., "Evaluation of DVE Landing Display Formats," Proc. of SPIE Vol. 8360, Airborne Intelligence, Surveillance, Reconnaissance (ISR) Systems and Applications IX, 2012.

[44] Doehler, H.-U., Schmerwitz, S., and Lueken, T., "Visual-conformal display format for helicopter guidance," Proc. of. SPIE Vol. 9087, Degraded Visual Environments: Enhanced, Synthetic, and, External Vision Solutions, Baltimore, USA, 2014.

[45] Doehler, H.-U., Ernst, J. M., and Lueken, T., "Virtual aircraft-fixed cockpit instruments," *Proc. of SPIE Vol. 9471,* Degraded Visual Environments: Enhanced, Synthetic, and External Vision Solutions, Baltimore, USA, 2015.

[46] Duda, H., Gerlach, T., Advani, S., and Potter, M., "Design of the DLR AVES Research Flight Simulator," Proc. of AIAA Modeling and Simulation Technologies Conference, Boston, MA, 2013.

[47] Eger, T., "Operational requirements for short-term solution in visual display specifically for Degraded Visual Environment (DVE)," Proc. of SPIE Vol. 8360, Airborne Intelligance, Surveillance, Reconnaissance (ISR) Systems and Applications IX, 2012.

[48] Eger, T., "Operational requirements for helicopter operations low level in degraded visual environment," Proc. of SPIE Vol. 8737, Degraded Visual Environments, Synthetic, and External Vision Solutions, 2013.

[49] Eisenkeil, F., Schafhitzel, T., Kuehne, U., and Deussen, O., "Real-time classification of ground from LIDAR data for helicopter navigation," Proc. of SPIE Vol. 8745, Signal Processing, Sensor Fusion, and Target Recognition XXII, May 2013.

[50] Eisenkeil, F., Schafhitzel, T., Kuehne, U., and Deussen, O., "Clustering and visualization of non-classified points from LiDAR data for helicopter navigation," Proc. of SPIE Vol. 9091, Signal Processing, Sensor/Information Fusion, and Target Recognition XXIII, June 2014.

[51] Eisenkeil, F., Ernst, J., Stadelhofer, R., Kuehne, U., and Deussen, O., "Traffic Visualization in Helmet-Mounted Displays in Synchronization with Navigation Displays," Proc. of IEEE/AIAA 34th Digital Avionics Systems Conference (DASC), Prague, Czech Republic, September 2015.

[52] Eisenkeil, F., "Computer Graphics Support in Head-Mounted Displays for Helicopter Guidance," PhD Thesis, University of Konstanz, Germany, April 2016.

[53] Endsley, M. R., "Toward a Theory of Situation Awareness in Dynamic Systems," *Human Factors: The Journal of Human Factors and Ergonomics Society, Vol. 37, No. 1, pp. 32–64*, March 1995.

[54] Endsley, M. R., and Jones, D. G., *Designing for Situation Awareness: An Approach to User-centered Design*, Chapter 3, pp. 31–41, Boca Raton, FL: CRC Press, 2012.

[55] Entzinger, J. O., "Analysis of Visual Cues for Human Pilot Control in the Final Approach and Landing," PhD Thesis, The University of Tokio, February 2010.

[56] Ernst, J. M., Doehler, H.-U., and Schmerwitz, S., "A concept for a virtual flight deck shown on an HMD," Proc. of SPIE Vol. 9839, Degraded Visual Environments: Enhanced, Synthetic, and External Vision Solutions, Baltimore, USA, 2016.

[57] Foote, B., and Melzer, J., "A History of Helmet Mounted Displays," Proc. of SPIE Vol. 9470, Display Technologies and Applications for Defense, Security, and Avionics IX; and Head- and Helmet-Mounted Displays XX, 2015.

[58] Garett, A., Aguilar, M., and Barniv, Y., "A Recurrent Neural Network Approach to Virtual Environment Latency Reduction," Proc. of the International Joint Conference on Neural Networks, IEEE, pp. 2288–2292, May 2002.

[59] Geiselman, E. E., and Havig, P. R., "Rise of the HMD: the need to review our human factors guidelines," Proc. of SPIE Vol. 8041, Head- and Helmet-Mounted Displays XVI: Design and Applications, 2011.

[60] Gibson, J. J., *The Ecological Approach to Visual Perception*, Psychology Press, Taylor & Francis Group, 1986.

[61] Godfroy-Cooper, M., Szoboszlay, Z., Kahana, A., and Rottem-Hovev, M., "Terrain and Obstacle Avoidance Displays for Low-Level Helicopter Operations in Degraded Visual environments," American Helicopter Society 72nd Annual Forum Proceedings, West Palm Beach, Florida, USA, May 2016..

[62] Gregory, R. L., *the intelligent eye*, Weidenfeld and Nicolson, London, 1970.

[63] Greiser, S., Lantzsch, R., Wolfram, J., Wartmann, J., Muellhaeuser, M., Lueken, T., Doehler, H.-U., and Peinecke, N., "Results of the pilot assistance system "Assisted Low-Level Flight and Landing on Unprepared Landing Sites" obtained with the ACT/FHS research rotorcraft," *Aerospace Science and Technology, Vol. 45, pp. 215–227*, Septmeber 2015.

[64] Gruenhagen, W., Muellhaeuser, M., Abildgaard, M., and Lantzsch, R., "Active Inceptors in FHS for Pilot Assistance Systems," 36th European Rotorcraft Forum, Paris, France, 2010.

[65] Gursky, B. I., Olsman, W. F. J., and Peinecke, N., "Development of a tunnel-in-the-sky display for helicopter noise abatement procedures," *CEAS Aeronautical Journal, Vol. 5, Issue 2, pp. 199-208*, June 2014.

[66] Haas, E. C., "Can 3-D Auditory Warnings Enhance Helicopter Cockpit Safety?," Proceedings of the Human Factors and Ergonomics Society 42nd Annual Meeting, 1998.

[67] Haisch, S., Heidenreich, K., and Gollnick, V., "Der Allwetter-Rettungshubschrauber – Neue Flugführungskonzepte fuer ein erweitertes Missionsspektrum," Deutscher Luft- und Raumfahrtkongress, pp. 621-628, Leipzig, Germany, 2000.

[68] Haisch, S., Hess, S., Jank, S., and Kreitmair-Steck, W., "Pilot Assistance for Rotorcraft," 35th European Rotorcraft Forum, Hamburg, Germany, 2009.

[69] Hardy, G. J., and Foote, B., "Flight Evaluation of an ISIE-11 Band Digital Night Vision Goggle Prototype," Proc. of SPIE Vol. 9471, Degraded Visual Environments: Enhanced, Synthetic, and External Vision Solutions, 2015.

[70] Hart, S. G., and Staveland, L. E., "Development of NASA-TLX (Task Load Index): Results of empirical and theroetical research," *In P. Hancock and N. Meshkati (Eds.) Human Mental Workload,* Amsterdam: North Holland Press, 1988.

[71] Hart, S. G., "NASA-Task Load Index (NASA-TLX); 20 Years Later," Proceedings of the Human Factors and Ergonomics Society 50th Annual Meeting, 904-908, Santa Monica: HFES, 2006.

[72] Heinecke, J. K., and Rash, C. E., "Image Intensification/Forward-Looking Infrared Sensor Comparison in Urban Combat in Operation Iraqi Freedom (OIF)," RTO-MP-HFM-141 (4), NATO, 2007.

[73] Helmholz, H., *Handbuch der physiologischen Optik*, 3. Band – Die Lehre von Gesichtswahrnehmungen, 3.Auflage, ergänzt und herausgegeben von A. Gullstrand, J. Kries und W. Nagel, Hamburg und Leipzig, Verlag von Leopold Voss, 1910.

[74] Hoffmann, D. M., Girshickm A. R., Akeley, K., and Banks, M. S., "Vergence-accommodation conflicts hinder visual performance and cause visual fatigue," *Journal of Vision, Vol. 8 No. 3 Article 33*, 2008.

[75] Hoh, R. H., "Investigation of outside visual cues required for low speed and hover," AIAA Conference Proceedings, 85-1808, USA, 1985.

[76] Hoh, R. H., Baillie, S., and Morgan, J. M., "Flight Investigation of the Tradeoff between Augmentation and Displays for NOE Flight in low Visibility," American Helicopter Society National Specialists' Meeting on Flight Controls and Avionics, Cherry Hill, N. J., October 1987.

[77] Hoh, R. H., "The Effects of Degraded Visual Cueing and Divided Attention on Obstruction Avoidance in Rotorcraft," Report DOT/FAA/RD-90/40, ADA380260, FAA, December 1990.

[78] Howard, I. P., and Rogers, B. J., *Seeing in Depth*, Volume 2: Depth Perception, Published by I. Porteous, Canada, 2002.

[79] Jennings, S., Craig, G., Carignan, S., Fischer, H., and Brulotte, M., "Development of NVG Test Maneuvers for Civilian Aircraft," Proc. of SPIE Vol. 6955, Head- and Helmet-Mounted Displays XIII: Design and Applications, USA, 2008.

[80] Jennings, S., Holst, P., Craig, G, and Cheung, B., "Rotary Wing Brown-Out Symbology: The DVEST Test," Proc. of SPIE Vol. 8383, Head- and Helmet-Mounted Displays XVII; and Display Technologies and Applications for Defense, Security, and Avionics VI, 2012.

[81] Johnson, W., "A History of Rotorcraft Comprehensive Analyses," NASA/TP-2012-216012, Ames Research Center, California, 2012.

[82] Jump, M., Padfield, G. D., and Lee, D. N., "Vehicle Guidance System," U.S. Patent No. 8,065,044 B2, The University of Liverpool, November 2011.

[83] Kaber, D. B., Alexander, A. L., Stelzer, E. M., Kim, S.-H., Kaufmann, K., and Hsiang, S., "Perceived Clutter in Advanced Cockpit Displays: Measurement and Modeling with Experienced Pilots," *Aviation Space and Environmental Medicine, Vol. 79, No. 11, pp. 1007–1018*, November 2008.

[84] Kahana, A., Sweet, B. T., Szoboszlay, Z., and Rottem-Hovev, M., "Terrain and Obstacle Avoidance Display for Low-Level Helicopter Operations in Degraded Visual Environments," American Helicopter Society 70th Annual Forum, Montréal, Canada, 2014.

[85] Kaiser, M. K., and Mowafy, L., "Visual Information for Judging Temporal Range," Proceedings of Piloting Vertical Flight Aircraft: A Conference on Flying Qualities and Human Factors, San Francisco, California, 1993.

[86] Kim, S.-H., Prinzel, L. J., Kaber, D. B., Alexander, A. L., Stelzer, E. M., Kaufmann, K., and Veil, T., "Multidimensional Measure of Display Clutter and Pilot Performance for Advanced Head-up Display," *Aviation Space and Environmental Medicine, Vol. 82, No. 11, pp. 1013–1022*, November 2011.

[87] Klausing, H., "Realisierbarkeit eines Radars mit synthetischer Aperatur durch rotierende Antennen," Dissertation, Universitaet Karlsruhe, 1989.

[88] Knabl, P. M., Doehler, H.-U., Schmerwitz, S., and Biella, M., “Integration of a helmet-mounted display for helicopter operations in degraded visual environment: a human factors perspective,” Human Factors and Ergonimics Society Europe Chapter Annual Meeting, Toulouse, France, October 2012.

[89] Knabl, P. M., and Peinecke, N., “Designing an obstacle display for helicopter operations in degraded visual environment,” Proc. of SPIE Vol. 8651, Human Vision and Electronic Imaging XVIII, 2013.

[90] Knabl, P., and Toebben, T., “Symbology Development for a 3D Conformal Synthetic Vision Helmet-Mounted Display for Helicopter Operations in Degraded Visual Environment,” *Engineering Psychology and Cognitive Ergonomics, Understanding Human Cognition, Springer, Vol. 8019, pp. 232-241*, 2013.

[91] Knabl, P., Schmerwitz S., Doehler, H.-U., Peinecke, N., and Vollrath, M., “Attentional issues with helmet-mounted displays in poor visibility helicopter flight,” 31st EAAP Conference, Valetta, Malta, 2014.

[92] Knabl, P., Schmerwitz S., Doehler, H.-U., Peinecke, N., and Vollrath, M., “Towards innovative helicopter helmet-mounted display designs: investigating flight performance and psychophysiological outcomes,” 11th International Symposium of the Australian Aviation Psychology Association (AAVPA), Australia, 2014.

[93] Knabl, P., “Towards Reducing Pilot Workload during Helicopter Flight in Degraded Visual Environment: An Evaluation of Helmet-Mounted Display Symbology with Special Regard to Attention Allocation”, Dissertation, DLR-Forschungsbericht, 2015-32, Braunschweig, 2015.

[94] Koenemann, T., and Dervailly, J., “HELIcopter Situation Awareness fuer eXtreme Missionsanforderungen (HELI-X),” Final Report, 20H1109A, Airbus Helicopters, Donauwoerth, Germany, 2015.

[95] Kooi, F. L., Meeuwsen, T., and de Graaff, M., “NVG Training Developments in The Netherlands,” RTO-MP-HFM-141 (28), NATO, 2007.

[96] Kooi, F., “A display with two depth layers: attentional segregation and declutter,” In *Human Attention in Digital Environments*, edited by Roda, C., pp. 245–258, Cambridge University Press, February 2011.

[97] Kooima, R., “Generalized Perspective Projection,” School of Electrical Engineering and Computer Science, Louisiana State University, (http://csc.lsu.edu/~kooima/articles/genperspective/, 08.12.2015), 2009.

[98] Koppe, W., “HELIcopter Situation Awareness fuer eXtreme Missionsanforderungen (HELI-X),” LuFo Abschlussbericht 20H1109G, Airbus DS Geo GmbH, Germany, 2015.

[99] Kreitmair-Steck, W., Haisch, S., Hess, S., and Jank, S., "EUROCOPTER Research on Pilot Assistance for Rotorcraft," Proc. of SPIE Vol. 7328, Enhanced and Synthetic Vision, 2009.

[100] Lam, T., and Cheng, V. H. L., "Simulation of Automatic Rotorcraft Nap-of-the-Earth Flight in Graphics Workstation Environment," AIAA Flight Simulation Technologies Conference, Guidance, Navigation, and Control, 1992.

[101] Langridge, R., Miles, K., and Luethy, J., "Terrain and Obstacle Data Manual," Edition 2.0, Eurocontrol, October 2011.

[102] Lee, D. N., "The Optic Flow Field: The Foundation of Vision," In Phil. Trans. of the Royal Society of London, Biological Sciences, Vol. 290, No. 1038, pp. 169–178, The Psychology of Vision, July 1980.

[103] Lee, D. N., "Tau in action development," 33rd Volume in the Minnesota Symposium on Child Psychology, Rieser, J. J., Lockman, J. J., and Nelsen, C. A. Eds., Hillsdale, N.J.: Erlbaum, April 2005.

[104] Lemoine, O., Francois, J.-M., and Point, P., "Contribution of TopOwl® Head Mounted Display System in Degraded Visual Environments," Proc. of SPIE Vol. 8737, Degraded Visual Environments: Enhanced, Synthetic, and External Vision Solutions, 2013.

[105] Lenhart, P. M., "Raeumliche Darstellung von Flugfuehrungsinformationen in Head-Mounted Displays," Dissertation TU Darmstadt, Ergonomia Verlag, Stuttgart, Germany, 2005.

[106] Lenhart, P. M., "Ein Head-Mounted-Display mit synthetischer Sicht," DGLR Bericht 2012-01, Fortschrittliche Anzeigesysteme für die Fahrzeug- und Prozessfuehrung, pp. 49–60, 2012.

[107] Li, H., Zhang, X., Shi, G., Qu, H., Wu, Y., and Zhang, J., "Review and analysis of avionic helmet-mounted displays," *Optical Engineering Vol. 52(11), 110901*, SPIE, November 2013.

[108] Lockett, H. A., "The Role of Tau-Guidance During Decelerative Helicopter Approaches," PhD Thesis, University of Liverpool, February 2010.

[109] Lueken, T., Peinecke, N., and Doehler, H.-U., "AllFlight – A Sensor Based Conformal 3D Situational Awareness Display for a Wide Field of View Helmet Mounted Display," 38th European Rotorcraft Forum, Amsterdam, The Netherlands, September 2012.

[110] Lueken, T., Ernst, J. M., and Doehler, H.-U., "Virtual Cockpit Instrumentation Using Helmet Mounted Display Technology," 41st European Rotorcraft Forum Conference Proceedings, Munich, Germany, 2015.

[111] Maha, F., and Jordan, D. R., "The impact of coloured symbology on cockpit eyes-out display effectiveness: a survey of key parameters," Proc. of SPIE Vol. 9470, Display Technologies

and Applications for Defense, Security, and Avionics IX: and Head- and Helmet-Mounted Displays XX, 2015.

[112] Malcolm, R., "The Malcolm Horizon – History and Future," In Peripheral Vision Horizon Display (PVHD), NASA Conference Puplication 2306, November 1984.

[113] McGrath, B., Drakunov, S., McKay, J., Ramiccio, J., and Rupert, A., "A Simple Short-Term Solution to Helicopter Spatial Disorientation During Operations in Degraded Visual Environment," American Helicopter Society 70th Annual Forum, Montréal, Canada, 2014.

[114] McGrath, B., Cox, J., McKay, J., and Rupert, A., "Mission Utility of a Tactile Display in Rotary Wing Operations," American Helicopter Society 71th Annual Forum, Virginia Beach, USA, 2015.

[115] McLeod, S.A., "Visual Perception Theory," retrieved from www.simplypsychology.org /perception-theories.html (18.04.2016), 2007.

[116] Melzer, J. E., and Moffitt, K., *Head Mounted Displays: Designing for the User*, chapter 3, pp. 55–82, McGraw-Hill, 1997.

[117] Melzer, J. E., "Toward the HMD as a *Cognitive Prosthesis*," Proc. of SPIE Vol. 6955, Head- and Helmet-Mounted Displays XIII: Design and Applications, 2008.

[118] Melzer, J. E., "Human-machine interface issues in the use of helmet-mounted displays in short conjugate simulators," Proc. of SPIE Vol. 8041, Head- and Helmet-Mounted Displays XVI: Design and Applications, 2011.

[119] Milgram, P., Takemura, H., Utsumi, A., and Kishino, F., "Augmented Reality: A class of displays on the reality-virtuality continuum," Proc. of SPIE Vol. 2351, Telemanipulator and Telepresence Technologies, 1994.

[120] Muensterer, T., Kress, M., and Klasen, S., "Sensor based 3D conformal cueing for safe and reliable HC operation specifically for landing in DVE," Proc. of SPIE Vol. 8737, Degraded Visual Environments: Enhanced, Synthetic, and External Vision Solutions, 2013.

[121] Muensterer, T., Schafhitzel, T., Strobel, M., Voelschow, P., Klasen, S., and Eisenkeil, F., "Sensor-enhanced 3D conformal cueing for safe and reliable HC operation in DVE in all flight phases," Proc. of SPIE Vol. 9087, Degraded Visual Environments: Enhanced, Synthetic, and External Vision Solutions, 2014.

[122] Muensterer, T., Kress, M., Fadljevic, D., Lupton, M., Passey, G., and Lamb, T., "Combining IR imagery and 3D lidar based symbology for a helicopter DVE support system," Proc. of SPIE Vol. 9471, Degraded Visual Environments: Enhanced, Synthetic, and External Vision Solutions, Baltimore, USA, 2015.

[123] Muensterer, T., Voelschow, P., Singer, B., Strobel, M., Kramper, P., and Buehler, D., "HMI aspects of the usage of ladar 3D data in pilot DVE support systems," Proc. of SPIE Vol.

9471, Degraded Visual Environments: Enhanced, Synthetic, and External Vision Solutions, Baltimore, USA, 2015.

[124] Nanda, S., and Pray, R., "A Technique for Correlating Images on Head Mounted Displays with Virtual Background Scenery," Proc. of the 47th Annual Southeast Regional Conference ACM-SE 47, March 2009.

[125] Open Geospatial Consortium, "OGC City Geography Markup Language (cityGML) Encoding Standard," edited by Groeger, G., Kolbe, T. H., Nagel, C., and Haefele, K.-H., April 2012.

[126] Padfield, G. D., Lee, D. N., and Bradley, R., "How Do Helicopter Pilots Know When to Stop, Turn, or Pull Up? (Developing guidelines for vision aids)," *Journal of the American Helicopter Society*, Vol. 48 (2), pp. 108–119, April 2003.

[127] Padfield, G. D., *Helicopter Flight Dynamics – The Theory and Application of Flying Qualities and Simulation Modelling*, Second Edition, Blackwell Publishing, 2007.

[128] Padfield, G. D., Clark, G., and Taghizad, A., "How Long Do Pilots Look Forward? Prospective Visual Guidance in Terrain-Hugging Flight," *Journal of the American Helicopter Society*, Vol. 52 (2), pp. 134–145, April 2007.

[129] Padfield, G. D., "The tau of flight control," Survey Paper, *The Aeronautical Journal*, Vol. 115, No. 1171, pp. 521–556, September 2011.

[130] Patterson, R., Winterbottom, M. D., and Pierce, B. J., "Perceptional Issues in the Use of Head-Mounted Visual Displays," AFRL-HE-AZ-TP-2007-03, Air Force Research Laboratory, Arizona, 2007.

[131] Peinecke, N., and Knabl, P. M., "Design Consideration for a Helmet-Mounted Synthetic Degraded Visual Environment Display" Proc. of the 31st Digital Avionics Systems Conference (DASC), IEEE/AIAA, 2012.

[132] Peinecke, N., "Detection of Helicopter Landing Sites in Unprepared Terrain," Proc. of SPIE Vol. 9087, Degraded Visual Environments: Enhanced, Synthetic, and External Vision Solutions, 2014.

[133] Peinecke, N., Knabl, P. M., Schmerwitz, S., and Doehler, H.-U., "An Evlauation Environment for a Helmet-Mounted Synthetic Degraded Visual Environment Display," Proc. of the 33rd Digital Avoinics System Conference (DASC), 2014.

[134] Peinecke, N., "Is OpenSceneGraph an Option for ESVS Displays?," Proc. of SPIE Vol. 9471, Degraded Visual Environments: Enhanced, Synthetic, and External Vision Solutions, Baltimore, USA, 2015.

[135] Peinecke, N., Chignola, A., Schmid, D., and Friedl, H., "The Glass Dome: Low-Occlusion Obstacle Symbols for Conformal Displays," Proc. of SPIE Vol. 9839, Degraded Visual Environments: Enhanced, Synthetic, and External Vision Solutions, Baltimore, USA, 2016.

[136] Perfect, P., Timson, E., White, M. D., Padfield, G. D., Erdos, R., Gubbels, A. W., and Berryman, A. C., "A Rating Scale for Subjective Assessment of Simulator Fidelity," 37th European Rotorcraft Forum Conference Proceedings, Gallarate, Italy, 2011.

[137] Pinkus, A. R., and Task, H. L., "Applied and Theoretical Aspects of Night Vision Goggle Resolution and Visual Acuity Assessment," RTO-MP-HFM-141 (17), NATO, 2007.

[138] Pope, S., "Air Ambulance Safety: A Closer Look," Flying Magazine, July 26, 2013.

[139] Pratt, A. B., "Weapon," U.S. Patent 1,183,492., May 1916.

[140] Preissner, J., "The influence of the atmosphere on passive radiometric measurements," Proc. of the Symbosium on Millimeter and Submillimeter Wave Propagation and Curcuits, AGARD CP 245, September, Munich, Germany, 1978.

[141] Qi, H., Moore, J. B., "Direct Kalman filtering approach for GPS/INS integration," *IEEE Transactions on Aerospace and Electronic Systems*, Vol. 38, Issue 2, pp. 687–693, April 2002.

[142] Rash, C. E., Bayer, M. M., Harding, T. H., and McLean, W. E., *Helmet-Mounted Displays: Sensation, Perception and Cognition Issues*, Rash, C. E., Russo, M. B., Letowski, T. R., and Schmeisser, E. T., Eds., chapter 4, pp. 109-174, U.S. Army Aeromedical Research Laboratory, Fort Rucker, 2009.

[143] Rash, C. E., Russo, M. B., Letowski, T. R., and Schmeisser, E. T., *Helmet-Mounted Displays: Sensation, Perception and Cognition Issues*, U.S. Army Aeromedical Research Laboratory, Fort Rucker, 2009.

[144] Rasmussen, J., "Skills, Rules, and Knowledge; Signals, Signs, and Symbols, and Other Distinctions in Human Perfromance Models," In IEEE Transactions on Systems, Man, and Cybernetics, Vol. SMC-13, Issue 3, pp. 257–266, 1983.

[145] Rehm, W., "Komponentenentwicklung im Rahmen eines Pilotenassistenzsystems fuer den Einsatz von HELIcoptern unter eXtremen Anforderungen," Final Report, 20H1109C, Airbus Group, Munich, Germany, 2015.

[146] Rogers, S. P., Asbury, C. N., and Szoboszlay, Z. P., "Enhanced flight symbology for wide field-of-view helmet-mounted displays," Proc. of SPIE Vol. 5079, Helmet- and Head-Mounted Displays VIII: Technologies and Applications, 2003.

[147] Rolland, J. P., Holloway, R. L., and Fuchs, H. "A comparison of optical and video see-through head-mounted displays," Proc. of SPIE Vol. 2351, Telemanipulator and Telepresence Technologies, 1994.

[148] Rolland, J. P., and Fuchs, H., "Optical Versus Video See-Through Head-Mounted Displays in Medical Visualization," *Presence: Teleoperators and Virtual Environments, Vol. 9, No. 3, pp. 287–309*, June 2000.

[149] Salmon, P. M., Stanton, N. A., Walker, G. H., Jenkins, D., Ladva, D., Rafferty, L., and Young, M., "Measuring Situation Awareness in complex systems: Comparison of measures study," *International Journal of Industrial Ergonomics Vol. 39, pp. 490–500*, 2008.

[150] Savage, J., Goodrich, S., Ott, C., Szoboszlay, Z., Soukup, J., Perez, A., and Burns, H. N., "Three-dimensional landing zone joint capability technology demonstration," Proc. of SPIE Vol. 9087, Degraded Visual Environments: Enhanced, Synthetic, and External Vision Solutions, 2014.

[151] Savage, J., Goodrich, S., and Burns, H. N., "Three-dimensional landing zone ladar," Proc. of SPIE Vol. 9839, Degraded Visual Environments: Enhanced, Synthetic, and External Vision Solutions, Baltimore, USA, 2016.

[152] Schmerwitz, S., Toebben, H., Lorenz, B., Iijima, T., and Kuritz-Kaiser, A., "Investigating the benefits of 'scene linking' for a pathway HMD: From laboratory flight experiments to flight tests," Proc. of SPIE Vol. 6226, Enhanced and Synthetic Vision, 2006.

[153] Schmerwitz, S., "Radarbasiertes Pilotenassistenzsystem zur visuellen Flugführung unter schlechten Sichtbedingungen," Dissertation, DLR-Forschungsbericht, 2010-29, Braunschweig, 2010.

[154] Schmerwitz, S., Knabl, P., Lueken, T., and Doehler, H.-U., "Drift Indication for Helicopter Approach and Landing," Proc. of SPIE Vol. 9471, Degraded Visual Environments: Enhanced, Synthetic, and External Vision Solutions, Baltimore, USA, 2015.

[155] Schmerwitz, S., Knabl, P., Lueken, T., and Doehler, H.-U., "Amplified Ego Motion Drift Indication for Helicopter Landing," 41st European Rotorcraft Forum, Munich, Germany, 2015.

[156] Schmerwitz, S., Knabl, P., Lueken, T., and Doehler, H.-U., "Amplifying the helicopter drift in a conformal HMD," Proc. of SPIE Vol. 9839, Degraded Visual Environments: Enhanced, Synthetic, and External Vision Solutions, Baltimore, USA, 2016.

[157] Schochlow, V., Santel, C., Weber, C., Vogt, J., and Klingauf, U., "Kollisionsvermeidung im Luftsport: Eine experimentelle Studie der Mensch-Maschine-Schnittstelle eines populären Kollisionswarnsystems in der Allgemeinen Luftfahrt," DGLR-Bericht 2012-01, Fortschrittliche Anzeigesysteme für die Fahrzeug- und Prozessfuehrung, pp. 157-173, 2012.

[158] Schuck, F., "Ein integriertes Auslegungskonzept zur Sicherstellung exzellenter Handling Qualities für Kleinflugzeuge," Dissertation, Technische Universitaet Muenchen, 2014.

[159] Schulz, K. R., Scherbarth, S., and Fabry, U., "Hellas: Obstacle warning system for helicopters," Proc. of SPIE Vol. 4723, Laser Radar Technology and Applications VII, 2002.

[160] Seidel, C., Samuelis, C., Wegner, M., Muensterer, T., Rumpf, T., and Schwartz, I., "Noval approaches to helicopter obstacle warning," Proc. of SPIE Vol. 6214, Laser Radar Technology and Applications XI, 2006.

[161] Seidel, C., Schwartz, I., and Kielhorn, P., “Helicopter collision avoidance and brown-out recovery with HELLAS,” Proc. of SPIE Vol. 7114, Electro-Optical Remote Sensing, Photonic Technologies, and Applications II, 2008.

[162] Singh, S., Cover, H., Stambler, A., et al., “Perception for Safe Autonomous Helicopter Flight and Landing,” American Helicopter Society 72nd Annual Forum, West Palm Beach, Florida, USA, 2016.

[163] Stelmash, S., Muensterer, T., Kramper, P., Samuelis, C., Buehler, D., Wegner, M., and Sheth, S., “Flight test results of ladar brownout look-through capability,” Proc. of SPIE Vol. 9471, Degraded Visual Environments: Enhanced, Synthetic, and External Vision Solutions, 2015.

[164] Stevens, J., Vreeken, J., and Masson, M., “European Helicopter Safety Team (EHEST): Mapping Safety Issues with Technological Solutions,” 37th European Rotorcraft Forum, Gallarate, Italy, 2011.

[165] Stevens, J., and Vreeken, J., “The Potential of Technologies to Mitigate Helicopter Accident Factors – An EHEST Study,” NLR-TP-2014-311, Amsterdam, The Netherlands, 2014.

[166] Sutherland, I. E., “The Ultimate Display,” Proceedings of IFIP Congress, pp. 506 – 508, 1965.

[167] Sutherland, I. E., “A head-mounted three dimensional display,” Proceedings of AFIPS Joint Computer Conferences, pp. 757–764, Washington D. C., 1968.

[168] Sweet, B. T, and Kato, K. H., “120 Hertz – The New 60 for Flight Simulation?,” Proc. of the IMAGE 2012 Confrerence, Scottsdale, Arizona, 2012.

[169] Sykora, B., “Rotorcraft Visual Situational Awareness Solving the Pilotage Problem for Landing in Degraded Visual Environments,” American Helicopter Society 65th Annual Forum, Grapevine, Texas, USA, 2009.

[170] Sykora, B., “BAE Systems Brownout landing aid system technology (BLAST) system overview and flight test results,” Proc. of SPIE Vol. 8360, Airborne Intelligence, Surveillance, Reconnaissance (ISR) Systems and Applications IX, May 2012.

[171] Szoboszlay, Z., and Ott, C., “Flight Evaluation of Fully-Masked Approaches to Landing using BOSS Displays in an EH-60L,” American Helicopter Society 68th Annual Forum, Ft. Worth, Texas, USA, 2012.

[172] Taylor, T., “Rotorcraft visual situational awareness (VSA): solving the pilotage problem for landing in degraded visual environments,” Proc. of SPIE Vol. 7328, Enhanced and Synthetic Vision, 2009.

[173] Tejada, F. R., Espada, B. P., Diaz, C. V., López, J. A. L., Desviat, P. V., Carrido, J. V., and Benavides, B. E., “Night Vision Training Capabilities in NATO: Trends and Challenges,” RTO-MP-HFM-141 (26), NATO, 2007.

[174] Thibaut, G., et al., "Airworthiness certification of rotorcraft Degraded Visual Environment Systems (DVES) and flight trials," Phase two report of NIAG SG 193, NIAG-D(2016)0001(PFP), January 2016.

[175] Tiana, C., and Muensterer, T., "Global vision systems regulatory and standard setting activities," Proc. of SPIE Vol. 9839, Degraded Visual Environments: Enhanced, Synthetic, and External Vision Solutions, USA, 2016.

[176] Toet, A., and Hogervorst, M. A., "Own the Night with Flying Colors: Towards Ergonomic Full Color Multiband Night Vision Systems," RTO-MP-HFM-141 (14), NATO, 2007.

[177] Tritschler, J. K., O'Conner, J. C., Arteche, D. R., Pritchard, J. A., Wallace, R. D., and Eksuzian, D., "Preliminary Investigation into Rotorcraft Pilot Strategy and Visual Cueing Effects in the Shipboard Environment," American Helicopter Society 71st Annual Forum, Virginia Beach, Virginia, USA, 2015.

[178] Tritschler, J. K., O'Conner, J. C., Klyde, D. H., and Lampton, A. K., "Analysis of Pilot Control Activity in ADS-33E Mission Task Elements," American Helicopter Society 72nd Annual Forum, West Palm Beach, Florida, USA, 2016.

[179] Turpin, T. S., Sykora, B., Neiswander, G. M., and Szoboszlay, Z. P., "Brownout Landing Aid System Technology (BLAST)," American Helicopter Society 66th Annual Forum, Phoenix, Arizona, USA, 2010.

[180] Velger, M., *Helmet-Mounted Display and Sights*, Artech House, Boston, 1998.

[181] Viertler, F., and Hajek, M., "Dynamic registration of an optical see-through HMD into a wide field-of-view rotorcraft flight simulation environment," Proc. of SPIE Vol. 9470, Display Technologies and Applications for Defense, Security, and Avionics IX; and Head- and Helmet-Mounted Displays XX, Baltimore, USA, April 2015.

[182] Viertler, F., and Hajek, M., "Requirements and Design Challenges in Rotorcraft Flight Simulations for Research Applications," Proc. of AIAA SciTech Modeling and Simulation Technologies Conference, Kissimmee, Florida, USA, January 2015.

[183] Viertler, F., Krammer, C., and Hajek, M., "Analyzing Visual Clutter of 3D-Conformal HMD Solutions for Rotorcraft Pilots in Degraded Visual Environment," 41st European Rotorcraft Forum, Munich, Germany, September 2015.

[184] Viertler, F., and Hajek, M., "Evaluation of Visual Augmentation Methods for Rotorcraft Pilots in Degraded Visual Environments," American Helicopter Society 72nd Annual Forum, West Palm Beach, Florida, USA, May 2016.

[185] Vincenzi, D. A., Deaton, J. E., Blickenderfer, E. L., Pray, R., Williams, B., and Buker, T. J., "Measurement and Reduction of System Latency in See-Through Helmet Mounted Display (HMD) Systems," Proc. of SPIE Vol. 7688, Head-and Helmet-Mounted Displays XV: Design and Applications, Bellingham, WA, USA, 2010.

[186] Voelschow, P., Muensterer, T., Strobel, M., and Kuhn, M., "Display of real-time 3D sensor data in a DVE system," Proc. of SPIE Vol. 9839, Degraded Visual Environments: Enhanced, Synthetic, and External Vision Solutions, Baltimore, USA, 2016.

[187] Voithenberg, M., "DeckFinder – High Precision Local Positioning System," www.deckfinder.net (08.12.2015), Ottobrunn, Germany.

[188] Vreeken, J., Haverdings, H., and Joosse, M., "Helicopter Flight in a Degraded Visual Environment," EASA.2011.02, Amsterdam, The Netherlands, May 2013.

[189] Waanders, T., Qian, Q., Scheiblhofer, R., van Noort, B., Koerber, R., Giere, A., Schubert, F., and Ziegler, V., "Miniaturized and Low-Cost Obstacle Warning System," 38th European Rotorcraft Forum, Amsterdam, 2012.

[190] Waanders, T., Muensterer, T., and Kress, M., "Sensor Supported Pilot Asssistance for Helicopter Flight in DVE," Proc. of SPIE Vol. 8737, Degraded Visual Environments: Enhanced, Synthetic, and External Vision Solutions, USA, 2013.

[191] Waanders, T., Scheiblhofer, R., Qian, Q., van Noort, B., Ziegler, V., Schubert, F., and Koerber, R., "Helicopter Rotorstrike Alerting System," 41st European Rotorcraft Forum, Munich, Germany, 2015.

[192] White, M., Perfect, P., Padfield, G. D., Gubbels, A. W., and Berryman, A., "Acceptance Testing of a Rotorcraft Flight Simulator for Research and Teaching: The Importance of Unified Metrics," 35th European Rotorcraft Forum Conference Proceedings, Hamburg, Germany, 2009.

[193] White, M. D., Perfect, P., Padfield, G. D., Gubbels, A. W., and Berryman, A. C., "Acceptance testing and commissioning of a flight simulator for rotorcraft simulation fidelity research," *Journal of Aerospace Engineering, Vol. 227(4), pp. 663-686*, 2012.

[194] Wickens, C. D., *Principles and Practice of Aviation Psychology*, edited by Tsang, P. S., and Vidulich, M. A., Chapter 5, pp. 147–200, CRC Press Taylor and Francis Group, 2003.

[195] Wickens, C. D., and Alexander, A. L., "Attentional Tunneling and Task Management in Synthetic Vision Displays," *The International Journal of Aviation Psychology, Vol. 19(2), pp. 182–199*, 2009.

[196] Wickens, C. D., Hollands, J. G., Banburry, S., and Parasuraman, R., *Engineering Psychology and Human Performance*, 4th Ed., Chapter 3–5, pp. 49–159, Pearson Education, Inc., 2013.

[197] Wickens, C. D., Hollands, J. G., Banburry, S., and Parasuraman, R., *Engineering Psychology and Human Performance*, 4th Ed., Chapter 11, pp. 346–376, Pearson Education, Inc., 2013.

[198] Wolff, D., *OpenGL 4.0 Shading Language Cookbook*, Chapter 5, pp. 149–185, Packt Publishing, July 2011.

[199] Yeh, M., Wickens, C. D., and Seagull, F. J., “Effects of Frame of Reference and Viewing Condition on Attentional Issues with Helmet Mounted Displays,” ARL-98-1/ARMY-FED-LAB-98-1, U.S. Army Research Laboratory, 1998.

[200] Zimmermann, M., and Peinecke, N., “Dynamic Landing Site Ranking for Helicopter Emergency Situations,” 41st European Rotorcraft Forum, Munich, Germany, 2015.

[201] Zimmermann, M., “Flight test results of helicopter approaches with trajectory guidance based on in-flight acquired LIDAR data,” Proc. of SPIE Vol. 9839, Degraded Visual Environments: Enhanced, Synthetic, and External Vision Solutions, Baltimore, USA, 2016.

[202] Zuckerman, J., *Perimetry*, Loppincott, Philadelphia, 1954.

Appendix

A.1 Subjective Rating Scales

The Cooper Harper Handling Qualities Rating (Figure A-1) always starts with the questions from the bottom left and the procedure continuous depending on the yes / no decision of the pilot. Finally, a rating between 1 and 10 will be obtained, which indicates the demand on the pilot in the selected task and within the applied usable cue environment (UCE).

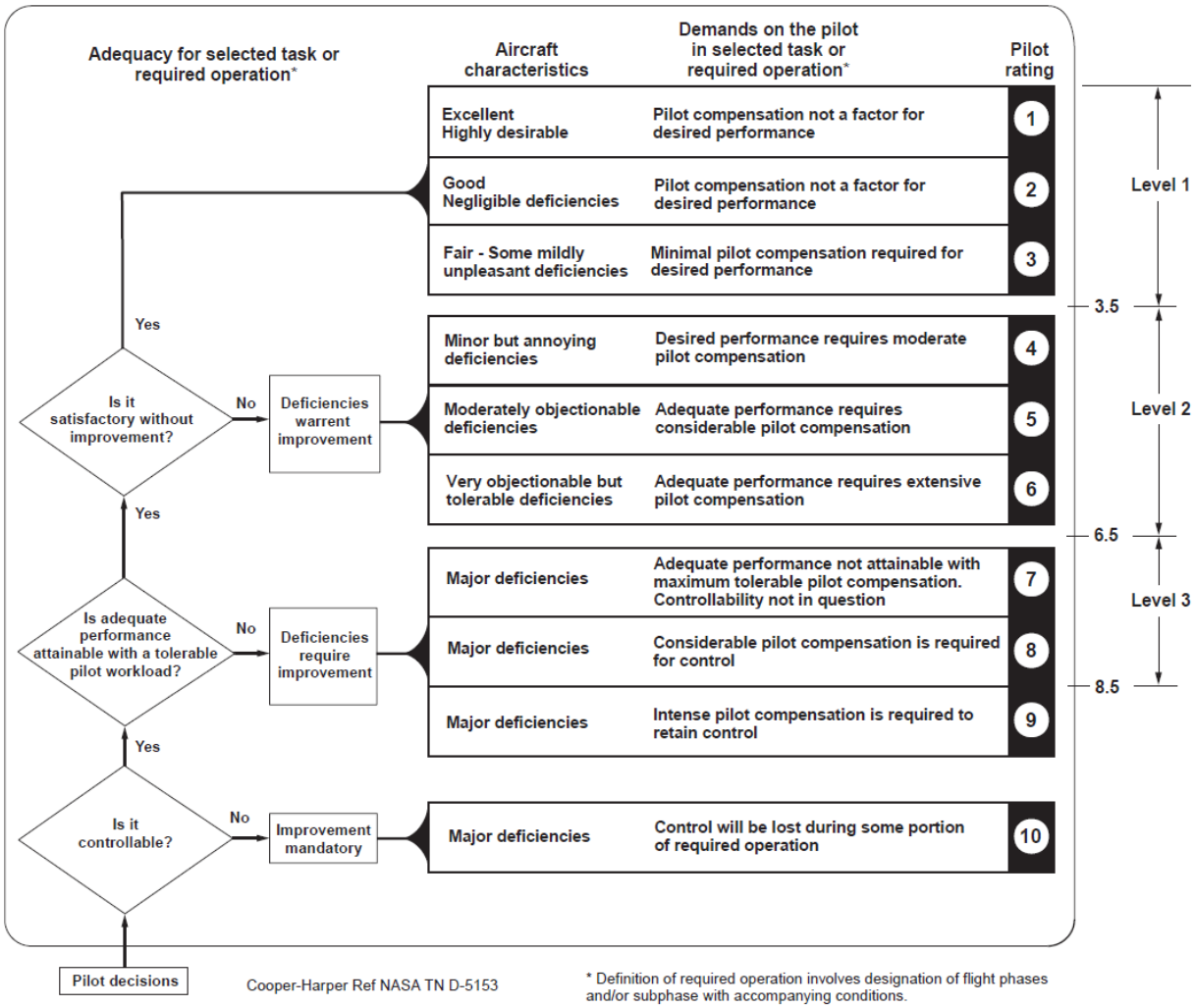

Figure A-1: Cooper-Harper Handling Qualities Rating (HQR) [5]

The assignment of the usable cue environment is based on the visual cue rating Figure A-2 for the stabilization effectiveness of the translational rate and the attitude. The rating is based on a scale from 1 to 5, which represents the possibility to make precise corrections ranging from good to poor. The lowest rating of all axis (translational and attitude) is used for the UCE determination, respectively.

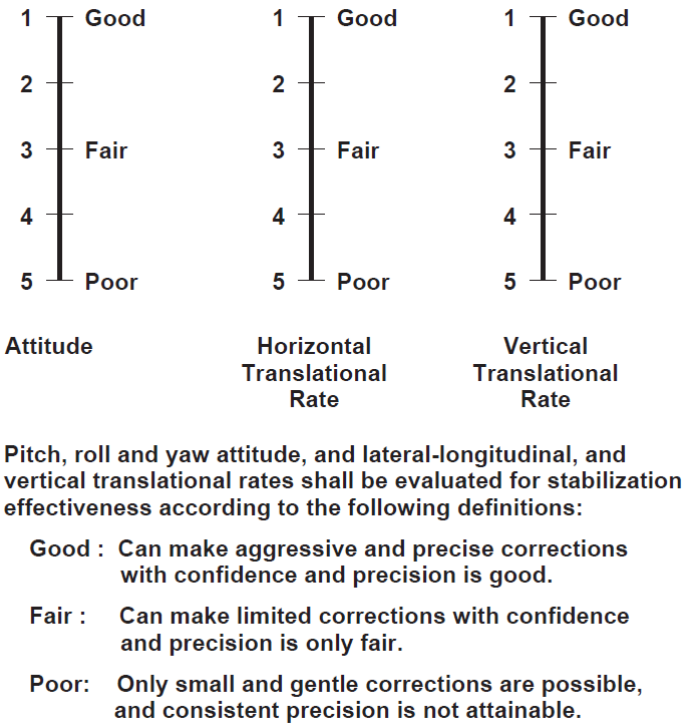

Figure A-2: Visual Cue Rating Scale [5]

Lastly, the NASA Task Load Index (TLX) rating was applied for the subjective pilot workload assessment. The evaluation contains six dimensions, which may contribute to the overall workload. Figure A-3 provides a definition of each dimension for the pilots.

RATING SCALE DEFINITIONS		
Title	**Endpoints**	**Descriptions**
MENTAL DEMAND	Low/High	How much mental and perceptual activity was required (e.g. thinking, deciding, calculating, remembering, looking, searching, etc.)? Was the task easy or demanding, simple or complex, exacting or forgiving?
PHYSICAL DEMAND	Low/High	How much physical activity was required (e.g. pushing, pulling, turning, controlling, activating, etc.)? Was the task easy or demanding, slow or brisk, slack or strenuous, restful or laborious?
TEMPORAL DEMAND	Low/High	How much time pressure did you feel due to the rate or pace at which the tasks or task elements occurred? Was the pace slow and leisurely or rapid and frantic?
PERFORMANCE	Good/Poor	How successful do you think you were in accomplishing the goals of the task set by the experimenter (or yourself)? How satisfied were you with your performance in accomplishing these goals?

EFFORT	Low/High	How hard did you have to work (mentally and physically) to accomplish your level of performance?
FRUSTATION LEVEL	Low/High	How insecure, discouraged, irritated, stressed and annoyed versus secure, gratified, content, relaxed and complacent did you feel during the task?

The scale to rate each of the six dimensions including 21 gradations:

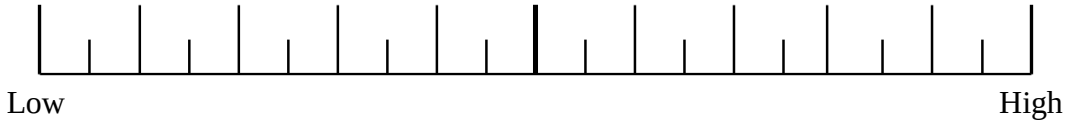

Figure A-3: NASA-TLX rating scale definitions [71]

A.2 Flight Path Tracking Results

The individual flight path tracking results of all sixteen pilots, who participated in the sense and avoid tasks, provide further impressions on the tracking accuracy and the obstacle avoidance maneuvers. Figure A-4 to Figure A-11 show the flown tracks in horizontal position with respect to the target flight path and the vertical altitude profile for both display types and all four visibility conditions. Three obstacles required a lateral avoidance maneuver and one obstacle (power line) required a vertical maneuver, either above or underneath it. For every visibility condition, the exact position and the sequence of the obstacle type appearance varied to ensure that pilots could not remember the appearance from one run to other. The target reference height was 100 feet above ground (≈ 30 m). The altitude profile varied slightly depending on the flown paths of each run.

In total, missed heading changes occurred only twice, while following the navigation markers presented on the HMD. This happened with the basic display type FG at 200 m (Figure A-6) and 400 m (Figure A-8) of visual range. At visibility conditions of 400 m or more, most pilots passed the power line above, while they were forced to fly below the cable wires at lower visual ranges in order to maintain ground visibility.

Visibility 100 m:

With the FG display type at 100 m of visual range, the pilots did not follow the first part of the flight track without the terrain visualization. The reason for this was that the northern corner of a lake was crossed by the target track. Without seeing the opposite shore of the lake at 100 m of visual range, the pilots followed the shore and got back on track after the crossing of the lake corner (Figure A-4: from 0 – 1000 m). As expected, initiation of the avoidance maneuver was very close to obstacles. Only three pilots passed the power line above. In general, the pilots flew at very low altitude and they were not able to maintain the reference height.

With the FGSA display type (Figure A-5), the flight path deviation was not observed because of the lake. Avoidance maneuvers were initiated earlier and distance to ground was higher. Ten out of the sixteen pilots decided to pass the power line above and thus, regarded it as being safer with the visual assistance.

Visibility of 200 m:

With the FG display type (Figure A-6), the number of flight path deviations around the north corner of the lake at the beginning of the task decreased. The avoidance maneuvers were more distinct and integrated smoother into the path following control strategy. More pilots decided to pass the power line above compared to the visibility of 100 m. One pilot lost the reference with the navigation markers before the second heading change. The reason could have been the small hill that had to be passed during this second heading change. Apart from that, all pilots could track the reference path very accurately.

With the FGSA display type (Figure A-7), the flight path tracking was very smooth and accurate. The avoidance maneuvers were initiated earlier compared to the FG display type. During the last 1500 m, a few pilots flew higher than the reference height. They did not recognize the descending terrain nor did they monitor the radar altitude sufficiently. However, they did not feel unsafe, even with less ground visibility, but with synthetic 3D-conformal augmentation.

Visibility of 400 m:

With both display types, the pilots could track the reference flight path accurately and smoothly. The height-above-ground was controlled according to the reference height in both cases. With the FG display type (Figure A-8), one pilot missed the first heading change and two other pilots have taken a shortcut during these heading changes. While two pilots passed the power line still underneath with the FG variant, all pilots passed it above with the FGSA display type. With the latter (Figure A-9), some pilots added a lateral maneuver to the vertical avoidance of the power line to cross it above the pole and not over the wire cables.

Visibility of 800 m:

At 800 m of visual range, the results of both display types are getting more and more identical (Figure A-10 and Figure A-11). In both cases, there were one or two pilots, who could not refrain from taking a shortcut at one of the heading changes. Flight path and height above ground tracking was smooth and accurate.

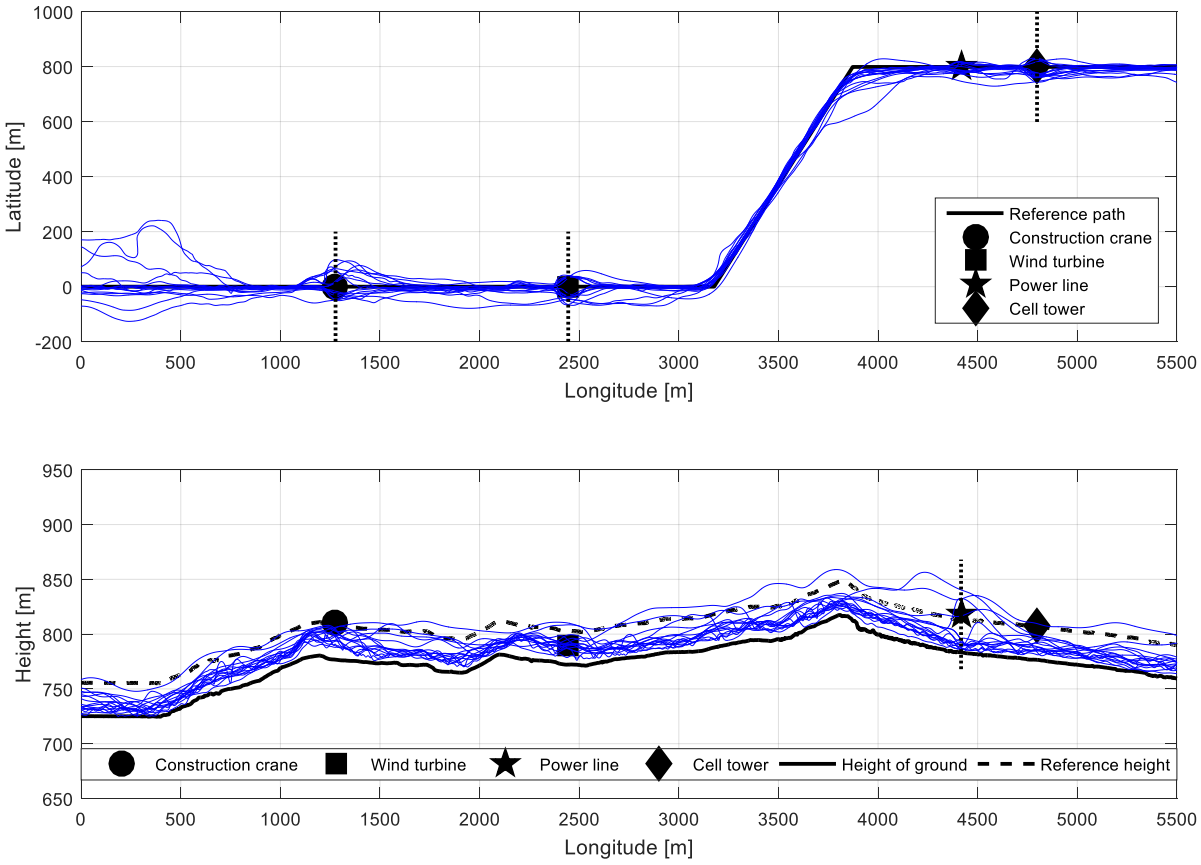

Figure A-4: Flight path tracking results for display type FG – 100 m visual range

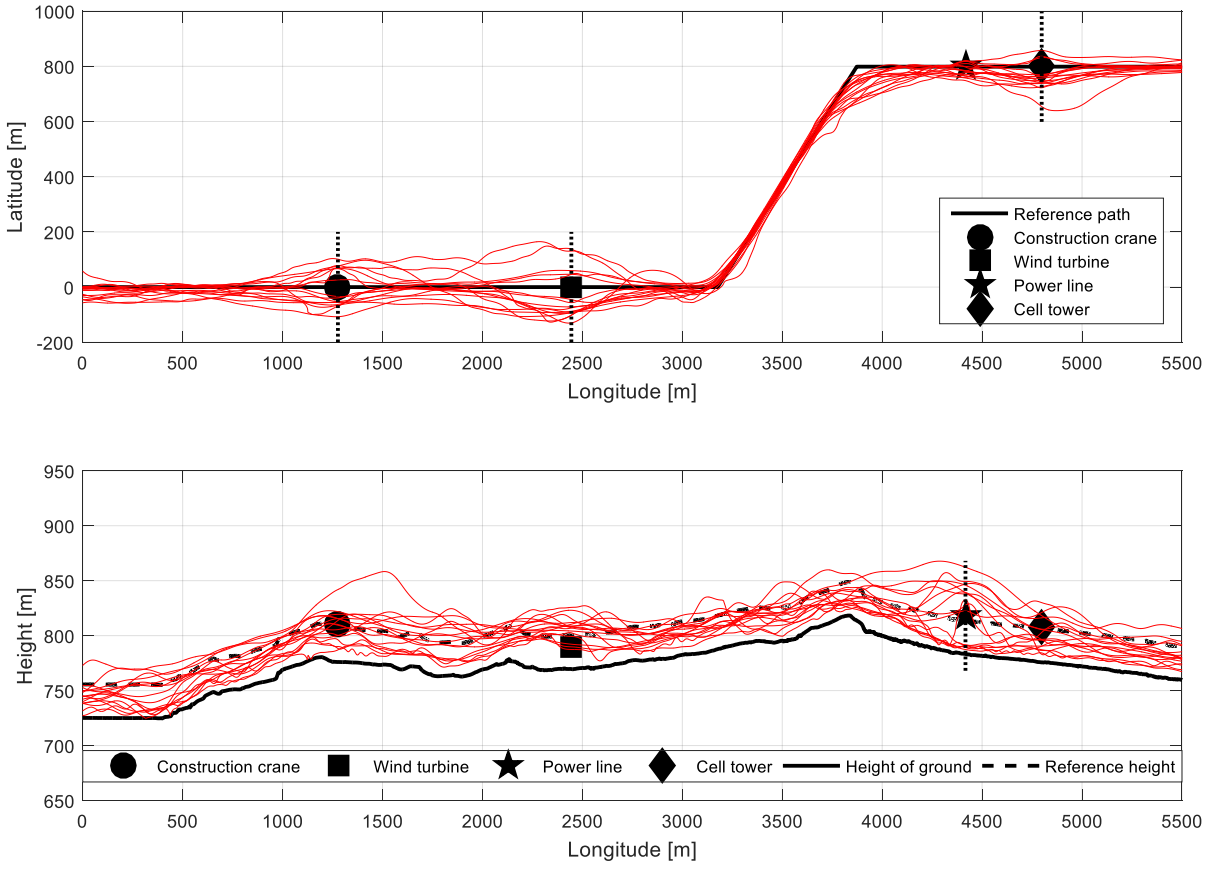

Figure A-5: Flight path tracking results for display type FGSA – 100 m visual range

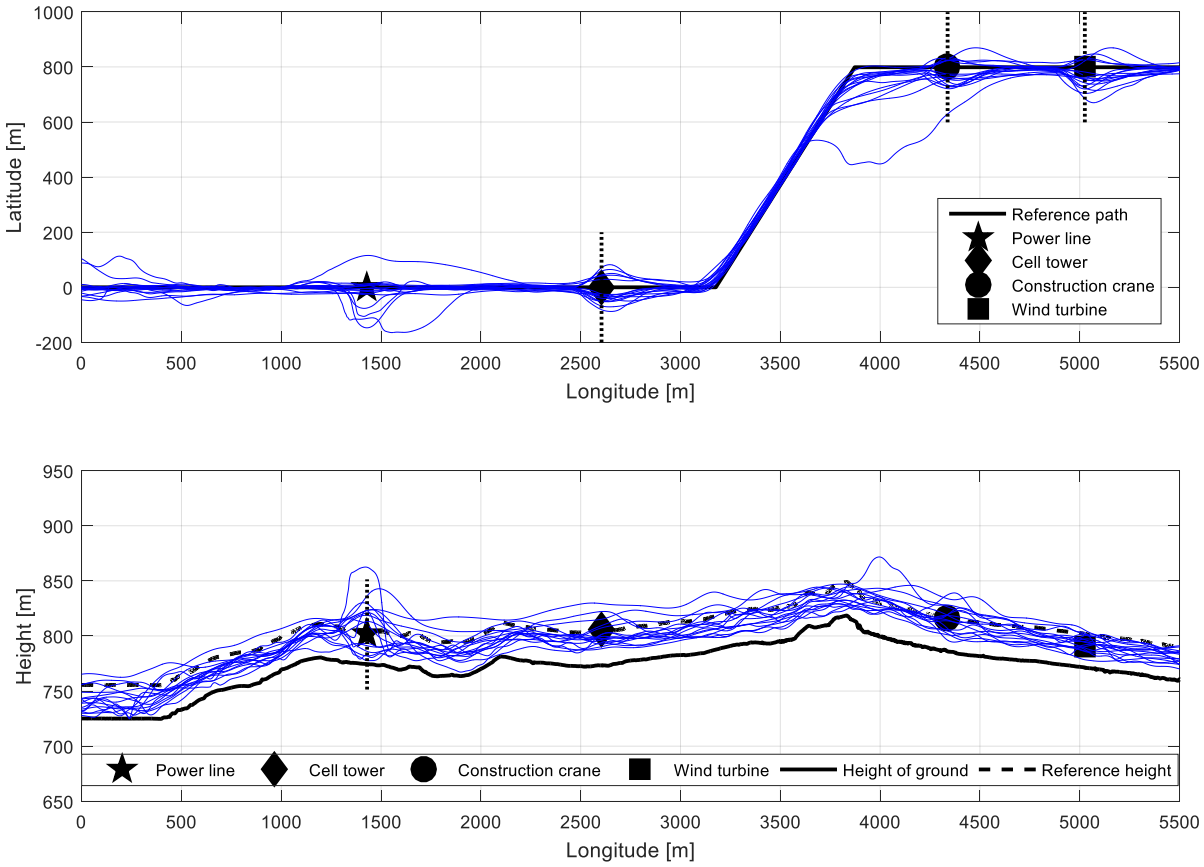

Figure A-6: Flight path tracking results for display type FG – 200 m visual range

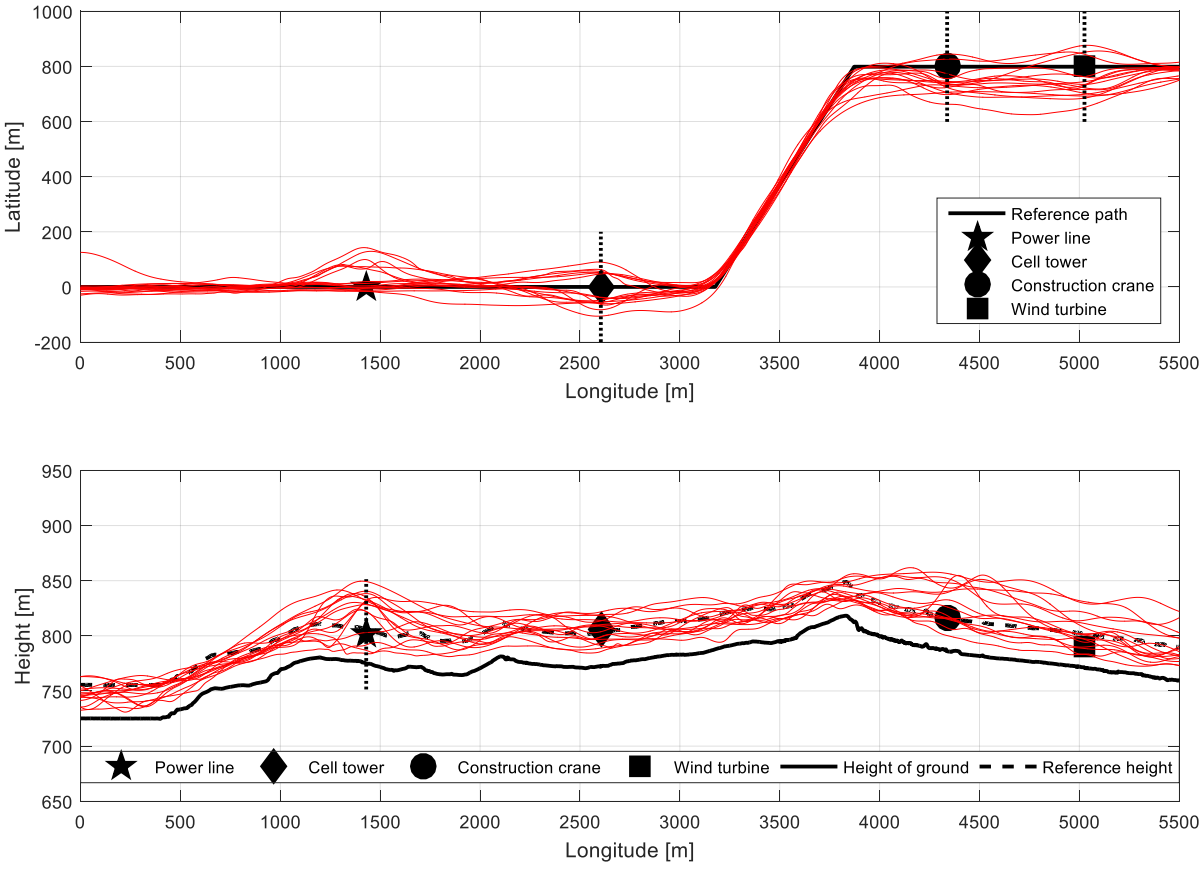

Figure A-7: Flight path tracking results for display type FGSA – 200 m visual range

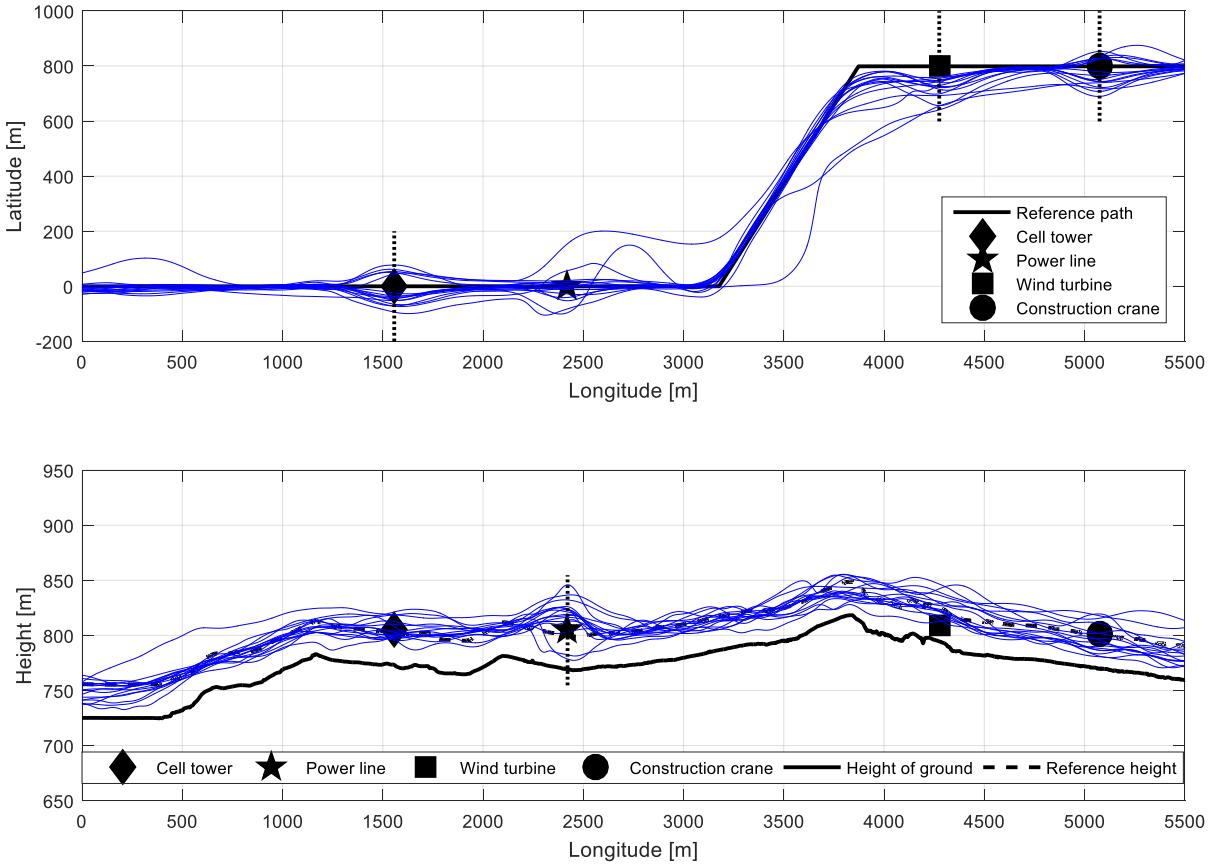

Figure A-8: Flight path tracking results for display type FG – 400 m visual range

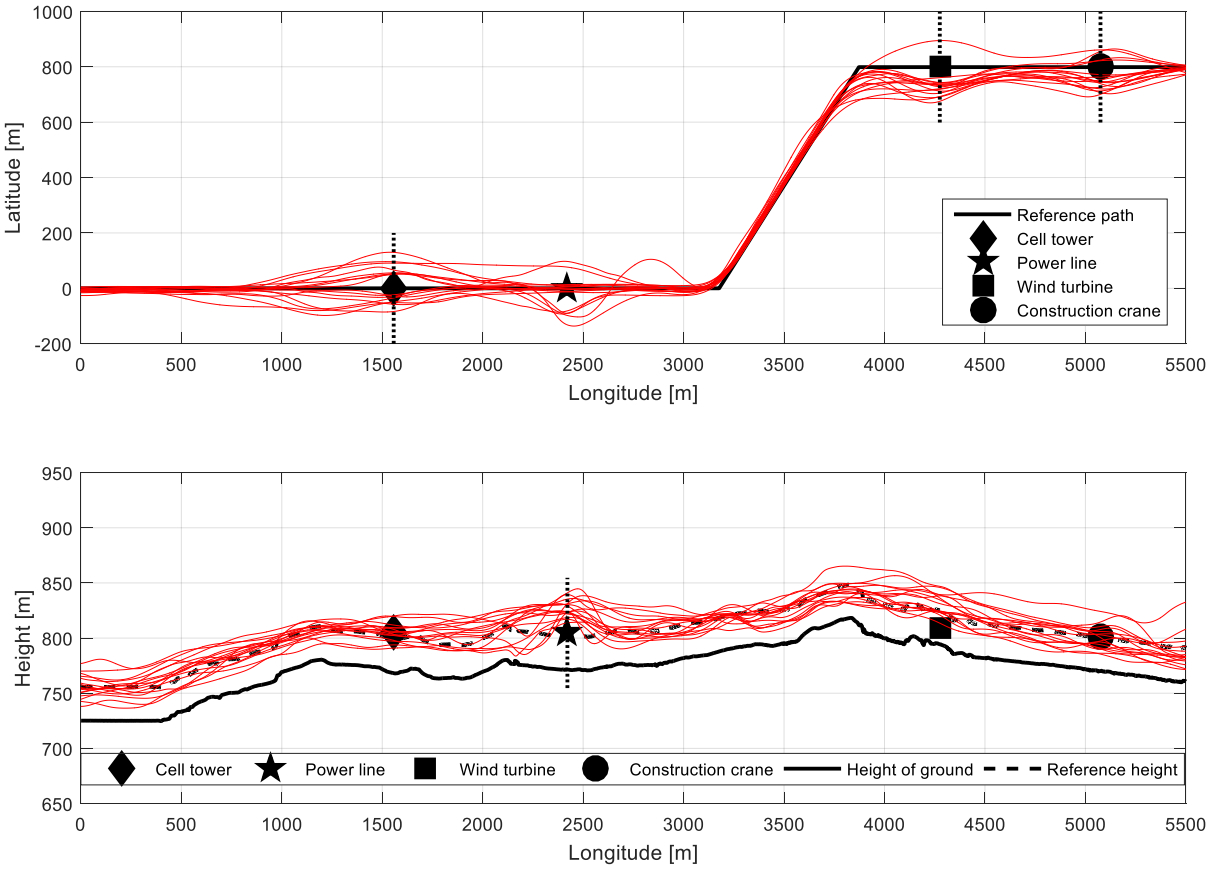

Figure A-9: Flight path tracking results for display type FGSA – 400 m visual range

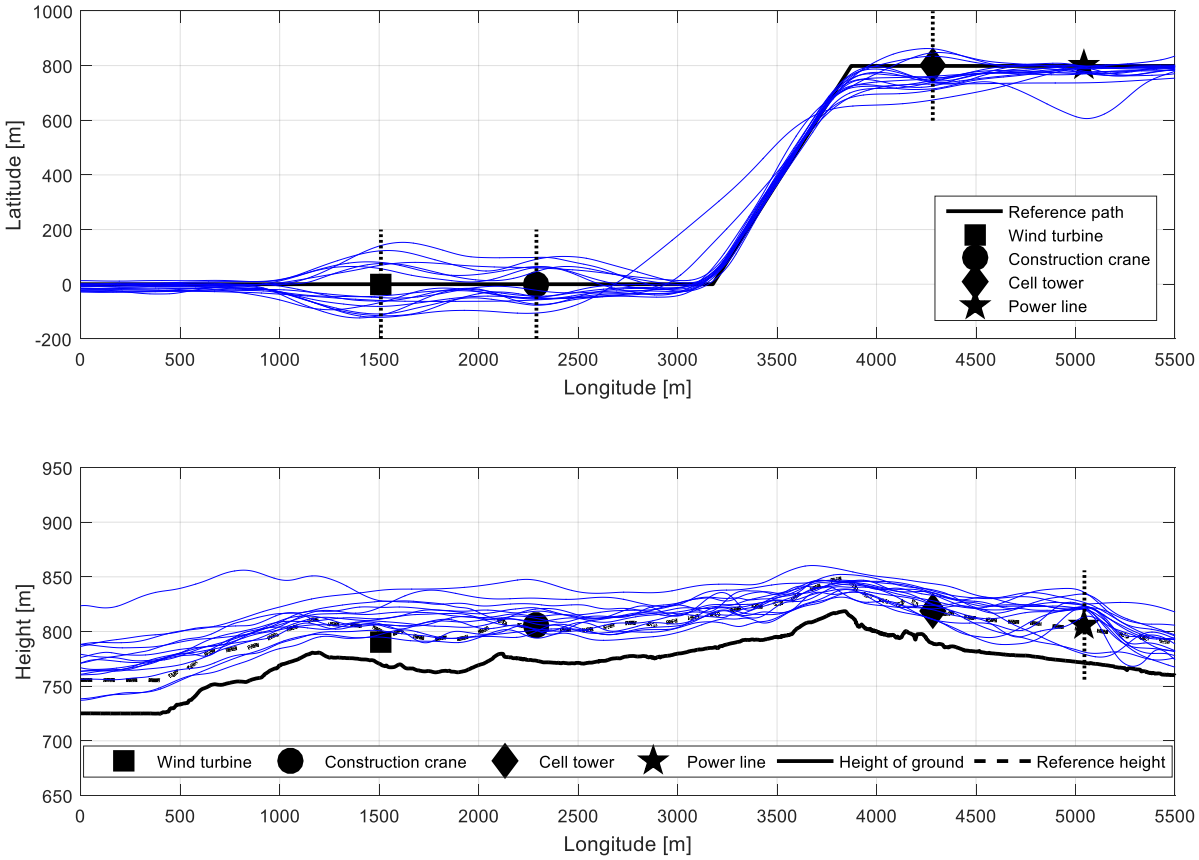

Figure A-10: Flight path tracking results for display type FG – 800 m visual range

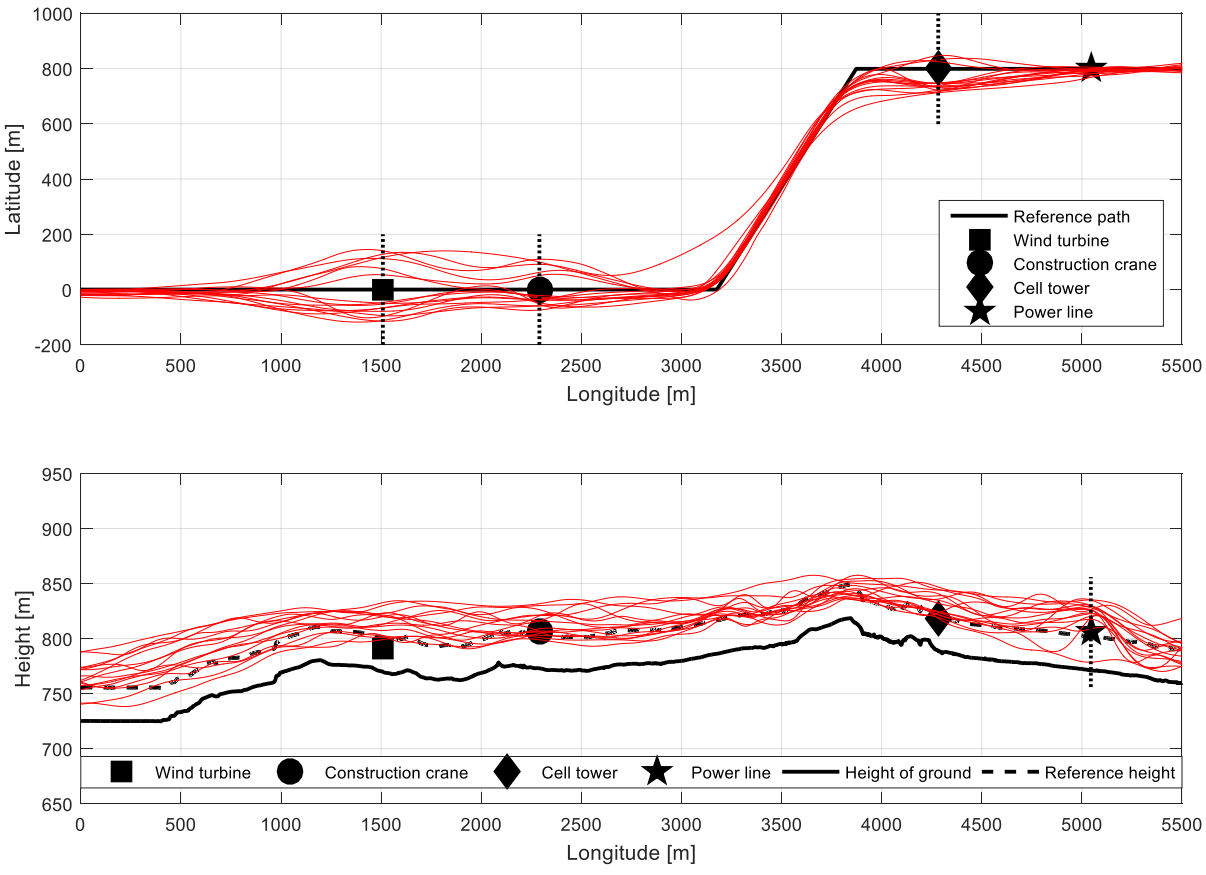

Figure A-11: Flight path tracking results for display type FGSA – 800 m visual range